

Barry S. Allen  
Vice President - Nuclear

419-321-7676  
Fax: 419-321-7582

May 14, 2012

L-12-196

Ms. Cynthia D. Pederson, Acting Administrator  
United States Nuclear Regulatory Commission  
Region III  
2443 Warrenville Road, Suite 210  
Lisle, IL 60532-4352

**SUBJECT:**

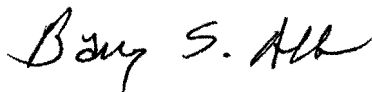
Davis-Besse Nuclear Power Station, Unit 1  
Docket Number 50-346, License Number NPF-3  
Submittal of Contractor Root Cause Assessment Report

On February 27, 2012, the FirstEnergy Nuclear Operating Company (FENOC) provided, via letter L-12-065, the Root Cause Analysis Report of the Davis-Besse Nuclear Power Station (DBNPS) Shield Building cracks to the Nuclear Regulatory Commission (NRC) in accordance with Confirmatory Action Letter 3-11-001. Following this submittal, during on-site NRC inspection activities, observations were identified with the content of both the FENOC Root Cause Analysis Report as well as the contractor root cause assessment report used to develop the FENOC Root Cause Analysis Report. These observations did not affect the overall conclusions or corrective actions being taken.

The contractor root cause assessment report by Performance Improvement International (PII) has been revised to incorporate these observations, and a non-proprietary version of the assessment report is enclosed. FENOC is in the process of revising our Root Cause Analysis Report based on the revised assessment report from PII, and will submit the revised Root Cause Analysis Report in the near future.

There are no regulatory commitments contained in this letter. If there are any questions or if additional information is required, please contact Mr. Patrick J. McCloskey, Manager, Site Regulatory Compliance, at (419) 321-7274.

Sincerely,



Barry S. Allen

GMW

RECEIVED MAY 15 2012

Davis-Besse Nuclear Power Station, Unit 1  
L-12-196  
Page 2 of 2

Enclosure: Performance Improvement International Root Cause Assessment, Davis-Besse Shield Building Laminar Cracking, Revision 2.1 (Redacted Version).

cc: NRC Document Control Desk  
DB-1 NRC/NRR Project Manager  
DB-1 Senior Resident Inspector  
Utility Radiological Safety Board

Enclosure

L-12-196

Performance Improvement International

Root Cause Assessment

Davis-Besse Shield Building

Laminar Cracking

Revision 2.1 (Redacted Version)

(1,091 pages follow)



**Performance Improvement International**

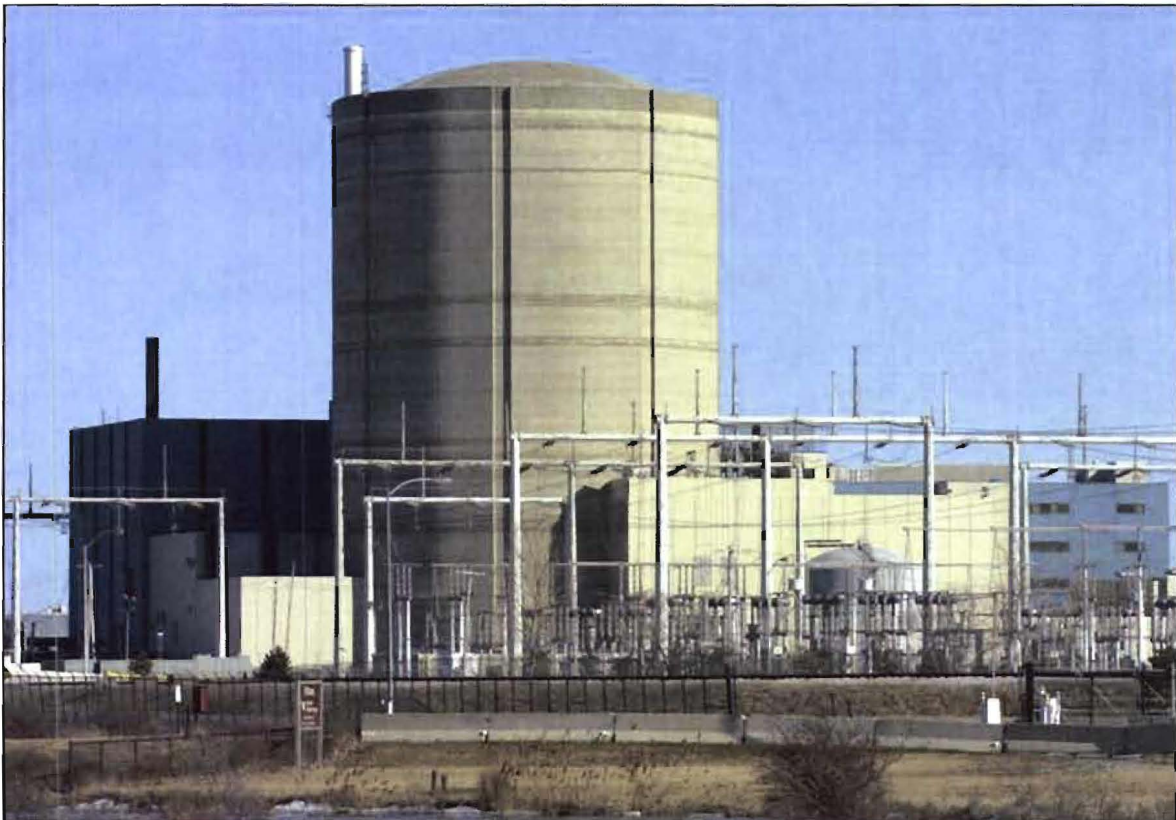
Providing a competitive advantage through research and applications

**REDACTED**

Root Cause Assessment

Davis-Besse Shield Building

Laminar Cracking



**Revision 2.1 REDACTED**

4/20/2012



This report is a Root Cause Assessment (RCA) of laminar cracking associated with the Davis-Besse Shield Building identified on October 10, 2011. The assessment was performed by Performance Improvement International (PII) at the request of First Energy Nuclear Operating Company (FENOC).

**Performance Improvement International:**

Chong Chiu, PhD, Team Leader

[REDACTED], PE

[REDACTED], PE

[REDACTED]

[REDACTED]

[REDACTED], PE

[REDACTED]

[REDACTED], Dr. Eng.


[REDACTED], PhD

[REDACTED], PE

[REDACTED], PhD, Reviewer

[REDACTED], PhD

Approved:

  
\_\_\_\_\_

Chong Chiu, PhD, Founder  
Performance Improvement International, LLC



## Table of Contents

<b>SUMMARY OF REVISIONS IN VERSION 2</b>	<b>1</b>
<b>I. INTRODUCTION</b>	<b>1</b>
SECTION 1.01 ISSUE	1
SECTION 1.02 REPORT STRUCTURE	1
<b>II. EXECUTIVE SUMMARY</b>	<b>2</b>
SECTION 2.01 LABORATORY TESTS AND EXAMINATION TO TEST FOR CONCRETE INTEGRITY	2
SECTION 2.02 CARBONATION	3
SECTION 2.03 THERMAL AND STRESS ANALYSIS	5
SECTION 2.04 ROOT CAUSE	5
SECTION 2.05 LAMINAR CRACKING SCENARIOS (PRIMARY AND SECONDARY)	6
SECTION 2.06 PREVENTION	8
<b>III. PLANT DESCRIPTION AND HISTORY</b>	<b>8</b>
SECTION 3.01 GENERAL DESIGN	8
SECTION 3.02 LAMINAR CRACK DISCOVERY	10
(A) CHARACTERIZATION OF LAMINAR CRACKS	11
<b>IV. FAILURE MODE PROCESS</b>	<b>11</b>
<b>V. GROUP 1: UNREFUTED FAILURE MODES – DESIGN &amp; ANALYSIS PHASE</b>	<b>12</b>
SECTION 5.01 UNREFUTED FAILURE MODES:	12
SECTION 5.02 FAILURE MODES 1.3 & 1.12:	13
(A) DISCUSSION	13
(B) FMS 1.3 – SHOULDER DESIGN AND REINFORCING STEEL ASSOCIATED WITH THE SHOULDER AREA: SUPPORTING EVIDENCE VERIFYING FAILURE MODE	14
(C) FMS 1.12 – SHOULDER DESIGN AND REINFORCING STEEL ASSOCIATED WITH THE SHOULDER AREA: SUPPORTING EVIDENCE VERIFYING FAILURE MODE	15
(D) CONCLUSION	15
SECTION 5.03 FAILURE MODE 1.5	15
(A) DISCUSSION	15
(B) FM 1.5 – HIGH CONCRETE STRESS AREAS ASSOCIATED WITH HIGH DENSITY OF HORIZONTAL REINFORCING STEEL: SUPPORTING EVIDENCE VERIFYING FAILURE MODE	16
(C) CONCLUSION	17
<b>VI. GROUP 2: FAILURE MODES – CONSTRUCTION &amp; FABRICATION PHASE</b>	<b>17</b>
SECTION 6.01 UNREFUTED FAILURE MODES	17
SECTION 6.02 FAILURE MODE 2.7:	17
(A) DISCUSSION	17
(i) THE TOP-DOWN MOISTURE PENETRATION	18
(ii) THE EXTERNAL-INTERNAL MOISTURE PENETRATION	19
(B) FM 2.7 – CONCRETE SEALANT: SUPPORTING EVIDENCE VERIFYING FAILURE MODE	21
(C) CONCLUSION:	22
<b>VII. GROUP 3: MAIN/SUB FAILURE MODES – OPERATIONAL PHASE</b>	<b>23</b>
SECTION 7.01 UNREFUTED FAILURE MODES	23



<b>SECTION 7.02</b>	<b>SUMMARY OF FAILURE MODES 3.6 (A) &amp; 3.6 (B):</b>	<b>23</b>
(A)	DISCUSSION	23
(B)	FAILURE MODE HYPOTHESIS	24
(I)	SUB-MODE 1: FM 3.6 (A) – FREEZING OF WATER NEAR OUTER REBAR MAT IN BLIZZARD CONDITIONS	24
(II)	SUB-MODE 2: FM 3.6 (B) – EXPANSION OF CONCRETE IN BLIZZARD CONDITIONS DUE TO INTERNAL ICE FORMATION	27
<b>VIII.</b>	<b>ANALYSIS INTRODUCTION</b>	<b>29</b>
<b>SECTION 8.01</b>	<b>ANALYSIS SUMMARY</b>	<b>29</b>
<b>IX.</b>	<b>ANALYSIS I, FM 3.6 (A): FINITE ELEMENT ANALYSIS OF DENSE REBAR CONDITION</b>	<b>30</b>
<b>SECTION 9.01</b>	<b>DENSE REBAR ANALYSIS</b>	<b>30</b>
(A)	“ENABLING EVENT” CONSIDERED	30
(B)	ANALYSIS DESIGN	30
(C)	SCENARIOS CONSIDERED	31
(D)	RESULTS SUMMARY	32
(E)	CONCLUSION	35
<b>X.</b>	<b>ANALYSIS II, FM 3.6 (B): FINITE ELEMENT ANALYSIS OF 1977 &amp; 1978 BLIZZARD CONDITIONS</b>	<b>36</b>
<b>SECTION 10.01</b>	<b>ANALYSIS</b>	<b>36</b>
<b>SECTION 10.02</b>	<b>COEFFICIENT OF THERMAL EXPANSION</b>	<b>39</b>
<b>SECTION 10.03</b>	<b>CIRCUMFERENTIAL TEMPERATURE DISTRIBUTION AT O.F. HORIZONTAL REBAR</b>	<b>40</b>
<b>SECTION 10.04</b>	<b>[REDACTED]</b>	<b>41</b>
(A)	[REDACTED]	43
(I)	1978 BLIZZARD CONDITION	44
(II)	1977 BLIZZARD CONDITION	48
<b>SECTION 10.05</b>	<b>CONCLUSION</b>	<b>51</b>
<b>XI.</b>	<b>ANALYSIS III: LAMINAR CRACKING DUE TO 1978 BLIZZARD CONDITIONS (FINITE ELEMENT CONCRETE [REDACTED] MODEL)</b>	<b>52</b>
<b>SECTION 11.01</b>	<b>BACKGROUND</b>	<b>52</b>
<b>SECTION 11.02</b>	<b>COEFFICIENT OF THERMAL EXPANSION</b>	<b>52</b>
<b>SECTION 11.03</b>	<b>[REDACTED]</b>	<b>53</b>
<b>SECTION 11.04</b>	<b>CIRCUMFERENTIAL TEMPERATURE DISTRIBUTION OF O.F. HORIZONTAL REBAR</b>	<b>54</b>
<b>SECTION 11.05</b>	<b>[REDACTED]</b>	<b>55</b>
<b>SECTION 11.06</b>	<b>DISCUSSION</b>	<b>58</b>
(A)	1978 BLIZZARD CONDITION	58
(B)	1977 BLIZZARD CONDITION	60
<b>SECTION 11.07</b>	<b>CONCLUSION</b>	<b>62</b>
<b>XII.</b>	<b>ANALYSIS IV: DAMAGE PROPAGATION INTO REGIONS WITH HIGH REBAR DENSITY</b>	<b>62</b>
<b>SECTION 12.01</b>	<b>BACKGROUND</b>	<b>62</b>
<b>SECTION 12.02</b>	<b>[REDACTED]</b>	<b>63</b>
<b>SECTION 12.03</b>	<b>CIRCUMFERENTIAL TEMPERATURE DISTRIBUTION AT O.F. REBAR</b>	<b>64</b>
<b>SECTION 12.04</b>	<b>DISCUSSION</b>	<b>64</b>
<b>SECTION 12.05</b>	<b>[REDACTED]</b>	<b>65</b>



(A) TOP 20' OF THE WALL LOCATION	65
(B) STEAM LINE LOCATION	66
<b>XIII. ANALYSIS V: INVESTIGATION FOR POTENTIAL LAMINAR CRACKING UNDER VARIOUS TEMPERATURE CONDITIONS</b>	<b>68</b>
SECTION 13.01 THERMAL STRESS SCREENING	68
SECTION 13.02 COMBINATION LOAD CASES	70
SECTION 13.03 ANALYSIS BASED ON MEASURED PROPERTIES	71
(A) CIRCUMFERENTIAL TEMPERATURE DISTRIBUTION AT O.F. HORIZONTAL REBAR	71
(B) [REDACTED]	73
SECTION 13.04 STRESS STATE DURING HOT SUMMER CONDITION	75
(A) STRESS ANALYSIS RESULTS SUMMARY	75
(B) SHOULDER 10 LOCATION ([REDACTED])	76
(C) AZIMUTH 225° LOCATION ([REDACTED])	80
SECTION 13.05 CONCLUSION	85
<b>XIV. ANALYSIS VI: INVESTIGATION OF POTENTIAL LAMINAR CRACK PROPAGATION GIVEN CURRENT SHIELD BUILDING CONDITION</b>	<b>86</b>
SECTION 14.01 ANALYSIS	86
SECTION 14.02 CONCLUSION	87
<b>XV. ROOT CAUSE AND CONTRIBUTING CAUSES</b>	<b>88</b>
<b>XVI. RECOMMENDATIONS TO PREVENT RECURRENCE</b>	<b>90</b>
<b>XVII. ADDITIONAL CONSIDERATIONS</b>	<b>92</b>
<b>APPENDIX I REFERENCE</b>	<b>I-1</b>
<b>APPENDIX II SUMMARY OF FINITE ELEMENT ANALYSES PERFORMED</b>	<b>II-1</b>
SECTION 2.01 SUMMARY	II-1
SECTION 2.02 [REDACTED]	II-1
(A) EXHIBIT 67 – DAVIS-BESSE CONTAINMENT TOWER [REDACTED] ANALYSIS	II-1
SECTION 2.03 [REDACTED]	II-2
(A) EXHIBIT 65 – DAVIS-BESSE THERMAL ANALYSIS	II-2
SECTION 2.04 [REDACTED]	II-2
(A) EXHIBIT 56 – STRUCTURAL AND THERMAL ANALYSIS INVESTIGATION	II-2
SECTION 2.05 [REDACTED]	II-3
(A) EXHIBIT 51 – FREEZING FAILURE AND REBAR SPACING SENSITIVITY STUDY	II-3
(B) EXHIBIT 73 – LAMINAR CRACKING DUE TO 1978 BLIZZARD	II-4
(C) EXHIBIT 75 – DAMAGE PROPAGATION INTO REGIONS WITH HIGH REBAR DENSITY	II-5
SECTION 2.06 [REDACTED]	II-5
(A) EXHIBIT 61 – STRESS STATE DURING THE 1978 AND 1977 BLIZZARDS	II-5
(B) EXHIBIT 62 – STRESS ANALYSIS DUE TO 105 MPH WIND LOAD	II-6
(C) EXHIBIT 64 – THERMAL STRESS ANALYSIS WITH GRAVITY AND WIND LOAD	II-7
SECTION 2.07 MODULUS OF ELASTICITY	II-7
<b>APPENDIX III UNCERTAINTY ANALYSIS</b>	<b>III-1</b>
<b>APPENDIX IV FAILURE MODE CHART</b>	<b>IV-1</b>
<b>APPENDIX V GROUP I FAILURE MODES</b>	<b>V-1</b>





<u>APPENDIX VI</u>	<u>GROUP 2 FAILURE MODES</u>	<u>VI-13</u>
<u>APPENDIX VII</u>	<u>GROUP 3 FAILURE MODES</u>	<u>VII-35</u>
<u>APPENDIX VIII</u>	<u>EXHIBITS</u>	<u>VIII-1</u>
<u>APPENDIX IX</u>	<u>RESUMES</u>	<u>IX-80</u>



## List of Figures

Figure 1: Plan View of the Davis-Besse Shield Building (8 Flutes & 16 Shoulders) .....	9
Figure 2: Rebar Schematic of Shield Building Shell and Architectural-Panel Shoulder Interface .....	14
Figure 3: High Density of Reinforcement at Outer Rebar Mat (Photo during Construction) .....	16
Figure 4: Top-Down Moisture Transport Mechanism .....	19
Figure 5: External-Internal Moisture Penetration.....	20
Figure 6: Freezing of Water near Outer Rebar Mat Sequence (FM 3.6, Sub-Mode 1).....	26
Figure 7: Outer-Expansion-Inner-Contraction Schematic (FM 3.6, Sub-Mode 2) .....	28
Figure 8: Laminar Cracking (Nominal 6" Spacing, 0.6% VF) .....	34
Figure 9: Debonding but No Laminar Cracking (Nominal 12" Rebar, 0.6% VF) .....	35
Figure 10: Plan View of the DBSB (Analysis of Flute 6, Shoulders 11 & 12) .....	38
Figure 11: Circumferential Temperature Distribution at the O.F. Horizontal Rebar Depth .....	41
Figure 12: ██████████ Geometry and Rebar .....	42
Figure 13: ██████████ Detail of Flute Region .....	42
Figure 14: ██████████ Detail of Flute Region with Mesh.....	43
Figure 15: Temperature (°F) during the Blizzard of 1978; Deformation Scale Factor 500X .....	45
Figure 16: Max Principal Stress (psi) during the 1978 Blizzard; Deformation Scale Factor 500X .....	45
Figure 17: Max Principal Stress during the 78 Blizzard; Deformation Scale Factor 500X; Wider Contour Range (+/- 1200 psi) .....	46
Figure 18: Radial Stress (psi) during the Blizzard of 1978; Deformation Scale Factor 500X.....	46
Figure 19: Hoop Stress (psi) during the Blizzard of 1978; Deformation Scale Factor 500X.....	47
Figure 20: Hoop Stress (psi) during the Blizzard of 1978; Deformation Scale Factor 500X; Wider Contour Range (+/- 1200 psi) .....	47
Figure 21: Vertical Stress (psi) during the Blizzard of 1978; Deformation Scale Factor 500X .....	48
Figure 22: Temperature (°F) during the Blizzard of 1977; Deformation Scale Factor 500X .....	49
Figure 23: Max Principal Stress (psi) during the Blizzard of 1977; Deformation Scale Factor 500X .....	49
Figure 24: Radial Stress (psi) during the Blizzard of 1977; Deformation Scale Factor 500X.....	50
Figure 25: Hoop Stress (psi) during the Blizzard of 1977; Deformation Scale Factor 500X.....	50
Figure 26: Vertical Stress (psi) during the Blizzard of 1977; Deformation Scale Factor 500X .....	51
Figure 27: Shield Building with Flute Numbers and ██████████ of ██████████ .....	53
Figure 28: Circumferential Temperature Distribution at the O.F. Horizontal Rebar Depth .....	55
Figure 29: ██████████; Geometry and Rebar .....	56
Figure 30: ██████████ Detail of Flute Region .....	56
Figure 31: ██████████; Detail of Flute Region with Mesh.....	57
Figure 32: Temperature (°F) during the Blizzard of 1978 .....	58
Figure 33: ██████████ during the 1978 Blizzard .....	59
Figure 34: Cracking Result during the 1978 Blizzard showing regions with DAMAGE > 0.7.....	59
Figure 35: Temperature (°F) during the Blizzard of 1977 .....	60
Figure 36: Cracking Result during the Blizzard of 1977 .....	61



Figure 37: Cracking Result during the 1977 Blizzard showing regions with DAMAGE > 0.7.....	61
Figure 38: Shield Building with Flute Numbers and Locations of [REDACTED].....	63
Figure 39: Temperature Contours (°F) in the Top 20' of the Wall .....	65
Figure 40: Cracking Result in Top 20' of the Wall showing regions with DAMAGE > 0.6 .....	66
Figure 41: Temperature Contours (°F) at Steam Line.....	67
Figure 42: Steam Line Area Cracking Result showing regions with DAMAGE > 0.6 .....	67
Figure 43: Circumferential Temperature Distribution at O.F. Horizontal Rebar.....	72
Figure 44: Shield Building Flute Numbers and Azimuth Locations.....	74
Figure 45: Temperature Distribution (°F) in the [REDACTED] in the Shoulder 10 Location .....	76
Figure 46: Max Principal Stress (psi) in the [REDACTED] in the Shoulder 10 Location .....	77
Figure 47: Radial Stress (psi) in the [REDACTED] in the Shoulder 10 Location .....	78
Figure 48: Hoop Stress (psi) in the [REDACTED] in the Shoulder 10 Location .....	79
Figure 49: Vertical Stress (psi) in the [REDACTED] in the Shoulder 10 Location.....	80
Figure 50: Temperature Distribution (°F) in the [REDACTED] at the Azimuth 225° Location .....	81
Figure 51: Max Principal Stress (psi) in the Shell Section [REDACTED] placed at the Azimuth 225° Location .....	82
Figure 52: Radial Stress (psi) in the Shell Section [REDACTED] placed at the Azimuth 225° Location .....	83
Figure 53: Hoop Stress (psi) in the Shell Section [REDACTED] placed at the Azimuth 225° Location .....	84
Figure 54: Vertical Stress (psi) in the Shell Section [REDACTED] placed at the Azimuth 225° Location.....	85
Figure 55: "Thin-Crack" region introduced as idealized the "Cracked" boundary at the OF Rebar.....	86
Figure 56: Summer Solstice Hot No Wind 7:30 pm, Constant Concrete CTE = 5.20 x10-6 in/in/°F.....	87



## List of Tables

Table 1: Comparison of 1977, 1978, & 1994 Blizzard Conditions (1978 Snowfall & Wind Velocity show Worst Case).....	24
Table 2: Results from Rebar Sensitivity Study for various Motivating Forces and Rebar Spacing.....	33
Table 3: .....	34
Table 4: [REDACTED].....	69
Table 5: [REDACTED].....	70
Table 6: Summer Solstice with Simulated 30'x30' "Crack" - Summary Results for Radial Stress @ EL 785' 10" (+ = Tension, - = Compression).....	87
Table 7: Root Cause/Contributing Factors and Corrective Action to Prevent Recurrence.....	91



## List of Exhibits

Exhibit 1: Mix Design .....	VIII-2
Exhibit 2: Lab Test Results from CTL.....	VIII-3
Exhibit 3: Lab Test Results from Twining .....	VIII-4
Exhibit 4: Spec C-26; Forming, Placing, Finishing, & Curing Concrete .....	VIII-5
Exhibit 5: QA and Procedures for Slip Form Construction .....	VIII-6
Exhibit 6: Technical Specification for the Shield Building .....	VIII-7
Exhibit 7: Freeze Thaw Tests, 1971 .....	VIII-8
Exhibit 8: NCR's Concrete Placement .....	VIII-9
Exhibit 9: Wall Inspection 2011, Part I.....	VIII-10
Exhibit 10: Wall Inspection 2011, Part II.....	VIII-11
Exhibit 11: Concrete Submittals .....	VIII-12
Exhibit 12: NCR – Interim Field Report, W2C and Temp. ....	VIII-13
Exhibit 13: NCR – Interim Field Report (Wrong Mix).....	VIII-14
Exhibit 14: NCR 57 – Wrong Cement Type .....	VIII-15
Exhibit 15: Slip Form Time Quantities Analysis .....	VIII-16
Exhibit 16: Rebar Cover Spacing (FENOC Document – Not Included as an Attachment to this Report) VIII-17	
Exhibit 17: Spec C-29 Reinforcing Steel .....	VIII-18
Exhibit 18: Wall Plumb Measurements .....	VIII-19
Exhibit 19: Out-of-Plumb Interim Field Reports.....	VIII-20
Exhibit 20: Slip-Form Records Summary.....	VIII-21
Exhibit 21: Guide for Preparation.....	VIII-22
Exhibit 22: ACI 546R-04 .....	VIII-23
Exhibit 23: Hydrodemolition of Concrete Surfaces and Reinforced Concrete.....	VIII-24
Exhibit 24: Hydrodemolition .....	VIII-25
Exhibit 25: MoDot Hydrodemolition and Repair of Bridge Decks .....	VIII-26
Exhibit 26: Test Report from WJE.....	VIII-27
Exhibit 27: 347R-63 Guide to Form Work .....	VIII-28
Exhibit 28: Fegles Drawing of Jack Bar Layout Plan.....	VIII-29
Exhibit 29: Permeability versus Water Cement Ratio .....	VIII-30
Exhibit 30: Irradiation Effect .....	VIII-31
Exhibit 31: MF-6, Rebar Detail by Fegles .....	VIII-32
Exhibit 32: ACI 515 Protective Systems .....	VIII-33
Exhibit 33: Corrosion Related Photos .....	VIII-34
Exhibit 34: Concrete Mix Summary for Below Grade.....	VIII-35
Exhibit 35: Concrete Strength Summary for Below Grade .....	VIII-36
Exhibit 36: Concrete Strength Summary for Above Grade .....	VIII-37
Exhibit 37: Earthquake Event .....	VIII-38



Exhibit 38: Shrinkage Crack Photos .....	VIII-39
Exhibit 39: C-0112 – Shield Building Details.....	VIII-40
Exhibit 40: C-0111 – Shield Building Wall Development .....	VIII-41
Exhibit 41: C-0110 – Roof Plan Wall Section Details .....	VIII-42
Exhibit 42: Entire Structure, 11-23 .....	VIII-43
Exhibit 43: Calc. C-CSS-099.20-054 R1 (FENOC Document – Not Included as an Attachment to this Report).....	VIII-44
Exhibit 44: Drawing C-0111a (FENOC Document – Not Included as an Attachment to this Report) ..	VIII-45
Exhibit 45: C-0100 Shield Building Foundation (FENOC Document – Not Included as an Attachment to this Report) .....	VIII-46
Exhibit 46: Shield Building Inspection Overview .....	VIII-47
Exhibit 47: E-0401 Lighting & Lightning (FENOC Document – Not Included as an Attachment to this Report).....	VIII-48
Exhibit 48: 1995 – 0395 Lightning (FENOC Document – Not Included as an Attachment to this Report) .....	VIII-49
Exhibit 49: Corrosion Related Photos (FENOC Document – Not Included as an Attachment to this Report).....	VIII-50
Exhibit 50: Calc. CSS 090.022-056 Rev 02 (FENOC Document – Not Included as an Attachment to this Report).....	VIII-51
Exhibit 51: Freezing and Rebar Spacing Study .....	VIII-52
Exhibit 52: Test Report from the University of Colorado .....	VIII-53
Exhibit 53: C-0109 Roof Plans and Details .....	VIII-54
Exhibit 54: C-200 .....	VIII-55
Exhibit 55: ACI 201.2R-08, Table 6.3 .....	VIII-56
Exhibit 56: Structural and Thermal Analysis Investigation .....	VIII-57
Exhibit 57: Temperature Dependent CTE .....	VIII-58
Exhibit 58: Carbonation Lab Testing.....	VIII-59
Exhibit 59: Test Report from the United States Bureau of Reclamation (USBR) .....	VIII-60
Exhibit 60: Test Report from the University of Colorado .....	VIII-61
Exhibit 61: Stress State during the 1977 and 1978 Blizzards .....	VIII-62
Exhibit 62: Stress Analysis due to 105 MPH Wind Load .....	VIII-63
Exhibit 63: CFD Analysis of Shield Building .....	VIII-64
Exhibit 64: Thermal Stress Analysis with Gravity and Wind Load .....	VIII-65
Exhibit 65: Thermal Analysis .....	VIII-66
Exhibit 66: Toledo 1978 Weather.....	VIII-67
Exhibit 67: CFD Analysis Summary .....	VIII-68
Exhibit 68: Debonding of Rebar/Concrete Lab Testing .....	VIII-69
Exhibit 69: M-284a .....	VIII-70
Exhibit 70: M-284b .....	VIII-71
Exhibit 71: Comparison of Toledo Blizzards.....	VIII-72



Exhibit 72: Water and Moisture Transfer into Concrete .....	VIII-73
Exhibit 73: Laminar Cracking due to 1978 Blizzard .....	VIII-74
Exhibit 74: Exhibit Not Used .....	VIII-75
Exhibit 75: Damage Propagation Analysis .....	VIII-76
Exhibit 76: Sample List and Activity for Lab Testing .....	VIII-77
Exhibit 77: Aggregate Size Distribution & Void Fraction Lab Testing .....	VIII-78
Exhibit 78: Microcrack Lab Testing .....	VIII-79



## Acronyms

**ABAQUS** – Finite Element Analysis Software

**ACI** – American Concrete Institute

**AGM** – [REDACTED]

**CDP** – Concrete Damaged Plasticity

**CFD** – Computational Fluid Dynamics

**CTE** – Coefficient of Thermal Expansion

**DBSB** – Davis-Besse Shield Building

**FEA** – Finite Element Analysis

**FEM** – Finite Element Methods/Modeling

**FENOC** – First Energy Nuclear Operating Company

**FM** – Failure Mode

**IR** – Impulse Response

**NASTRAN** – Finite Element Analysis Program

**NDE** – Nondestructive Evaluation

**NRC** – Nuclear Regulatory Commission

**PII** – Performance Improvement International

**VF** – Void Fraction

**WDR** – Wind-Driven Rain





## Summary of Revisions in Version 2

The RCR was revised to include comments and responses following NRC and FENOC review. The main changes are summarized below:

1. Item 15: Were fracture surfaces or concrete voids tested near the subsurface laminar crack surfaces for the presence Ettringite as was done along the outer surface of the SB core bores to confirm moisture intrusion (e.g. Ettringite)? If not, why was this test not done to confirm that moisture had penetrated to location/depth of laminar cracks? If this testing was done provide the results.
  - a. PII: (ADDED TO F.M. 3.9 – Discussion - Moisture Migration)
2. Item 19: Why did the observed laminar cracking propagate "through" the coarse aggregate Instead of around the aggregate? Does this suggest any information about the rate of crack propagation?
  - a. PII: (ADDED TO Section 2.01 –Laboratory Tests and Examination to Test for Concrete Integrity – 1st paragraph – PAGE 3)
3. Item 20: With the conclusion that the laminar subsurface cracking was not exposed to air, what caused the trace amounts of carbonation identified on the transverse and longitudinal crack surfaces?
  - a. PII: (See the Carbonation Failure Mode.)
4. Item 21: States that the lack of micro-cracks on the fracture surfaces eliminates a progressive aging failure mechanism or fatigue. However, in PII report; Exhibit 2; page 20 Figure 6b for cores A and D identified micro-cracks and Exhibit 2 Page 30 describes these cracks. Explain the presence/cause of these micro-cracks and why they are not considered or discussed in your conclusions in the RCR on page 25?
  - a. PII: (ADDED TO Section 2.01 –Laboratory Tests and Examination to Test for Concrete Integrity –3<sup>rd</sup> paragraph).
5. Item 26: Provide and explain the input assumptions for the finite element analyses performed by your vendor (Exhibits 61 and 73) associated with the 1977 and 1978 blizzards events. Also, identify how sensitive your analysis conclusions were to each input assumption (e.g. sensitivity study).
  - a. PII: (ADDED TO Appendix II, Section 2.05 – Exhibit 73 discussion; last bullet) (ADDED TO Appendix II, Section 2.06 – Exhibit 61 discussion; last bullet)
6. Item 27: Provide and explain the input assumptions for the finite element analysis performed by your vendor (Exhibit 62) associated with wind loading and the 1998 tornado event. Also, identify how sensitive your analysis conclusions were to each input assumption (e.g. sensitivity study).
  - a. PII: (ADDED TO Appendix II, Section 2.06 – Exhibit 62 discussion; last bullet) Item 46: PII states "The second most likely scenario is that during the blizzard, water intruded from the cracks in the dome of the structure and trapped in small gaps between the rebar and concrete. Upon freezing, the volume expansion of ice produced significant radial stresses that resulted in the observed cracking." Is this scenario also identified and explained in the FENOC RCR? If so where? If not, why not? Could a third environmental scenario (e.g. wind-driven rain & freezing conditions, moisture intrusion and loading) existed after completion of the SB wall, but prior to dome installation (May 1971-August 1975) generated sufficient forces at inner rebar mat to cause laminar cracks? Was this investigated? Explain.
    - a. PII: (ADDED TO main report, Section 2.05 – top of page 7) This mechanism was explained in Section 6.02 Failure Mode 2.7 on page 15 and by Fig. 4 on page 16.
8. Item 47: PII states "Shield Building expanded due to crystallization of the diffused, moisture trapped in the concrete." And on Pg 24 "when an excessive amount of ice forms in pores, the ice generates cracks in concrete." What concrete tests were performed to confirm this assumption that freezing and crystallization of ice in pores causes internal cracking damage the SB concrete? If no tests were done explain. Were SB concrete tensile and compressive properties tested in the areas assumed affected by ice crystallization? Explain.
  - a. PII: (ADDED TO main report, Section 2.05 – top of page 7)



9. Item 48: PII, report shows picture of standing water between roof dome and parapet and picture stating "freeze-thaw damage in the roof concrete." It appears this condition would allow water to intrude/collect in the parapet to roof joint and if followed by freezing conditions, ice would expand within this joint. What effect would this have on the stress applied to the SB structures? Was this condition analyzed by FE techniques? If not, why not? It appears if ice forms within this joint it would create radial stress on the parapet and top of SB wall, at roof (and tensile loads on inside SB wall near roof). Were any examinations (other than visual) performed on the roof or parapet? If not why not. Were any type of examinations conducted at the inside surface of the SB wall just below the parapet to identify cracking? If not why not? What actions proposed preclude this scenario from causing further cracking (e.g. is top surface sealing identified)?
  - a. PII: (ADDED TO main report, Section 6.02 – bottom of page 17)
10. Item 49: Why does this section of the report discuss 2-3 inch penetration for wind driven rain, but other tests used in your FE analysis were based on work at UC Boulder that show 3-4 inch penetration with 90 mph winds?
  - a. PII: (ADDED TO main report, Section 6.02 – top of page 21)
11. Item 50 (Exhibit 61): PII judged the 1977 blizzard to be the "second worst" in terms of environmental factors which can cause laminar cracking. Could this laminar cracking have been caused by the 1977 blizzard since according to Exhibit 61 of the PII report stresses during this blizzard approached the tensile strength of the concrete and may exceed this level when modeling accuracy is considered? Also; identify the expected FE model accuracy for this application and how it was determined (e.g. benchmarked)?
  - a. PII: (ADDED TO main report, Section 2.04 – middle of page 6)
12. Item 51: The equation for cracking parameter  $S_c$  uses a concrete tensile strength of 973 psi. This is not consistent with roof cause and other PII report sections that indicate 600 psi is a more representative number. Why was this number used and what impact does it have on the analysis and conclusions?
  - a. PII: (ADDED a note to Appendix III – near center of page III-1)
13. Item 52: FM 2:12 discusses Out of Plumb condition of SB walls (original construction field report No. 5), but did not investigate effect of this condition on the friction forces at the slip forms: Specifically, the out of level condition can create higher friction forces on slip forms which can cause internal laminar tears/cracking the uncured concrete at the reinforcement steel. Identify and provide the tests/analysis performed to rule out this potential cause as the initiation site for the laminar cracking observed. If no investigation of this potential cause was performed identify planned corrective actions. Reference "Slip forming of Vertical, Concrete Structures Friction between concrete and slipform panel" by Kjell Tore Fossa - Dr. Thesis- Section Below from Chapter 2, pg 33 of this document."

Delamination of the concrete in the cover zone is concrete separated or displaced from the substrate: A vertical crack in the cover zone parallel to the reinforcement and sometimes invisible on the surface, is delamination of concrete. Delamination is also areas where the concrete in the cover zone is lifted together with the panel and makes the cover deficiency on the wall face clearly visible.

Delamination is often related to:

  - Problems during start up,
  - Geometry changes,
  - Area above embedment plates and block outs
  - the slipform is not in level"
  - a. PII: (Discussed in Appendix VI, FM 2.12 – Discussion)
14. Item 54: PII, modeling suggests that SB laminar cracking initiated by debonding at the interface of concrete/ rebar along the outer reinforcement; however core bore laminar crack depths exist away from the rebar mat depth. How is this possible explain?
  - a. PII: (note added to Analysis I, section 9.01 – page 33 before table 3)
15. Item 55: PII model suggests crack propagation by freezing the void fraction available in the concrete. What modeling was done to evaluate crack propagation which did not occur by freezing (e.g.: laminar cracking identified in the MS room near areas that have been confirmed to remain above 100F during operation)? If no modeling can explain this crack propagation identify why this crack exists.



- a. PII: (note added to Analysis I, section 9.01 – page 32 before table 2)
16. Item 56: Why was the thermal conductivity of the SB concrete 50% higher than the highest range expected for concrete? Did this contribute to an increased depth of freezing such that the area susceptible to cracking was at the outer rebar mats?
- a. PII: (note added to Analysis I, section 10.02 – page 39 end of 3rd paragraph)
17. Item 57: It does not appear that the FE stress analysis of the SB incorporated the abnormally high thermal conductivity measured for the SB (exhibit 59): Instead, only the measured coefficient of thermal expansion was included in the FE analysis. Why didn't the FE analysis account for the uniquely high thermal conductivity measured for the SB concrete? What effect would it have on the analysis to account for this parameter?
- a. PII: (note added to Analysis III, section 11.02 – page 52 3rd paragraph)
18. Item 58: How was the tensile strength of the SB concrete range of (836 to 962) used in this analysis determined? Why was the tensile strength representative of the concrete properties in 1977 and 1978? Explain?
- a. PII: (note added to Section 2.01 Laboratory Tests and Examination to Test for Concrete Integrity – page 2)
19. Item 59: Can a radial/bending loads induced by off-center loads applied on the dome (e.g. uneven snow loads or unbalanced dead load for dome/parapet) be transmitted to the top of the shield building wall? If not explain. If so should this have been incorporated into the FE models?
- a. PII: (Response added in new section XVII Additional Comments item 1 before Appendix I – page 92-93)
20. Item 60: Why was this location and size of crack on the SB selected to evaluate crack propagation? Is it the highest stress location for this type of cracking, explain?
- a. PII: (Response added in new section XVII Additional Comments item 2 before Appendix I – page 92-93)
21. Item 61: Why wasn't the maximum design loading in the lowest margin areas of the SB assumed for this crack growth analysis (e.g. seismic loads/design wind loads including tornado driven missile impacts)? If the design loading was considered could the cracks propagate? (e.g. What combination of design and service loads could cause the existing cracks to propagate?)
- a. PII: (Response added in new section XVII Additional Comments item 3 before Appendix I – page 92-93)
22. Item 62: States "Therefore it is not believed that the increased magnitudes in either the radial or maximum principal stresses are sufficient to propagate cracks that may have formed under normal thermal and environmental conditions, such as winter and summer." What is the magnitude of the stress amplification assumed at the tip of the laminar crack front? And what is the level of tensile stress (mode I) or shear stress (mode II) is required to drive this crack based upon the stress concentrations? Work in Sweden that indicates non-linear FE models have been used to predict cracking of reinforced concrete under shear loads. Why wasn't a similar FE model developed to evaluate the potential for growth of the existing cracking? Why isn't a more refined FE model or other applicable analysis needed as part of the corrective actions to monitor crack growth to ensure monitoring plans are adequate?
- a. PII: (note added before XV. Root Cause and Contributing Causes – page 87)
23. Item 63: Ice could not form in the main steam line room areas, where laminar cracking was identified. How did laminar cracking propagate into this area without ice formation and how long did this propagation take? (e.g. minutes, hours, days, weeks?) Based on Exhibit 75 sub model near top of aux building roof, the cracking is not predicted to propagate once the crack has initiated due to differential thermal expansion and freezing process, so why did the crack propagate into the main steam line room? If this cannot be explained based upon the model developed why not?
- a. PII: (Response added in new section XVII Additional Comments item 4 before Appendix I – page 92-93)
24. Item 64: What was the exact number used as an input to the finite element model for the maximum depth of penetration where moisture levels would generate expansion of material vice contraction, (e.g. exceeded relative humidity of 93%). How sensitive is this model to this assumed moisture penetration depth? Specifically, if the depth is one inch less or one inch more, will it change the predicted crack initiation depth or growth rate? 7 JANUARY 5/4/12 GPH
- a. PII: (Response added in new section XVII Additional Comments item 5 before Appendix I – page 92-93)
25. ■ Item 1 & 2: Finite element analysis evaluated a set of parameters that resulted in laminar cracking – necessary parameters. Explain the engineering judgment and assumptions that concluded 1978 blizzard conditions (rain, wind, temperature) resulted in the finite element analysis necessary parameters that resulted in shield building laminar cracking.



Explain how 1978 blizzard conditions can explain cracking in the entire shield building. For example, if blizzard wind was in a single direction, how was water driven into all flute shoulders explained? *3/21/12*

- a. PII: (Response added in new section XVII Additional Comments item 8 before Appendix I)
26. ■ Item 3: Cracking postulated at 600 psi radial stress is one component of stress tensor. Clarify how this failure stress was developed. What is the significance with respect to actual tensile stress magnitude? *3/21/12*
- a. PII: (Response added in new section XVII Additional Comments item 7 before Appendix I)
27. ■ Item 4: Provide clarification with respect to shield building crack initiation, crack growth, and crack arrest. Why are the computer results reasonable and reflective of identified cracking?
- a. PII: (Response added in new section XVII Additional Comments item 8 before Appendix I). *10/21/12*



## I. Introduction

### *Section 1.01 Issue*

First Energy Nuclear Operating Company's (FENOC) Davis-Besse Nuclear Power Station discovered laminar cracking along the outer rebar mat of the Shield Building during the installation of an access opening for the Reactor Vessel Head Replacement. This occurred during the 17 Mid-Cycle Outage.

FENOC subsequently contracted Performance Improvement International (PII) to perform a comprehensive technical root cause assessment to identify the cause or causes of the observed laminar cracking. This report provides the results of PII's technical root cause assessment as well as the recommended corrective actions to prevent reoccurrence.

### *Section 1.02 Report Structure*

This report is intended to be a single point reference document that includes the detailed information needed to understand the circumstances and conclusions associated with the Shield Building's laminar cracking. The report has a pyramidal structure. Section 2, the Executive Summary, provides detailed summary and overall conclusions. Section 3 provides a brief description of the Davis-Besse Shield Building (DBSB) and a detailed discussion about the observed laminar cracking. The first step in the analysis process is to identify potential Failure Modes (FMs) in order to determine the overall scope of the issues to be investigated. A total of 45 potential FMs in three general groups were identified to encompass the scope of possible contributors to the laminar cracking event. This report provides a discussion of the confirmed failure modes grouped by topic area. Section 4 discusses in detail the failure mode process and the individual failure modes that contributed to the observed Shield Building cracking. Section 5 through Section 7 discusses the unrefuted (supported) failure modes that most likely or did not contribute to the laminar cracking event. Section 8 through Section 14 discusses the methodology and results from the comprehensive Finite Element Analyses that were performed based on the confirmed failure modes. Conclusions that are associated to conditions that caused the cracking event, conditions that could not have caused the cracking event, and conditions that do not support the current Shield Building cracking to propagate are discussed in these sections. Based on the discussion in Sections 8 – 14, Section 15 discusses the root cause of the event and



Section 16 provides recommendations to prevent recurrence of the issue. Navigating through this document is facilitated by use of hyperlink and cross-reference functions.

## II. Executive Summary

In equipment failure analysis, a root cause is typically defined as the main contributing factor that leads to the damage of an engineering system. A root cause must possess the following two characteristics to be considered valid: 1) It can be eliminated to prevent recurrence and 2) It is under the control of management.

In determining the root cause of the laminar cracking located at the outer rebar mat of the Davis-Besse Shield Building (DBSB), Performance Improvement International examined every potential mode-of-failure that could have conceivably led to the observed damage. PII's root cause investigation searched for all potential sources, spanning from the inception of the building's design to the present-day operational conditions. Consequently, over a period of four months, PII experts in conjunction with FENOC, VATIC, and MPR collegially developed an exhaustive list of 45 failure modes that could have plausibly contributed to the laminar cracking of the DBSB, either individually or in concert.

The 45 failure modes analyzed are associated with 3 main phases: the Design & Analysis Phase, the Construction & Fabrication Phase, and the Operational Phase. Laboratory tests and examinations as well as Finite Element Analyses (FEA) were conducted extensively, which either supported or refuted the developed list of failure modes. To assure that the Shield Building was not in any immediate jeopardy, two of the failure modes investigated instantly were the integrity of the concrete used in the Shield Building and the stress-state, in the confirmed damaged regions, caused by thermal effects.

### *Section 2.01 Laboratory Tests and Examination to Test for Concrete Integrity*

PII performed extensive analyses of fracture-surface characterization and measurements of concrete material properties. Laboratory tests performed on concrete cores extracted from the Shield Building show that the concrete has both high compressive and tensile strength characteristics. Strength increase in concrete is larger at early ages and stabilizes after a few years; on the other hand, the strengths of concrete can decrease over time due to aging related



deterioration mechanisms such as freeze-thaw cycles and chemical attacks. There was no available data to determine the strength development rate for the SB wall concrete.

Based on established strength development rates from long term research it is plausible to assume that between 1978 and the present the concrete may gain very little.

By using current strength to model 1977 and 1978 we took a conservative approach.

The strength range of 836 to 962 was only used to set the stress contour limits for the figures in the Exhibit. The value 900 psi was chosen to represent approximate stress needed to be exceeded to crack the concrete and used as a visual indicator in the stress contour figures only.

Furthermore, examination of the core bores revealed that the cracks propagated through the aggregate which demonstrates a strong bond between the cement paste and aggregate. The propagation of cracks through aggregates is common in mature concrete. In cases like this one, the location and direction of the stresses and resultant cracks is predetermined and, depending on the orientation of the aggregates, may make propagation through the aggregate the 'path of least resistance'. It is possible that propagation through the aggregate requires less energy than through the interface around it.

This cracking through the aggregate does not provide any reliable information about the rate of crack propagation.

The core-bores showed no signs of micro-cracking which, in combination with factors to be discussed in subsequent sections, eliminates a fatigue / progressive failure mechanism. The micro-cracks observed in the CTL report (Exhibit 2) are not representative of the areas observed by PII. The cores observed by PII were from locations exposed to repetitive loading and not the near-surface concrete observed by CTL.

In addition, there is no observable material degradation in all other aspects of the concrete, such as concrete placement, creep coefficient, young's modulus of elasticity, heat capacity, thermal diffusivity, air entrainment, or freeze-thaw resistance.

### *Section 2.02 Carbonation*

To answer the question of whether we have a problem with carbonation at the Davis-Besse shield building it was necessary to evaluate the environmental conditions, observed carbonation and extent of corrosion.



- Observed carbonation - Laboratory tests by CTL Group (Exhibit 2) found that: "Paste along the outer surface of the cores... is fully carbonated to a depth of 5 to 8 mm." It also noted that "Carbonation in the body of the cores exhibits a mottled pattern with small areas of carbonated and non-carbonated paste; however, this feature does not appear to affect the overall integrity and performance of the concrete. Paste along the fracture surfaces of both cores, associated with those crack locations identified in the core holes, exhibits the same mottled carbonation pattern observed in the body of the cores; however, the paste does not appear to have carbonated due to exposure along the fracture surfaces."
- Observations of 83 fracture surfaces by PII (Exhibit 58) noted similar pattern of carbonation on 23 samples. This thin layer may be related to exposure after the cores were cut and is not considered an indication of deep significant carbonation. The source of carbon dioxide at the observed fracture carbonation is unclear. The carbon dioxide could have been introduced into the fracture dissolved in water, through limited surface cracks or by exposure to air prior to testing.

Since the depth of cover to main reinforcement was 3 inches, the observed rate of carbonation is considered very slow and does not present a problem for the structure. In some locations, cover to outer surface of rebar was found to be as low as 1 inch (25.4mm). This reduced cover is likely the result of exceptional conditions (such as reinforcement overlaps, bundling, or misaligned forms), and is not a problem considering that carbonation reached less than a third of the reduced cover in 40 years.

Research found that "The carbonation induced corrosion cannot start until the carbonation depth reaches a certain critical level of depth from the steel rebar. This critical carbonation depth has been calculated as 80% of the total depth of concrete cover."

A review of durability reported on the expected carbonation depth for different concretes was conducted, and concluded that concrete similar to the Davis-Besse concrete (high strength with outdoor exposure) was expected to have carbonation depth of 5 mm after 25 years. The rate of carbonation is a function of the square root of time, indicating that future carbonation will be significantly slower (approximately 7 mm after 50 years and





10 mm after 100 years). These values are a close match to Davis-Besse, where 8 mm carbonation was observed after 40 years.

- Extent of corrosion – Failure Mode (FM) 3.10 - Corrosion of Rebar - evaluated the potential and extent of corrosion at the Davis-Besse shield building. The conclusion was that no significant corrosion of reinforcing bars existed.

Based on the above it is concluded that carbonation of concrete is not a problem at the Davis-Besse shield building.

### *Section 2.03 Thermal and Stress Analysis*

The unique configuration of the architectural-panel shoulders (refer to Figure 1 for a schematic) and areas of high density rebar (the top of the Shield Building and main steam line areas) were investigated for their vulnerability. Extensive thermal analysis and stress analysis were undertaken using finite element analysis (FEA), looking at typical and worst case winter and summer conditions to which the Shield Building could potentially be exposed. These analyses did not singularly produce high enough stresses to overcome the tensile capacity of the concrete. Based on these results, PII concluded that cyclic stresses are most likely not responsible for initiating the observed laminar cracking. These analyses indicate that a major event capable of creating significant radial stresses would be required to produce the observed laminar cracking. Considering the aforementioned, PII concluded that the fracture was therefore initiated and propagated by substantial stresses beyond what would be anticipated by the design intent of the Davis-Besse Shield Building.

### *Section 2.04 Root Cause*

As it became clear that an atypical event was required to produce the observed laminar cracking, all known *abnormal events* occurring during the Operational Phase of the Davis-Besse Shield Building were supported or refuted. Correspondingly, all known abnormal events (earthquakes, lightning, etc.) were refuted except blizzard conditions for which the DBSB is susceptible. Based on the evidence, PII extensively investigated the damage mechanism which is founded on internal ice formation within the wall of the Davis-Besse structure during severe blizzards.



Out of the top 3 blizzards to which the Davis-Besse Shield Building has been subjected, the root cause investigation found that the most likely triggering event is The Toledo Blizzard of 1978. Only this scenario had the existing combination of wind, moisture and temperature extremes to generate the significant stresses required to produce the observed laminar cracking. To confirm, the second worst blizzard, occurring in 1977, was also analyzed using finite element thermal and stress analysis. The results show that the radial stresses do not exceed the tensile capacity of the concrete and therefore most likely could not have contributed to the observed crack. The 1977 Blizzard stress analysis suggests that the peak max principal stress approached the tensile strength. However, the area of high stress is limited to a very small area (See Figures 14 - 17). The stress contours during the 1978 Blizzard (shown in Figures 7 - 13) show a significantly larger area subjected to high stresses. The difference in the stress results during the two Blizzards is significant and larger than the expected uncertainty in modeling. This is based on engineering judgement. There was no sensitivity analysis performed.

As supported by thermal and stress analysis as well as laboratory tests and examination, the common factor for all unrefuted failure modes is moisture intrusion under severe blizzard conditions. Therefore, the most likely root cause of the laminar cracking observed in the Davis-Besse Shield Building is the *inadequate sealing of the building surface to prevent moisture intrusion during a severe blizzard.*

The other two contributing factors that, considered alone do not qualify as a root cause, are 1) the structural design of the shoulders and 2) dense spacing of the outer horizontal rebar mat in some areas of the building. Given severe blizzard conditions that allow for significant moisture penetration and subsequent internal ice formation, these two contributing factors intensify radial stresses to the point of structural damage.

#### *Section 2.05 Laminar Cracking Scenarios (Primary and Secondary)*

The primary, most likely scenario, which led to the observed laminar cracking in the Davis-Besse Shield Building, is described in what follows. During the 1978 blizzard, a significant amount of moisture penetrated the wall of the Shield Building. In addition, the Shield Building concrete was also subjected to below freezing temperatures. With the combination of moisture



penetration and below freezing temperatures, the outer layers of the Shield Building expanded due to crystallization of the diffused moisture trapped in the concrete. The volume expansion in the outer layer of the concrete, especially in the thick shoulder areas, produced significant radial stresses, which initiated and propagated the laminar cracking in the outer rebar mat. This theory could not be confirmed by direct testing since the limited number of strength tests precluded the possibility of making a statistically significant analysis of such damage. A very large number of tests throughout the structure would have been required and there is no guarantee that the tests would be sensitive enough to identify such variation. The variation in the tests performed points to this problem.

The test procedure and test data are shown in Exhibit 52 Fig. 5.

The second most likely scenario is that during the blizzard, water intruded from the cracks in the dome of the structure and trapped in small gaps between the rebar and concrete. Upon freezing, the volume expansion of ice produced significant radial stresses that resulted in the observed cracking. This mechanism was explained in Section 6.02 Failure Mode 2.7 on page 16 and by Fig. 4 on page 17.

A third environmental scenario assumed that wind-driven rain & freezing conditions, moisture intrusion and loading existed after completion of the SB wall, but prior to dome installation (May 1971-August 1975) and generated sufficient forces at inner rebar mat to cause laminar cracks. This scenario was also addressed in Section 6.02 Failure Mode 2.7 on page 16 and by Fig. 4 on page 17 of the PII Report. Historical records relative to significant snow storms in the Toledo area were reviewed dating back to 1870. Prior to the 1977 blizzard, there was only one major snow storm that struck on December 1st 1975. However, this blizzard was accompanied by milder temperatures (above 20 deg F), relatively weak winds, and was of very short duration (less than 2 days).

The necessary conditions for this laminar cracking event are listed as follows:

1. The exposed unsealed concrete surface of the Shield Building allows moisture penetration.
2. A significant amount of water is diffused into the concrete



3. The environmental temperature is well below freezing point of water for a long period of time so that the temperature near the outer mat rebar behind the shoulders (~3-18 inches deep into the Shield Building) could drop below the freezing point.
4. The design of flute-shoulders which caused discontinuity in the structure and the lack of radial reinforcing steel in the shoulder areas to resist radial stresses.
5. Tensile strength of the concrete is lower than the radial stresses produced in some areas near the outer rebar mat

#### *Section 2.06 Prevention*

To eliminate any possibility of repeat conditions as further degradation, one or more of the necessary conditions stated above would have to be eliminated. Among the necessary conditions stated above, the only practical condition that could be prevented is the moisture intrusion prior to and during a severe blizzard. As such, PII recommends FirstEnergy consider applying a weather-proof concrete sealant to the outside and top surface of the Shield Building.

As a conservative measure, PII recommends performing confirmation monitoring at a few selected locations to ensure that the proposed corrective action effectively prevent further crack propagation. This confirmation monitoring shall be performed on a periodic basis, such as once per refueling outage. If the cracks are confirmed not to propagate after three times of confirmation monitoring, the efforts of further monitoring may be suspended.

### III. Plant Description and History

#### *Section 3.01 General Design*

The Shield Building is a reinforced concrete structure of right cylinder configuration with a shallow dome roof. An annular space is provided between the steel Containment Vessel and the interior face of the concrete Shield Building of approximately 4 feet 6 inches width to permit construction operations and periodic visual inspection of the steel Containment Vessel. The volume contained within this annulus is approximately 678,700 cubic feet. The containment vessel and Shield Building are supported on a concrete foundation set on a firm rock structure. With the exception of the concrete under the containment vessel, there are no structural ties between the containment vessel and the Shield Building above the foundation slab.



The Shield Building has a height of 279 feet 6 inches measured from the top of the foundation ring to the top of the dome. The inside radius of the Shield Building is 69 feet 6 inches and the thickness of the Shield Building wall is approximately 2 feet 6 inches. The Shield Building exterior has eight vertical architectural flute reveals that are spaced 45 degrees apart. The architectural flute reveals consist of shoulders that extend another 1 foot 6 inches outward and gradually taper back to the outer cylindrical wall of the Shield Building while reaching a point of tangency 17 feet 11 inches from the centerline of the flute. Figure 1 shows a plan view of the Davis-Besse Shield Building. Numbers 1 – 8 refer to the Flute regions of the building:

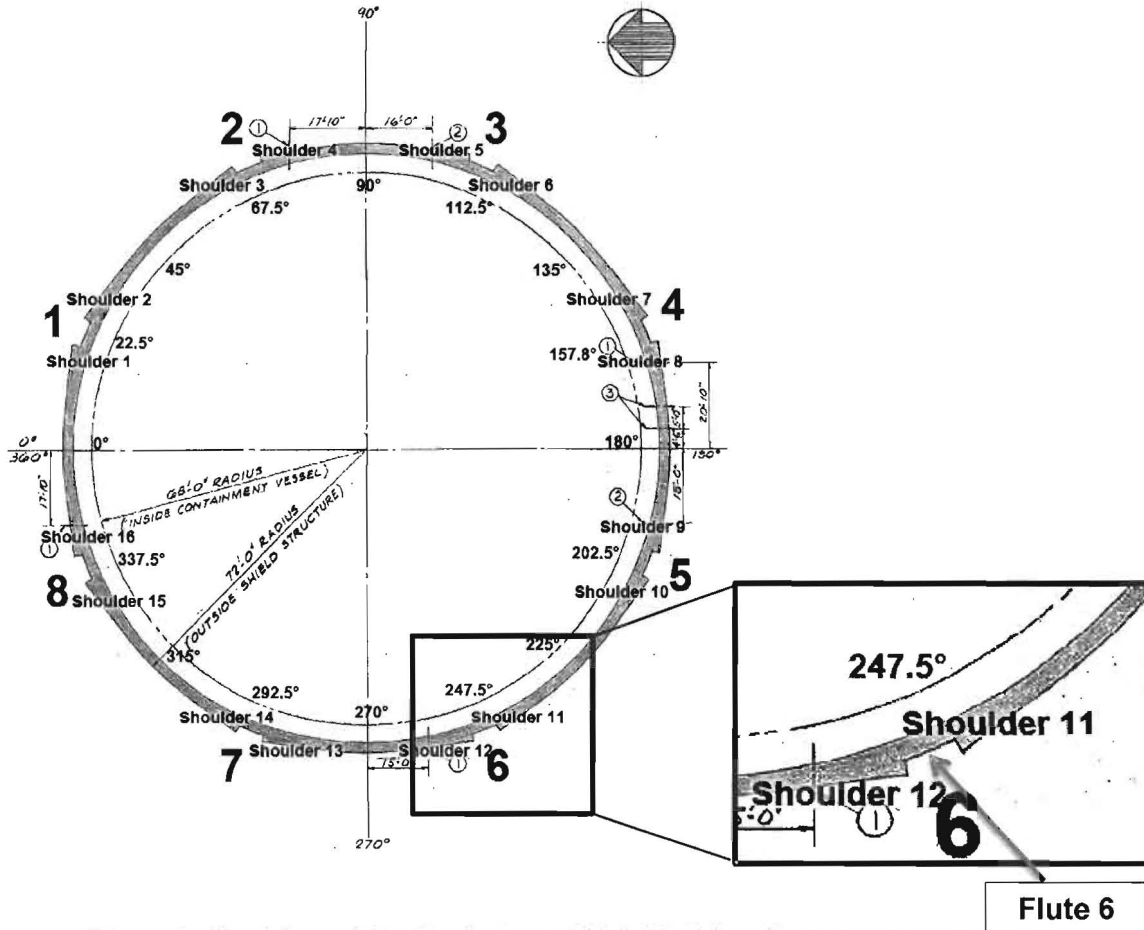


Figure 1: Plan View of the Davis-Besse Shield Building (8 Flutes & 16 Shoulders)



The Shield Building is designed to provide biological shielding during normal operation and from hypothetical accident conditions. The Shield Building provides radiation shielding, a means for collection and filtration of fission product leakage from the containment vessel following a hypothetical accident, and provides environmental protection for the containment vessel from adverse atmospheric conditions including extreme winds, tornadoes, and tornado-borne missiles. Besides the emergency ventilation system, the Shield Building also interfaces with station lightning protection, and station drainage.

The Shield Building is a structure consisting of concrete, and reinforcing steel, with other minimal miscellaneous embedded material. The Shield Building was designed in accordance with American Concrete Institute (ACI) 307-69, Specification for the Design and Construction of Reinforced Concrete Chimneys, and checked by the Ultimate Strength Design Method in accordance with ACI 318-63, Building Code Requirements for Reinforced Concrete.

#### *Section 3.02 Laminar Crack Discovery*

During the installation of an access opening to the Davis-Besse Nuclear Power Station's Shield Building, during the 17-Mid-Cycle outage, a crack was observed along the entire left edge of the opening as well as on the left side of the top and bottom opening edge. The location of the crack is in the shoulder area below the surface of the concrete and tends to run along the edge of the outer-face reinforcing steel mat. Investigation of the right side of the opening and the entire wall thickness did not reveal any additional crack-like indications.

Initial chipping along the left edge was performed to determine the extent of cracking. This chipping revealed that the extent of cracking quickly dissipated. Chipping was also performed along the top edge of the access opening, however, the crack indication continued.

Nondestructive evaluation (NDE), using Impulse Response (IR), was used to identify the extent of cracking. Subsequently, concrete core bores were performed to confirm the locations of the laminar crack identified by NDE techniques, and also to establish the areas of solid concrete. These examinations revealed similar cracking in each flute shoulder inspected. The cracks in the flute shoulder area are well defined and generally bounded by the flute shoulder horizontal steel reinforcing hooks. Cracking was also identified outside of the flute shoulders at the top of



the Shield Building wall and local cracking around the blockouts for the main steam line penetrations.

(a) **Characterization of Laminar Cracks**

Based on the investigation performed, the following conclusions can be made:

- The crack is considered a circumferential laminar crack and not a radial through-thickness directional crack.
- The width of the crack is very tight, generally less than 0.01 inches
- The crack passed through the coarse aggregate
- The location of the crack is limited to the outer reinforcing (rebar) mat
- The cracking is prevalent in the flute shoulder areas.
- The crack is also prevalent in the higher-density reinforcing areas along the outer face rebar at the top of the Shield Building and along the outer face rebar around the blockouts for the main steam line room penetrations.
- Cracking is more prevalent in the South and Southwest quadrant of the Shield Building
- Cracking is less prevalent in the flute areas and the shell areas (between the shoulder areas)

#### IV. Failure Mode Process

Performance Improvement International's investigation efforts identified three major categories (phases) that house all potential failure modes. These phases are: the Design & Analysis Phase; the Construction & Fabrication Phase; and the Operational Phase. An extensive literature review was conducted (Grieve et al. 1987; Mehta and Monteiro 1993; Neville 1995; Young et al. 1998; Naus and Graves 2007; Li et al. 2009), and 45 possible failure modes were identified. Each of the possible failure modes was extensively investigated and evaluated as to its likelihood.



In general, each failure mode was scientifically refuted or supported by laboratory tests & examinations or by state-of-the-art Finite Element Analysis. Some failure modes did not need to be scientifically tested as deductive reasoning based on existing evidence was sufficient enough to either support or refute their mode of failure. Unless there is positive refuting evidence against a given failure mode, it is considered as a possible contributing factor. The failure modes without positive refuting evidence, hereafter called unrefuted failure modes, are further quantitatively analyzed to understand their relative importance and contribution to the observed laminar cracking.

After exhaustively investigating the cause of the laminar cracking, PII concluded that the damage to the Davis-Besse Shield Building was most likely a result of internal ice formation within the wall of the building due to moisture transport and below freezing temperatures. Investigation confirmed that the root cause of the observed laminar cracking is inadequate sealing of the concrete surface to prevent moisture intrusion during severe blizzards. There are however contributing factors that, once the internal formation of ice has occurred, facilitate crack propagation, they are:

1. Shoulder Design and Reinforcing Steel Associated with the Shoulder Area.
2. High density of horizontal reinforcing steel rebar located in the top 20 feet of the Shield Building and in some localized areas (i.e. – penetration blockouts)

All 45 failure modes, along with their verified supporting or refuting evidence can be found in Appendices 4 – 7.

## V. Group 1: Unrefuted Failure Modes – Design & Analysis Phase

### *Section 5.01 Unrefuted Failure Modes:*

- FM 1.3** Rebar Interaction with Flute/Shoulder
- FM 1.5** Excessive Density of Rebar
- FM 1.12** Inadequate Shoulder Reinforcement Details





Section 5.02 Failure Modes 1.3 & 1.12:

(a) Discussion

The shoulders were not adequately considered in the structural analysis of the Shield Building for the unforeseen extreme set of unique environmental conditionals that ultimately caused the observed cracking; however, the building along with its architectural panels was properly designed and analyzed for all known load cases. As such, the reinforcing steel mat in the shoulder area is independent of the main outside reinforcing steel mat with the exception of the horizontal reinforcing steel anchored only at the ends of the shoulder area. This results in a discontinuity since the shoulder reinforcing steel mat is not sufficiently tied to the shell outside reinforcing steel mat. Any stress in the main outer reinforcing steel mat would tend to cause differential stress between the shoulder areas and the Shield Building shell area. The original design of the Shield Building did not consider this structural discontinuity and any affects it might have on the building's structural capacity.

The following figure illustrates the shoulder/shell interface showing the shell's outer rebar mat and the rebar in the architectural panel which ties the panel to the shell.

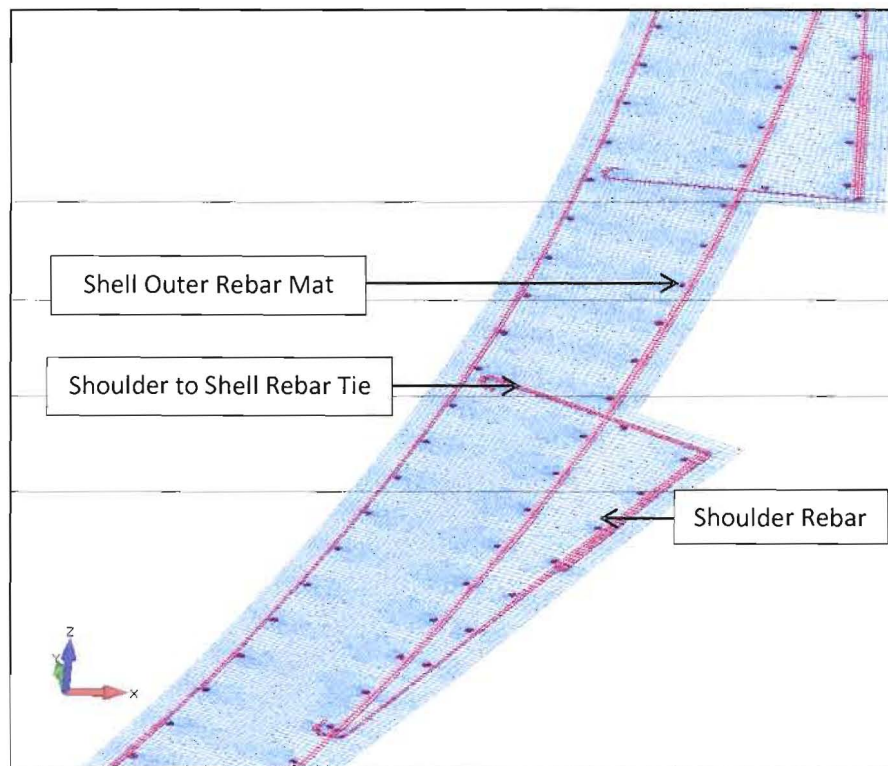


**Figure 2: Rebar Schematic of Shield Building Shell and Architectural-Panel Shoulder Interface**

**(b) FMs 1.3 – Shoulder Design and Reinforcing Steel Associated with the Shoulder Area:  
Supporting Evidence Verifying Failure Mode**

- Cracks are predominate in the shoulder area
- Cracks are predominately located between the horizontal rebar anchor points. (results in approximately 10 foot spacing)
- The shoulder vertical and horizontal rebar are #8@12 spacing.
- The vertical rebar are not tied to the main outside reinforcing steel mat
- The horizontal rebar are tied to the main outside reinforcing steel mat only at the ends.

There is approximately 10 foot horizontal span in which the shoulder concrete is not connected to the main outside reinforcing steel



(c) **FMs 1.12 – Shoulder Design and Reinforcing Steel Associated with the Shoulder Area:  
Supporting Evidence Verifying Failure Mode**

The shoulder areas were reinforced with #8 rebar spaced at 12 inches in each direction. The horizontal rebar were provide with a tie (i.e. hooks) at each end into the main reinforcing of the Shield Building wall. The distance between these tie points was about 10 feet. This left a considerable span where only concrete was available to resist loads at the cylinder/shoulder interface. This relatively large span is the area where the laminar cracks have been identified, Ref. Drawing C-111A.

(d) **Conclusion**

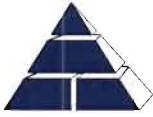
The lack of adequately spaced ties between the shoulder reinforcement and the main cylinder appear to be the one potential failure that could have prevented the cracking. Therefore, this failure mode is considered to be a cause for the identified laminar cracks.

*Section 5.03 Failure Mode 1.5*

(a) **Discussion**

Reinforcing steel bars around the Shield Building are made up of many individual bars. Stresses are transmitted from one reinforcing steel bar to the next bar through the concrete in the immediate area surrounding the lap splice. Areas with high density of reinforcing steel are usually associated with concrete high stress areas. In addition the concrete spacing between the reinforcing bars is also reduced in areas of high density of reinforcing steel. Although the ACI Code does not limit the amount of steel, and by itself high density reinforcing steel does not cause cracking, it may contribute to the propagation of a crack once it has initiated. The top 20 feet of the Shield Building can be considered an area of high stress associated with high density of horizontal reinforcing steel. It should also be noted that although higher density reinforcing may contribute to crack propagation once initiated, it is not a violation of past or current ACI standards.

The cracking observed around the main steam line penetration blackout area also can be considered an area of high stress with high density of reinforcing steel. Additional reinforcing



steel were added to compensate for the interruption of bars around the temporary blackout opening.

There are locations, such as the top 20 feet of the walls where the nominal spacing of the horizontal rebar is 6". With lap splices and normal construction tolerances, this can lead to regions where there is less than 2" of clear concrete spacing between the horizontal rebar. It was also observed that in some locations the vertical rebar was adjusted on either side of the jacking bars in order to accommodate the hydraulic jacking heads used during the slip-forming operation. The following figure illustrates the high density rebar that exists in the outer rebar mat at some locations of the Shield Building.



**Figure 3: High Density of Reinforcement at Outer Rebar Mat (Photo during Construction)**

**(b) FM 1.5 – High Concrete Stress Areas Associated with High Density of Horizontal Reinforcing Steel: Supporting Evidence Verifying Failure Mode**

- Laminar cracks were observed at the top of the Shield Building
- Laminar cracks were observed around the construction opening adjacent to the shoulders
- Laminar cracks were observed around the main steam line penetration adjacent to the shoulders



### (c) Conclusion

PII conducted a rebar sensitivity study through Finite Element Analysis, the specifics of which are discussed in Exhibit 51. The study confirms that laminar cracking occurs in high density reinforcement zones while laminar cracking is absent under the same motivating conditions in areas of less dense rebar.

## VI. Group 2: Failure Modes – Construction & Fabrication Phase

### Section 6.01 Unrefuted Failure Modes

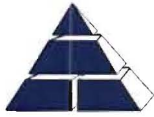
#### FM 2.7 Concrete Sealant

### Section 6.02 Failure Mode 2.7:

#### (a) Discussion

There are two types of moisture transport processes in the Davis Besse Shield Building that provide sufficient moisture to be entrapped in the concrete. One may be called “Top-down moisture penetration”, and the other may be called “External-internal moisture penetration”. The top-down penetration results in high moisture content near rebar regions and what we call the sub-mode 1 laminar cracking, as will be described in FM 3.6. The external-internal transport causes high moisture content in the outer layer of concrete, which leads to what we call the sub-mode 2 delamination cracking which will be described in FM 3.6 as well. The following section describes the two types of moisture transport processes in Davis-Besse Shield Building.

A Third theory involved freezing of water that penetrated into roof/parapet joint, causing radial stresses. However, the two potential mechanisms identified preclude cracking on the inside since it is not exposed to the same deep freezing conditions as the outside. Three ‘full-depth’ cores showed no indication of cracking on the inside of the wall, and the construction opening that originally identified the laminar cracking showed no crack at the IF rebar. Cracking was only found at the OF rebar



#### (i) The top-down moisture penetration

The top-down moisture transport process assumes that the water comes from the top of the structure and slowly penetrates down within the concrete wall. During the construction of the Shield Building, the wall was built first and the dome was subsequently constructed two years and four months later. So, the jacking bars, dense rebar, and top of the concrete wall were all exposed to the environment. Moreover, initial defects may be generated by the jacking bars and dense rebar, together with the large aggregate used in the concrete. These factors resulted in the potential for high porosity concrete near the rebar and jacking bars allowing for water penetration. Due to the heterogeneous characteristics of concrete, the water comes down along random paths of least resistance which may tend to explain the sporadically distributed cracks in the wall. This moisture transport mechanism is illustrated in Figure 4.

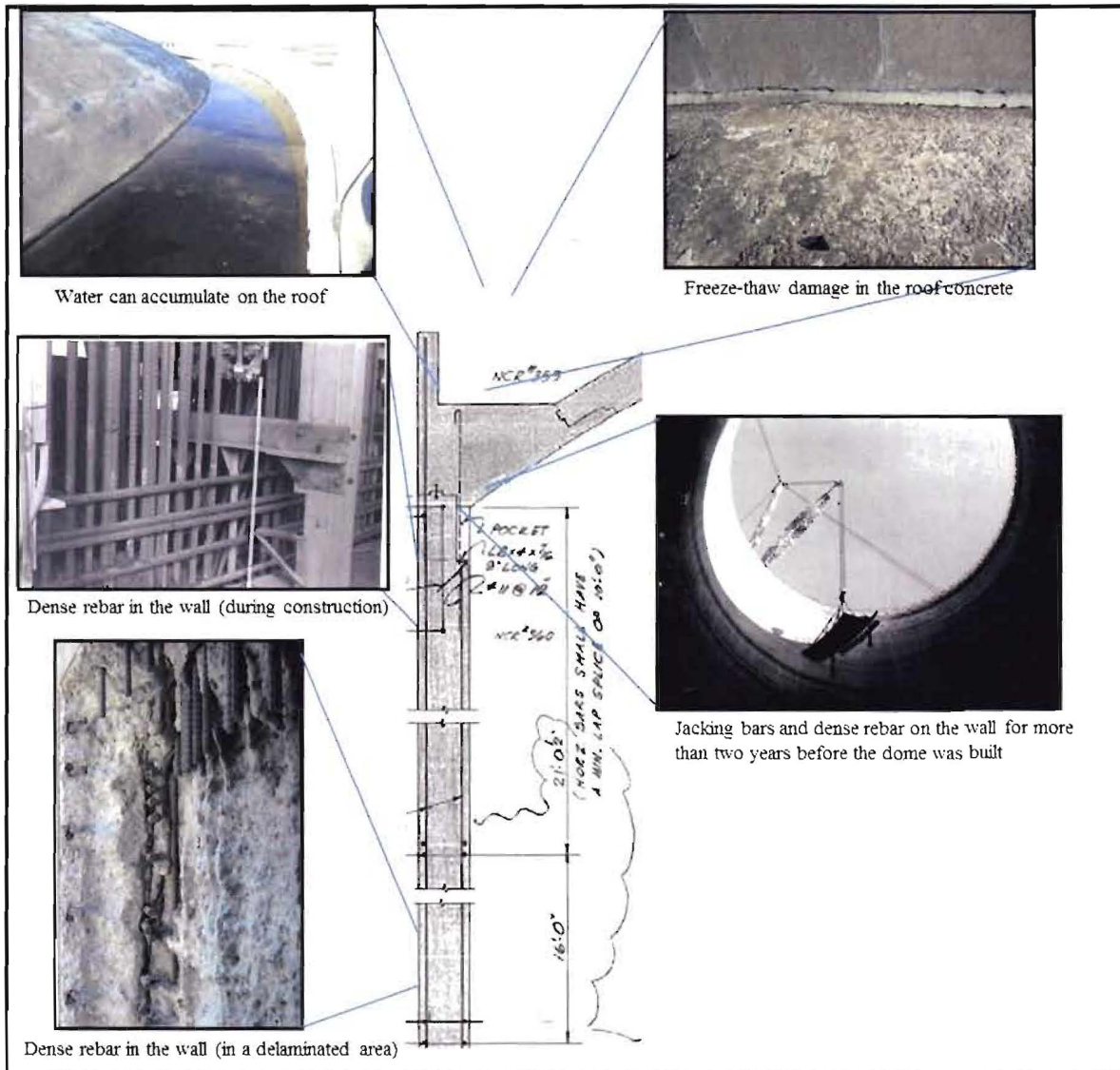


**Figure 4: Top-Down Moisture Transport Mechanism**

**(ii) The external-internal moisture penetration**

This moisture transport process is illustrated in Figure 5. It assumes that the moisture comes from the side surface of concrete wall and slowly penetrates into the wall. For above ground concrete structures like Davis Besse Shield Building, there is hardly any liquid water in the porous system in concrete under an arid environment, and the water vapor diffusion is a dominant process. During a blizzard, the effect of wind-driven rain is an important factor to



consider. On the outer surface of concrete wall, the rain water is pressed by the wind pressure and penetrates into concrete. The liquid water penetration is a dominant process which is driven by the wind pressure on the surface.

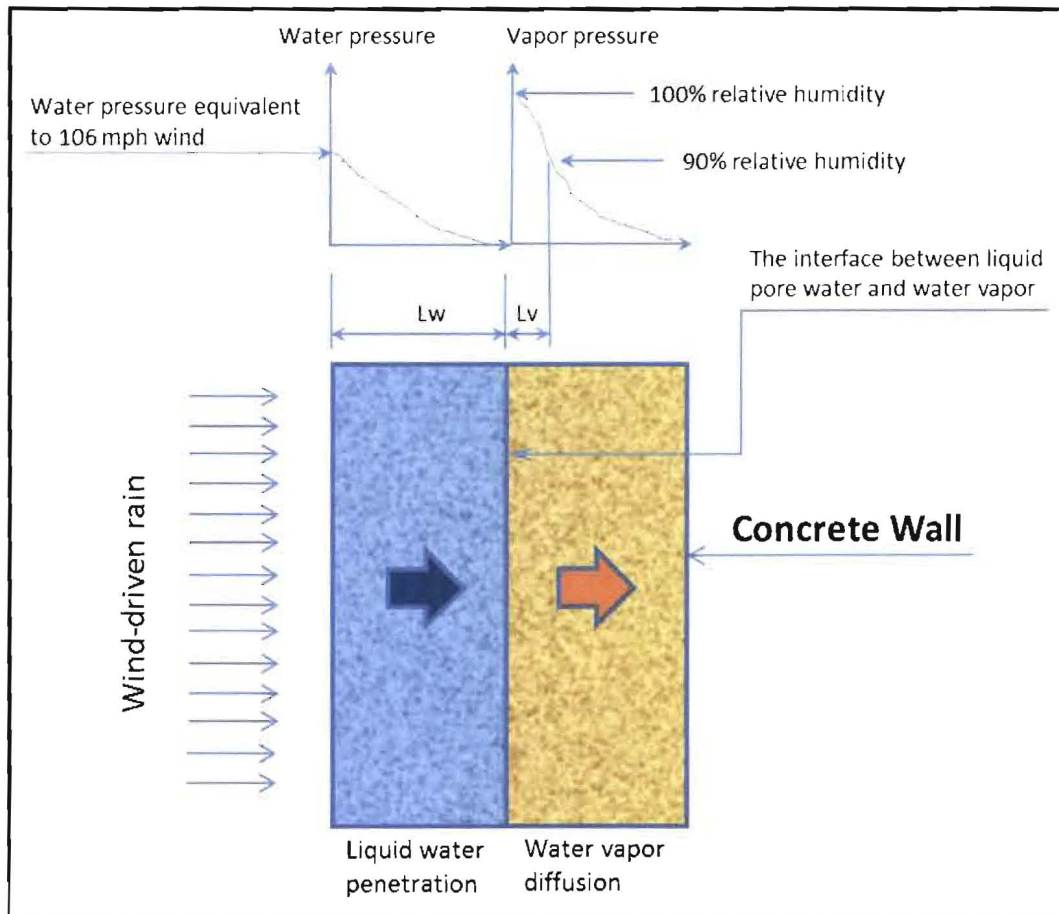


Figure 5: External-Internal Moisture Penetration

Figure 5 shows the two transport processes in a concrete wall during a blizzard. The blue region represents the outer layer of concrete in which pores are saturated by liquid water, which may be called water region, and the yellow region stands for the inner layer where vapor water is dominant, which may be called vapor region. The entire depth of the water region is shown in Figure 5 as  $L_w$  (on the left), which is important in the study conducted. The partial depth of the vapor region, say higher than 90% pore relative humidity is shown as  $L_v$  (on the right), which is also important for our study. The depth of the water region  $L_w$  is much higher than that of vapor





region  $L_v$ . The sum of the two depths is called  $L_m$ , ( $L_m = L_w + L_v$ ), representing the depth of concrete with high moisture content.

Exhibit 72 shows that the water penetration depth depends on permeability of concrete and it can vary in a very large range. For solid concrete without distress, the 1D analytical results showed that the penetration depth could be 2 - 3 inches under a strong wind-driven rain. With surface distress such as microcracks and 2D moisture penetration, the depth of high moisture region could be higher. Moreover, the moisture trapped in the concrete could continue to penetrate into the concrete after the blizzard, resulting in a higher depth of the high moisture region.

Therefore, in the 1978 models, the depth of moisture penetration is considered approximately 3 to 4 inches in locations subjected to 1D moisture diffusion.

As a summary, based on preliminary and approximate analyses for solid concrete without major distress, the depth of high moisture region  $L_m$  is about 2 to 3 inches after a few days of WDR. This may be considered as a reference or guideline for determining the depth of high moisture region in the concrete wall. The present results are based on 1-D analysis. The concrete in shoulder areas is subjected to 2-D moisture penetration, and thus the high moisture region  $L_m$  in shoulder areas may be higher than that in the wall between shoulders.

#### (b) FM 2.7 – Concrete Sealant: Supporting Evidence Verifying Failure Mode

ACI 515.1 R-79 (not available during construction) is ‘A Guide to the Use of Waterproofing, Damp-proofing, Protective, and Decorative Barrier Systems for Concrete.’ Section 2.2 sets the standard-of-care for using water proofing and makes the case for applying water-proofing or damp-proofing to the wall:

“2.2-When waterproofing is used

Waterproofing is normally used to prevent leakage of water into, through, or out of concrete under hydrostatic pressure. **If freezing and thawing conditions exist, as in above-grade applications** or if water is carrying aggressive chemicals which attack reinforcing steel or concrete, **then the waterproofing barrier will be used to prevent**



**leakage into the concrete...** Waterproofing is also used to minimize unsightly carbonates or efflorescence.

2.2.1 Water leakage into and through concrete - Water may be forced through concrete by hydrostatic pressure, water vapor gradient, capillary action, **wind-driven rain**, or any combination of these. This movement is aggravated by porous concrete, cracks or structural defects, or joints that are improperly designed or installed... Waterproofing membranes are intended primarily to prevent the passage of water in liquid form. They also retard the passage of water vapor in varying degrees depending on the type of membrane..."

According to Davis-Besse specification C-38 (Exhibit 5):

**"9.2 Curing**

The Shield Building concrete, except as otherwise approved by the CONSTRUCTION MANAGER, shall be cured by the liquid membrane method. The liquid membrane curing compound shall conform to Clear Seal No. 150 as manufactured by Grace and Company, Cambridge, Massachusetts, or approved equal. Application shall be in accordance with the manufacturer's instructions. The liquid membrane shall be applied to all slip-form wall surfaces. The membrane shall be applied to within 2 feet (two feet) of the bottom of the slip-form after the concrete surface has been finished."

The product used is no longer available, but similar sealants have limited life and are mainly intended to prevent moisture evaporating during the curing phase of the concrete cure. This curing compound can be assumed to be ineffective after 12 months.

**(c) Conclusion:**

If the concrete was to achieve high moisture content, facilitated by methods described in the previous section, followed by sub-freezing conditions, it could create a situation where an icing condition would exist. This icing condition could be a contributor to concrete cracking if the moisture content was sufficiently high and widespread. The lack of a Concrete Sealant was a contributing cause to the Laminar Cracks.



## VII. Group 3: Main/Sub Failure Modes – Operational Phase

### Section 7.01 Unrefuted Failure Modes

#### 3.6 (a) Freezing of Water near Outer Rebar Mat in Blizzard Conditions

#### 3.6 (b) Expansion of Concrete due to Internal Ice Formation in Blizzard Conditions

### Section 7.02 Summary of Failure Modes 3.6 (a) & 3.6 (b):

#### (a) Discussion

PII considered a number of abnormal-event failure modes that either could have or did occur during the operational life of the Davis-Besse Shield Building (DBSB) such as earthquakes, tornados, lightning, and physical or chemical attacks. All abnormal events were refuted except for the extreme weather conditions attributed to the Toledo Blizzard of 1978. Dubbed the *Great Blizzard of 1978*, it was the state of Ohio's worst blizzard in recorded history. The blizzard lasted for three days, spanning from January 25<sup>th</sup> – January 27<sup>th</sup>, with maximum wind speeds reaching 105 mph and 850mb atmospheric temperatures recorded as low as -24° F (see Exhibit 65 for temperature discussion).

The top three blizzards in recorded Ohio history in terms of freezing temperature and duration, occurring near the Davis-Besse Power Plant, were determined to be the 1977, 1978, and 1994 blizzards. Snowfall and wind velocity are two critical factors in determining the moisture content near the surface of the Shield Building. The moisture content is the critical factor involved in the process leading to significant radial stresses that produce cracking. From the below table, it is obvious that the 1978 Blizzard is the worst case. Based on PII's engineering judgment, the second worst blizzard is the 1977 case.



**Table 1: Comparison of 1977, 1978, & 1994 Blizzard Conditions (1978 Snowfall & Wind Velocity show Worst Case)**

<b>EVENT</b>	<b>SNOWFALL 20 DAYS PRIOR (INCHES)</b>	<b>SNOWFALL DURING (INCHES)</b>	<b>MAX WIND (MPH)</b>	<b>LOW TEMPERATURE (° F)</b>
<b>BLIZZARD 1977</b>	9.1	4	84 (gust) 78 (avg., est.)	-2, (surface)
<b>BLIZZARD 1978</b>	21.5	12	105	-5, (surface)
<b>BLIZZARD 1994</b>	11.9	3.5	45(avg., est.)	-17, (surface)

**(b) Failure Mode Hypothesis**

This failure mode hypothesizes that during the 1978 Toledo Blizzard, water diffused into the concrete partly due to wind induced pressure and subsequent internal ice formation occurred due to the below freezing temperatures. As a consequence, two failure modes which will be discussed in detail, one main and one secondary, could have resulted from the water/ice-concrete interaction. The requisite for one or the other of these failure modes to be valid depends upon 1) The extent of the diffusivity of water into concrete and 2) The effects of the coefficient of thermal expansion (CTE) in the low temperature range. Investigation shows that the established moisture penetration and CTE values are in the range to cause crack propagation during 1978 Blizzard conditions. Both of these requisites are discussed in detail in [Exhibit 72](#) and [Exhibit 57](#), respectively.

**(i) Sub-Mode 1: FM 3.6 (A) – Freezing of Water near Outer Rebar Mat in Blizzard Conditions**

This sub-mode can explain the laminar cracking in the shoulders. Recall that there is a discontinuity at the shoulder/shell interface of the Shield Building. Any stress in the main outer reinforcing steel mat, as caused by concrete expansion due to internal ice formation for example, would tend to cause differential stress between the shoulder areas and the Shield Building shell area. The damage process is shown in Figure 6 by three stages and explained below:



1. As the environmental temperature drops below the freezing point during the beginning stage of a blizzard, the trapped water (from diffusion processes) near the horizontal outer mat rebar at the flute and mid-panel locations freezes first. This is because in these two areas, the horizontal rebar are closest to the cold surface (~ 3 inches), as shown in the upper figure of Figure 6. However, the moisture in the pores of the concrete behind the shoulders remains in liquid or vapor states (no ice) because the shoulder keeps this area warmer due its thickness.
2. As the blizzard continues, the temperature continues to drop well below the freezing point of water. At this point, the water trapped near the outer mat horizontal rebar between the two first-freezing areas starts to freeze, i.e., in the areas directly behind the thick shoulders from the surface. The moisture behind the shoulder diffuses towards the ice fronts, which are located near the surface of the flute and shell wall. The diffusion directions of moisture are shown in the middle figure of Figure 6. The moisture diffusion is driven by the maximum temperature gradient from the hottest area to the coldest area as well as by the maximum free energy gradient from the area with higher free energy (vapor and liquid) to the area with lower free energy (ice).
3. When the diffusing moisture reaches the ice fronts, it turns into ice. This is shown in the third figure (the enlarged area) in Figure 6. So, the ice fronts move from both sides (the flute and the shell wall) toward the middle of the shoulder. Due to the formation of ice at both ends of the shoulder which acts as a dam, high pressure is generated in the shoulder areas as the water continues to migrate to the ice fronts resulting in the crack initiation in the shoulder.

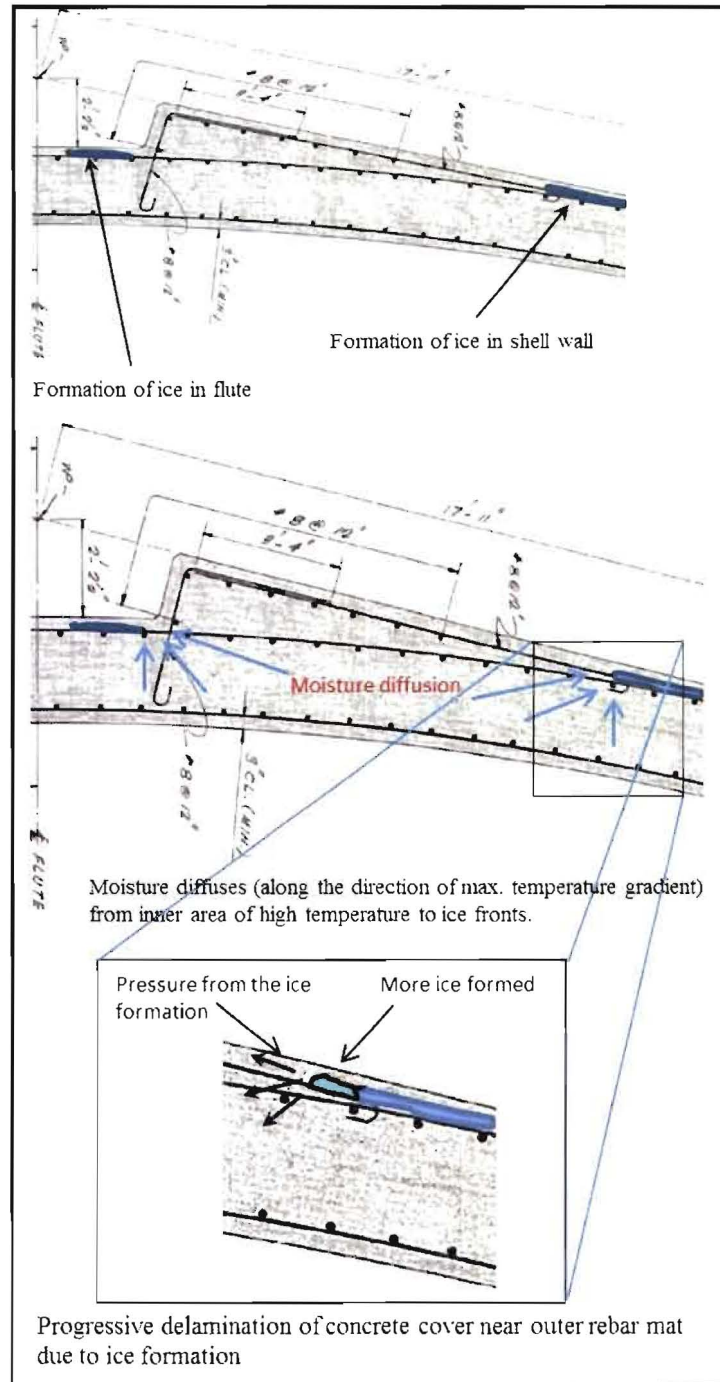


Figure 6: Freezing of Water near Outer Rebar Mat Sequence (FM 3.6, Sub-Mode 1)



The moisture diffusion and ice formation process in the shoulder area were not simulated by any finite element models because, as stated earlier, the moisture diffusion process is driven by two field variables: temperature and moisture. The two field variables are fully coupled. Moreover, the formation of ice in the pores of concrete changes moisture diffusivity of concrete since ice crystals in pores block the pathway of moisture and thus reduces the diffusivity. On the other hand, when an excessive amount of ice forms in pores, the ice generates cracks in concrete and thus increases the diffusivity of concrete (Eskandari-Ghadi et al. 2012; Xi and Nakhi 2005). Furthermore, the effect of high wind pressure on the outer surface of the Shield Building makes the numerical modeling of the moisture penetration process into concrete a very complicated task. Currently available commercial finite element programs cannot handle such a sophisticated multi-physics problem.

This failure mode would exist only under the following conditions in a severe blizzard:

1. A significant amount of water is diffused into the gaps between outer mat rebar and the concrete due to wind induced surface pressurization.

The environmental temperature is well below freezing point of water for a long period of time so that the temperature near the out mat rebar behind the shoulders (~2-12 inches deep into the Shield Building) could drop below the freezing point

#### **(ii) Sub-Mode 2: FM 3.6 (B) – Expansion of Concrete in Blizzard Conditions due to Internal Ice Formation**

Under low temperatures, concrete may expand (instead of contract) during a cooling period. This expansion is caused by the formation of ice in the concrete. During a severe cooling process, the temperature of the concrete in the outer layer of a cylindrical-type wall, such as the DBSB, is lower than that of the inner layer. Therefore, ice formation in the outer layer of the wall results in an expansion while the absence of ice formation in the inner layer of the wall leads to continuous contraction. This special outer-expansion-and-inner-contraction deformation pattern can result in a tensile stress in the radial direction of the wall. Thus, laminar cracking may occur in the case of excessively high radial tensile stress.



For illustration purposes, Figure 7 shows a general schematic of the outer-expansion-and-inner-contraction phenomenon. Due to the structural configuration of the DBSB, this phenomenon causes significant stresses in the shoulder areas, as will be demonstrated in subsequent sections of this report.

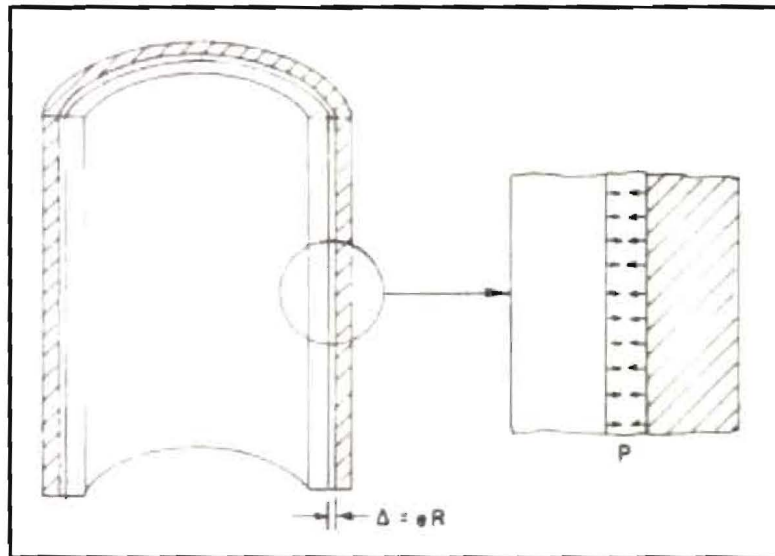


**Figure 7: Outer-Expansion-Inner-Contraction Schematic (FM 3.6, Sub-Mode 2)**

Extensive finite element analyses were performed to study the response of the DBSB due to internal ice formation during blizzard conditions. The results showed that this sub-mode can be used to explain the increase in radial stress and damage development in the wall during the blizzard. This sub failure-mode will be discussed in detail in the subsequent finite element analysis section.





## VIII. Analysis Introduction

### *Section 8.01 Analysis Summary*

To analyze the laminar cracking, PII used state-of-the-art concrete stress- and fracture-analysis modeling techniques to evaluate the contributions of volume expansion due to ice freezing, thermal stress, and high density reinforcing steel. These modeling techniques were originally developed as a part of the Crystal River-3 (CR-3) root cause investigation and calibrated against the Crystal River-3 fracture and temperature data. Note that the CR-3 root cause investigation was extensively reviewed by the US Nuclear Regulatory Commission (NRC) over a period of more than one year and has received no negative comments from the NRC.

The findings of PII's analysis results are summarized below:

1. There are high stresses near the thick portions of the shoulders due to differential volume expansion amplified by the structural discontinuity,
2. The radial stresses located in the shoulder areas under extreme rain-wind-temperature conditions exceed the tensile capacity of the concrete. These stresses are a result of ice driven concrete volume expansion, due to high internal moisture content, under prolonged extremely low temperature conditions preceded with rain storms. These conditions were encountered shortly before and during the 1978 Toledo blizzard.
3. There is inadequate radial reinforcing steel in the shoulder area to resist high concrete tensile stresses in the radial direction. Due to the lack of radial reinforcing steel, the concrete tensile stresses exceed the tensile capacity of the concrete producing laminar cracks near the outer reinforcing steel mat.
4. The thermal stresses resulting from the hottest weather conditions (104°F), under which the thermal stresses are the greatest, would be approximately 300 psi. This stress is significantly below the tensile capacity of the concrete; therefore this condition probably did not initiate or propagate the laminar cracks.
5. Laminar cracks happen in areas of dense rebar (6" spacing) when subjected to high moisture content and cold temperatures and NOT in areas of sparse rebar (12" spacing).



## IX. Analysis I, FM 3.6 (A): Finite Element Analysis of Dense Rebar Condition

### *Section 9.01 Dense Rebar Analysis*

A set of analyses was performed to quantify the propensity to propagate a laminar crack due to freezing of water under the horizontal rebar. The study was done using a wide range of rebar densities, as this seems to be a key factor in the observed extent and therefore the propagation of the laminar cracks.

Specifically, the issue is the density of rebar in 2 dimensions (not 3 dimensions) in the outer face (OF) rebar mat. There are locations, such as the top 20 feet of the walls where the nominal spacing of the horizontal rebar is 6". With laps and normal construction tolerances, this can lead to regions where there is less than 2" of clear spacing between the horizontal rebar. It was also observed that in some locations the vertical rebar were adjusted on either side of the jacking bars in order to accommodate the hydraulic jacking heads used during the slip-forming operation. An example of this is shown in Figure 3.

#### (a) "Enabling Event" Considered

In these models, the "enabling event" is a freezing failure in which the "sides" of the shoulders freeze first and trap moisture in the centers of the shoulders. The "sides" of the shoulders include the regions where the shoulders transition into the walls, including the flute valleys and the tangential transition to the base cylinder. The shoulders can insulate the OF rebar mat and delay changes in temperature in the middle of the shoulders. As the concrete near the outer surface of the building freezes, temperature and pore pressure gradients may form in the concrete. These gradients would drive water "side" to "side", hence the "side-to-side" label (See Figure 6 for details).

#### (b) Analysis Design

The moisture ingress is not modeled explicitly. The ingress of moisture is an assumption for this set of analyses (See Section 7.02, FM 3.6 (A) for more explanation). [REDACTED]



The horizontal bars are frozen from the outside in, [REDACTED] Water expands about 9% when it freezes, [REDACTED]

Only a small subset of the elements in the models is assigned a [REDACTED] That subset is [REDACTED] under the horizontal rebar [REDACTED]

Using these values, it was found that laminar cracks form in regions with rebar spacing of 6" or less. The 0.6% and 1% values are referred to as the void fraction (VF) or "air content" that is filled with water. Note that the Davis-Besse concrete was measured to have a void fraction of roughly 5%, and the void fraction is generally higher under the horizontal rebar (See Exhibit 2 and Exhibit 26).

[REDACTED]

[REDACTED]

**(c) Scenarios Considered**

Five sets of different rebar spacing scenarios were modeled. They included:



- 1) <6" – Tightly-spaced rebar with a pattern based on the figure above. In this scenario, the vertical rebar have a variable spacing from 2" to 6". The horizontal bars have a nominal spacing of 6" with laps. This results in a clear spacing between bars of 0.6" to 4.6".
- 2) 6" nominal – Both horizontal and vertical bars have a nominal 6" spacing, including laps, which creates a clear spacing between bars of 2.6" in some locations and 4.6" in others.
- 3) 6"H/12"V – Horizontal bars are spaced with the same nominal 6" including laps. The vertical bars are given a nominal 12" spacing, including laps.
- 4) 12" nominal – Both horizontal and vertical bars have a nominal 12" spacing, including laps.
- 5) >12" – Both horizontal and vertical bars are placed 12" from each other, but no laps are included and the bars are 8" from the boundary edges of the model, simulating a scenario with bars that are more sparse than 12".

#### (d) Results Summary

The results are summarized in the Table 2.

The “motivating force” is the void fraction of elements treated as ice, e.g. 0.6% and 1% of the [REDACTED]. The “rebar spacing” variable is summarized above and presented in the legend, and the “extent of cracking” is a scale from 0 to 3 that serves to simplify the extent of the damage observed in each model. The meaning of each level from 0 to 3 is described in the third legend following the table below. A level of “3” is a complete delamination along the OF rebar mat similar to the center of shoulder 9 at the top of the shield building. A level of “0” is no damage.

What the results show is that there is a clear trend toward more damage with tighter rebar spacing. The models with all 12" rebar spacing showed no laminar cracks at all.

Accordingly, the laminar cracking identified in the MS room near areas that have been confirmed to remain above 100F during operation can be explained by a weakened plane in the concrete, created by the presence of very high density rebars in the OF rebar mat plane. This plane allows a crack to propagate with relatively little motivating force.



**Table 2: Results from Rebar Sensitivity Study for various Motivating Forces and Rebar Spacing**

Case	Motivating Force	Rebar Spacing	Extent of Cracking
Case 1	0	<6"	0
	0.6	<6"	1
	1	<6"	3
Case 2	0	6"	0
	0.6	6"	1
	1	6"	3
Case 3	0	6" H/ 12" V	0
	0.6	6" H/ 12" V	1
	1	6" H/ 12" V	3
Case 4	0	12"	0
	0.6	12"	0
	1	12"	0
Case 5	0	>12"	0
	0.6	>12"	0
	1	>12"	0

Note that the models' suggestion that SB laminar cracking initiated by debonding at the interface of concrete/ rebar along the outer reinforcement may appear to conflict with the observation that some core bore laminar crack depths exist away from the rebar mat.

However, in concrete, cracks that initiate at the concrete/rebar interface may 'wander' through the 'path of least resistance' as it propagates. Variation in localized material strength could readily cause such crack 'wandering'. It is likely that these cores encountered such condition.



Table 3:



Motivating Force		Extent of Cracking		Rebar Spacing	
0	No Force	0	No Laminar Cracks	<6"	Sub 6" Spacing (e.g. 2", 4")
0.6	0.6% 	1	Sparse, Up To 12" x 12"	6"	Nominal 6" Spacing of all Bars, with Laps
		2	Continuous Up To 24" x 24"	6" H /12" V	Nominal 6" Spacing Horizontal Nominal 12" Spacing Vertical
1	1% 	3	Extensive, Larger than 24" x 24" with Localized Double Cracks	12"	Nominal 12" Spacing of all Bars, with Laps
				>12"	Wider than 12" Spacing

Figure 8 & Figure 9 respectively show laminar cracking due to water freezing near dense rebar and laminar cracking that is absent due to water freezing near sparse rebar.

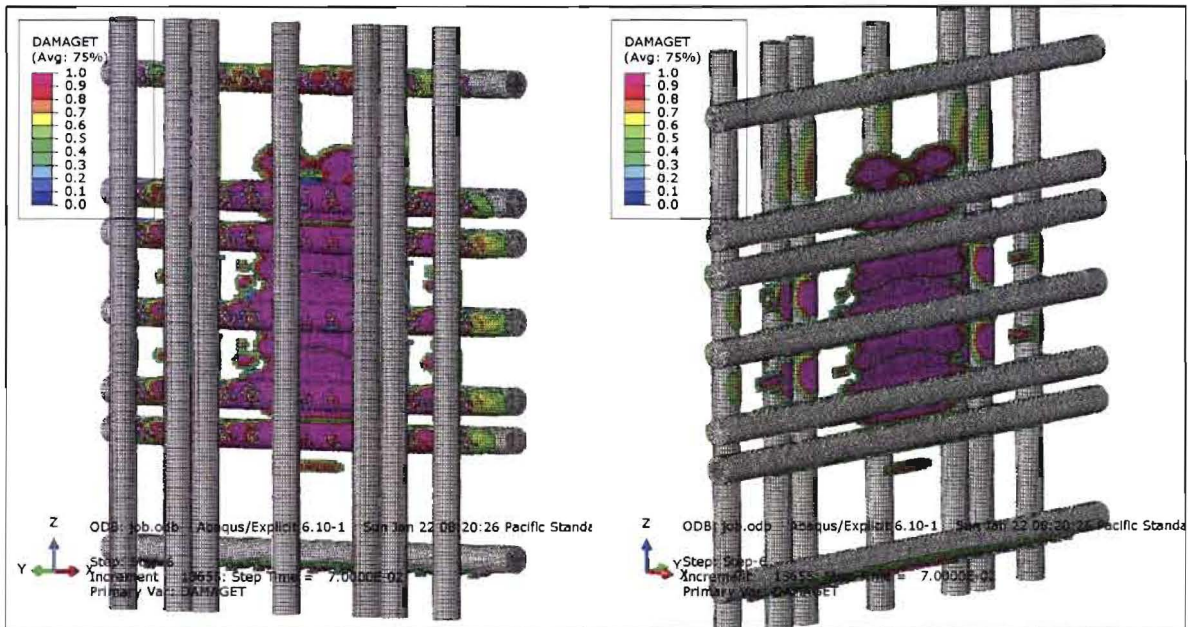


Figure 8: Laminar Cracking (Nominal 6" Spacing, 0.6% VF)

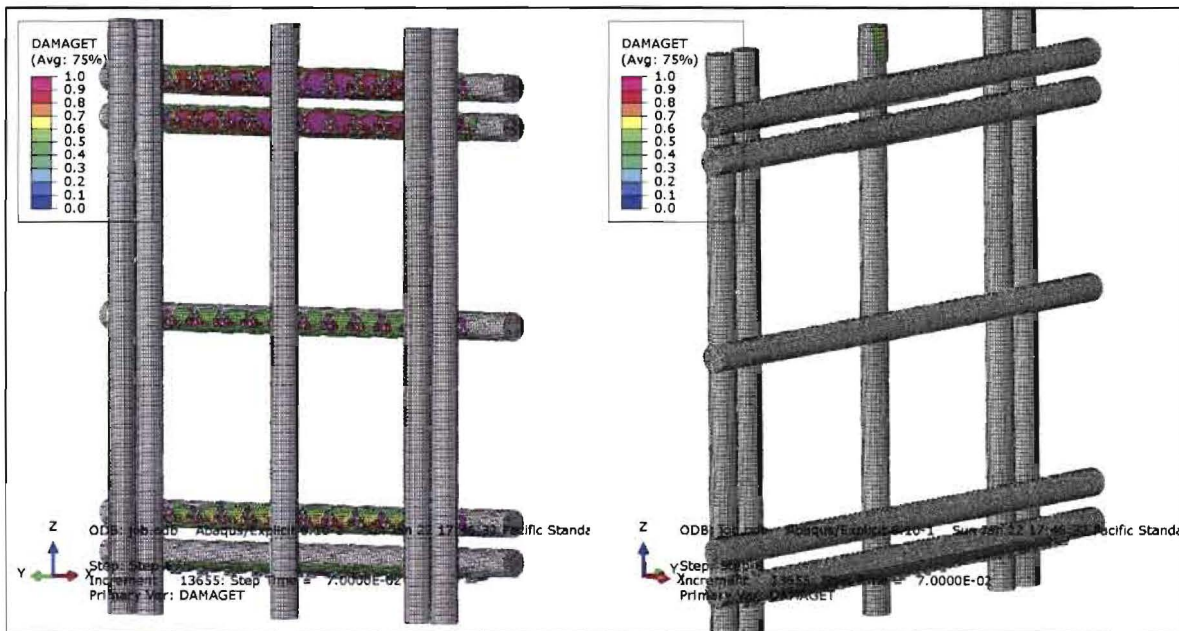


Figure 9: Debonding but No Laminar Cracking (Nominal 12" Rebar, 0.6% VF)

(e) Conclusion

This study shows and establishes the following:

- Only a small fraction of the voids under the rebar need to fill with water and freeze in order to get laminar cracks. And, for a given motivating force, there are large laminar cracks that form in regions with dense rebar and none form in regions with sparse rebar.
- Freezing of ice under the horizontal rebar is a plausible failure mode. The cracks are reproducible and [REDACTED] and then further testing shows that there is no failure in regions with sparse rebar
- For the same motivating force, there are large laminar cracks that form in regions with dense rebar and do not form in regions with sparse rebar. With a given motivating force, [REDACTED] [REDACTED], all of the models with 6" spacing of rebar showed the development of some laminar cracks, while none of the models with all 12" spacing showed any laminar cracking.

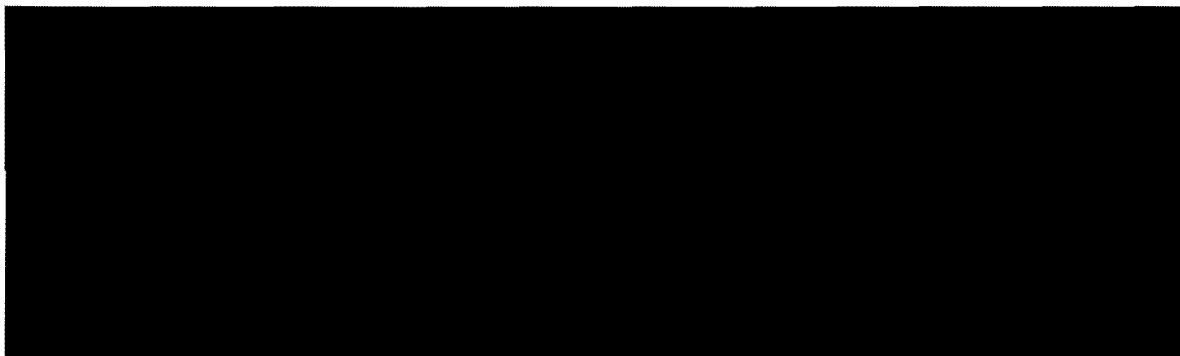


- Establishes that rebar spacing is a probable contributing factor because the tighter rebar spacing can facilitate crack propagation along the plane of weakness. In regions with wider rebar spacing, damage is less likely because of the absence of this contributing factor.

X. Analysis II, FM 3.6 (B): Finite Element Analysis of 1977 & 1978  
Blizzard Conditions

*Section 10.01 Analysis*

Numerous finite element analysis models were developed to examine the behavior of the DBSB under several weather conditions. For purposes of this failure mode, extreme weather conditions, using the 1977 & 1978 Toledo Blizzard as a case study was examined. Finite element analysis experts worked in concert with aggressive scientific application to determine the structural response of the DBSB to the conditions associated with the 1978 Toledo Blizzard. Detailed analysis reports, referenced in Exhibits 56, 63, 65, 66, 67, and 71, may be reviewed for an in-depth scientific understanding of the analyses performed; however, the highlights from these analyses will be discussed in what follows.



two. The purpose of the transient thermal analysis was to determine the temperature distribution throughout the DBSD. [REDACTED]



details of the wind and thermal modeling can be found in Exhibits 65 & 67.





Initially, thermal transient analyses were conducted using the Crystal River CR3 thermal properties. A total of 32 thermal conditions were examined which included the summer/winter solstices and spring/autumn equinoxes with either windy or calm conditions as well as average hot/cold ambient temperatures. These are summarized in Table 4 of Section 13.

[REDACTED]

[REDACTED] Those conditions were then identified that maximized the tensile radial stresses. Once the DBSB thermal properties became available, thermal analyses were repeated for those six cases that produced the highest radial stresses (Table 5). An additional two thermal transient analyses were performed for ambient conditions that corresponded to the 1977 and 1978 blizzards.

[REDACTED]

[REDACTED]

temperature conditions discussed in this section of the report reference the predicted temperatures for the 1977 and 1978 blizzard conditions (Exhibit 65).

[REDACTED]



The following figure shows the region studied in detail, shoulder numbers 11 & 12.

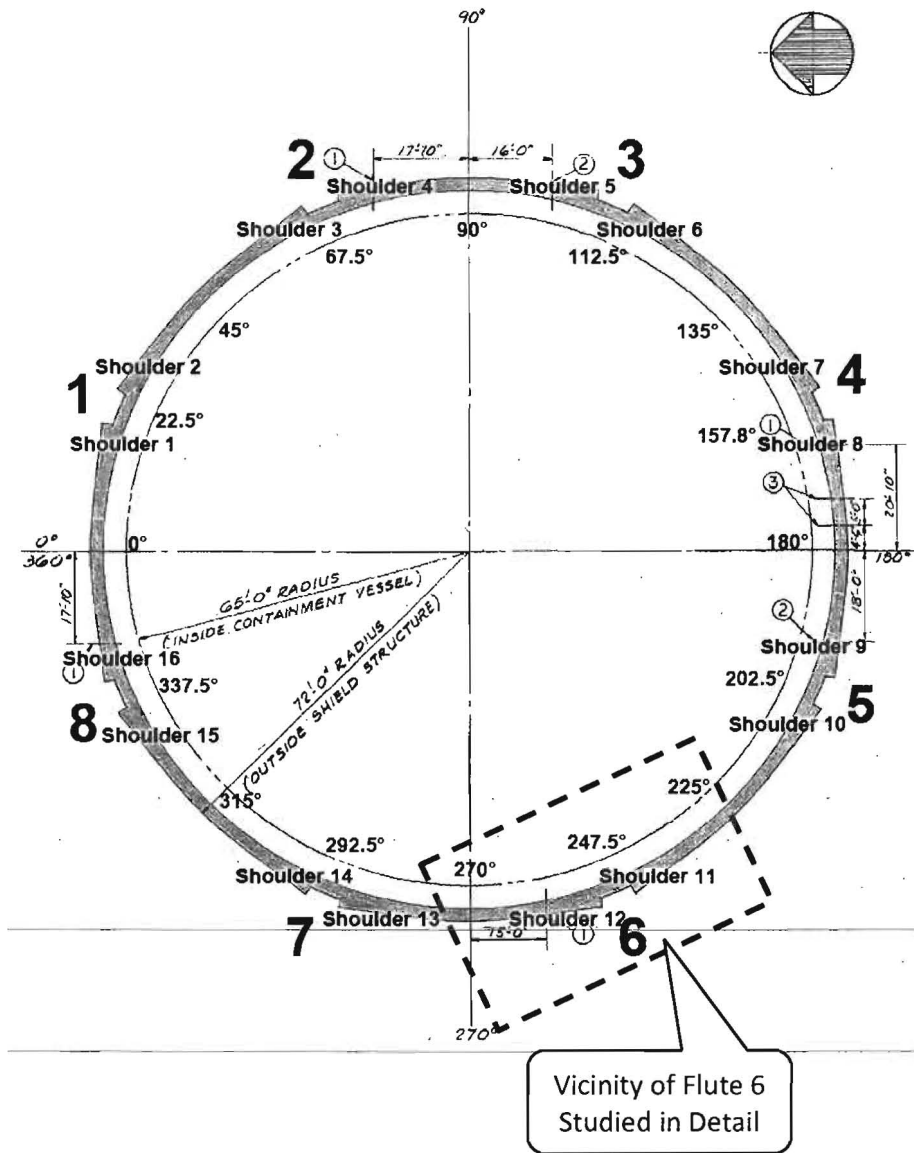
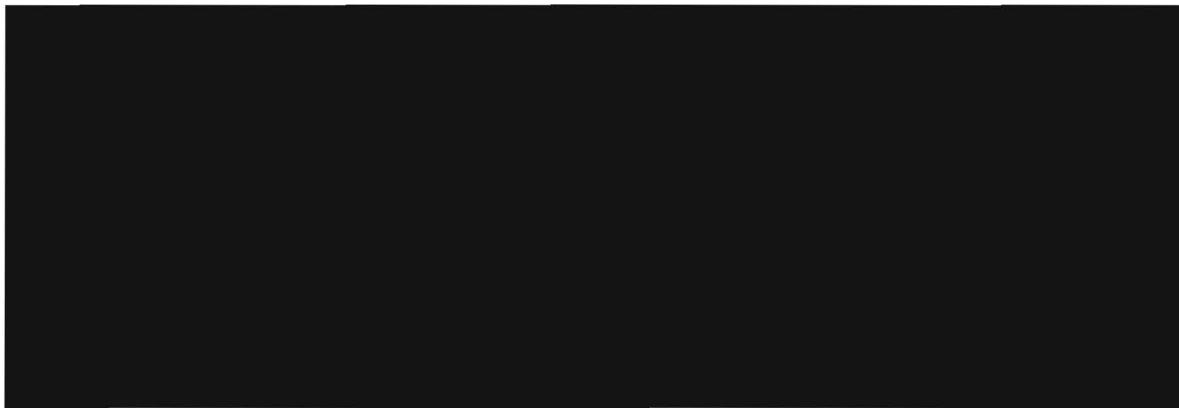


Figure 10: Plan View of the DBSB (Analysis of Flute 6, Shoulders 11 & 12)



### *Section 10.02 Coefficient of Thermal Expansion*

The coefficient of thermal expansion (CTE) of high moisture concrete is a highly nonlinear function of temperature. This is associated with the 9% volume expansion of the freezing of entrapped water. The freezing of water in small pores in concrete takes place at temperatures lower than 32°F due to surface tension, which prevents the formation of ice at 32°F; the water in concrete freezes at varying temperatures depending on the pore size. This nonlinear dependence of the CTE with temperature is shown in Exhibit 57 and used as an input to the finite element analysis presented here.



██████████ The thermal properties of concrete reported in Exhibit 59 depend on many parameters such as moisture content of concrete and type of aggregate. The important thermal parameter is the thermal diffusivity which includes the effects of both conductivity and specific heat.

Tests of moisture penetration were also performed at the University of Colorado at Boulder, which showed that a ██████████ water penetration up to 3 or 4 inches is possible when there are winds in excess of 90mph (such as during the 1978 blizzard). The 1978 models are



[REDACTED] f penetration is approximately 3 to 4 inches [REDACTED]

[REDACTED]

[REDACTED] The 1977 models assume that the moisture depth of penetration is roughly half the 1978 case due to significantly less wind and precipitation in the 1977 case. Exhibit 66 and Exhibit 71 summarize some key meteorological data during and prior to the blizzards of 1977 and 1978.

*Section 10.03 Circumferential Temperature Distribution at O.F. Horizontal Rebar*

[REDACTED]

[REDACTED] (See Exhibit 65) The temperature profiles around the Shield Building at the outer face horizontal rebar are shown in Figure 11.

[REDACTED]

[REDACTED]

The figure shows 8 sets of double peaks for each temperature profile. The double peaks represent the warmer temperature under the shoulders. The temperature is warmer under the shoulders because there is a thicker layer of concrete at those locations which reduces the heat loss to the exterior during the blizzards.

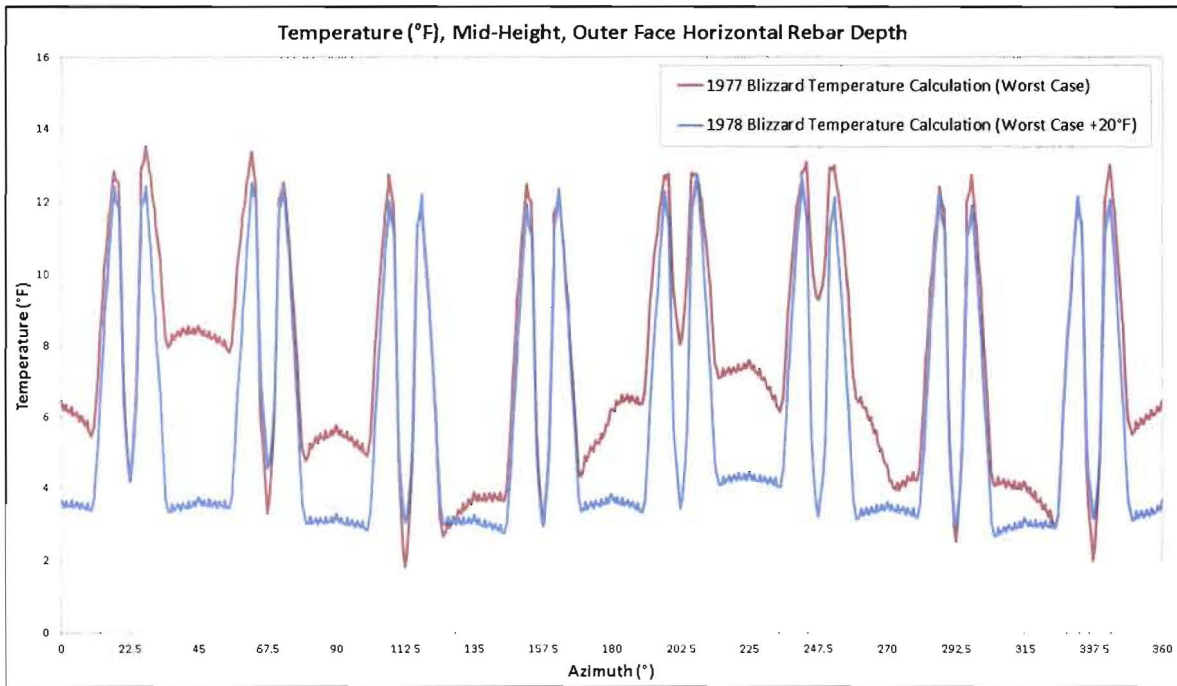


Figure 11: Circumferential Temperature Distribution at the O.F. Horizontal Rebar Depth

Section 10.04 [REDACTED]

The [REDACTED] includes concrete and steel rebar at nominal (as designed)

Figure 12, Figure 13, and Figure 14 depict the geometry and finite element mesh of the [REDACTED]

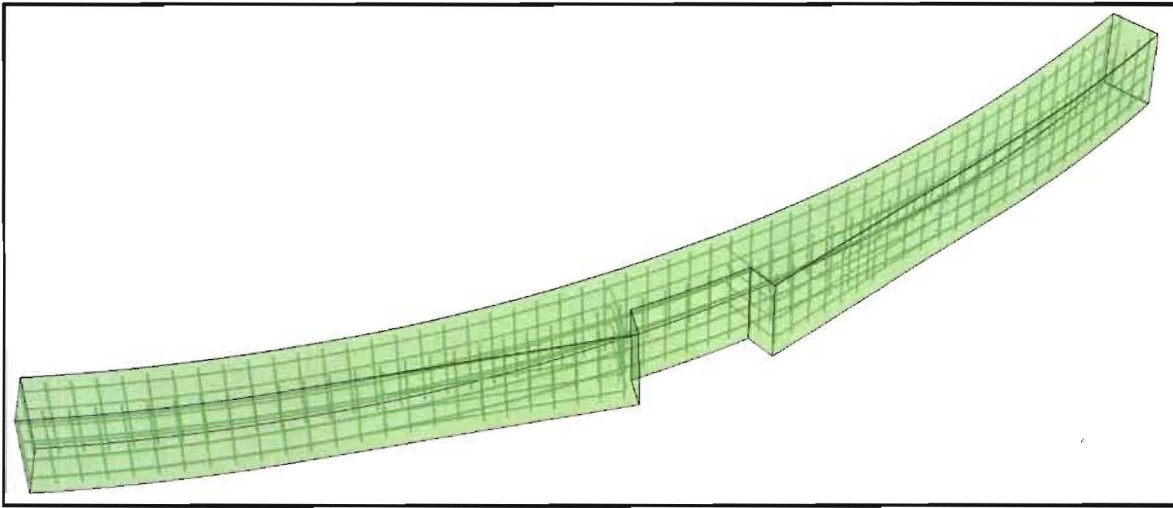


Figure 12: [REDACTED] Geometry and Rebar

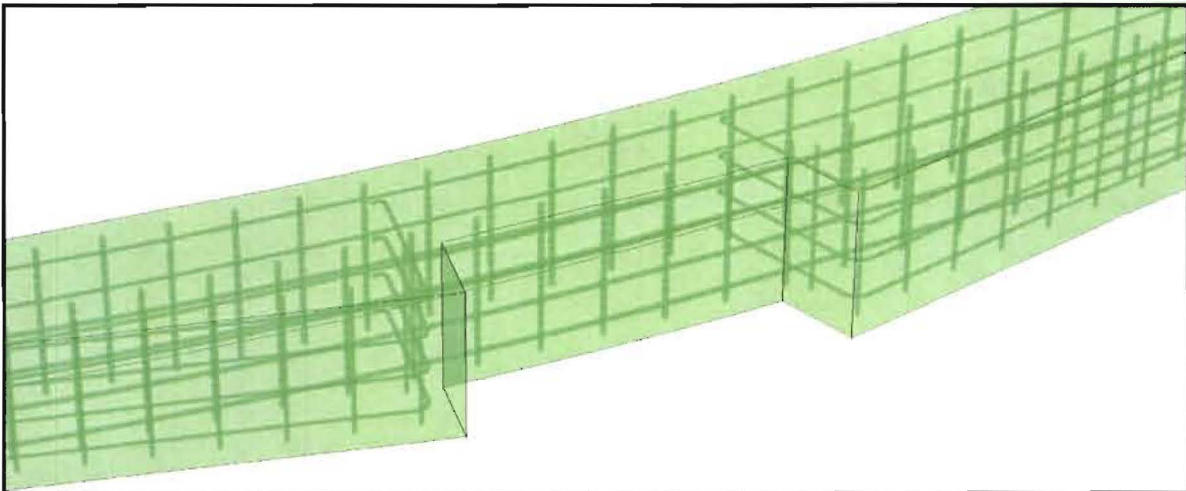


Figure 13: [REDACTED] Detail of Flute Region



Figure 14: [REDACTED] Detail of Flute Region with Mesh

(a) [REDACTED]

This section summarizes the results from the [REDACTED]. The result from the [REDACTED] [REDACTED] is used to make predictions about the delamination propensity due to the two blizzard conditions. This model does not attempt to make predictions of stress concentration effects around the included reinforcing bars due to lack of detail at the concrete/steel interface.

The tensile strength of the Davis-Besse concrete is in the range of 836 to 962 psi. The contours in the stress figures in this section are assigned an upper limit of 900 psi. A tensile stress exceeding 900 psi is indicated by light grey contours in the stress figures. The interpretation of any light grey area in the contour plots below is that damage may occur in that area. The damage that results from any tensile stress above the strength of the concrete depends on 3D stress state as well as the strain energy available to open the crack. Low strain energy results in microcracks and high strain energy results in more microcracking and eventually a structural crack.

In order to determine the size of the resulting crack, a separate Abaqus [REDACTED] [REDACTED] analysis was performed. [REDACTED]  
[REDACTED]



analysis of the 1978 blizzard is presented in a separate section of the Root Cause Analysis Report.

The stress contour results shown in this section can be summarized as follows:

- Higher tensile stress and larger stressed areas is predicted in the 1978 blizzard compared to the 1977 blizzard
- Blizzard of 1978:
  - Tensile stresses high enough to damage the concrete is predicted
  - The high stresses are distributed over large areas in the observed crack locations under the thick sections of the shoulders and not in the thinner sections in the flute and panels
- Blizzard of 1977:
  - Tensile stresses are lower or equal to the strength of the concrete
  - The highest tensile strength are confined to small areas under the thick sections of the shoulders

**(i) 1978 Blizzard Condition**

The result due to the 1978 blizzard is shown in Figure 15 through Figure 21. The temperature contours can be seen in Figure 15 and the stress results is shown in Figure 16 through Figure 21.



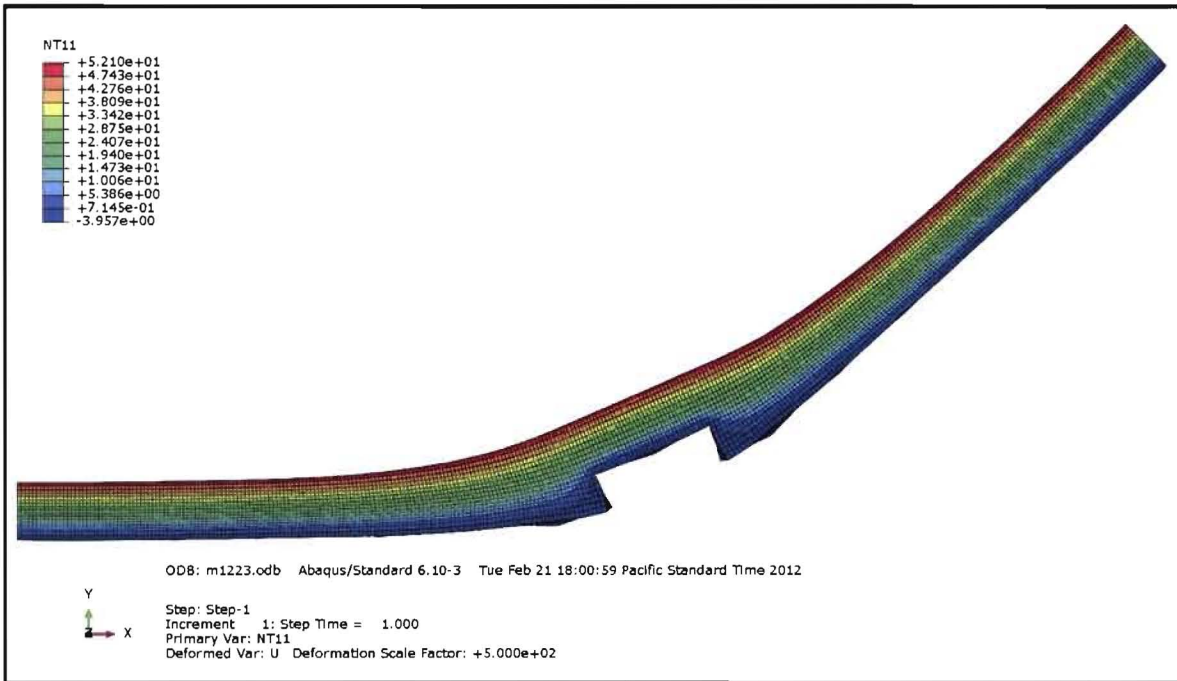


Figure 15: Temperature (°F) during the Blizzard of 1978; Deformation Scale Factor 500X

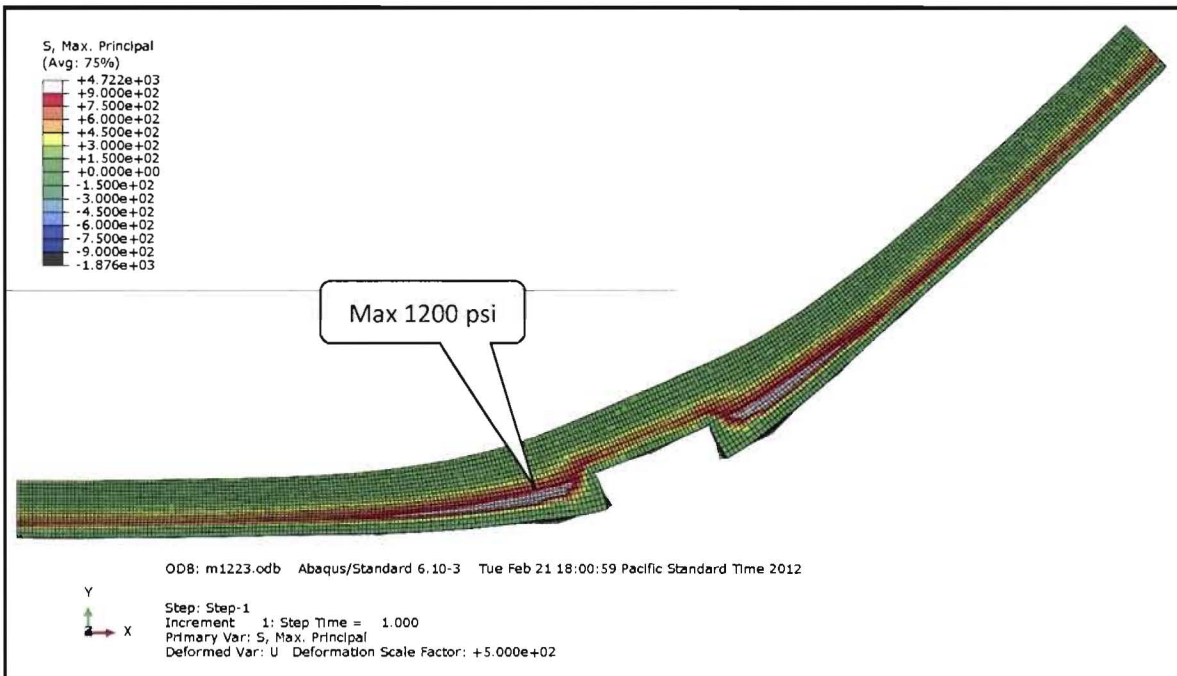


Figure 16: Max Principal Stress (psi) during the 1978 Blizzard; Deformation Scale Factor 500X

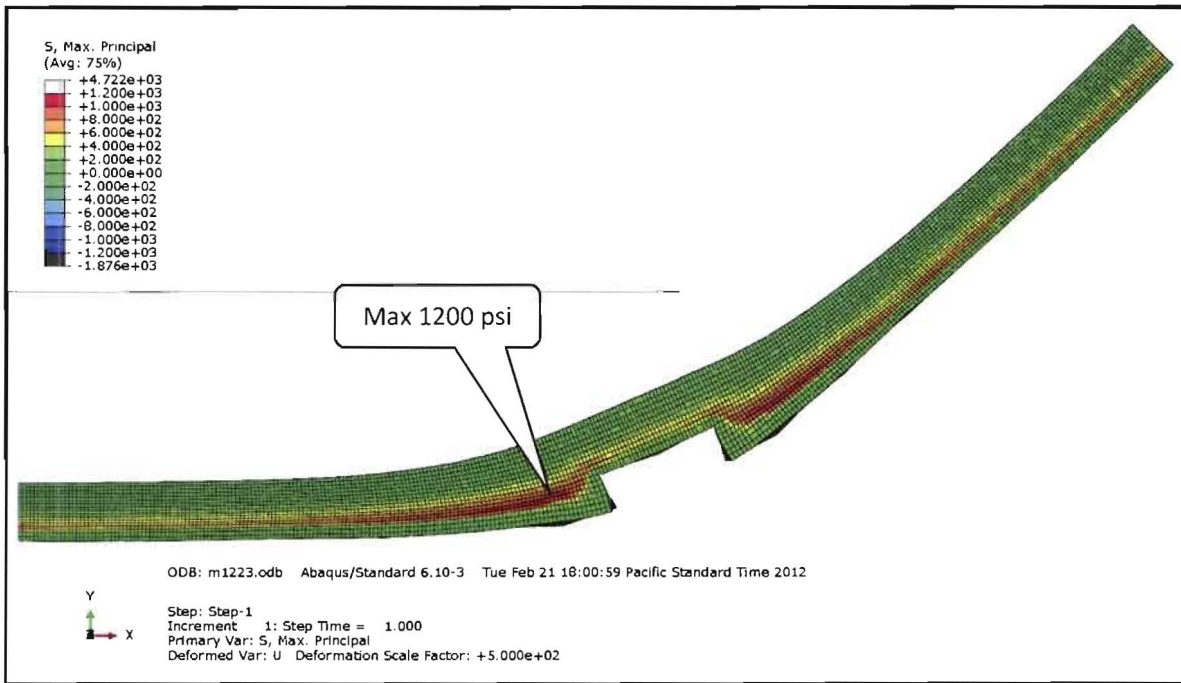


Figure 17: Max Principal Stress during the 78 Blizzard; Deformation Scale Factor 500X; Wider Contour Range (+/- 1200 psi)

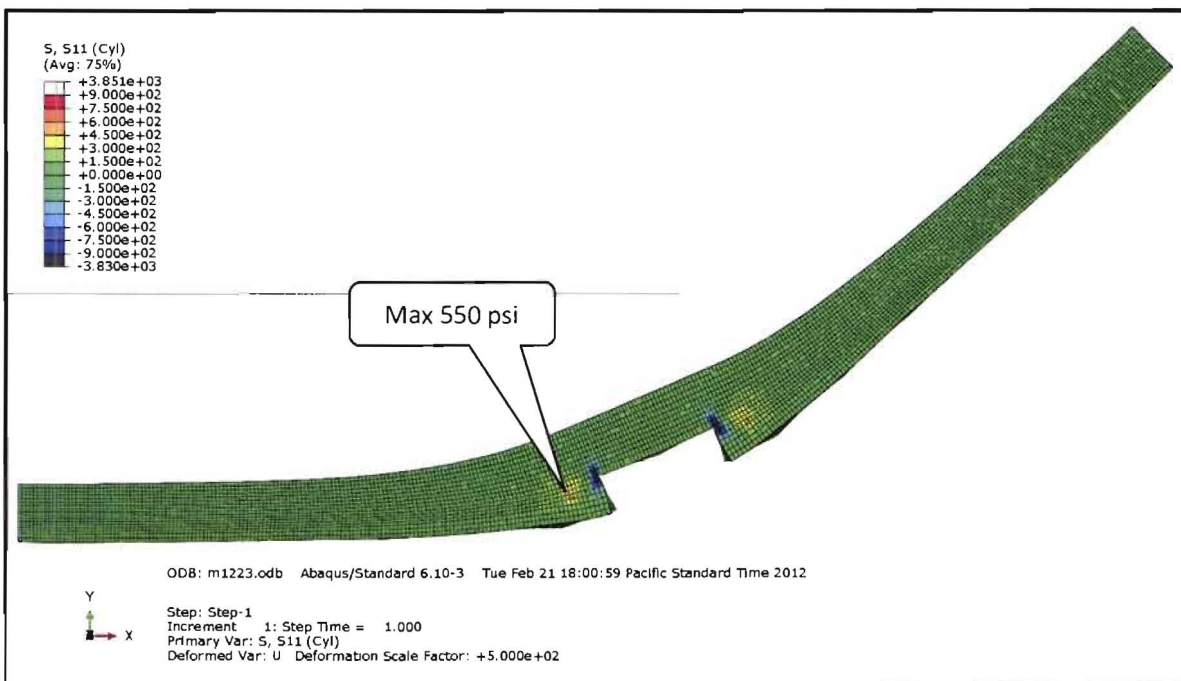


Figure 18: Radial Stress (psi) during the Blizzard of 1978; Deformation Scale Factor 500X

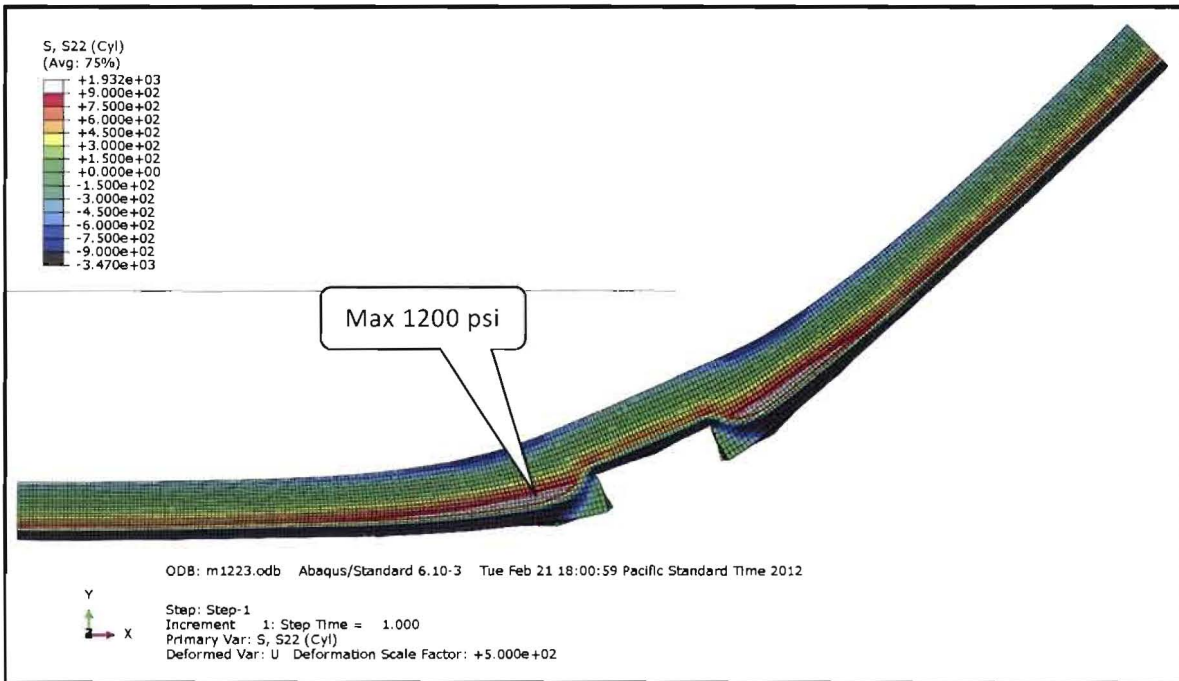


Figure 19: Hoop Stress (psi) during the Blizzard of 1978; Deformation Scale Factor 500X

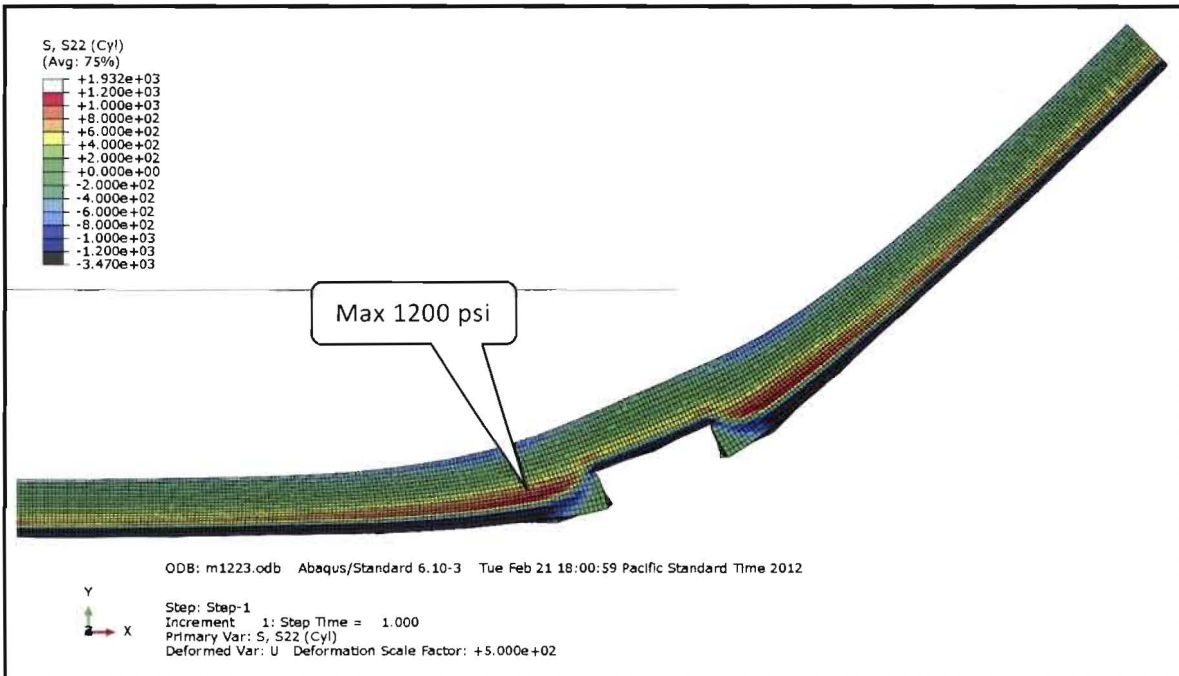


Figure 20: Hoop Stress (psi) during the Blizzard of 1978; Deformation Scale Factor 500X; Wider Contour Range (+/- 1200 psi)

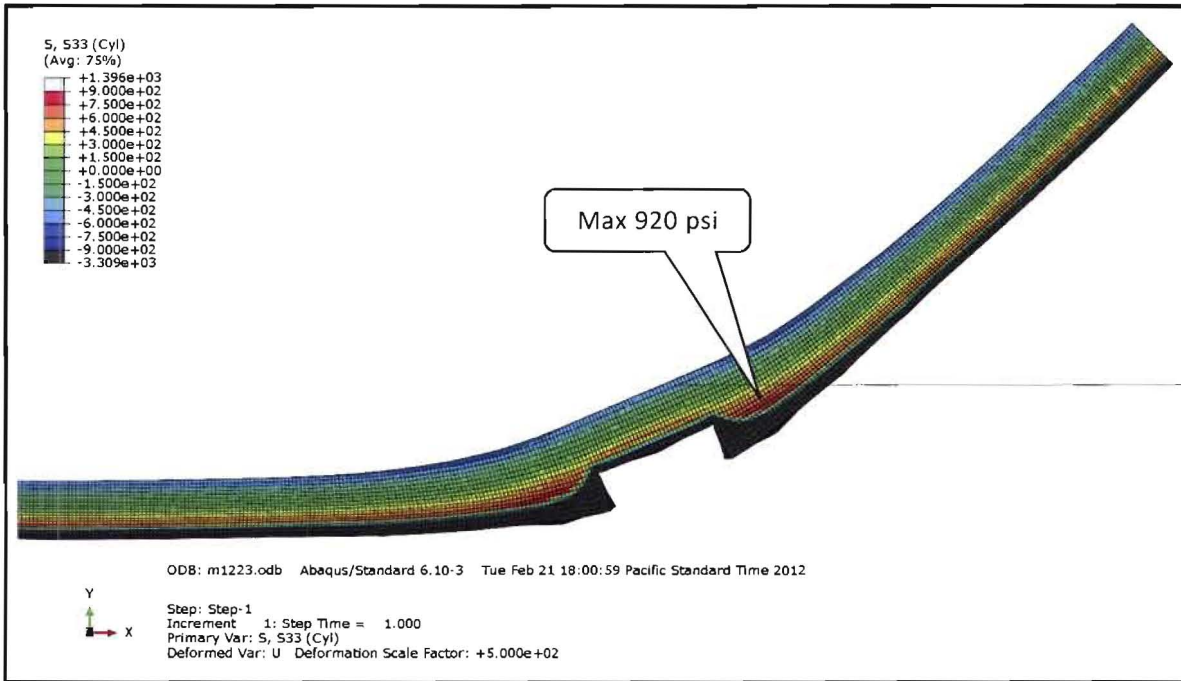


Figure 21: Vertical Stress (psi) during the Blizzard of 1978; Deformation Scale Factor 500X

### (ii) 1977 Blizzard Condition

The result from the [REDACTED] due to the 1977 blizzard condition is shown in this section. Figure 22 depicts the temperature distribution in the model. Figure 23 through Figure 26 show the stress state in the max principal, radial, hoop, and vertical directions, respectively.

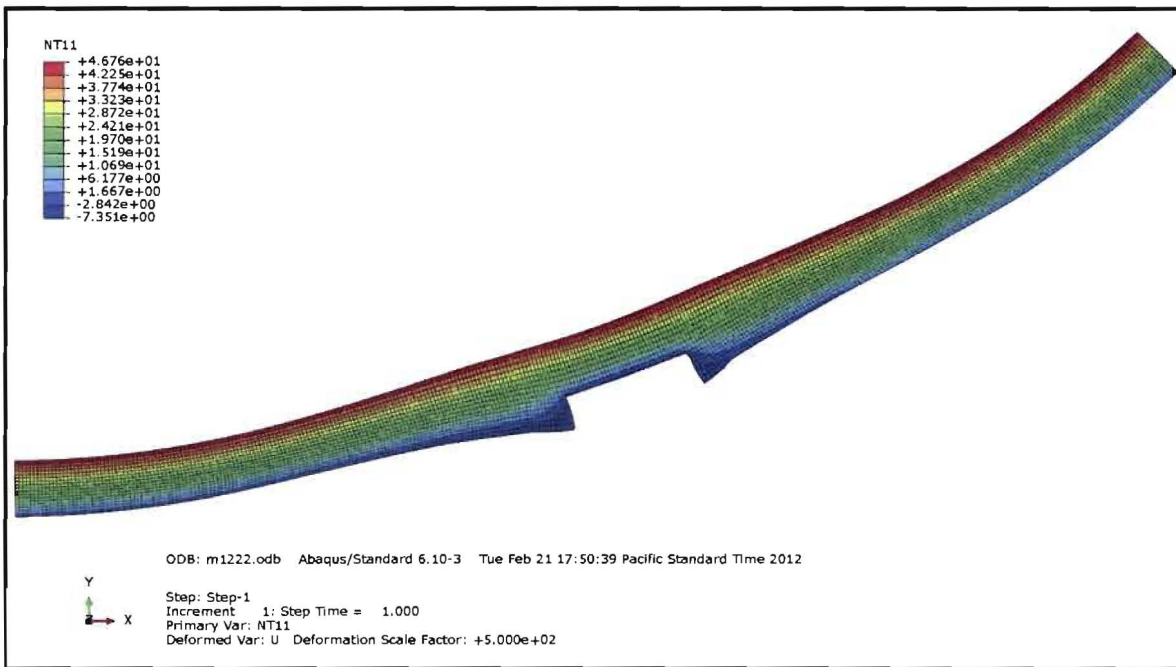


Figure 22: Temperature (°F) during the Blizzard of 1977; Deformation Scale Factor 500X

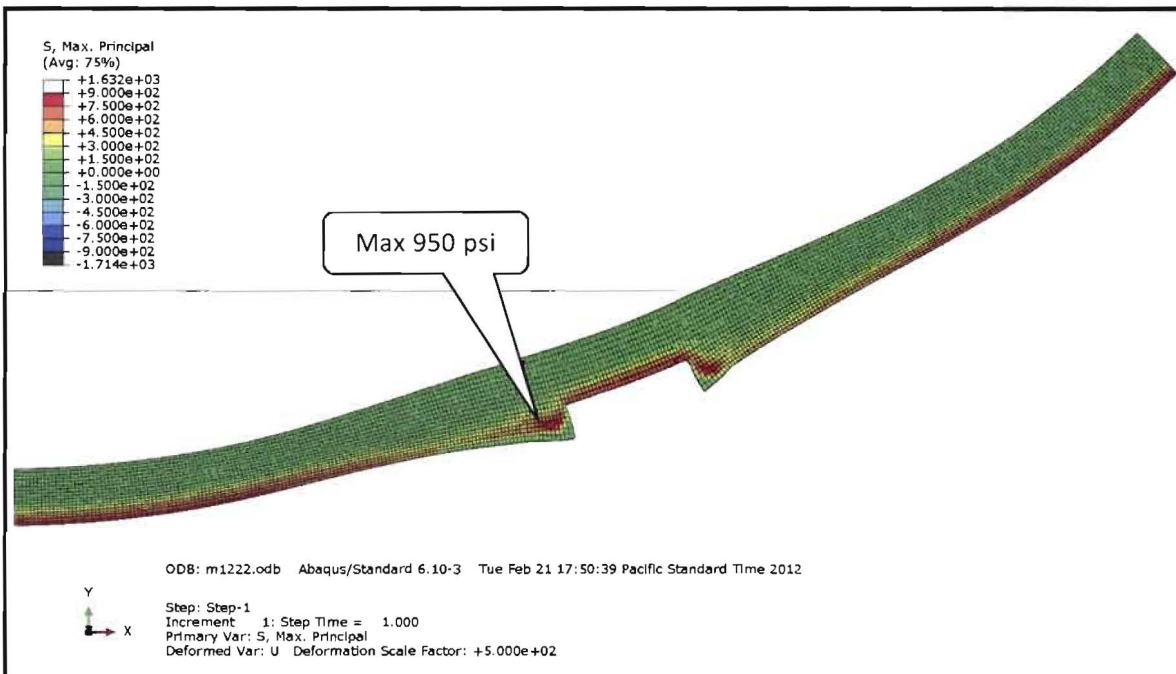


Figure 23: Max Principal Stress (psi) during the Blizzard of 1977; Deformation Scale Factor 500X

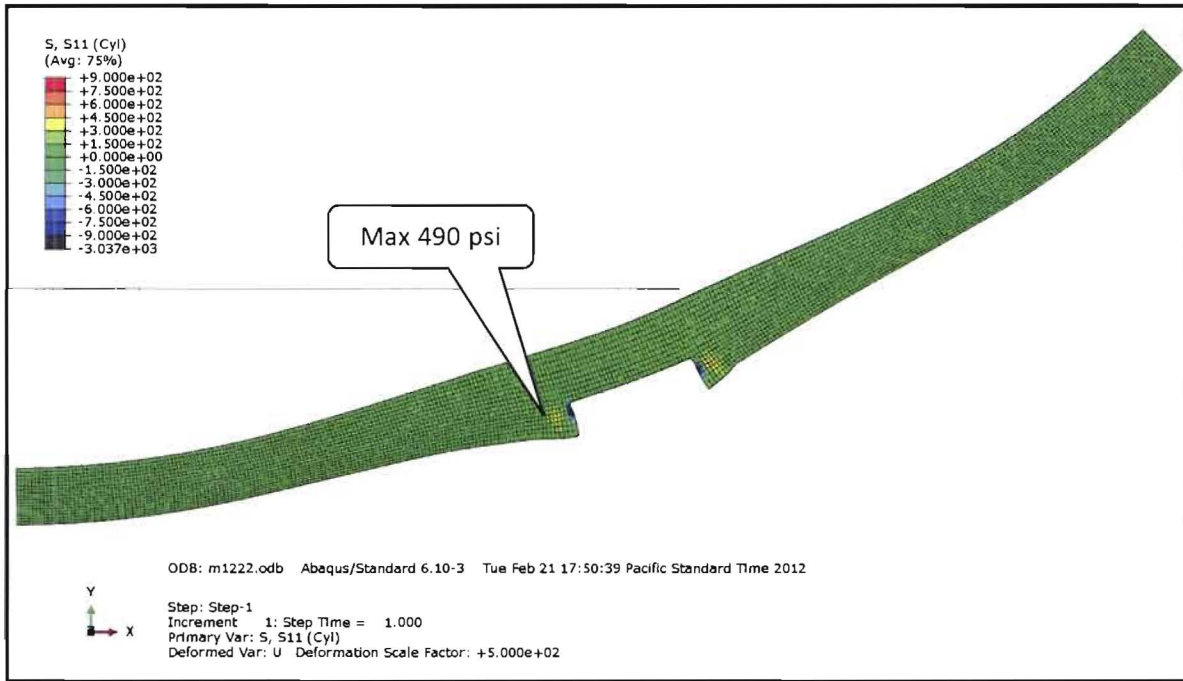


Figure 24: Radial Stress (psi) during the Blizzard of 1977; Deformation Scale Factor 500X

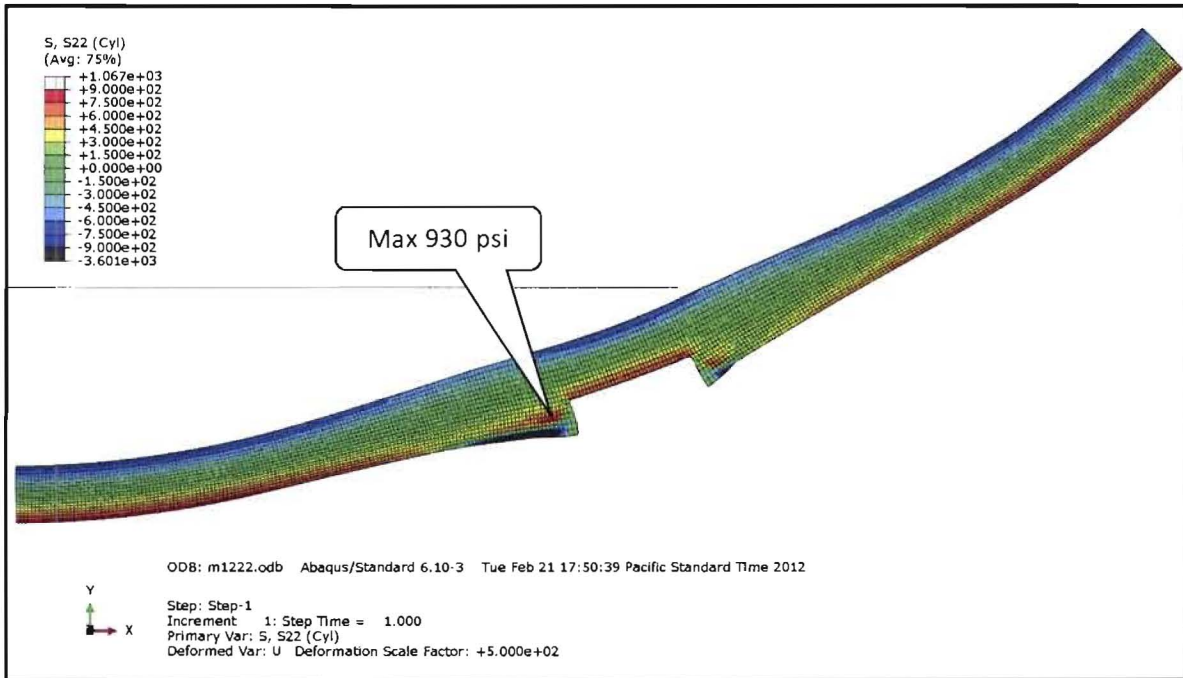


Figure 25: Hoop Stress (psi) during the Blizzard of 1977; Deformation Scale Factor 500X

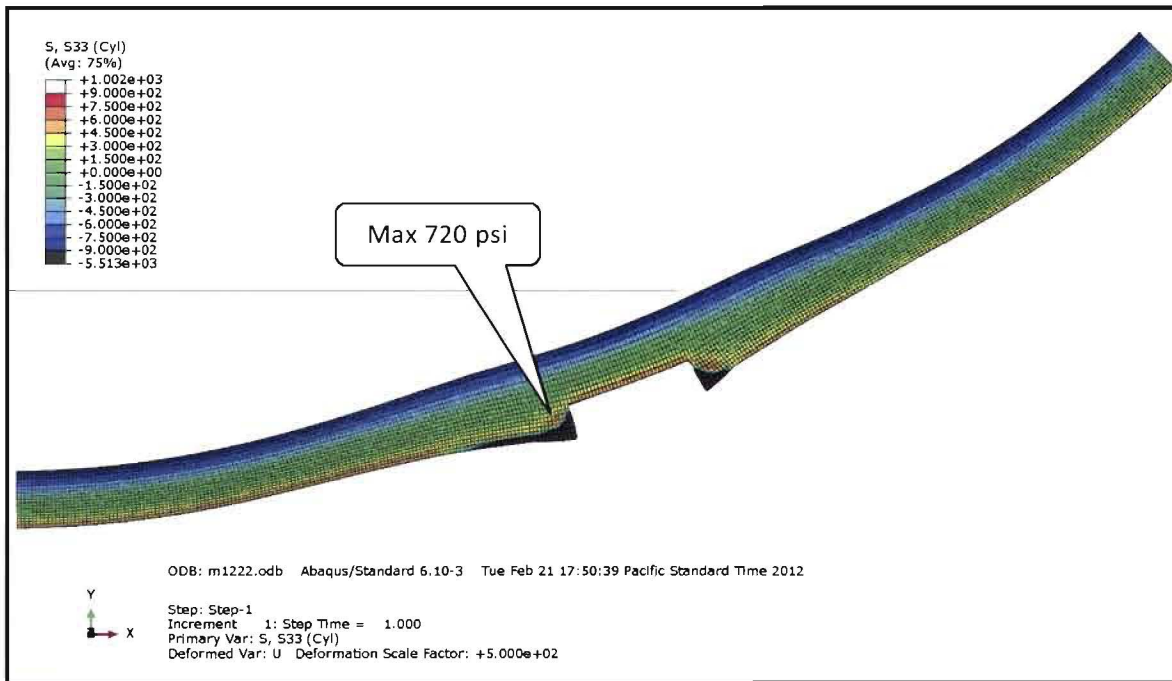
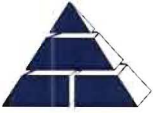


Figure 26: Vertical Stress (psi) during the Blizzard of 1977; Deformation Scale Factor 500X

### Section 10.05 Conclusion

The results of the analysis presented in this report can be summarized as follows:

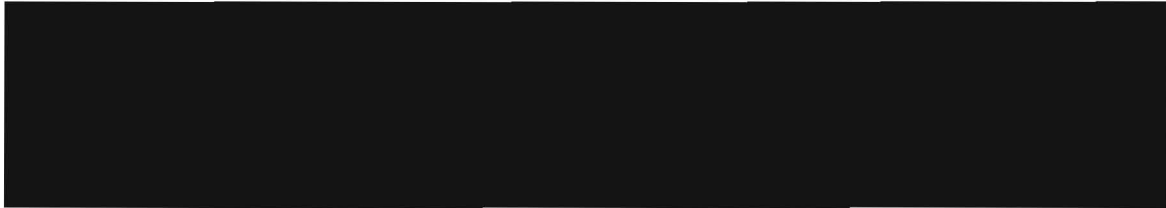
- The blizzard of 1978 produced stresses above the tensile strength in the hoop direction, likely resulting in damage. The area exceeding the tensile strength is confined to a circumferential plane at the depth of the outer face main cylindrical wall under the raised shoulders.
- The 1977 blizzard shows significantly lower stress compared to the blizzard of 1978. The hoop stress approached the tensile strength of the concrete and it is limited to a small area. For these reasons only minor damage, if any, is predicted.



## XI. Analysis III: Laminar Cracking Due to 1978 Blizzard Conditions (Finite Element [REDACTED] Cracking Model)

### *Section 11.01 Background*

Expansion of concrete due to freezing of entrapped moisture was studied in the [REDACTED]



[REDACTED] The raised shoulders and the flute geometry are included in the model.

### *Section 11.02 Coefficient of Thermal Expansion*

The Coefficient of Thermal Expansion (CTE) discussion found in [Section 10.01](#) applies for this analysis as well. Again, the CTE of concrete with high moisture content is a highly nonlinear function of temperature. This is associated with the 9% volume expansion of the freezing of entrapped water.

Once more, the models assume that there are two outermost contour regions with a saturation of 93% (see [Exhibit 57](#) Figure 4). The calculation of the saturated depth is discussed in detail in [Exhibit 72](#) “Water and Moisture Transfer into Concrete”. The rest of the structure is assigned the linear CTE of 5.2e-6, as found and discussed in [Exhibit 59](#) and [Exhibit 56](#) Figure 2.1.4 (Material Properties for Davis-Besse [REDACTED]).

The thermal conductivity and specific heat of DB concrete were used as inputs for the FE thermal analysis. The thermal diffusivity was calculated by the FE program based on the input values for thermal conductivity and specific heat. In the linear thermal analysis for temperature distributions in the concrete structure, the important thermal parameter is the thermal diffusivity which is in the typical range for concrete, as shown in [Exhibit 59](#). One can see from [Exhibit 59](#) that both thermal conductivity and specific heat of DB concrete have abnormally higher values than the typical values shown in the literature. Thermal diffusivity = Thermal-conductivity/(specific heat x density). When the thermal conductivity and specific heat were





used to calculate the thermal diffusivity, the effect of the two abnormally higher values was canceled, resulting in the normal value of the thermal diffusivity for DB concrete.

Section 11.03

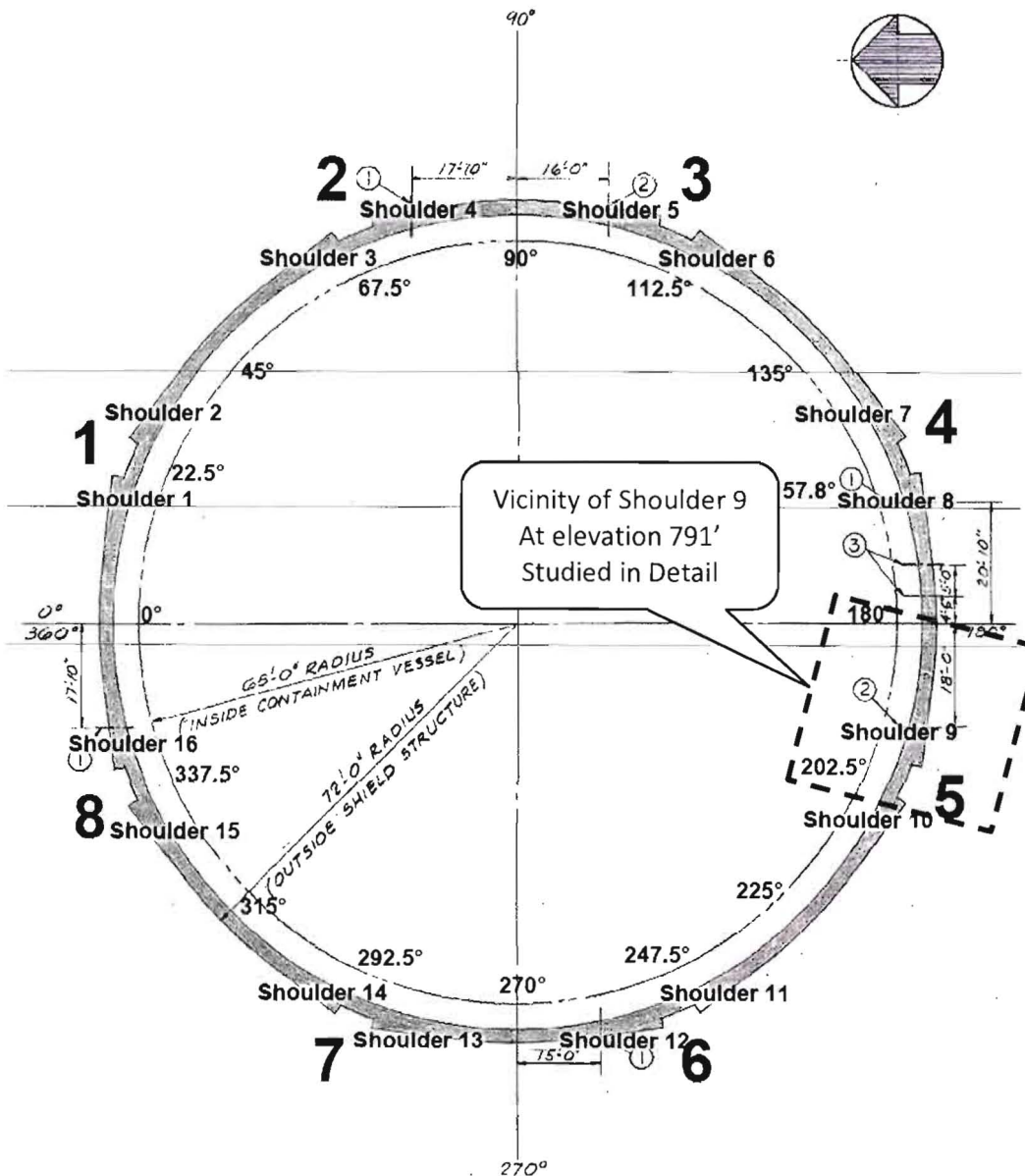


Figure 27: Shield Building with Flute Numbers and



[REDACTED]

[REDACTED] Depth of penetration is discussed in Exhibit 72.

*Section 11.04 Circumferential Temperature Distribution of O.F. Horizontal Rebar*

The temperature distribution in [REDACTED] presented here were calculated in separate heat transfer analysis an [REDACTED] (See Exhibit 65) The temperature profiles around the Shield Building at the outer face horizontal rebar are shown in Figure 28.

The models presented here use the worst case temperatures calculated for the 1978 blizzard with an offset of +20°F to simulate nominal temperatures. In this case, nominal temperatures will produce the most expansion and therefore the worst case stress condition for the building. The +20°F offset brings the 1978 temperature gradients into rough equivalence with the lowest recorded ground temperatures during the 1978 blizzard (see Exhibit 66), which would be the expected low temperature condition assuming heavy cloud cover rather than a clear night sky (see Exhibit 65).

The 1977 blizzard model uses the worst case temperatures calculated for the 1977 blizzard with no temperature offset because the worst case 1977 temperatures are already in the range that will maximize expansion and cracking.

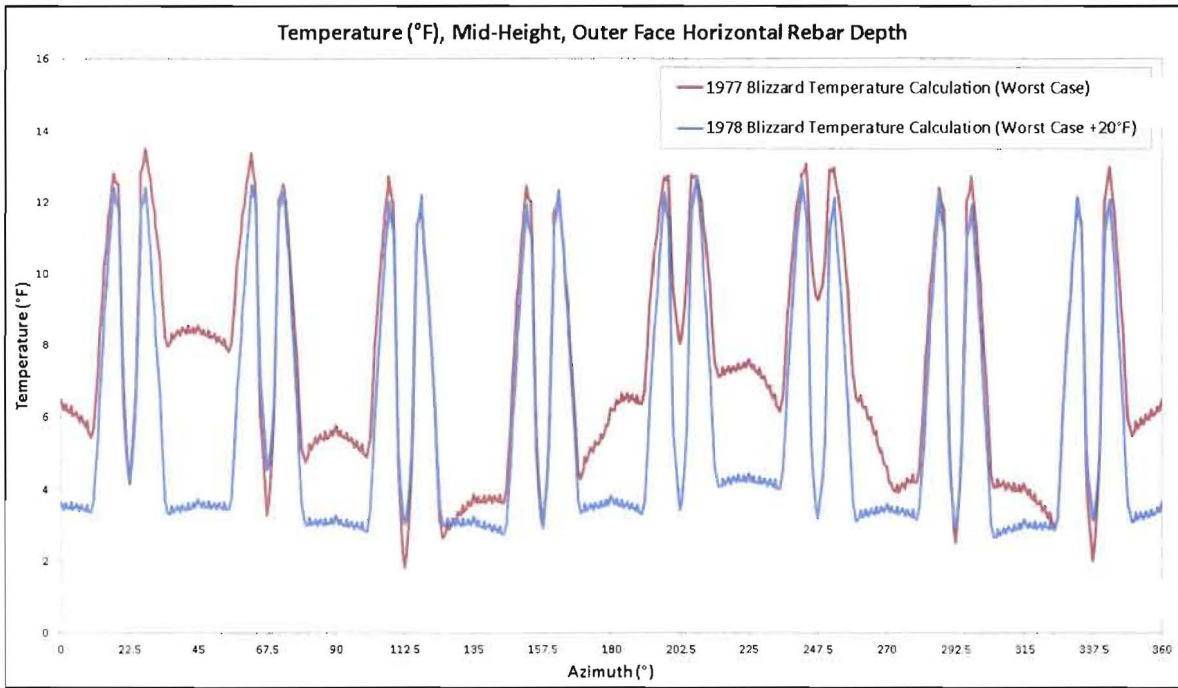


Figure 28: Circumferential Temperature Distribution at the O.F. Horizontal Rebar Depth

Section 11.05



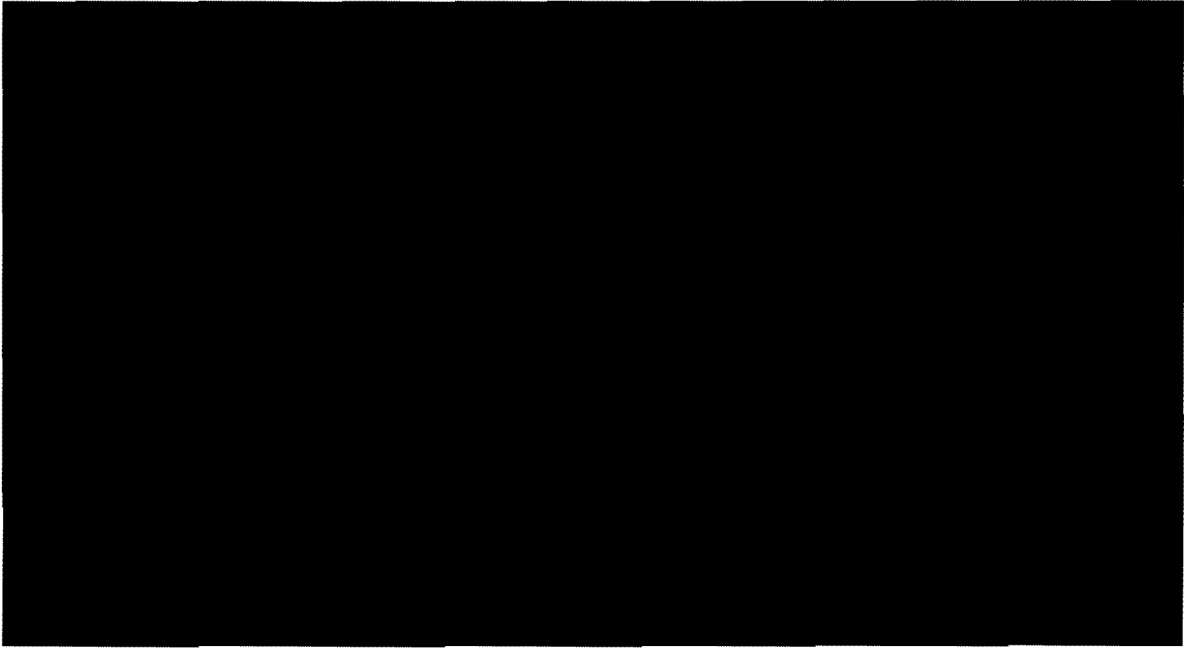


Figure 29: [REDACTED] Geometry and Rebar



Figure 30: [REDACTED] Detail of Flute Region

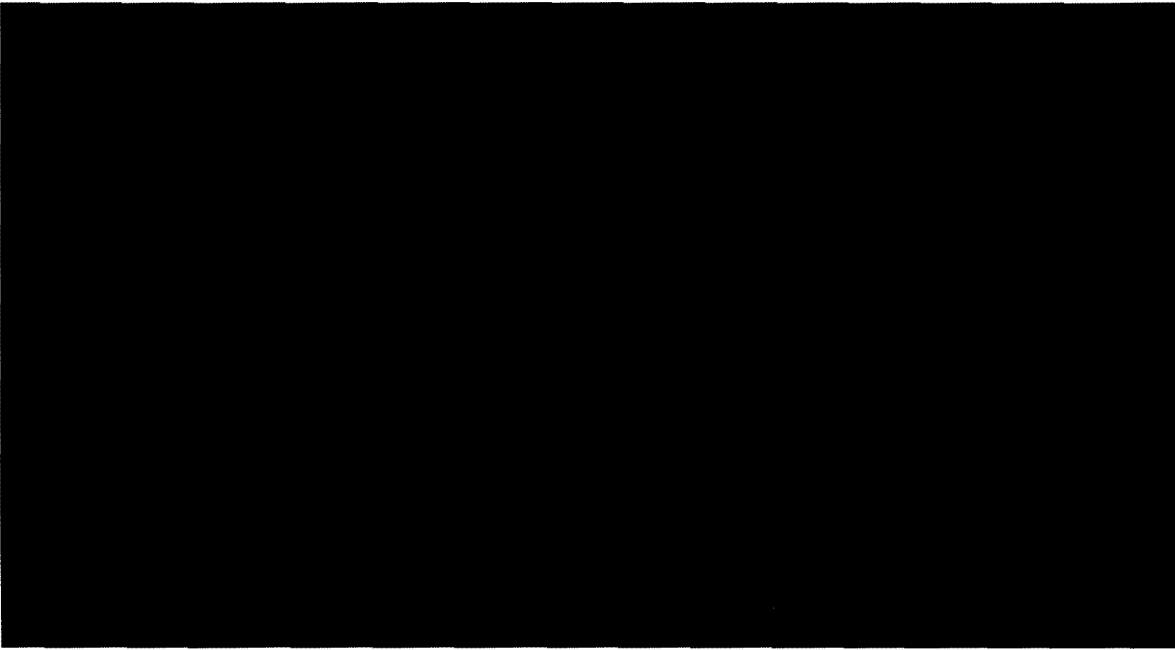


Figure 31: [REDACTED] Detail of Flute Region with Mesh



### Section 11.06 Discussion

The result from the [REDACTED] is used to make predictions about the delamination propensity due to the two blizzard conditions, given the assumptions of the model.



The damage that results from any tensile stress above the strength of the concrete depends on the 3D stress state as well as the strain energy available to open the crack. Low strain energy results in microcracks and high strain energy results in a structural crack.

#### (a) 1978 Blizzard Condition

The result due to the 1978 blizzard is shown in Figure 33 and Figure 34. The temperature contours can be seen in Figure 32 and the cracking result is shown in Figure 33.

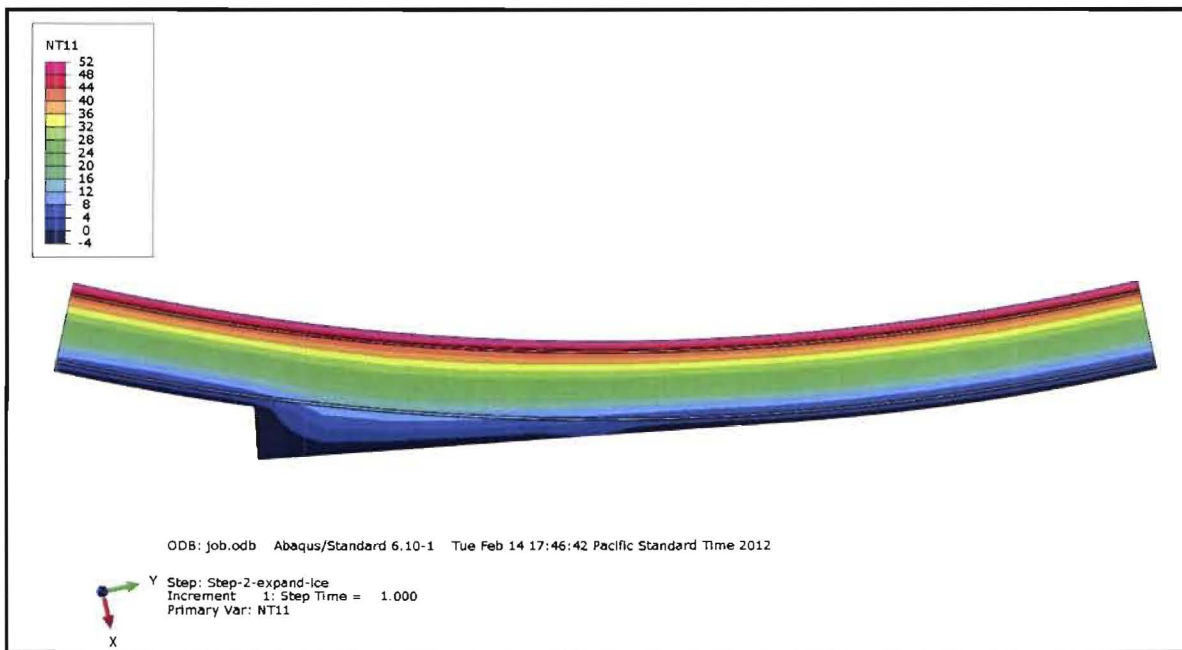


Figure 32: Temperature (°F) during the Blizzard of 1978

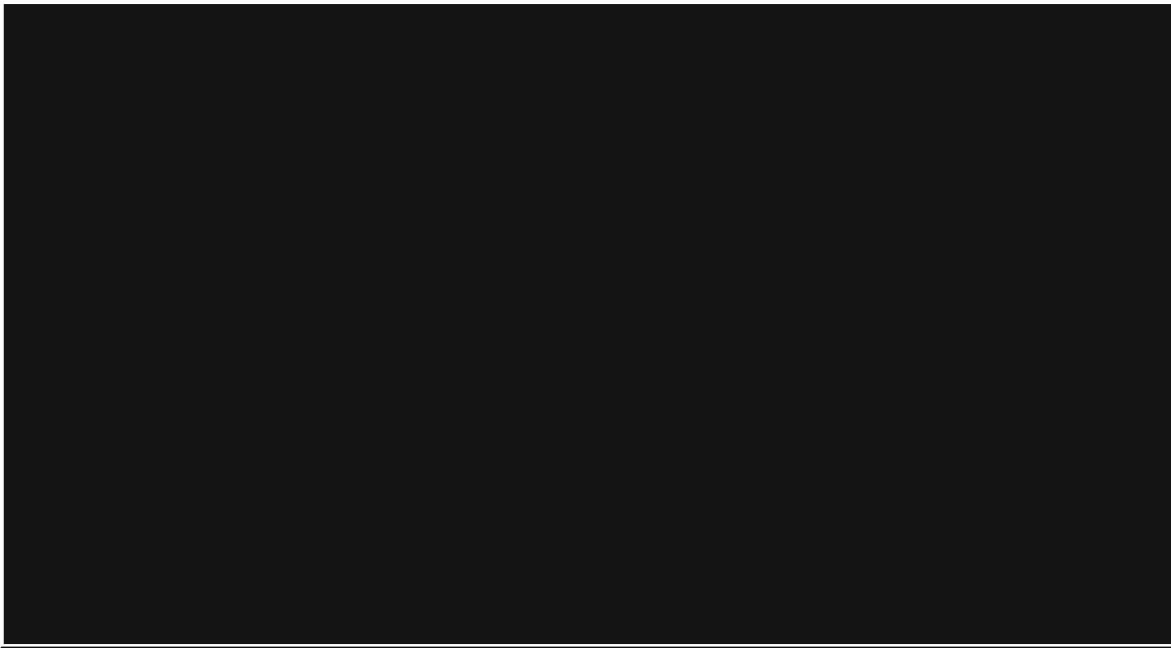


Figure 33: [REDACTED] during the 1978 Blizzard

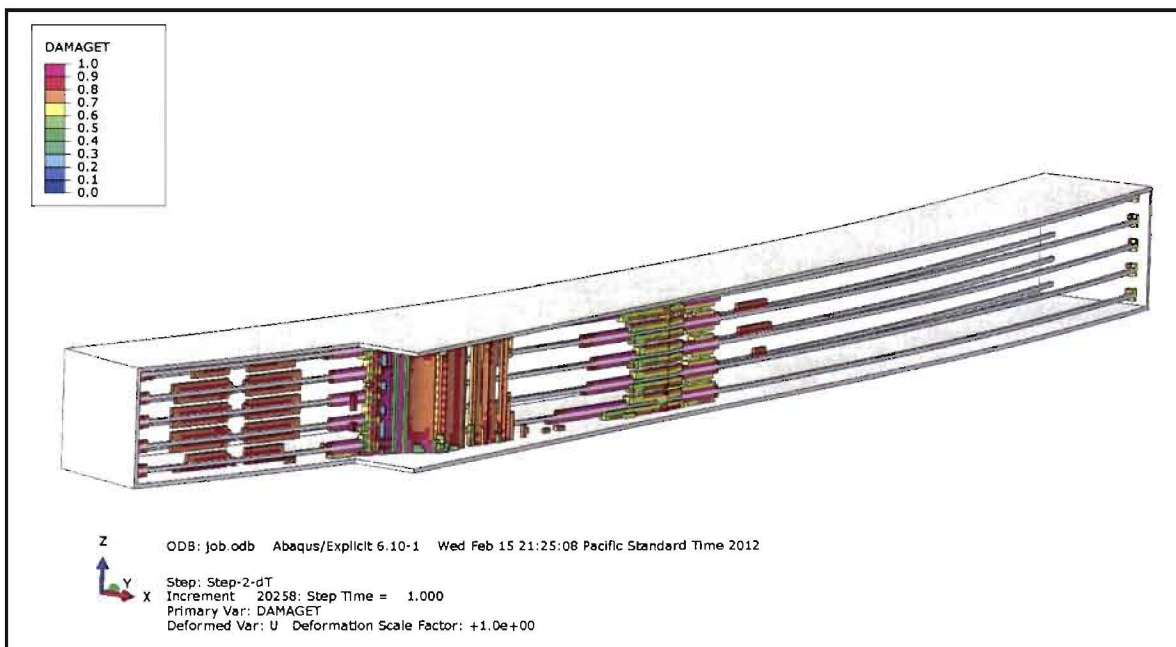


Figure 34: Cracking Result during the 1978 Blizzard showing regions with DAMAGE > 0.7



(b) 1977 Blizzard Condition

The result from the Cracking [REDACTED] due to the 1977 blizzard condition is shown in this section. Figure 35 depicts the temperature distribution in the model. Figure 36 and Figure 37 show the cracking result.

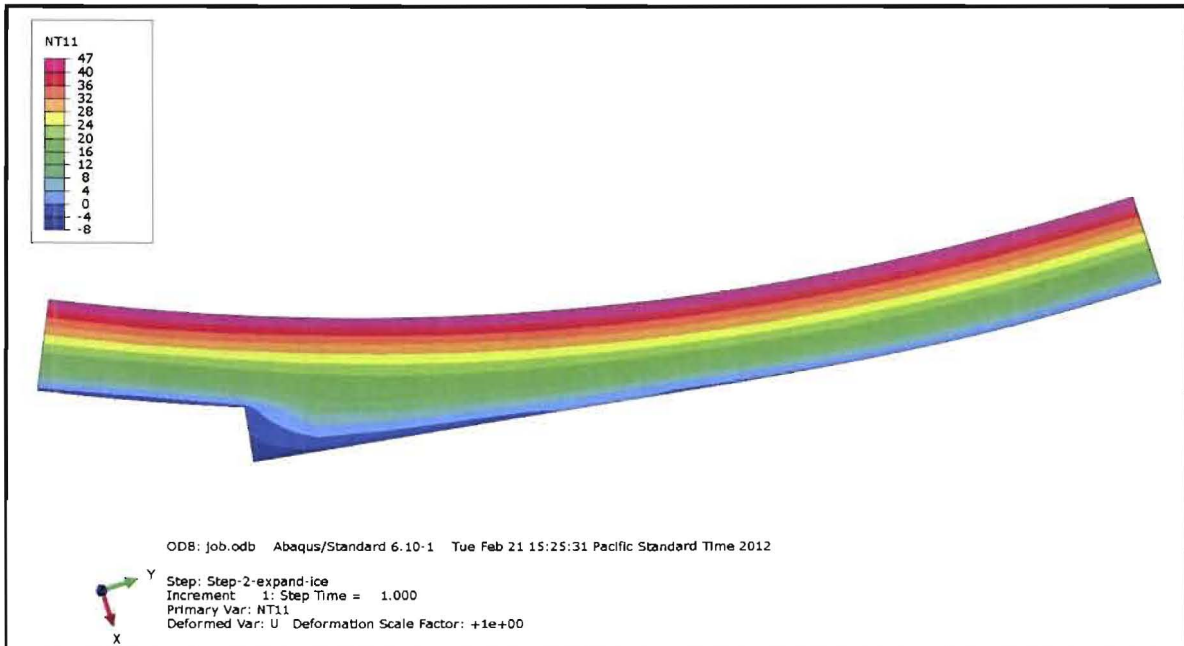


Figure 35: Temperature (°F) during the Blizzard of 1977





Figure 36: [REDACTED] during the Blizzard of 1977

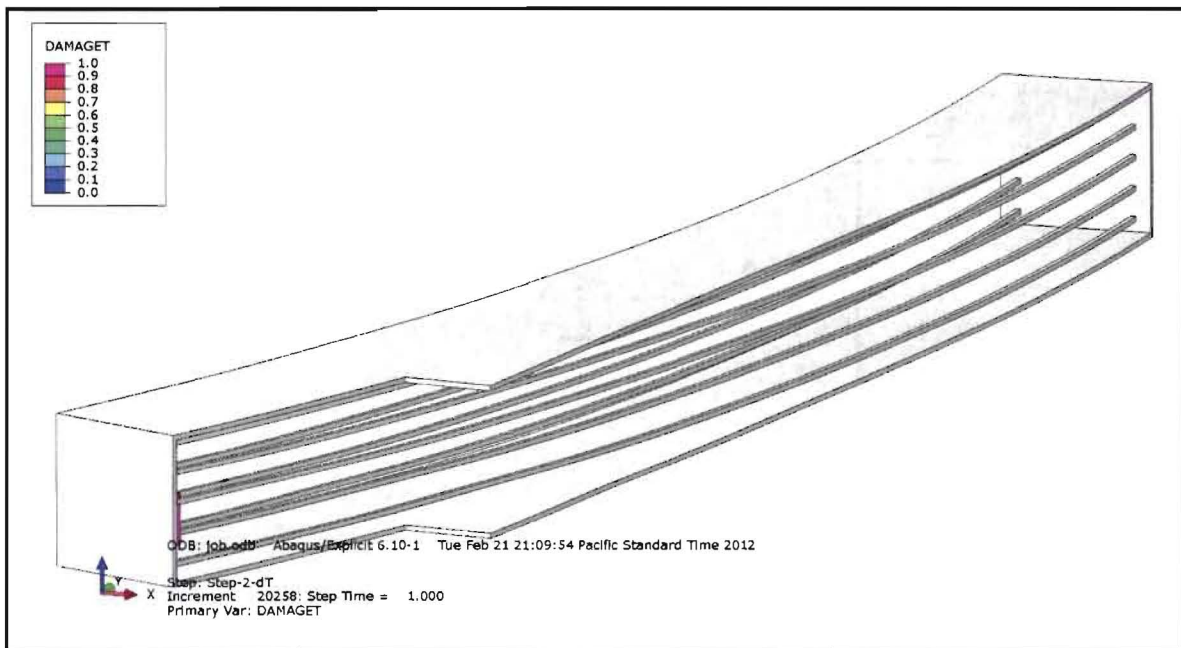


Figure 37: Cracking Result during the 1977 Blizzard showing regions with DAMAGE > 0.7



### Section 11.07 Conclusion

The cracking model results shown in this section can be summarized as follows:

- The blizzard of 1978 scenario results in laminar cracking near the OF rebar mat.
- The blizzard of 1977 shows some damage (microcracking) relatively close to the surface of the shoulders, and significantly less damage compared to the blizzard of 1978.

○



•



Laminar cracks developed most prominently at the OF rebar mat under the thick shoulder regions and not in the thinner sections in the flute and shell.

## XII. Analysis IV: Damage Propagation into Regions with High Rebar Density

### Section 12.01 Background

Expansion of concrete due to freezing of entrapped moisture was studied in the





\_\_\_\_\_ This analysis uses the same CTE discussed in previous sections (Sections 10 & 11).

Section 12.02 \_\_\_\_\_

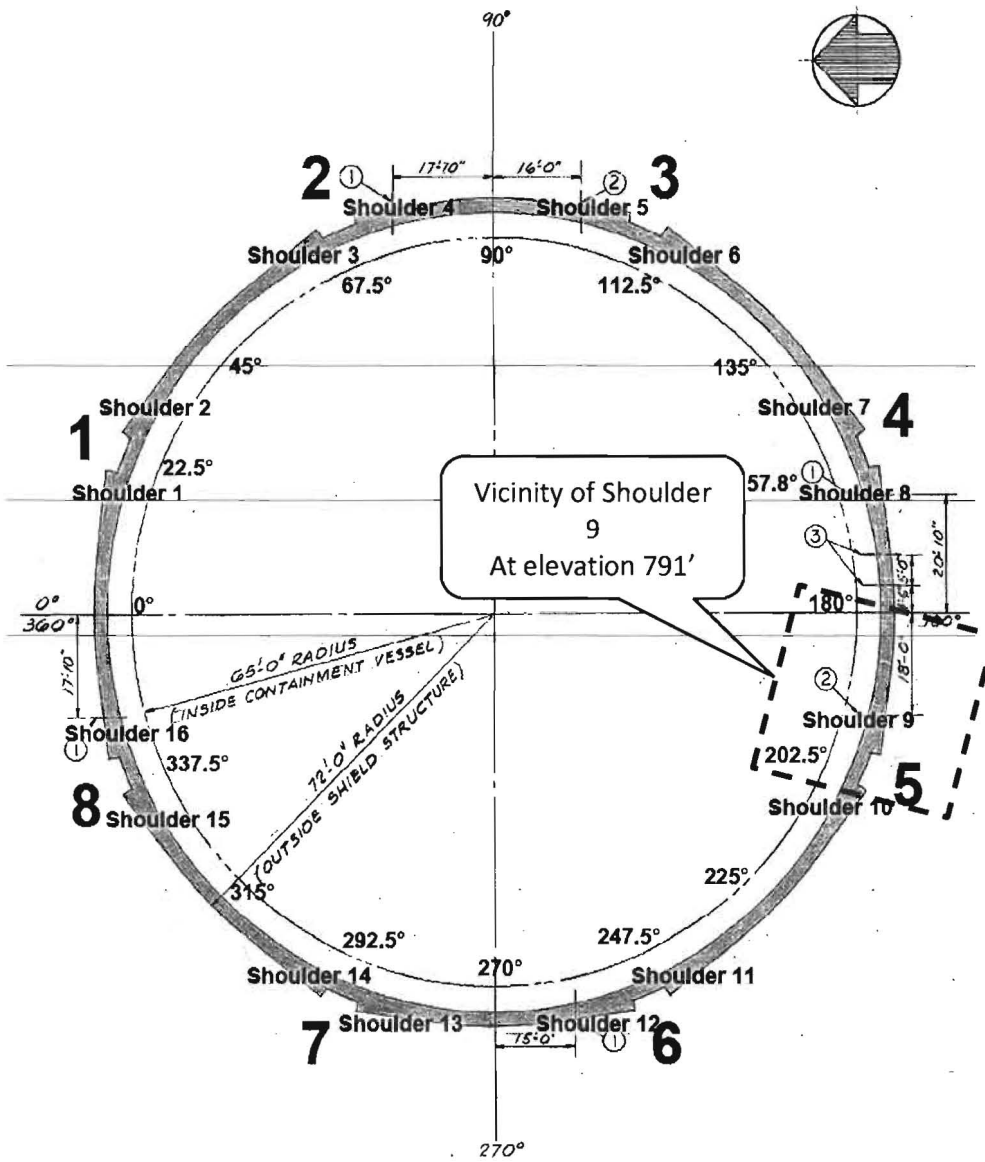
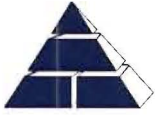


Figure 38: Shield Building with Flute Numbers and \_\_\_\_\_



### *Section 12.03 Circumferential Temperature Distribution at O.F. Rebar*

The temperature distribution in the [REDACTED] here were calculated in separate heat transfer analysis and [REDACTED] (See Exhibit 65) The temperature profiles around the Shield Building at the outer face horizontal rebar are shown in Figure 28. The models presented here use the worst case temperatures calculated for the 1978 blizzard with an offset of +20°F to simulate nominal temperatures. In this case, nominal temperatures will produce the most expansion and therefore the worst case stress condition for the building. The +20°F offset brings the 1978 temperature gradients into rough equivalence with the lowest recorded ground temperatures during the 1978 blizzard (see Exhibit 66), which would be the expected low temperature condition assuming heavy cloud cover rather than a clear night sky (see Exhibit 65).

### *Section 12.04 Discussion*

The result from the [REDACTED] is used to make predictions about the delamination propensity due to blizzard conditions, given the assumptions of the model.



The damage that results from any tensile stress above the strength of the concrete depends on the 3D stress state as well as the strain energy available to open the crack. Low strain energy results in microcracks and high strain energy results in a structural crack.



## Section 12.05

The results shown in this section can be summarized as follows:

- The locations of the cracking remain confined to the observed crack locations at the OF rebar mat, both under the thick sections of the shoulders and in locations where the horizontal rebar is spaced on 6" centers.
  - The model in the top 20' of the walls shows some damage in the flute valley, which is in line with observation.
  - The model near the Aux building roof shows less damage in the flute valley, which is also in line with observation.
- Overall, the results show good agreement with observed cracking in the areas studied.

### (a) Top 20' of the Wall Location

The results at the top 20' location, perturbed by the 1978 blizzard are shown in Figure 39 and Figure 40. The 20°F offset temperature contours can be seen in Figure 39 and the cracking results are shown in Figure 40.

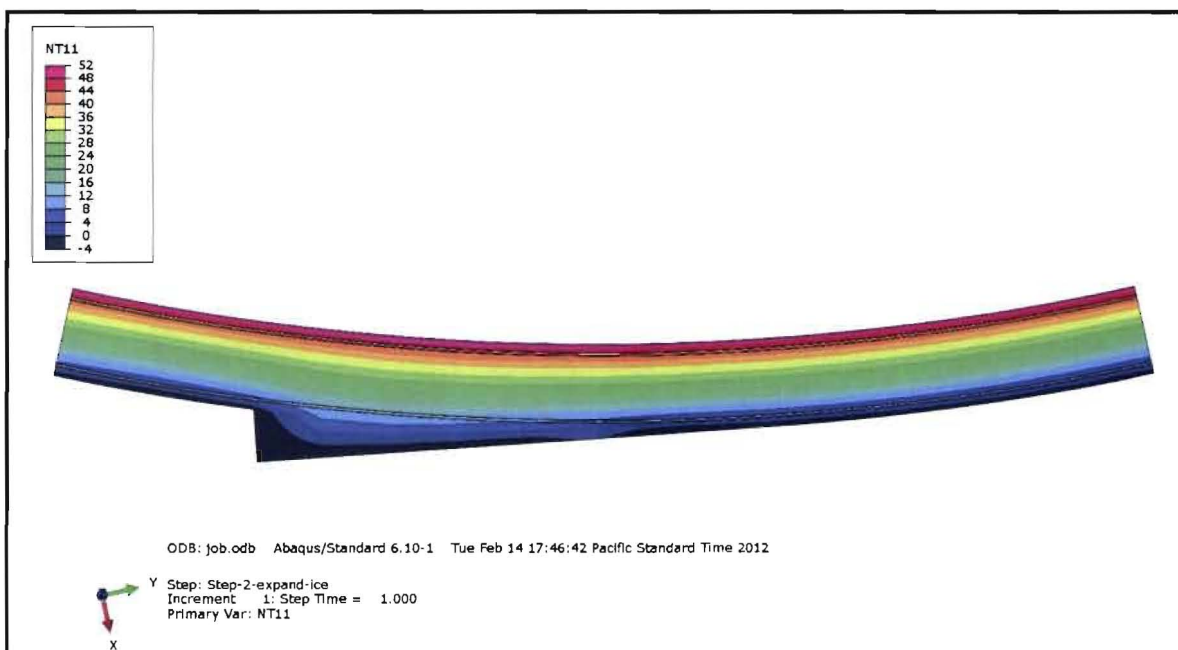


Figure 39: Temperature Contours (°F) in the Top 20' of the Wall

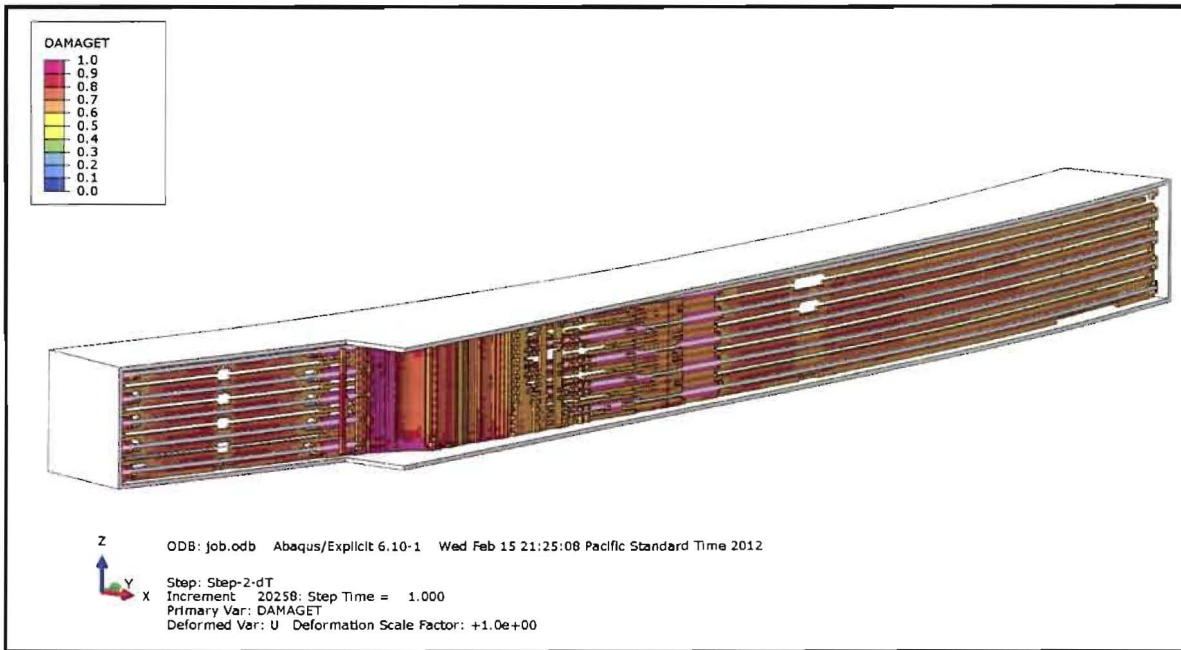


Figure 40: Cracking Result in Top 20' of the Wall showing regions with DAMAGE > 0.6

### (b) Steam Line Location

The results at the steam line location, perturbed by the 1978 blizzard are shown in Figure 41 and Figure 42. The 20°F offset temperature contours are in Figure 41 and the cracking results are shown in Figure 42.

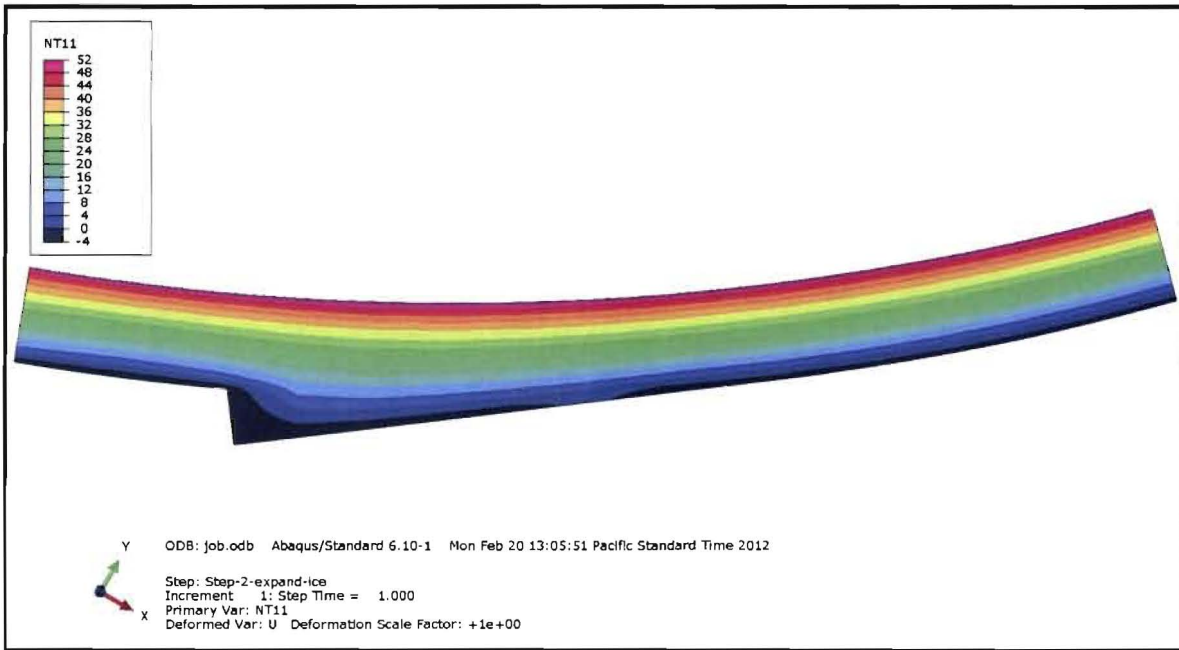


Figure 41: Temperature Contours (°F) at Steam Line

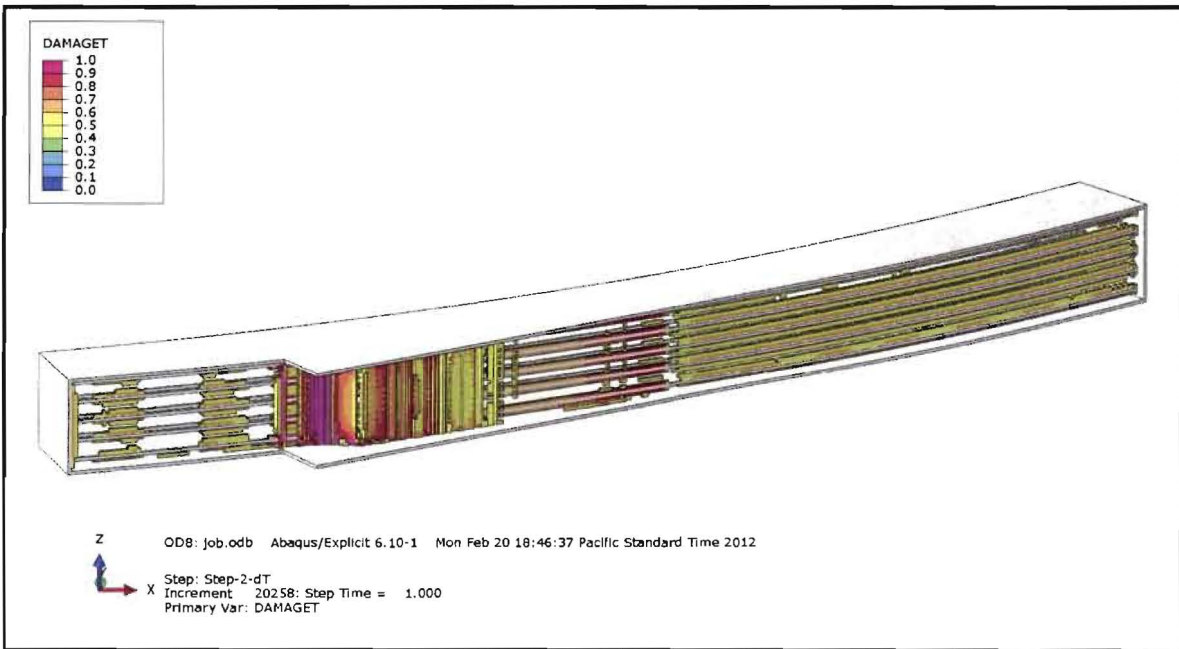


Figure 42: Steam Line Area Cracking Result showing regions with DAMAGE > 0.6



### XIII. Analysis V: Investigation for Potential Laminar Cracking under Various Temperature Conditions

As previously discussed, numerous finite element analyses models were developed to examine the behavior of the DBSB under the extreme conditions of the 1978 Toledo Blizzard. The same aggressive scientific analysis was also employed for several additional weather conditions to which the DBSB is exposed. As stated earlier, the analysis exhibits attached to this report may be reviewed for an in-depth scientific understanding of the analyses performed and corresponding results. The highlights from these analyses will be discussed in what follows.



#### *Section 13.01 Thermal Stress Screening*

In order to understand the effect of the various thermal conditions that the containment structure may be subjected to, a screening analysis was performed. The screening analysis was performed using preliminary material properties before the official material properties were obtained.

The screening analysis considered a total of 32 thermal conditions. [redacted] summer and winter [redacted] the spring and [redacted] windy and calm [redacted] as well as average and hot/cold ambient temperatures. Table 4 [redacted]



[redacted] In many instances several locations were analyzed to find the location of the highest radial stress. [redacted]



In order to understand the relative effect of the 32 different thermal conditions the gravity and wind load was excluded from the screening analysis. The six thermal conditions resulting in the highest radial stress in the screening analysis is analyzed with gravity and wind pressure loads in the next section.





Table 4:  
is Incl

[Redacted]

[Redacted]



*Section 13.02 Combination Load Cases*

The result of the screening analysis identified the thermal conditions most likely resulting in the highest radial stress. [REDACTED]

[REDACTED] These combination load cases were again solved with the preliminary material properties since the official values had not yet been obtained.

[REDACTED]

Table 5: [REDACTED]  
St [REDACTED]

[REDACTED]



### Section 13.03 Analysis Based on Measured Properties

The six cases predicted to result in the maximum radial stress is analyzed using measured material properties from samples taken from the Davis-Besse containment structure. The material properties used for the analysis are summarized in a separate section in the Root Cause Analysis Report (Exhibit 56, Figure 2.1.4: Material Properties for Davis-Besse [REDACTED]).

The conditions analyzed using the measured material properties are the same six conditions presented in Table 5. They are listed below along with the time of day determined to produce the highest radial stress. The time of day was determined using a [REDACTED] which is detailed in Exhibit 56 – [REDACTED] are

[REDACTED]

- [REDACTED]
- [REDACTED]
- [REDACTED]
- [REDACTED]
- [REDACTED]
- [REDACTED]

#### (a) Circumferential Temperature Distribution at O.F. Horizontal Rebar

The temperature profiles for the six conditions resulting in the highest radial stress based on the screening analysis are shown in Figure 7. The temperature profiles are plotted in the circumferential direction around the shield building at the outer face horizontal rebar depth.

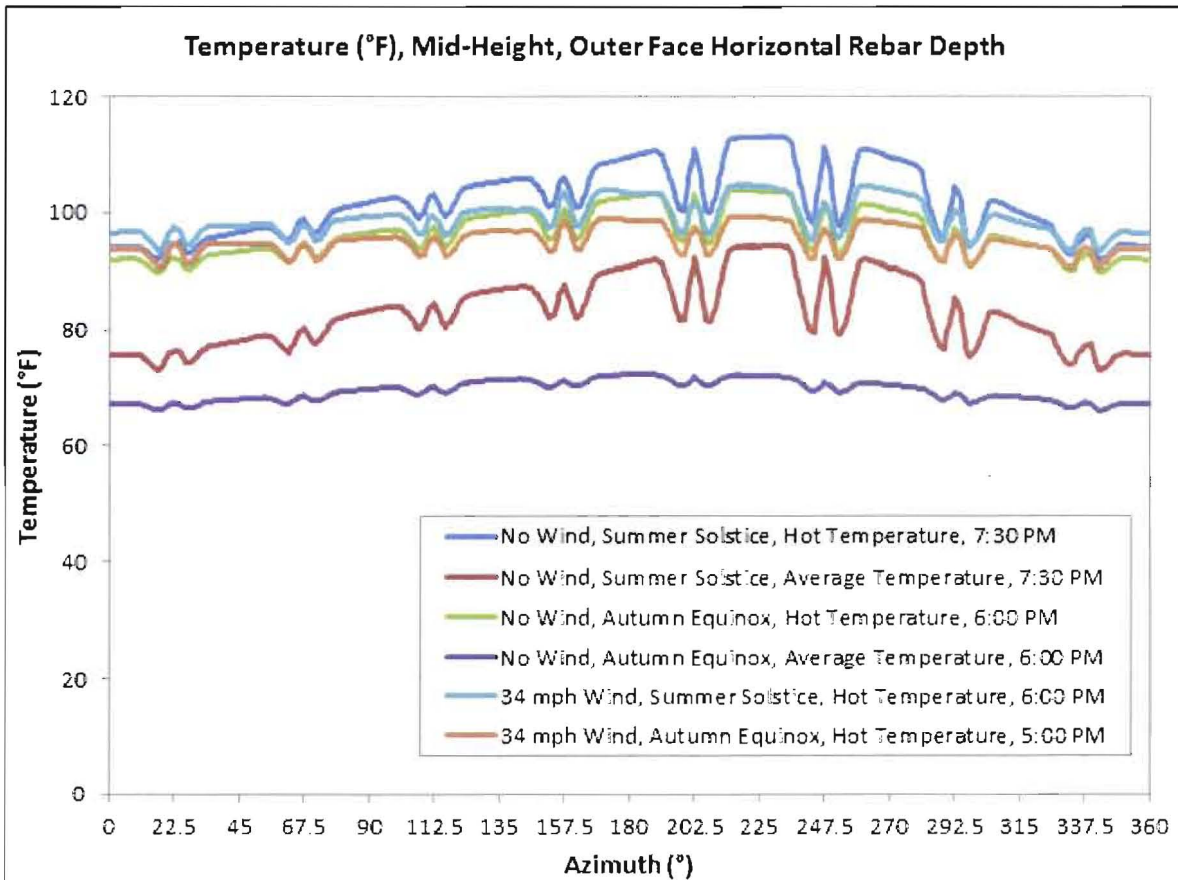


**Figure 43: Circumferential Temperature Distribution at O.F. Horizontal Rebar**

For each of the six temperature profiles shown in Figure 43 eight set of double valleys can be seen. The valleys represent the lower temperature under the thick sections of the shoulders. These areas are covered by thicker layer of concrete so it takes longer for them to heat up due to the hot exterior conditions. Figure 43 also shows that the azimuth 225° location corresponds to the hottest location around the structure. The condition resulting in the hottest temperature at the outer face horizontal rebar depth is labeled “No Wind, Summer Solstice, Hot Temperature, 7:30 PM.” This is the temperature condition studied in detail [REDACTED] following sections.



(b) [REDACTED] Locations

The [REDACTED] The south to south-west side has the highest thermal gradient do to the solar heating during the day. The Flute/Shoulder [REDACTED] in Shoulder 10 and the [REDACTED] in the middle of the panel at azimuth 225. Again, Figure 44 shows the location of the flutes, shoulders, and the azimuth convention for the Davis-Besse containment structure.

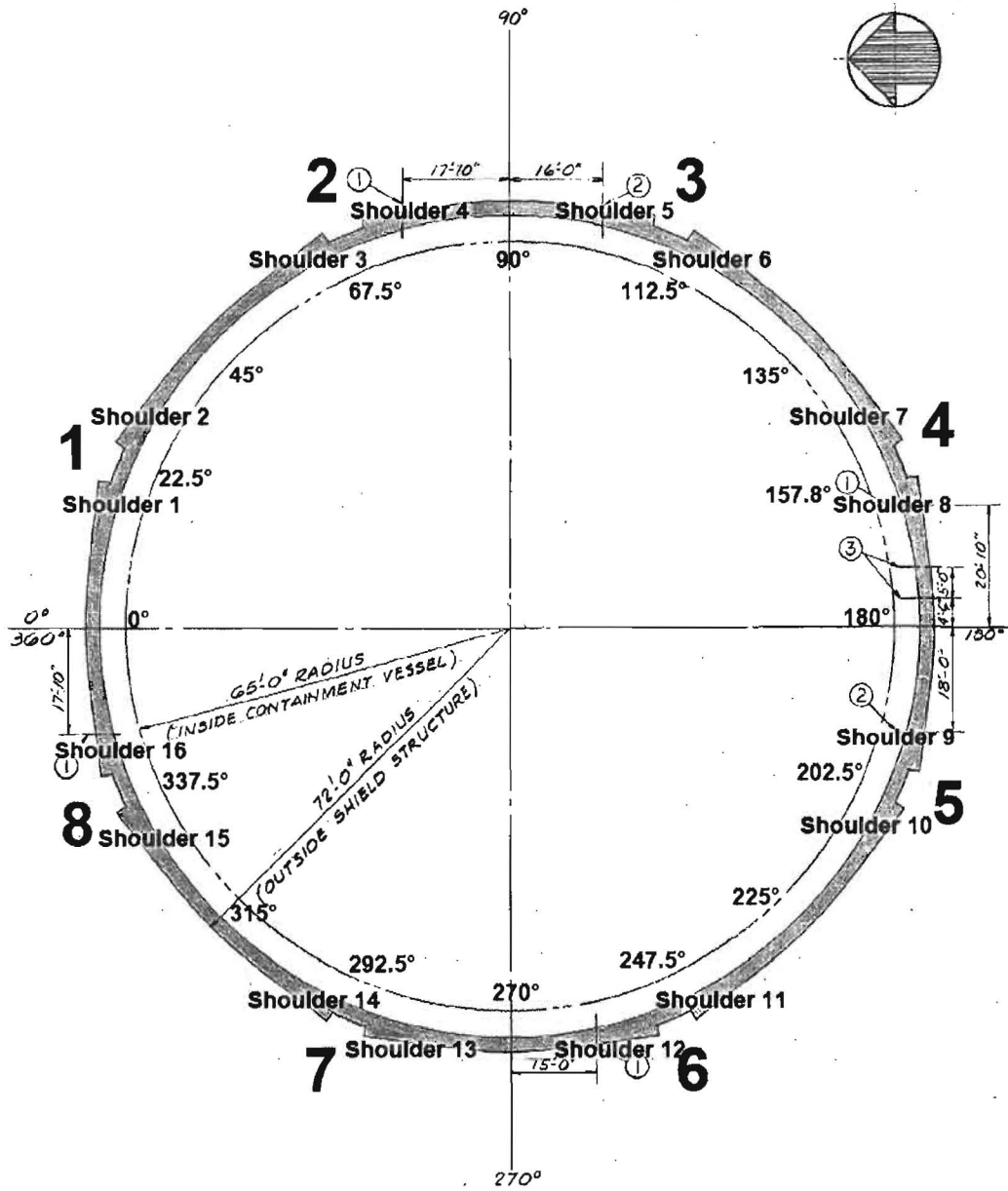
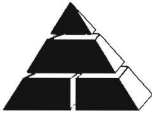


Figure 44: Shield Building Flute Numbers and Azimuth Locations



#### Section 13.04 Stress State during Hot Summer Condition

The results shown in this section describes the detailed stress state in the hottest location around the structure for the hot summer condition (No Wind, Summer Solstice, Hot Temperature, 7:30 PM)

Figure 45 through Figure 49 show the results from the shoulder 10 location using the [REDACTED] Figure 50 through Figure 54 depict the same results from the azimuth 225° location using the [REDACTED]

For each of the two locations the result is presented in five figures. The first figure shows the temperature distribution and the following four figures depict the stress state:

1. Temperature Distribution
2. Max Principal Stress
3. Radial Stress
4. Circumferential (Hoop) Stress
5. Vertical Stress

The stress state is presented at the mid-height section of [REDACTED] [REDACTED] The contour range is set to +/- 300 psi for all the stress figures so that they can be compared more easily.

##### (a) Stress Analysis Results Summary

The maximum stress in the [REDACTED] is confined to the top and bottom of the outer face horizontal rebar. The maximum tensile stress is about 300 psi and not enough to crack the concrete.



(b) Shoulder 10 Location

The temperature distribution, max principal stress, radial stress, hoop stress, and vertical stress in shoulder 10 are depicted in Figure 45 through Figure 49, respectively. Figure 45 shows that the shoulder surface is hotter than the flute surface. This is the result of more solar exposure on the shoulder surface compare to the flute valley. Also, there is more surface area at the corner of the shoulder resulting in higher temperature during the hot ambient condition.

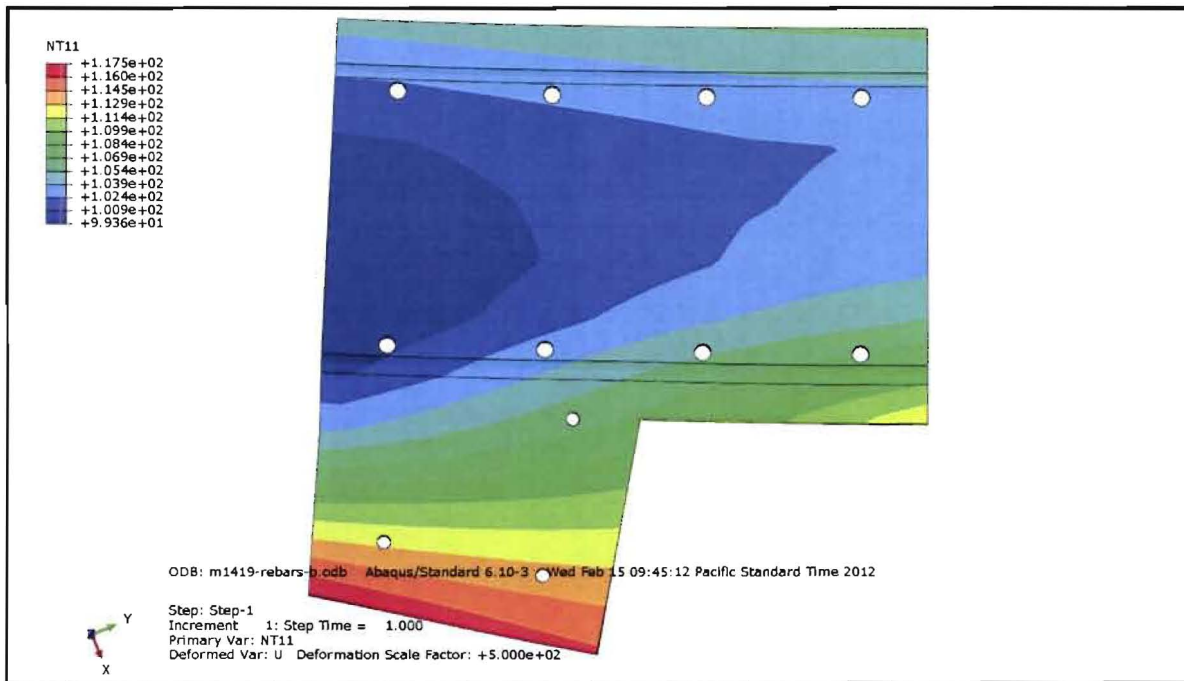


Figure 45: Temperature Distribution (°F) in Shoulder 10 Location

Figure 46 through Figure 49 depict the stress state using the max principal stress and the three stress components in a cylindrical coordinate system located at the containment structure center. The max principal and radial stresses are highest at the outer face horizontal rebar. The figures







Comparing the stress in the three radial, hoop, and vertical directions (Figure 47 through Figure 49 respectively) indicates that the radial component has the highest tensile stress. As shown in Figure 47, the radial tensile stress is below 300 psi which is less than the tensile strength of the concrete. It is concluded that the hot summer temperature condition is not capable of delaminating the structure in the flute/shoulder location.



Figure 46: Max Principal Stress (psi) in the [redacted] laced in the Shoulder 10 Location

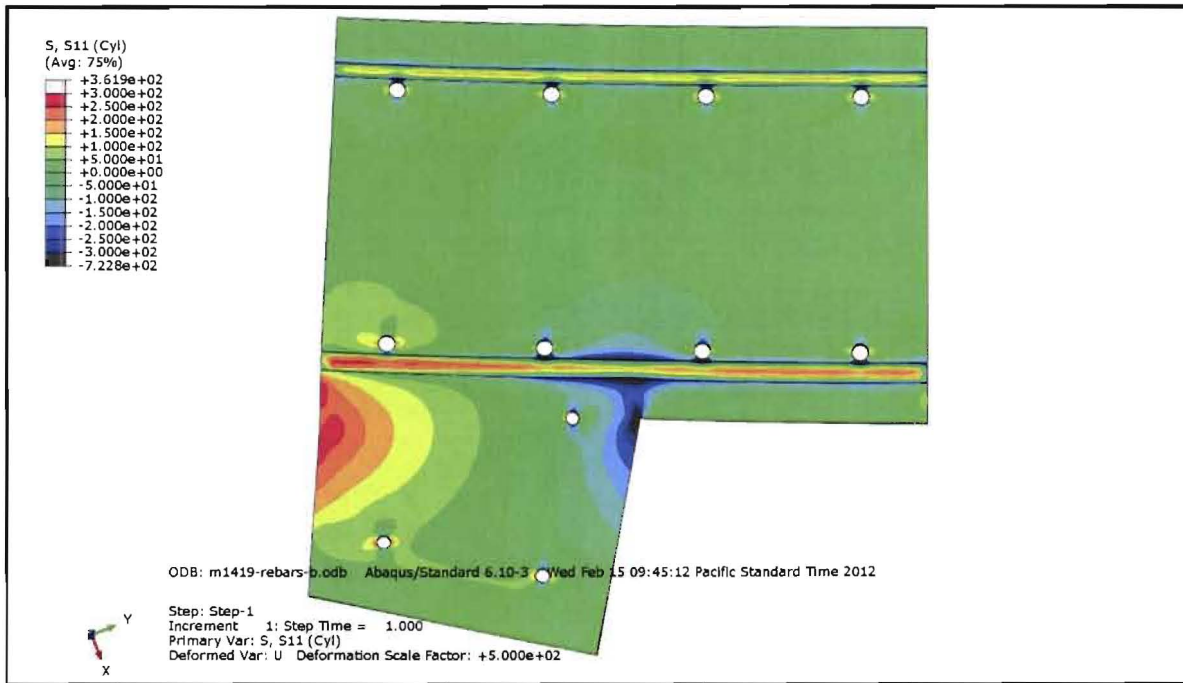
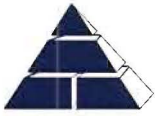


Figure 47: Radial Stress (psi) in the [redacted] laced in the Shoulder 10 Location



Figure 48: Hoop Stress (psi) in the [REDACTED] placed in the Shoulder 10 Location

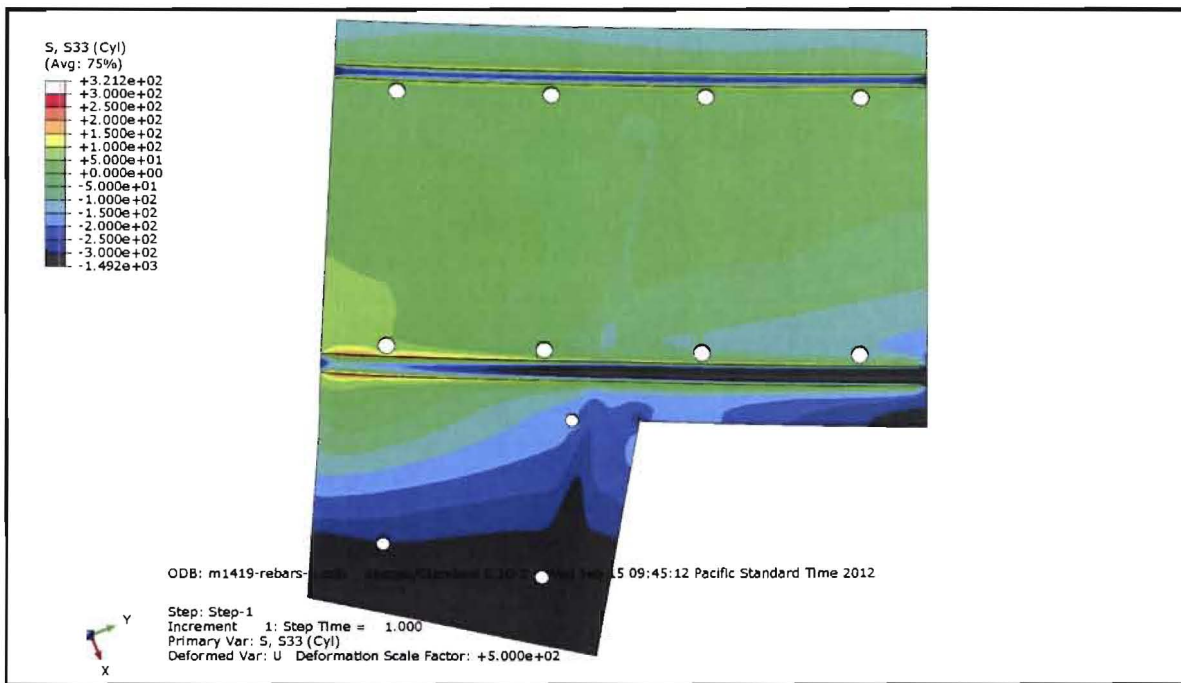


Figure 49: Vertical Stress (psi) in the [redacted] placed in the Shoulder 10 Location

(c) Azimuth 225° Location ([redacted])

The temperature distribution, max principal stress, radial stress, hoop stress, and vertical stress in the shell area at azimuth 225° are shown in Figure 50 through Figure 54, respectively. Figure 50 shows that the exterior surface is hotter than the interior. This is the result of the hot ambient daytime condition and the colder nighttime condition.

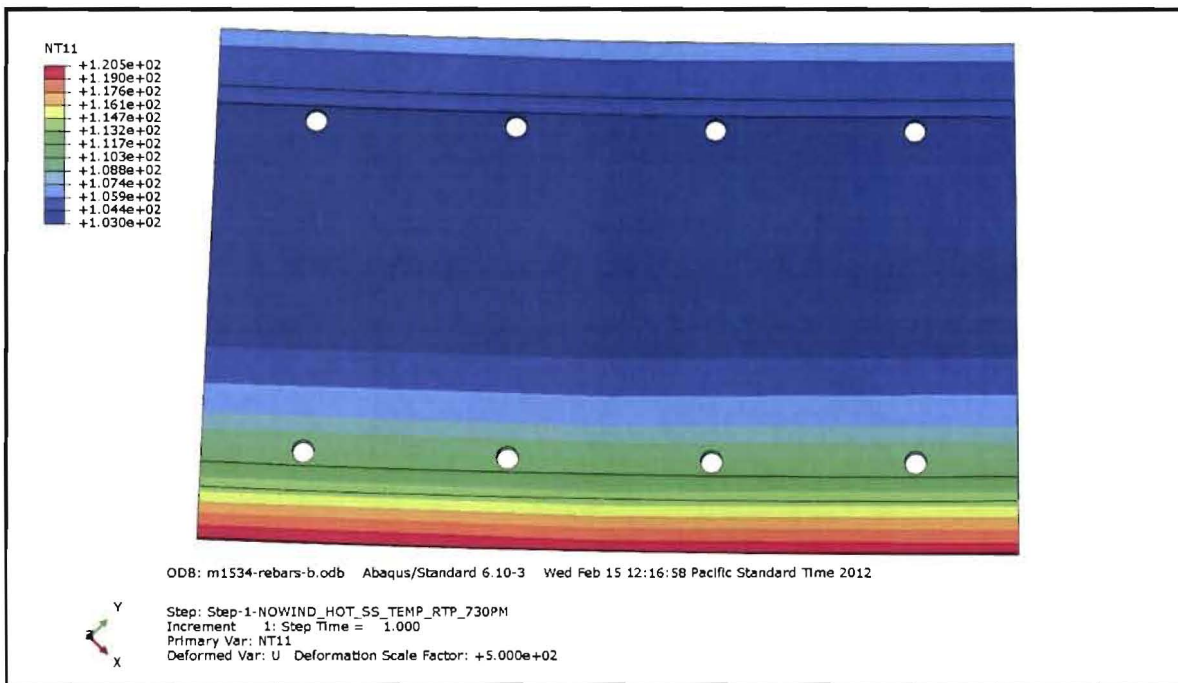


Figure 50: Temperature Distribution (°F) in the [redacted] placed at the Azimuth 225° Location

Figure 51 through Figure 54 depict the stress state using the max principal stress and the three stress components in a cylindrical coordinate system located at the containment structure center. The max principal and radial stresses are highest at the outer face horizontal rebar depth (see Figure 51 and Figure 52). Comparing the stress in the radial, hoop, and vertical directions (Figure 52 through Figure 54, respectively) indicates that the radial component has the highest tensile stress. As shown in Figure 52, the radial stress is below 300 psi which is less than the strength of the concrete. It is concluded that the hot summer temperature condition is not capable of delaminating the structure in the shell section location (middle of a panel). Furthermore, Figure 53 and Figure 54 show that the hotter exterior surface temperature results in compression stresses in both the hoop and vertical directions due to expansion of the outer layer.

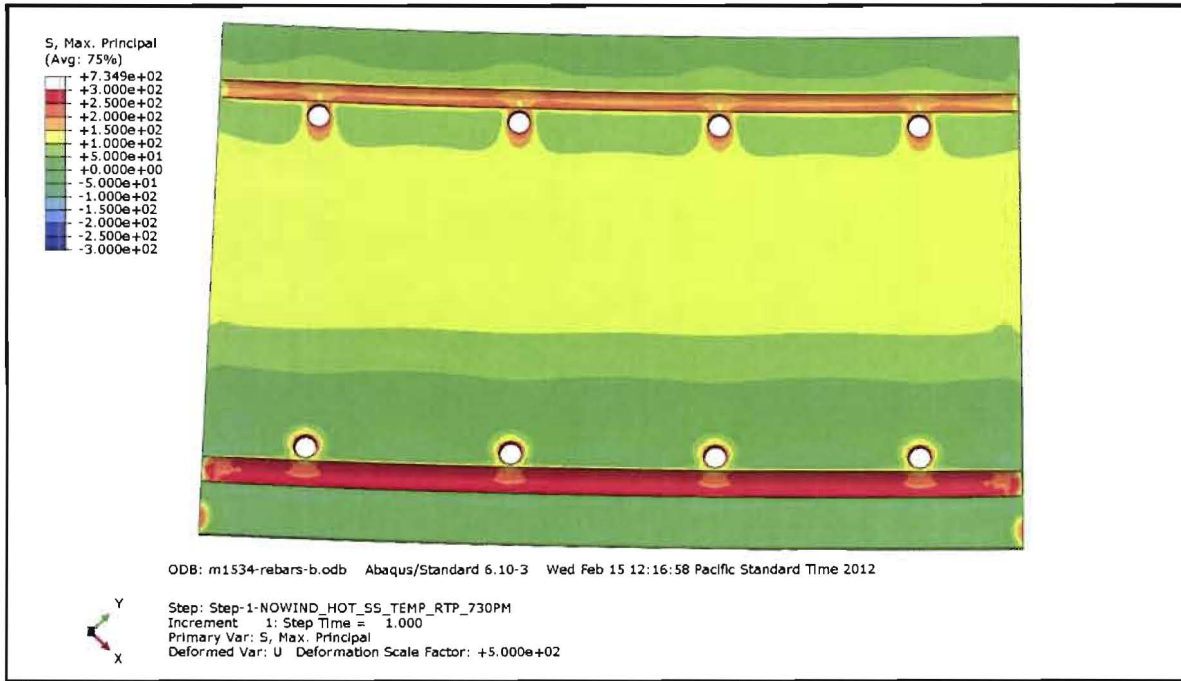


Figure 51: Max Principal Stress (psi) in the [redacted] placed at the Azimuth 225° Location

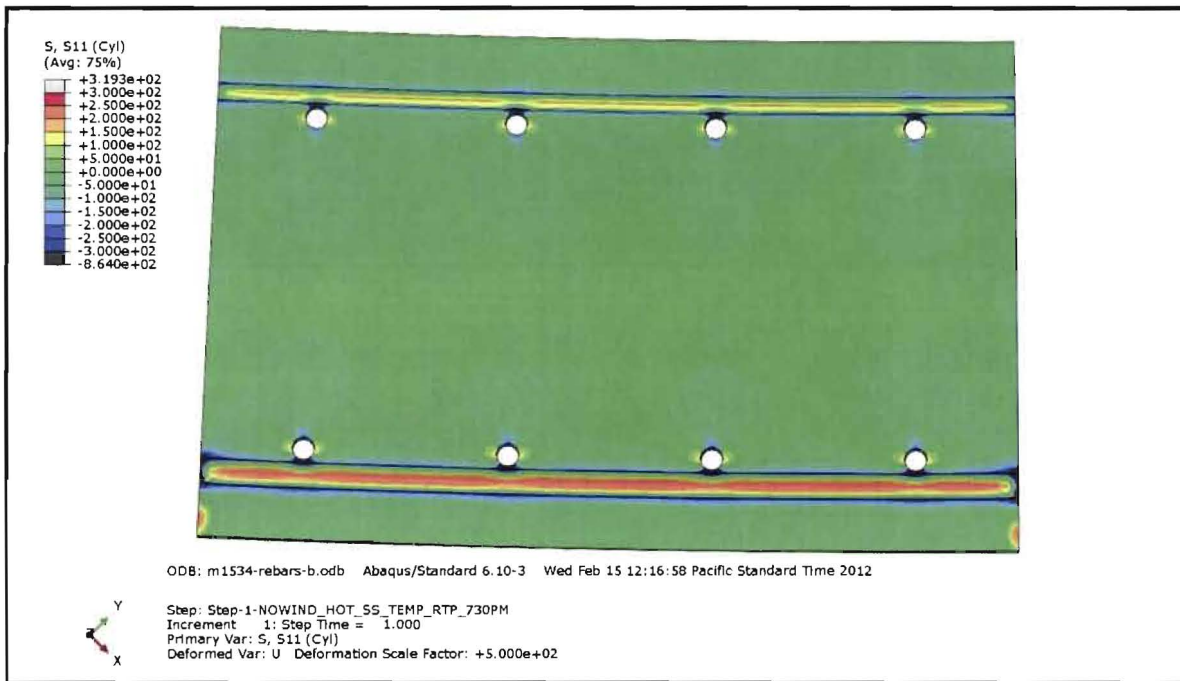


Figure 52: Radial Stress (psi) in the [REDACTED] placed at the Azimuth 225°  
Location

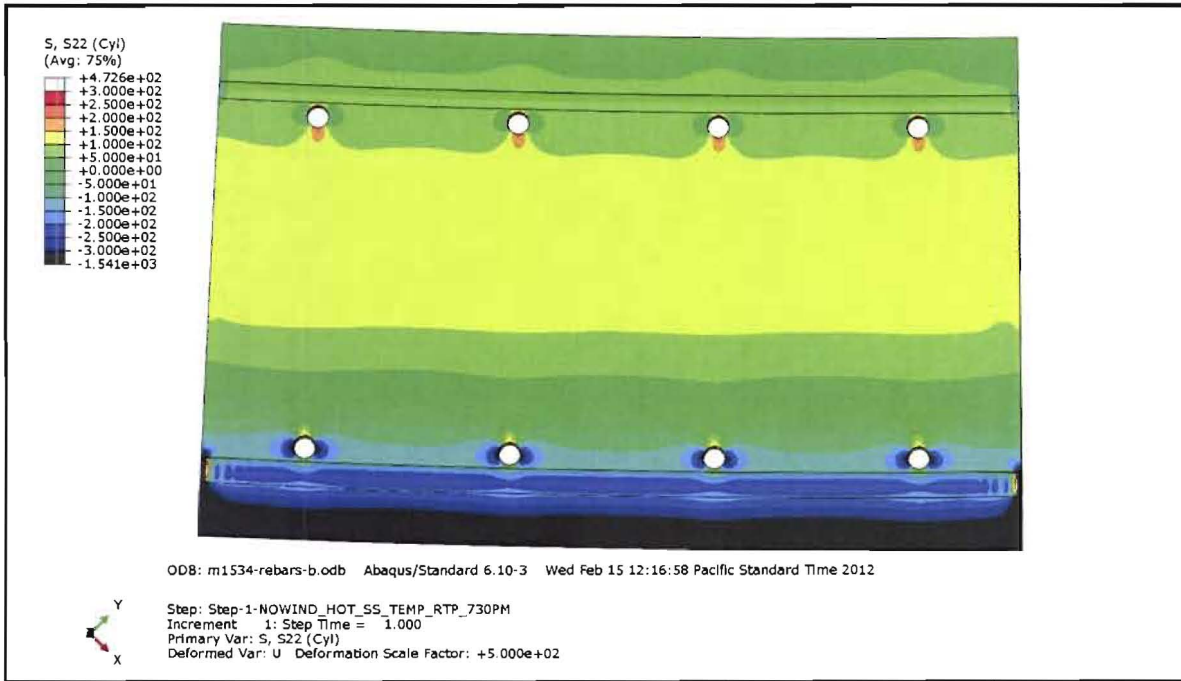


Figure 53: Hoop Stress (psi) in the [REDACTED] placed at the Azimuth 225° Location



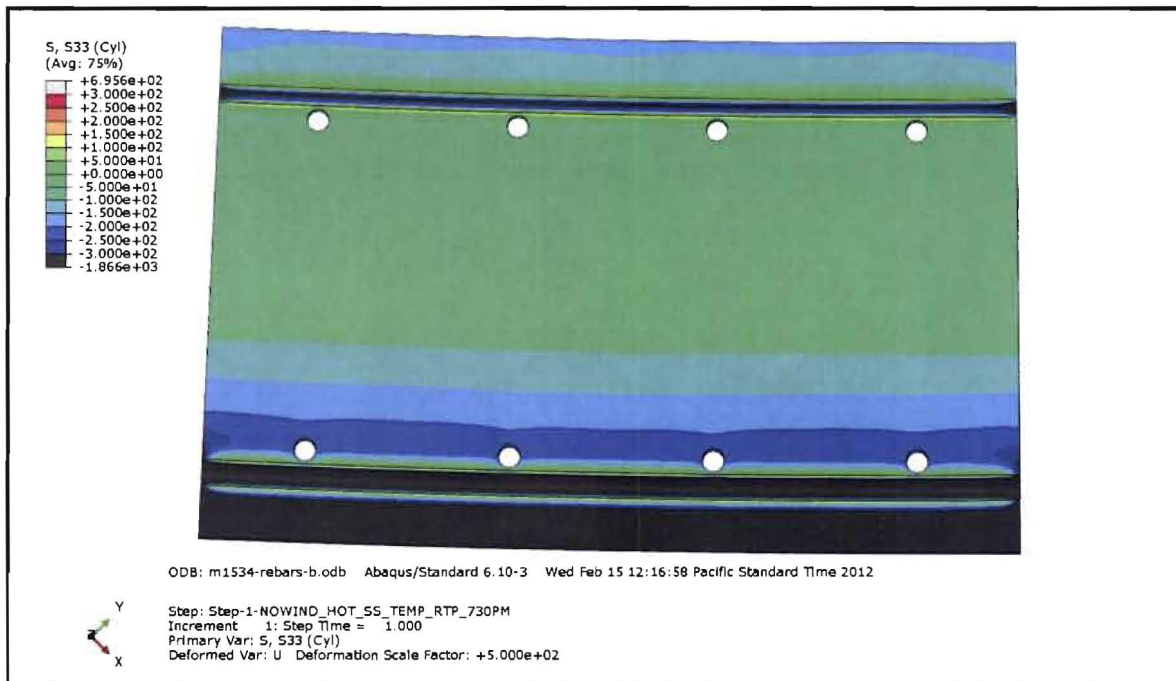


Figure 54: Vertical Stress (psi) in the [REDACTED] placed at the Azimuth 225°

### Section 13.05 Conclusion

The results of the analysis presented in this report can be summarized as follows:

- The temperature and wind conditions found to maximize the radial stress are not sufficient to delaminate the structure alone
- Thermally induced radial stresses is maximized at the hot summer temperatures
- At the location of the outer face horizontal rebar, the maximum radial stress due to temperature gradients, gravity, and wind is about 300 psi



#### XIV. Analysis VI: Investigation of Potential Laminar Crack Propagation given current Shield Building Condition

##### Section 14.01 Analysis

A Finite Element Analysis was performed using the NASTRAN 3D Model to investigate the potential for existing-crack propagation. The NASTRAN 3D Model idealized a 30 ft. by 30 ft. cracked section of the DBSB centered with respect to the southwest flute (Flute Number 6). Figure 55 shows an illustration of the NASTRAN idealization and Figure 56 shows a detailed region of the flute and shoulder highlighting the difference in stresses due to the existing crack.

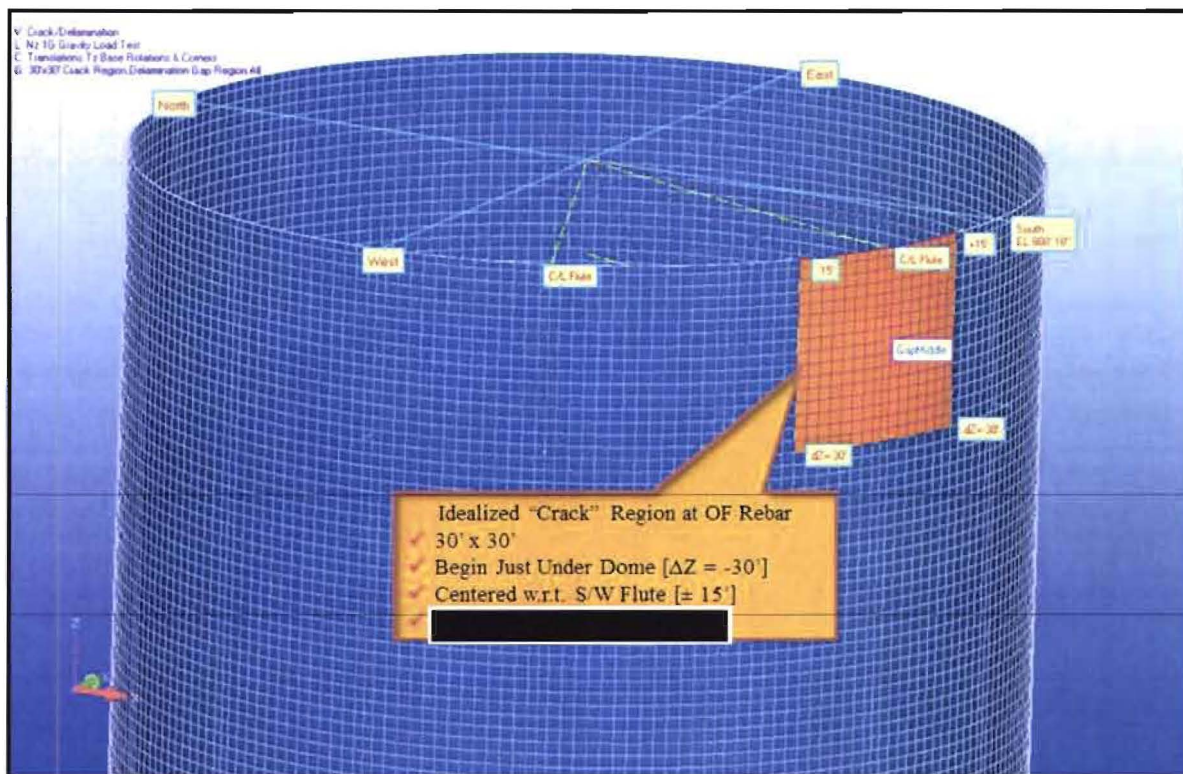


Figure 55: "Thin-Crack" region introduced as idealized the "Cracked" boundary at the OF Rebar

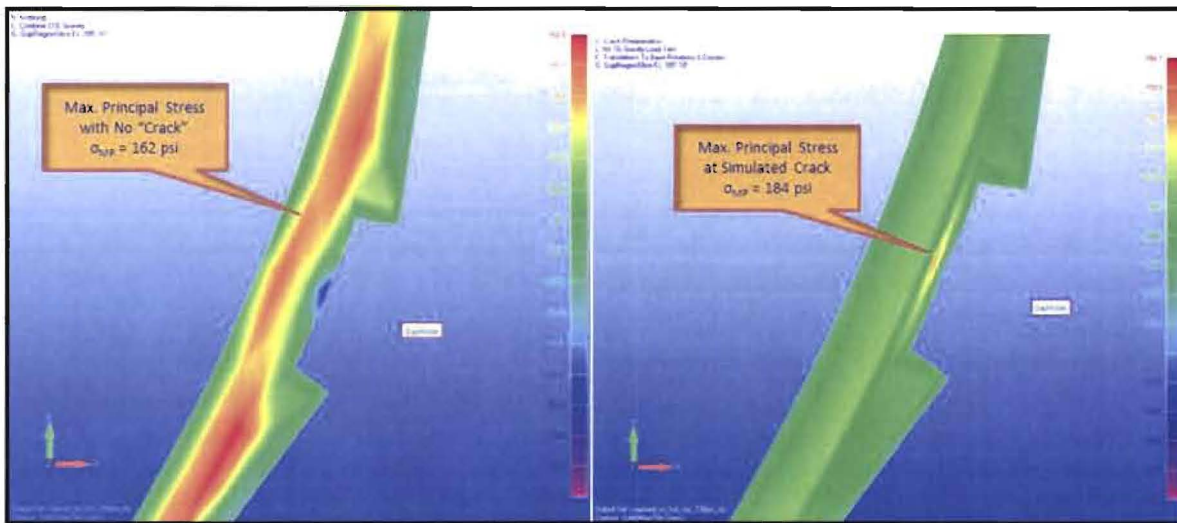


Figure 56: Summer Solstice Hot No Wind 7:30 pm, Constant Concrete CTE =  $5.20 \times 10^{-6}$  in/in/°F

#### Section 14.02 Conclusion

As summarized in Table 6 the magnitude of maximum principal stresses increased a slight amount from  $\sigma_{MP} = 162$  psi (No crack) to  $\sigma_{MP} = 184$  psi (w/crack). There is only a marginal increase in the magnitude of radial stress, from  $\sigma_R = 76$  psi (No crack) to  $\sigma_R = 92$  psi (w/crack).

Table 6: Summer Solstice with Simulated 30'x30' "Crack" - Summary Results for Radial Stress @ EL 785' 10"  
(+ = Tension, - = Compression)

ID	Case Description	2D Nastran Plane-Strain	3D Nastran	Peak Stress Values at "Crack"
		Time Slice Peak Stress	Radial Stress	
9	Summer Solstice Hot No Wind;	7:30 PM	+ 76 psi	+ 162 psi
10	Summer Solstice Hot No Wind; Crack	7:30 PM	+ 92 psi	+ 184 psi

Therefore it is not believed that the increased magnitudes in either the radial or maximum principal stresses are sufficient to propagate cracks that may have formed under normal thermal and environmental conditions, such as winter and summer.

The stress concentrations, mode I and mode II stresses are calculated by the solver in the cracking models.



The PII proprietary modeling techniques have been validated in thick-walled reinforced concrete silos. PII has the only modeling technology that has successfully predicted the cracking at Crystal River 3, including the SGR opening delamination, the detensioning cracks, and the retensioning cracks. No other modeling technology has been more validated for this purpose.

## XV. Root Cause and Contributing Causes

As stated in the beginning of this report, a root cause must possess the following two characteristics to be considered valid: 1) It can be eliminated to prevent recurrence and 2) It is under the control of management.

As supported by thermal and stress analysis as well as laboratory tests and examination, the common factor for all unrefuted failure modes is moisture intrusion under severe blizzard conditions. Therefore, the most likely root cause of the laminar cracking observed in the Davis-Besse Shield Building is the *inadequate sealing of the building surface to prevent moisture intrusion during a severe blizzard.*

The other two contributing factors that, considered alone do not qualify as a root cause, are 1) the structural design of the shoulders and 2) dense spacing of the outer horizontal rebar mat in some areas of the building. Given severe blizzard conditions that allow for significant moisture penetration and subsequent internal ice formation, these two contributing factors intensify radial stresses to the point of structural damage.

This most-likely failure scenario, which is able to explain all the general characteristics of the cracking pattern states that, during a blizzard which is preceded by a rain storm, the rain/snow diffuses into the structure due to the surface static pressure produced by high velocity winds. The moisture content of the concrete may increase to a level of 90% or greater during this process. Moreover, because the wind direction near the Davis-Besse Power Plant is more prevalent from the southwest direction, the moisture level in the southwest side of the concrete will be higher than the northeast side of the concrete. The high winds associated with the blizzard are also a significant contributor as it increases the heat loss on the concrete surface. Note that during a



typical blizzard, the exact wind direction may change from time to time due to the swirling action of the wind.

As the environmental temperature drops during the blizzard, the temperature of the concrete also drops, with the outside surface having a lower temperature than areas deep into the concrete.

When the concrete temperature reaches 23 °F or below, the moisture in the concrete starts going through the crystallization process and eventually forms into ice. The volume expansion of ice makes the volume of concrete greater near the surface of the Shield Building, thus producing large radial stresses.

Due to the discontinuity of the shoulder and shell interface of the Shield Building, the radial stresses are the highest near the outer rebar mat and near the areas of the thicker portion of the shoulders. In addition, the radial stresses are higher in the outer rebar mat where there is a higher density of horizontal or vertical rebar.

Radial stresses are significant enough to initiate laminar cracks when the concrete has high moisture content with very cold temperatures. Cracks will propagate in the areas where the concrete tensile strengths are lower than the radial stresses and will stop when the radial stresses redistribute themselves in the process of crack propagation or the crack propagates into a high material strength area.

The necessary conditions for this laminar cracking event are listed as follows:

1. The exposed unsealed concrete surface of the Shield Building allows moisture penetration.
2. A significant amount of water is diffused into the concrete
3. The environmental temperature is well below freezing point of water for a long period of time so that the temperature near the outer mat rebar behind the shoulders (~3-18 inches deep into the Shield Building) will drop below the freezing point of water.
4. The design of flute-shoulders which caused discontinuity in the structure and the lack of radial reinforcing steel in the shoulder areas to resist radial stresses.
5. Tensile strength of the concrete is lower than the radial stresses produced in some areas near the outer rebar mat



The supporting evidence of this most-likely failure scenario is listed below:

- The crack is considered a circumferential laminar crack and not a radial through-thickness directional crack.
- The width of the crack is very tight, generally less than 0.01 inches, indicating the damaging force is highest and concentrated at the fracture surface
- The crack passed through the coarse aggregate, indicating the initiating force is large and not cyclic
- The location of the crack is limited to the outer reinforcing (rebar) mat
- The cracking is prevalent in the flute shoulder areas.
- The crack is also prevalent in the higher reinforcing areas at the top of the Shield Building and along the blockouts for the main steam line room penetrations
- Cracking is more prevalent in the South and Southwest quadrant of the Shield Building
- Cracking is less prevalent between the shoulder areas

Our conclusions and recommendations are based on the limited samples made available to PII and the finite element models developed by PII's best effort, within the four month investigation. Additional samples and further numerical studies will certainly help to resolve more detailed issues (such as the laminar cracking in Shoulder 9), but will not change our conclusions and recommendations.

## XVI. Recommendations to Prevent Recurrence

To prevent recurrence, one or more of the five necessary conditions for the most likely failure scenario has to be prevented. Among the five necessary conditions stated above, the only practical condition is to prevent the moisture intrusion into the concrete prior to and during a



severe blizzard. As such, PII recommends FirstEnergy consider applying a weather-proof concrete sealant to the outside surface of the Shield Building.

The following table summarizes the logic for the corrective action.

**Table 7: Root Cause/Contributing Factors and Corrective Action to Prevent Recurrence**

<b>Necessary Condition</b>	<b>Any Corrective Action to Prevent Recurrence</b>
Rain storm proceeding a blizzard which helps diffuse water into concrete to significantly raise its moisture content	Applying Weather Proof Sealant on the concrete surface will prevent the concrete from reaching the critical saturation point
A severe blizzard which is capable of reducing concrete temperature significantly to a level much below the freezing point of the water	Not practical to insulate the Shield Building or prevent the adverse effects of high winds and low temperatures.
The design of flute-shoulders which caused discontinuity in structure	Not practical to remove the flute shoulders to remove the discontinuity
The high density of rebar which increases the radial stresses	Not practical to redesign the required reinforcing steel
The tensile strength is lower than the radial stresses produced near the outer rebar mat	Not practical to install additional radial reinforcing steel to resist the increase in concrete radial stresses.

As a conservative measure, PII recommends performing confirmation monitoring at a few selected locations to ensure that the proposed corrective action effectively prevent further crack propagation. This confirmation monitoring shall be performed on a periodic basis, such as once per refueling outage. If the cracks are confirmed not to propagate after three times of confirmation monitoring, the efforts of further monitoring may be suspended.



## XVII. Additional Considerations

The following are responses to issues raised after the report was finalized in its current form.

1. The moisture penetration test procedure and test data are shown in Exhibit 52 Fig. 3. The analysis was shown in Exhibit 72. The tests, performed at the University of Colorado at Boulder, followed the procedure detailed in Exhibit 52 since there is no ASTM standard test appropriate for this purpose.
2. Six core-bores revealed evidence of multiple laminar cracks in the same area of the outside face reinforcement. Performance Improvement International (PII) considers these to be a part of a single delamination process. As explained elsewhere, cracks in concrete follow the path of least resistance and may diverge an inch or two to bypass a large piece of strong aggregate. A crack may also split under the same condition and continue on both sides of the aggregate for a short distance. Another possibility is that two distinct cracks, originating to the left and right of the core, follow a slightly different path due to localized stronger aggregates. These cracks will either converge or one will terminate beyond the stronger area.
3. An uneven snow load could transfer load to the top of the SB wall, but it wouldn't be any worse than the entire roof filling up with water. A previous vendor did a calc on the latter and the stresses were relatively small. This also wouldn't explain why there was cracking all the way down the wall, so it was never considered as a significant contributor to the laminar cracking.
4. [Exhibit 56] [Page 79]. The size and location for the 30'x30' simulated "crack" was selected to approximate the same location as the physically observed 30' crack.
5. The thermal transient analysis conditions were chosen as the design load conditions because these thermal loads are the only conditions that produce radial stresses of any significant magnitude tending to open pre-existing cracks. Wind, seismic and tornado loads do not produce any significant stresses of any nature at the location of 30' "crack".
6. The presence of laminar cracks in the steam room does not contradict the freezing mechanism. In places where there is a very high density of rebar in a single plane (and therefore a very low density of concrete in that plane, like a perforated paper towel) it is possible for a crack to propagate due to initiation of cracking in an adjacent region. Based on the IR mapping data provided by Davis-Besse, the cracks around the main steam lines coincide with regions of very high-density rebar and have arrested near the boundary of these regions. This is entirely compatible with the most likely failure mode identified.
7. The exact depth of penetration used as input to the FE model varies. In "1D" areas, it is 4" or less. In "2D" areas, it is 14" or less. An inch one way or the other would shift the crack location about an inch -- but a rigorous sensitivity study was not performed since we are not modeling growth rate.





8. A qualitative elimination analyses was performed for all possible events. The analysis concluded that the blizzard of 1978 was the only event that can possibly generate the damage. The externally necessary conditions are high speed wind driven rain which facilitated a large amount of moisture penetrated into the concrete. The internally (intrinsically) necessary condition is the expansive nature of the concrete upon the formation of ice under low temperatures. The blizzard of 1978 produced a “perfect storm” that combined all necessary conditions and make them sufficient to generate the damage. All necessary parameters (external loading parameters and internal material parameters) are random variables to a certain extent, such as wind speed, wind direction, temperature, coefficient of thermal expansion, compressive strength, and modulus of elasticity of concrete. Therefore, general trends of structural responses are more important than a specific response to a combination of input parameters. In order to simulate the general trend of the damage process by the FE method, the necessary parameters used as inputs for the FE analyses are either average values of test data obtained from the concrete cores available to PII during the project period or typical values collected based on our extensive literature search. The general trend of stress output of the FE analyses showed that the blizzard of 1978 was highly likely the event to cause large laminar cracks like those found in Davis-Besse shielding building.

The blizzard of 1978 was the only event that produced a “perfect storm”. Large forces were needed to propagate cracks through the aggregate and only two motivating forces were found to be capable of this – ice freezing and differential expansion due to ice freezing. In order for this scenario to happen, there need to be high winds and precipitation driving moisture into the concrete. The temperature outside has to drop to well below freezing. The blizzard of 1978 was the only event found to have all these factors in sufficient magnitude to cause large laminar cracks like those found at Davis-Besse.

2D moisture penetration in the shoulders (due to a high surface area to volume ratio) leads to more differential expansion under the shoulders. The presence of weak planes in the concrete (due to very high rebar density) gives the cracks a “perforated” path to propagate. Damage in the flute shoulders is concentrated on the southwest side of the building, which coincides with the predominant wind direction. Other parts of the building will still get wet. Based on the IR mapping, the laminar cracks that are not on the southwest side of the building are limited to regions with weak planes of concrete (due to high density rebar). Weak planes of concrete will require less force to initiate cracks. Therefore, the observed result is expected.

9. The cracking models consider the entire stress tensor when calculating damage. This is done internally by the code. In all other models (non-cracking models), the failure stress being considered (regardless of its direction or magnitude) is strictly a means of comparison. The failure stress is not used as an input to any of the models other than the cracking models. The cracking models used a failure stress of 600 psi, which is not limited to radial stress.



10. The models that have been run to date produce results that are reflective of the observed damage based on IR mapping data. The laminar cracks occur in essentially the same locations in the models and in reality, including in the shoulders on the southwest side of the building and in regions with very high planar rebar density, such as in the top 20' of the building and around the main steam line penetrations.



## Appendix I Reference

1. Lori King. *The Containment Tower at Davis-Besse Nuclear Power Station*. 2011. Photograph. Toledo Blade, Toledo. Web. 27 Feb 2012.  
<[http://www.toledoblade.com/image/2011/10/13/300x\\_b1\\_a4-3\\_cCM\\_z/davis-besse-crack.jpg](http://www.toledoblade.com/image/2011/10/13/300x_b1_a4-3_cCM_z/davis-besse-crack.jpg)>.
2. Xi, Y. and Nakhi, A. (2005) "Composite Damage Models for Diffusivity of Distressed Materials", *J. of Materials in Civil Engineering*, ASCE, May/June, 17(3), 286-295.
3. Eskandari-Ghadi, M., Zhang, W.P., Xi, Y., and Sture, S. (2012) "Moisture Diffusivity of Concrete at Low Temperatures", submitted to *Journal of Engineering Mechanics, ASCE*, accepted for publication, will appear in 2012.
4. Grieve, R., Slater, W.M., and Rothenburg, L. (1987) "Deterioration and Repair of Above Ground Concrete Water Tanks in Ontario, Canada", *Research Report to Ontario Ministry of the Environment*, Golder Associates and W.M. Slater & Associates, Inc.
5. Li, Z.J., Leung, C., and Xi, Y. (2009) Structural Renovation in Concrete, Taylor & Francis, London, 356p.
6. Mehta, P.K., and Monteiro, P.J.M. (1993) Concrete: Structure, Properties, and Materials, Prentice Hall Inc., Englewood Cliff, NJ 07632.
7. Naus, D.J., and Graves, H.L. (2007) "Primer on Durability of Nuclear Power Plant Reinforced Concrete Structures – A Review of Pertinent Factors", Report to U.S. Nuclear Regulatory Commission, NUREG/CR-6927, ORNL/TM-2006/529.
8. Neville, A.M. (1995) Properties of Concrete, 4<sup>th</sup> edition, Pearson.
9. Young, J.Y., Mindess, S., Gray, R.J., and Bentur, A. (1998) The Science and Technology of Civil Engineering Materials, Prentice Hall, Upper Saddle River, NJ 07458



## Appendix II Summary of Finite Element Analyses Performed

### Section 2.01 Summary

This document describes all analysis performed by the PII computational analysis team. The report submitted to the Root Cause Analysis from each analyst is summarized below.

### Section 2.02 [REDACTED]

(a) Exhibit 67 – Davis-Besse Containment Tower [REDACTED] Analysis  
The [REDACTED] performed for this report includes:

- No surrounding buildings
  - 34mph from the Northwest (summer)
  - 34mph from the Southwest (winter)
  - 72mph from the Southwest (winter)
- Surrounding buildings
  - 34mph from the Northwest (summer)
  - 72mph from the Southwest (winter)
  - 105mph from the Southwest (winter)
- Tornado
  - Category F2
  - Traveled from the Northwest to Southeast

Boundary Conditions for the problem consisted of:

- Winter
  - Ambient temperature of -13°F.
  - Temperature of the containment tower remained at a constant 7°F.
- Summer
  - Ambient temperature of 104°F.
  - Temperature of the containment tower remained at a constant 130°F.

The results from this analysis are input the Nastran [REDACTED] It includes:

- Pressure distributions on the surface
- Heat transfer coefficients
- Vorticity shedding calculated on the 72mph case



There are no conclusions of this analysis alone. The results of the [REDACTED] are used in Exhibit 65 – Davis-Besse Thermal Analysis

Section 2.03 [REDACTED]

Role: Heat transfer analysis using Nastran Finite Element Analysis

**(a) Exhibit 65 – Davis-Besse Thermal analysis**

This analysis serves the purposes of assessing the seasonal and daily variations in the temperature of the outer concrete shield building of the Davis-Besse reactor. The results of this analysis are used as inputs for subsequent thermal stress analysis. There are no conclusions of this analysis alone. The results of this analysis are used in the following Exhibits:

- Exhibit 56 – Structural and Thermal Analysis Investigation
- Exhibit 54 – Thermal Stress Analysis with Gravity and Wind Load
- Exhibit 61 – Stress Analysis at Cold Conditions and High Moisture Content
- Exhibit 62 – Stress Analysis due to 105 mph Wind Load

Section 2.04 [REDACTED]

Role: Structural analysis using Nastran Finite Element Software

**(a) Exhibit 56 – Structural and Thermal Analysis Investigation**

**(i) [REDACTED]**

These models serve the dual purposes of:

1. Calculating temperature distributions throughout the Shield Building resulting from the thermal transient response due to the various environmental conditions
2. Thermal stress analysis at critical time intervals during the 24 hour time periods of each environmental condition.

The [REDACTED] also provide a cross check and quality assurance with [REDACTED]  
[REDACTED]

A revised version of the [REDACTED] introduced a simulated crack 30' x 30' to evaluate the state of stress in the simulated crack region.

The Results of the [REDACTED] are:



- The highest magnitude of radial stress is in the thick portion of the architectural flutes during the summer months. The south-west facing architectural flutes experience a higher degree of radial stress. The magnitude of radial stress is not sufficient to cause cracks.
- As a result of the thermal temperature gradients across the wall section the outer layers of concrete to the outer face rebar show the highest magnitudes of tension stress. From the outer face rebar layer moving further toward the center of the shield building wall the magnitude of tension stresses reduces to levels that would clearly not initiate cracks.
- Result from the [REDACTED] Nastran Model with simulated 30' × 30' crack is that stress developed due to thermal stress from the environmental conditions would not further propagate the simulated crack.

(ii) [REDACTED]

These models are used to identify peak time intervals during 24 hour/1 hour individual time slices where the magnitudes of radial stresses are highest.

The Results of the [REDACTED] re:

- Identifies the time of day during the 24 hour time period when magnitude of radial stresses is highest.
- Peak radial stresses around regions where known stress concentration factor (SCF) effects are known to exist will produce high stresses that could initiate cracks.
- The state of stress surrounding these SCF points would not propagate.

Section 2.05 [REDACTED]

Role: Structural analysis using Abaqus Finite Element software

**(a) Exhibit 51 – Freezing Failure and Rebar Spacing Sensitivity Study**

This study shows that only a small fraction of the voids under the rebars need to fill with water and freeze in order to get laminar cracks. And, for a given motivating force, there are large laminar cracks that form in regions with dense rebar and none form in regions with sparse rebar.



This study shows that freezing of ice under the horizontal rebars is a plausible failure mode by establishing the conditions under which this modality matches the observed failures and then further testing the mode to show that there is no failure in regions with sparse rebar.

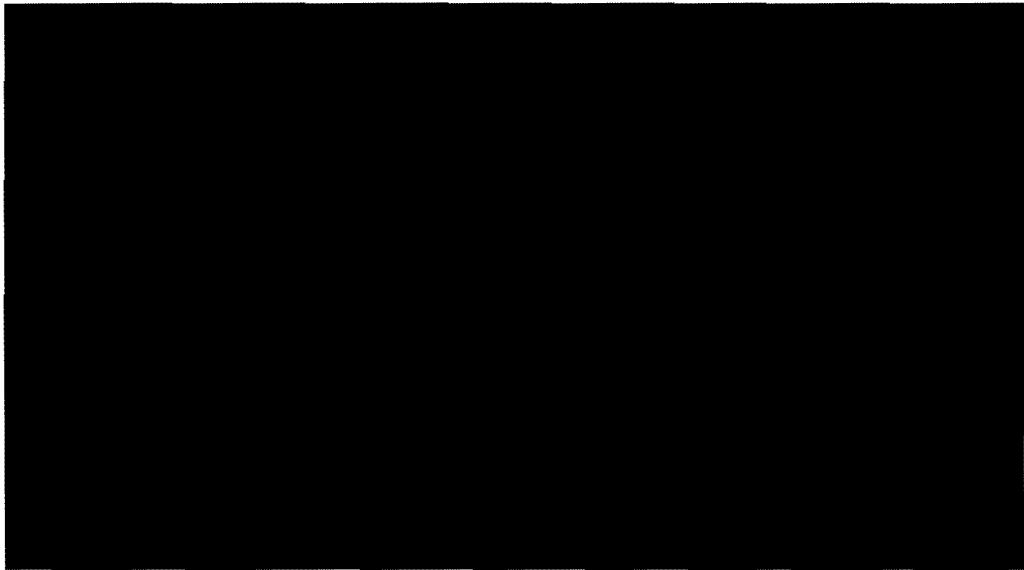
This study shows that for the same motivating force, there are large laminar cracks that form in regions with dense rebar and do not form in regions with sparse rebar. With a given motivating force, [REDACTED] all of the models with 6" spacing of rebar showed the development of some laminar cracks, while none of the models with 12" spacing of both horizontals and verticals showed any laminar cracking.

This study establishes that rebar spacing is a probable contributing factor because the tighter rebar spacing can facilitate crack propagation. In regions with wider rebar spacing, damage is less likely because of the absence of this contributing factor.

**(b) Exhibit 73 - Laminar Cracking due to 1978 Blizzard**

- The blizzard of 1978 scenario results in laminar cracking near the OF rebar mat.
- The blizzard of 1977 shows some damage (microcracking) relatively close to the surface of the shoulders, and significantly less damage compared to the blizzard of 1978.

○





- The [REDACTED] [REDACTED] Laminar cracks developed most prominently at the OF rebar mat under the thick shoulder regions and not in the thinner sections in the flute and shell.
- Assumptions: For the assumed depth of penetration of water (3-4”), PII performed a Rilem tube test and got a number very similar to our assumption (2-3”). For the strength we assumed 600-900 psi and tensile tests showed a range of 500-1000 psi. For the strain energy, we performed a calibration to a known crack. The elastic stiffness is validated by test data as well. Moreover, our conclusions are based on a reasonable set of input parameters that result in a plausible failure scenario. There is reasonable assumptions information, but we have determined that all other possible failure modes are not credible. Traditional sensitivity studies were not performed since this analysis is not a design basis analysis.

**(c) Exhibit 75 – Damage Propagation into Regions with High Rebar Density**

- The locations of the cracking remain confined to the observed crack locations at the OF rebar mat, both under the thick sections of the shoulders and in locations where the horizontal rebar is spaced on 6” centers.
  - The model in the top 20’ of the walls shows some damage in the flute valley, which is in line with observation.
  - The model near the Aux building roof shows less damage in the flute valley, which is also in line with observation.
- Overall, the results show good agreement with observed cracking in the areas studied.

Section 2.06 [REDACTED]

Role: Structural analysis using Abaqus Finite Element software

**(a) Exhibit 61 – Stress State during the 1978 and 1977 Blizzards**

This analysis compares the stresses during the 1978 and 1977 blizzards assuming 93% moisture content in the outer few inches of the structure. The results of the analysis can be summarized as follows:





- The blizzard of 1978 produced stresses above the tensile strength in the hoop direction, likely resulting in damage. The area exceeding the tensile strength is confined to a circumferential plane at the depth of the outer face main cylindrical wall under the raised shoulders.
- The 1977 blizzard shows significantly lower stress compared to the blizzard of 1978. The hoop stress approached the tensile strength of the concrete and it is limited to a small area. For these reasons only minor damage, if any, is predicted.
- Assumptions: For the assumed depth of penetration of water (3-4”), PII performed a Rilem tube test and got a number very similar to our assumption (2-3”). For the strength we assumed 600-900 psi and tensile tests showed a range of 500-1000 psi. For the strain energy, we performed a calibration to a known crack. The elastic stiffness is validated by test data as well. Moreover, our conclusions are based on a reasonable set of input parameters that result in a plausible failure scenario. There is reasonable assumptions information, but we have determined that all other possible failure modes are not credible. Traditional sensitivity studies were not performed since this analysis is not a design basis analysis.

**(b) Exhibit 62 – Stress Analysis due to 105 mph Wind Load**

The wind pressure during the 1978 blizzard was considered in this analysis

- The wind pressure does not produce stresses capable of delaminating the structure.
- The 105 wind pressure load results in a max principal stress of about 55 psi
- The 105 wind pressure load results in a radial stress of less than 1 psi
- Assumptions: The pressure loads due to the 105 mph wind were calculated in a separate [REDACTED] model and mapped to the Abaqus [REDACTED] Model. The assumptions and modeling details are provided in Exhibit 67. Page 15, Figure 23 shows the surface pressure contours due to the 105 mph wind speed. Since the stresses are benign (<1 psi) there is no need to perform a sensitivity study. Even a factor of 2 difference in any input parameter will not result in a significant stress change.



**(c) Exhibit 64 – Thermal Stress Analysis with Gravity and Wind Load**

This analysis considers various temperature, gravity and wind conditions and the influence on the radial stress. The results of the analysis are:

- The temperature and wind conditions found to maximize the radial stress are not sufficient to delaminate the structure alone
- Thermally induced radial stresses is maximized at the hot summer temperatures
- At the location of the outer face horizontal rebar, the maximum radial stress due to temperature gradients, gravity, and wind is about 300 psi

**Section 2.07 Modulus of Elasticity**

The average compressive strength test data obtained at University of Colorado at Boulder showed that  $f'_c = 7571$  psi (See Exhibit 52). Considering the large deviation of compressive strength test data from 5,444 psi to 10,508 psi and only one specimen available for testing modulus of elasticity (the result was  $E_c = 5.9E06$  psi, See Exhibit 3), it was decided that the modulus of elasticity of concrete be calculated using the ACI formula for normal weight concrete, assuming  $f'_c = 7500$  psi, which results in  $E_c = 4.94E06$ . This value was used in all finite element models.



## Appendix III Uncertainty Analysis

The laminar cracking phenomenon is a structure wide issue. The crack develops at some weak point in the susceptible region and then propagates throughout the rest of the susceptible area. The overall result is sensitive to the overall average parameter to determine the ultimate extent of the crack.

The overall cracking parameter is made up as follows:

$S_c = F_t / (E * M_t * T)$ , where  $F_t$  is the tensile strength (~ 973 psi +/- 6%)

$E$  is modulus of elasticity (~ 5.5 Msi +/- 8%)

$M_t$  is the modulus of thermal expansion (~ 5.20 E-6/F)

$T$  is the temperature gradient seen by the concrete when it cracked. Solving, a 34 °F gradient is needed to precipitate cracking.

**Note:** The measured  $F_t$  value of 973 psi was replaced with 'effective strength' of 600 psi for the cracking models since experience shows that it is necessary to use a lower "effective" strength in the cracking models for multiple reasons.

The uncertainty on any one of the physical parameters of the concrete is about +/- 8% each and taken together would give an uncertainty of about 13%. The uncertainty in the modeled distributions of temperature and stress are on the order of 30% for steady state cyclic fatigue calculations. It is much higher for transient temperature and stress conditions during a blizzard condition.

As a result, we consider the uncertainty in steady state calculations to be on the order of +/- 35% which is sufficient to conclude that small amplitude cyclic phenomena are not responsible for the laminar cracking observed. It is not possible to make as firm a conclusion about the identified root cause because of the highly transient nature of the event. It is only possible to make comparisons about relative damage predicted by the model and verify that the observed damage is similar in nature. Thus the computer models provide a qualitative verification of the root cause conclusion.

The more limiting parameter is the calculation of the temperature gradient in a severe transient condition such as the Blizzard of 1978. The uncertainties associated with the calculation of this

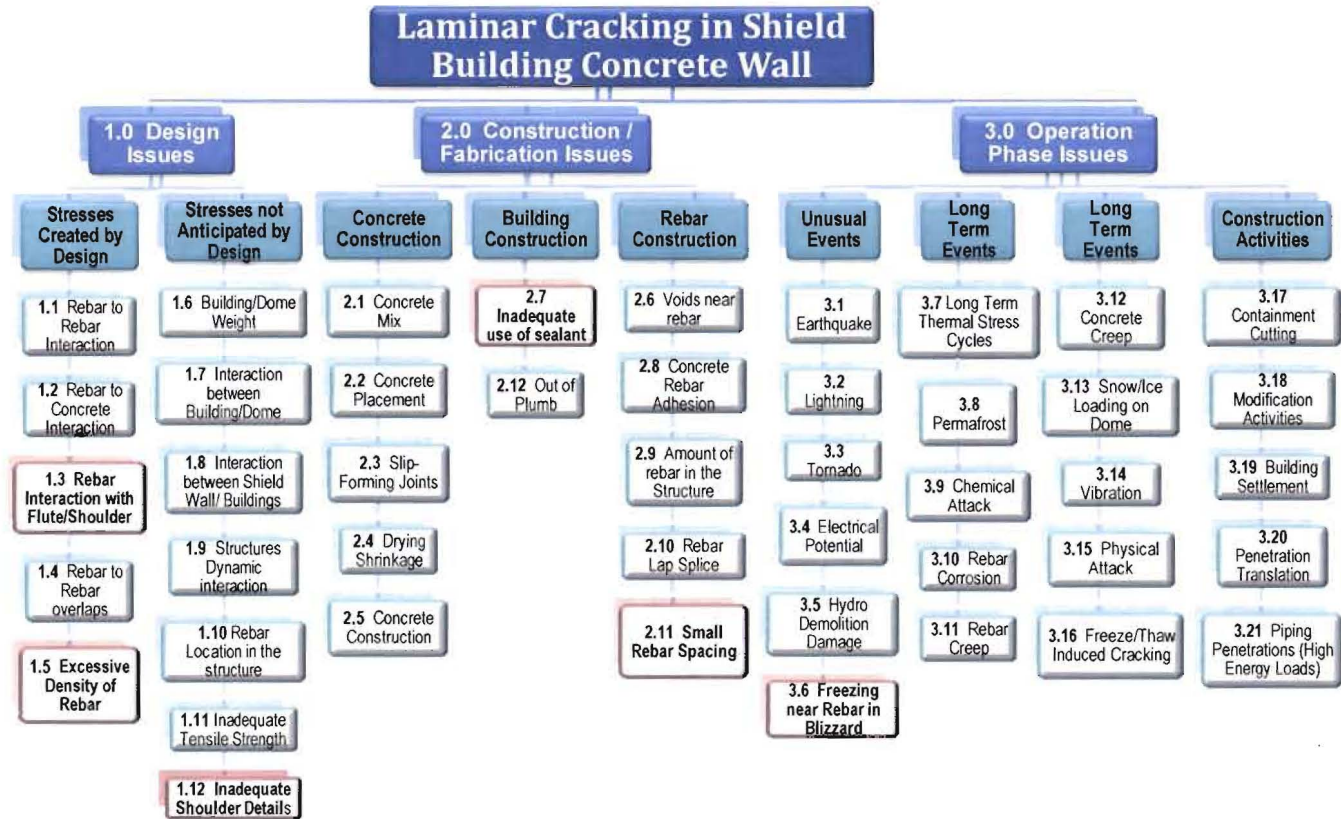


parameter are very large indeed. For that reason the calculation is not meant to be a quantitative assessment.





## Appendix IV Failure Mode Chart





## Appendix V Group I Failure Modes

### FM 1.1 – Rebar to rebar Interaction

<b>Description:</b> This failure mode will review the potential for rebar to rebar interaction to have caused/contributed to the laminar cracking issue.
<b>Data to be collected and analysed:</b> Construction drawings: Exhibit 43 - Calculation C-CSS-099.20-054 Exhibit 44 – Calculation C-CSS-099.20-056 Exhibit 41 - C-0110 Roof plan wall section details
<b>Verified Supporting Evidence:</b> None
<b>Verified Refuting Evidence:</b> Per Drawing C-110, the majority of the rebar is as follows: Shell area Inside face: Horizontal     either #11 @ 6", or #11@ 12", or #8 @ 12" depending on location Vertical       either #10 @ 12" spacing or #11 @ 12" depending on location Shell area Outside face: Horizontal     either #11@6" spacing or #11@12" depending on location Vertical       either #11@ 12" or #10@8" spacing depending on location Shoulder area: Horizontal     #8 @ 12" Vertical       #8 @ 12"  The above rebar is the typical pattern. Additional rebar have been added at penetrations and at the construction opening. This additional rebar is considered localized and not typical. Additional rebar is also present at the top 20 foot of the shield building. The rebar spacing is not unusual for this type of construction The specified rebar lap splice length is consistent with or more conservative than the ACI Code requirements The stresses in the rebar and concrete are approximately ½ of the allowable values There is NO Supporting Evidence that this is a contributor
<b>Discussion:</b> None
<b>Conclusion:</b> Rebar to rebar interaction was not a cause of the Laminar Cracks



## FM 1.2 – Rebar to Concrete Interaction

<b>Description:</b> This failure mode will review the potential for rebar to concrete interaction to have caused/contributed to the laminar cracking issue.
<b>Data to be collected and analysed:</b> Construction drawings: Exhibit 41 - C-0110
<b>Verified Supporting Evidence:</b> None
<b>Verified Refuting Evidence:</b> See FM 1.1 and Exhibit 41 for rebar design requirements The stresses in the rebar and concrete are approximately $\frac{1}{2}$ of the allowable values. The specified rebar lap splice length is consistent with or more conservative than the ACI Code requirements.  There is NO supporting evidence that this is a contributor
<b>Discussion:</b> None
<b>Conclusion:</b> Rebar to Concrete interaction was not a cause of the Laminar Cracks



## FM 1.3 – Rebar Interaction with Flute Shoulder

**Description:**

This failure mode will review the potential design deficiency on rebar detailing that could lead to rebar interaction with the Flute/Shoulder to have caused/contributed to the laminar cracking issue.

**Data to be collected and analysed:**

Exhibit 41 - C-0110 Roof plan wall section details

**Verified Supporting Evidence:**

- Cracks are predominate in the shoulder area
- Cracks are predominately located between the horizontal rebar anchor points. (results in approximately 10 foot spacing)
- The shoulder vertical and horizontal rebar are #8@12 spacing.
- The vertical rebar are not tied to the main outside reinforcing steel mat
- The horizontal rebar are tied to the main outside reinforcing steel mat only at the ends.
- There is approximately 10 foot horizontal span in which the shoulder concrete is not connected to the main outside reinforcing steel

**Verified Refuting Evidence:**

None

**Discussion:**

Refer to FM 1.12 for additional discussion

**Conclusion:**

Rebar interaction with flute shoulder may be cause of the Laminar Cracks





## FM 1.4 – Rebar to Rebar Overlap

**Description:**

This failure mode will review the potential for rebar to rebar lap splice to have caused/contributed to the laminar cracking issue. Some of the rebar in the wall were extended (spliced) by overlapping instead of mechanical connectors. These overlap connections need to be spaced correctly with sufficient overlap in order to transfer stresses between rebar.

**Data to be collected and analysed:**

Exhibit 41 - C-0110 Roof plan wall section details  
Exhibit 43 - Calculation C-CSS-099.20-054

**Verified Supporting Evidence:**

None

**Verified Refuting Evidence:**

Reference Drawing C- 110, the specified rebar lap splice length is consistent with or more conservative than the ACI Code requirements

The stresses in the rebar and concrete are approximately  $\frac{1}{2}$  of the allowable values.

The lap splice lengths specified on Drawing C-110 exceed the minimum length of lap splices required by American Concrete Institute (ACI) 318-1963. The specified length of the lap splices ensures that the required load transfer is very low as identified in Calculations C-CSS-99.20-054 and 056.

There is NO Supporting Evidence that this is a contributor

**Discussion:**

None

**Conclusion:**

Rebar to rebar overlap did not cause the Laminar Cracks



## FM 1.5 – Excessive density of rebar

<b>Description:</b> This failure mode will examine the potential for excessive rebar density to have caused the identified laminar cracks.
<b>Data to be collected and analysed:</b> Construction drawings: Exhibit 44 - C-0111A Exhibit 41 - C-0110 Exhibit 51 – Rebar density sensitivity study by PII
<b>Verified Supporting Evidence:</b> <ul style="list-style-type: none"><li>• Laminar cracks were observed at the top of the shield building</li><li>• Laminar cracks were observed around the construction opening</li><li>• Laminar cracks were observed around the main steam line penetration</li><li>• A 'Rebar Spacing Sensitivity Study' was performed by PII (exhibit 51). The study established that higher density of rebar could lead to more laminar cracking under a given stress condition.</li></ul>
<b>Verified Refuting Evidence:</b> See rebar requirement in the Rebar to Rebar Interaction section. The normal detail is #10 bar or #11bar@12" spacing. Additional rebar was added at the construction opening and at blockout areas to compensate for the rebar interrupted by the opening. In addition, at the top 20' of the shield building, the rebar density increase to #11bar@ 6" spacing.  However, The majority of the cracks were observed in the shoulder areas where the rebar density is not excessive and very normal for that type of construction.
<b>Discussion:</b> A study to evaluate freezing failure and rebar spacing (exhibit 51) found that for a given motivating force, large laminar cracks form in regions with dense rebar and not in regions with sparse rebar.
<b>Conclusion:</b> Excessive density of rebar is a contributor to the Laminar Cracks



## FM 1.6 – Building Dome Weight

<b>Description:</b> This potential failure mode will examine the effect of the Building and dome weight as a cause/contributor to the identified laminar cracking.
<b>Data to be collected and analysed:</b> See FM 1.7
<b>Verified Supporting Evidence:</b> None
<b>Verified Refuting Evidence:</b> See FM 1.7
<b>Discussion:</b> None
<b>Conclusion:</b> See FM 1.7



## FM 1.7 – Interaction between Building/Dome

<b>Description:</b> This potential failure mode will examine the interaction between the Shield Building dome and walls as a cause/contributor to the identified laminar cracking.
<b>Data to be collected and analysed:</b> Construction drawings: Exhibit 43 - Calculation C-CSS-099.20-054, Attachment C p. 11 Exhibit 53 – Drawing C-109 Exhibit 41 – Drawing C-110
<b>Verified Supporting Evidence:</b> None
<b>Verified Refuting Evidence:</b> The weight of the dome is over 5000 kips, Ref. Calculation C-CSS-099.20-054. However, the circumference of the shield building is approximately 450 feet with 30 inch thick walls. This results in a compressive force of less than 50 psi. The weight of the 225 foot wall results in a compressive force of less than 250 psi The reinforcing at the top of the shield building is substantial. However, per ACI 307 Section 4.1.4 the amount of reinforcement in the top 7.5 feet is doubled what is needed to account for the load. The structural analysis shows that the stress in the rebar and concrete are approximately ½ of the allowable values. There is nothing unusual with the rebar in this area. Therefore, this potential cause is refuted.
<b>Discussion:</b> None
<b>Conclusion:</b> Interaction between Building/Dome was not a cause of the Laminar Cracks



## FM 1.8 – Interaction between Building/Wall

<b>Description:</b> Interaction between the Shield Building and the adjacent Auxiliary Building could have exerted forces that potentially caused some of the laminar cracks.
<b>Data to be collected and analysed:</b> Construction drawings: Exhibit 44 - Drawing C-111A Exhibit 45 - C-0100 Shield Bldg Foundation Exhibit 51 - C-0200 rev 30
<b>Verified Supporting Evidence:</b> None
<b>Verified Refuting Evidence:</b> There has been no seismic activity at the Davis-Besse site which could have caused any interaction between structures. Also, the Auxiliary Building is founded on bedrock as is the Shield Building. This eliminates any potential for differential settlement to have caused interaction. The as-found cracks are primarily located away from the direct interface between these two structures (Exhibit 44 - Drawing C-111A). The Shield Building and Aux building are isolated by an expansion joint. (See Drawing C-200) This makes it highly unlikely that interaction between the two buildings caused any of the laminar cracks.
<b>Discussion:</b> None
<b>Conclusion:</b> Interaction between Building/Wall was not a cause of the Laminar Cracks



## FM 1.9 – Structures Dynamic interaction

<b>Description:</b> Structures Dynamic Interaction could have exerted forces that potentially caused some of the laminar cracks.
<b>Data to be collected and analysed:</b> See FM 1.8
<b>Verified Supporting Evidence:</b> None
<b>Verified Refuting Evidence:</b> See FM 1.8
<b>Discussion:</b> None
<b>Conclusion:</b> Structures Dynamic interaction was not a cause of the Laminar Cracks



## FM 1.10 – Rebar Location in the structure

<b>Description:</b> The potential for the rebar location in the structure to have caused or contributed to the laminar cracking will be reviewed.
<b>Data to be collected and analysed:</b> Construction drawings: Exhibit 41 – Drawing C-110
<b>Verified Supporting Evidence:</b> None
<b>Verified Refuting Evidence:</b> The rebar location is consistent with good engineering / fabrication practices with the exception of how the shoulder area is tied back to the shield building shell area. Refer to Failure Mode 1.3 for the Rebar Interaction with the Flute /Shoulder.
<b>Discussion:</b> Refer to FM 1.12 for additional discussion
<b>Conclusion:</b> Rebar Location in the structure was not a cause of the Laminar Cracks



## FM 1.11 – Inadequate Concrete Tensile Strength

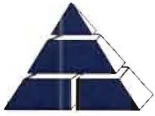
<b>Description:</b> This potential failure mode will examine the potential for inadequate tensile strength in the concrete as a cause/contributor to the identified laminar cracking.
<b>Data to be collected and analysed:</b> Exhibit 3 - Lab Test results from Twining Laboratories Exhibit 52 – Lab test results from University of Colorado at Boulder
<b>Verified Supporting Evidence:</b> None
<b>Verified Refuting Evidence:</b> The minimum specified compressive strength is 4000 psi. The design tensile strength of the concrete is a function of this minimum compressive strength. A common design expression (ACI 318-89) is: $f_t = 6.7 (f_c)^{0.5} \text{ or } 6.7(4000)^{0.5} = 424 \text{ psi}$ Average Splitting Tensile Strength ( $f_{st}$ ) from tests performed on shield building core samples (Exhibit 3 and 52) exceeded 900 psi.
<b>Discussion:</b> None
<b>Conclusion:</b> Inadequate tensile strength did not cause the Laminar Cracks





## FM 1.12 – Inadequate Shoulder Detail

<b>Description:</b> This potential cause for the laminar cracks is the potential of inadequate shoulder reinforcement details.
<b>Data to be collected and analysed:</b> Construction drawings: Exhibit 44 - C-0111A Exhibit 41 - C-0110
<b>Verified Supporting Evidence:</b> The shoulder areas were reinforced with #8 rebar spaced at 12 inches in each direction. The horizontal rebar were provide with a tie (i.e. hooks) at each end into the main reinforcing of the Shield Building wall. The distance between these tie points was about 10 feet. This left a considerable span where only concrete was available to resist loads at the cylinder/shoulder interface. This relatively large span is the area where the laminar cracks have been identified, Ref. Drawing C-111A. Various loading (thermal, creep shrinkage, etc.) have been shown to develop stresses that could account for these cracks. The lack of adequately spaced ties between the shoulder reinforcement and the main cylinder appear to be the one potential failure that could have prevented the cracking. Therefore, this failure mode is considered to be a cause for the identified laminar cracks.
<b>Verified Refuting Evidence:</b> None
<b>Discussion:</b> None
<b>Conclusion:</b> Inadequate shoulder detail was a major cause for the Laminar Cracks



## Appendix VI Group 2 Failure Modes

### FM 2.1 – Concrete Mix

#### **Description:**

Concrete mix design controls the physical properties of the concrete and its performance in the structure.

The mix components analysed here include the aggregate type, aggregate properties and cement type. Mix-dependent properties include workability, design and actual strength, durability, and air content and distribution.

Description of issues and conclusions follow.

#### **Data to be collected and Analysed:**

Concrete mix design was evaluated based on data from original mix-design, visual and microscopic investigation of the hardened concrete, review of inspection and NCR (Non-Conformance Report) records. Analysis of delivery tickets and test reports was performed.

Exhibit 1 is original mix design

Exhibit 11 is original submittals including mix design and material properties

Exhibit 2 is a Petrographic analysis by CTL.

Exhibit 8 is a report on four NCRs during concrete placement.

Exhibit 26 is a report on Petrographic Studies of Concrete from Containment Structure by WJE.

Exhibit 34 - Concrete mix summary for Below Grade wall

Exhibit 35 - Concrete Strength summary for Below Grade wall

Exhibit 36 - Concrete Strength summary for Above Grade wall

#### **Verified Refuting Evidence:**

##### **Aggregates**

Aggregates used were in compliance with the project specifications of 1.5" MSA (Maximum Size Aggregate). Exhibit 11 provides complete information on the original aggregates. Petrographic analysis by CTL (exhibit 2) identified the aggregate as "composed of limestone, dolomitic limestone, argillaceous limestone, and other carbonate rocks. Particles range from dense to moderately porous." Microscopy inspection found no indication of reactive aggregates or weak inclusions. The aggregate is hard and appears to be well distributed in the matrix.

It is concluded that the aggregates were not a cause of the laminar cracking.

##### **Cement Type**

Two cement types were used in the structure. Type II cement was used in the below-grade part and in the top 4 feet of the wall (as detailed in NCR – Exhibit 8). The choice of Type II for use below grade may have been influenced by concern for potential durability issues.

Type I cement was used for the rest of the structure. This choice may be related to the higher early strength requirements of slip-forming operation.

These two cement types have similar strength properties after the first month and should provide the same long-term performance.

It is concluded that the choice of cement type had no effect on physical properties of the hardened concrete and was not a cause of the laminar cracking.



## Strength

A total of ninety-two (92) cylinder sets from original construction were analyzed. Eighteen sets were for concrete using the Type II cement (Exhibits 34-35) and seventy four (74) were for Type I cement (Exhibit 36). Figure 1 below summarizes the results. Note the first 19 tests and 3 of the last are for concrete with Type II cement – resulting in lower seven day strength but comparable later strength.

Twenty-eight (28) days strength averaged 5750 psi with seven (7) days strength averaging 4100 psi. As expected, the concrete with Type II cement was slower to gain strength, but by day 28 all concrete exceeded the design requirements of 4000 psi.

Average strength at 90 days reached 7075 psi with Standard Deviation (StD) of 505, maximum strength of 8100 psi, and minimum value of 5884 psi.

Due to the nature of the placement (slip-forming) and the limited records it was not possible to determine where each load was placed and attempt to correlate strength results with observed distress.

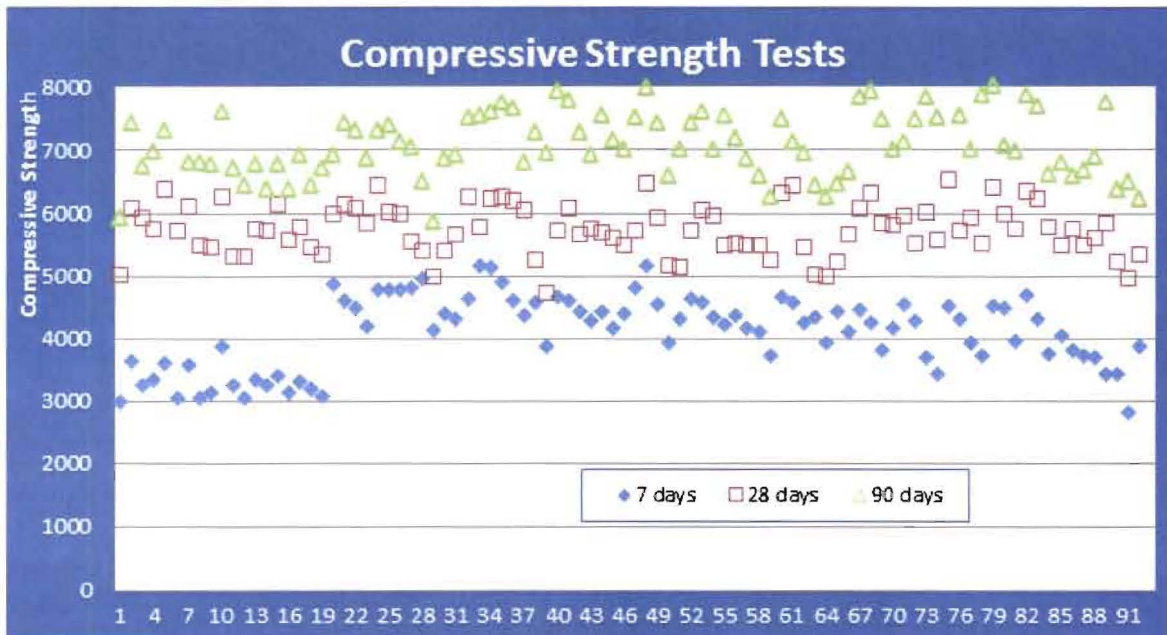


Figure 1 – Compressive Strength tests of concrete in containment wall below and above grade

Project specifications (exhibit 4) required that "Concrete for slip-form work shall conform to ACI Standard "Recommended Practice for Cold Weather Concreting" (ACI 306-66). The concrete shall attain a minimum ultimate compressive strength of 1200 psi in two days when type II cement is used and 1600 psi in two days when type I cement is used."

A freezing test reported in January 1971 (Exhibit 7) found 2 days strength averaged 2310 psi and 28 days strength following 14 freezing cycles exceeded 4600 psi.

It is concluded that concrete strength was in compliance with requirements and was not a cause of the laminar cracking. It is possible that the wide range of strength results explains why areas with similar



load conditions exhibit different distress levels.

### **Durability**

There are no indications of any durability related distress to the structure. Microscopic analysis of concrete cores did not detect any distress related to reactive aggregates or attack by external chemical agents (Exhibit 2 – CTL Lab Test Report). The petrographer's report states: "Based on Petrographic examination, no materials related causes for the cracks and microcracks are observed... concrete does not exhibit deleterious chemical reactions involving aggregates and paste... nor other forms of chemical or physical deterioration."

The chloride content of the shield building concrete is insignificant and could not contribute to corrosion of the reinforcing bars.

Visual inspections of the outside face of the wall did not reveal any durability related distress.

It is concluded that durability issues did not cause the laminar cracking.

### **Air content**

All the concrete used in the structure was specified with air entrainment range of 3-6% (Exhibit 1). Sixty Nine (69) tests on fresh concrete averaged 5.2% air with StD of 0.5%, maximum value of 6% and minimum value of 3.3%.

Air measurements in a core (Exhibit 2 page 16 of 20 – CTL Lab Test Report) were reported as "effectively non-air entrained." Another core from the same report (page 19 of 20) found varying levels of air-entrainment ranging from 1 to 5%. Petrographic Studies of Concrete from Containment Structure by WJE (Exhibit 26) reached similar conclusion. They noted that even though the total air content met industry standards, the specific surface and spacing factor did not meet the requirements. However, they concluded that the apparent lack of freeze-thaw damage may be explained by the high density (low permeability) and high strength typical of concrete with low water/cement ratio.

Analysis to measure effect of air on the compressive strength shows no significant effect of air content on the strength at 7, 28 and 90 days. (See Figure 2)

Visual inspection of external concrete wall shows no indication of freeze-thaw damage after forty years exposure. Visual inspection of concrete on top of the structure detected an area of the walkway with shallow surface spalling typical to freeze-thaw damage. This location is exposed to standing water, ice, and snow, and is expected to experience substantially harsher exposure than the rest of the structure. This level of damage after 40 years exposure is considered insignificant.

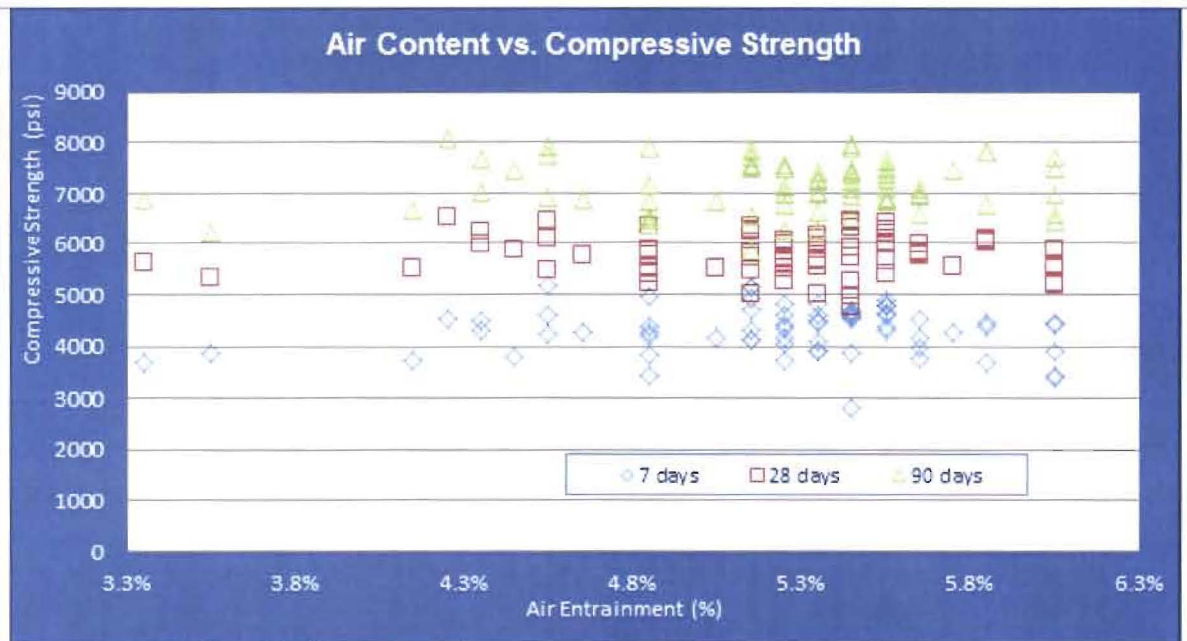


Figure 2 – Air content vs. Compressive Strength of concrete in containment wall

### Workability

Workability in concrete construction is specified by Slump values. Average Slump at the truck unloading point, calculated from inspection reports, was 4" with a maximum value of 6". The concrete mix design (exhibit 1) specified maximum slump of 5-6" while the specification C-38 (exhibit 5) required maximum 5" slump at point of placement. The measured slump values are in compliance and another indication that the concrete placed was within acceptable limits.

Even the lower range of slump measured can be consolidated properly with the mechanical vibrators used in the wall construction.

It is concluded that workability was not a cause of the laminar cracking.

### Verified Supporting Evidence:

None

### Discussion:

See above

### Conclusion:

The investigation of the concrete mix design, resultant properties, and lab test results show that the concrete used in the Shield Building is sound, of good quality, high strength, and consistent with the construction specifications. Therefore, the concrete mix can be eliminated as a cause for the delamination.



## FM 2.2 – Concrete Placement

### **Description:**

Concrete placement may determine its performance and properties. It can affect the void structure, rate of strength gain, adhesion, consolidation, moisture resistant and other properties. Description of issues and conclusions follow.

### **Data to be collected and Analysed:**

Concrete placement was evaluated based on original job specifications, review of inspection and NCR (Non-Conformance Report) records, review of photographic evidence, and analysis of industry standards and good construction practices.

Exhibit 4 (Specification C-26 - TECHNICAL SPECIFICATIONS FOR THE FORMING, PLACING, FINISHING AND CURING OF CONCRETE) provided guidelines for placing the concrete in the wall.

Exhibit 5 (Specification C-38 - QUALITY ASSURANCE AND CONSTRUCTION PROCEDURES REACTOR SHIELD WALL SLIP FORM CONSTRUCTION METHOD)

Exhibit 6 (Specification C-38 - TECHNICAL SPECIFICATIONS FOR THE SHIELD BUILDING No 7749-C-38) includes description and instruction for the slip-form work.

Exhibit 8 – report on four NCRs during concrete placement.

Exhibits 12 and 13 are Interim Field Reports regarding temperature, mix and water content issues.

### **Verified Refuting Evidence:**

#### **Methodology**

Specification C-26 (Exhibit 4) provided guidance for all phases of mixing, conveying, placing, finishing and curing the concrete. It required compliance with ACI 301, ACI 304, ACI 318, ASTM C-94, and as indicated in the specification. Thorough review of project documents, including daily inspection records, NCRs, and delivery tickets did not show any significant issues with the methodology of placing concrete in the wall. Specification C-38 (exhibit 5) provides additional details and clarifications:

“The concrete is placed directly into the forms from a specially designed round concrete bucket, in approximately 9" layers evenly around the form, and then vibrated with electric vibrators, The bucket is hoisted to the deck area by means of an electrically controlled, free-standing tower crane after being loaded from a charging hopper. At the foundation level, the charging hoppers will be fed by concrete conveyors loaded from the ready-mix trucks.”

#### **Segregation**

Segregation in concrete is a phenomenon where heavier particles sink and lighter ones rise during placement and consolidation. It can create areas of different properties that may lead to stress concentration and non-uniform behavior of the concrete.

Specification C-26 (exhibit 4) stated:

“Concrete shall not be dropped through dense reinforcing steel which might cause segregation of the coarse aggregate. In such cases spouts, elephant trunks, or other suitable means shall be used. In any event, concrete shall not be dropped free through dense reinforcing from a height of more than 6 feet except as otherwise approved by the CONSTRUCTION MANAGER...”

Visual inspection of cores did not reveal any significant segregation in the wall concrete.

It can be concluded that segregation was not a cause of the laminar cracking.



### **Ambient Temperature**

Ambient temperature, either high or low, can have deleterious effect on concrete unless steps are taken to protect it. Specification C-26 Section 11 (Exhibit 4) provided guidelines for cold and hot weather concreting.

Thorough review of project documents, including daily inspection records, NCRs, and delivery tickets did not show any significant problems when concrete was placed at temperatures as low as 0°F.

It is concluded that the ambient temperature was not a cause of the laminar cracking.

### **Concrete Temperature**

Concrete temperature is critical when placing during cold weather since a minimum temperature is required to get the chemical reactions started. Once started, these reactions will normally produce enough heat to keep the process going. Specification C-26 Section 11 (Exhibit 4) provided guidelines for required temperature range of the concrete. (Exhibit 4 - section 11.3.3 states:

“slip-form concrete which shall have a minimum placing temperature of 85F and a minimum placing temperature of 70 F.”).

Exhibit 8 refers to a placement of low-temperature concrete during winter operations. Exhibit 12 details tests and analysis performed to confirm that the low temperature did not impact the strength properties.

It is concluded that the concrete temperature was not a cause of the laminar cracking.

### **Excessive Water**

The total water content of the concrete is the main parameter determining its strength and durability.

Exhibits 8 and 12 detail an occurrence where 48 cu. yds were placed with water to cement ratio exceeding the design mix. Analysis and tests led to the conclusion that the strength properties were acceptable. The concrete was accepted.

It is concluded that excess water was not a cause of the laminar cracking.

### **Wrong Mix**

Exhibits 8 and 13 detail an occurrence where 6 cu. yds of concrete mix C 1-3 were placed in error. Analysis and tests led to the conclusion that fly-ash was not used and the strength properties were acceptable. The concrete was accepted.

It is concluded that wrong mix was not a cause of the laminar cracking.

### **Concrete Cover**

Reinforcing steel cover is intended to transfer the load between reinforcement and concrete, provide confinement, and protect the reinforcement from the environment. A requirement for minimum cover of solid concrete over any embedded steel is intended to ensure that the steel is properly protected from corrosion. The alkaline nature of concrete provides such protection.

Interaction of permeable concrete with air can, over time, cause carbonation of the cement paste and loss of alkalinity.

Laboratory tests (exhibit 2) found that:

“Paste along the outer surface of the cores... is fully carbonated to a depth of 5 to 8 mm.”

Since cover to main reinforcement was 3 inches, this rate of carbonation is very slow and does not



present a problem for the structure. In some locations, cover to outer surface of rebar was found to be as low as 1 inch (24.5mm). This observed cover is likely the result of exceptional conditions (such as overlaps, bundling, or misaligned forms), and is not a problem considering that carbonation reached less than a third of the depth in 40 years.

The report also found that chloride content is insignificant.

It is concluded that concrete cover is not considered a cause of the laminar cracking.

### **Curing**

Concrete requires presence of sufficient amount of moisture to facilitate the chemical reactions and to delay drying shrinkage until the concrete achieved sufficient strength to resist cracking.

Specification C-26 (exhibit 4) lists six acceptable curing methods that the superintendent can use individually or together.

Exhibit 6 provided the following guideline:

“The Shield Building concrete, except as otherwise approved by the CONSTRUCTION MANAGER, shall be cured by the liquid membrane method... The liquid membrane shall be applied to all slip-form wall surfaces. The membrane shall be applied to within 2 feet (two feet) of the bottom of the slip-form after the concrete surface has been finished.”

Review of project documents did not locate a description of the method actually used during the slip-forming operations.

Thorough review of project documents, including daily inspection records, NCRs, and other communications did not show any problem with the curing.

### **Placing Limitations**

Specification C-26 (exhibit 4) states that:

“Concrete shall be deposited in horizontal layers of not greater depth than 24 inches, and shall not be allowed or caused to flow a distance, within the forms, of more than 5 feet from point of deposition.”

Thorough review of project documents, including daily inspection records, NCRs, and other communications did not show any problem with the placing limitations.

It is concluded that placing limitations did not cause the laminar cracking.

### **Verified Supporting Evidence:**

None

### **Discussion:**

See above

### **Conclusion:**

The placement methods did not cause the Laminar Cracks





## FM 2.3 – Slip-forming joints

**Description:**

Cold joints in concrete construction are joints where fresh concrete is placed over hardened concrete. In these situations it is possible to have poor adhesion, reduced load transfers, and leaks through open joints.

**Data to be collected and Analysed:**

Exhibit 20 - slip-form records summary

Exhibit 15 – hand written summary of slip-form records.

Exhibit 4 - Spec C-26 forming placing finishing curing concrete

Exhibit 5 - QA and procedures slip form construction - Vendor Document 7749-C-38-3-1

Exhibit 46 – Overview and close-up of shield building showing mortar lines

**Verified Supporting Evidence:**

None

**Verified Refuting Evidence:**

Exhibits 15 and 20 include a summary of data taken from slip-form records.

- Normally, three daily shifts poured concrete continuously.
- Concrete was placed in the forms in uniform layers that were vibrated to create a solid interface without any breaks or cold joints (see FM 2.5 for discussion of procedures).
- Slip form records indicate breaks in the sequence on:
  1. May 1 – One shift
  2. May 2 – No pours
  3. May 8-9 – No pours
  4. May 15-16 – No pours
- The above indicates three times that cold joints were created in the structure.

Exhibit 4 provides the following instructions for cold joints:

“All concrete surfaces to receive new concrete shall be wet down two hours prior to placing concrete. All horizontal surfaces be thoroughly covered with approximately 1/2 inch of mortar immediately before the concrete is placed. For congested areas the mortar may be forced ahead of the concrete. The mortar shall have the same cement-sand ratio as used in the concrete being placed. The provision requiring placement of 1/2” mortar on horizontal construction joints may be waived by the CONSTRUCTION MANAGER on slip-form work when in his judgment the CONTRACTOR demonstrates that a satisfactory joint can be obtained without the use of mortar.”

Exhibit 2 includes additional specifications for cleaning and preparing the hardened concrete for placement of new concrete.

Exhibit 46 is recent photos of the shield building. Darker lines on the surface appear to be the mortar beds used to tie hard and fresh concrete when needed. It appears that the construction manager used



this treatment on cases (other than the three above) when setting concrete required it.

Close observations did not detect any sign of crack or open joint or any indication of moisture movement (Efflorescence).

It is concluded that cold-joints were treated according to job specifications and were not a problem.

**Discussion:**

Above

**Conclusion:**

Slip-forming joints were not a cause of the Laminar Cracks



## FM 2.4 – Drying Shrinkage

**Description:**

Concrete goes through a process of water loss, mostly in the first months of exposure to the environment. The resultant reduction in volume – shrinkage – can cause stresses in restrained concrete. In the case of a wall where the exposed surfaces are not restrained the stresses are parallel to the face and may cause radial cracks.

**Data to be collected and Analysed:**

Visual observations of cracking in the containment wall

**Verified Supporting Evidence:**

None

**Verified Refuting Evidence:**

Tight radial cracks were observed in multiple locations along the wall and the parapet (Exhibit 38). These cracks were barely visible and appeared old and inactive. There was no indication of moisture movement (no efflorescence, staining, etc.).

**Discussion:**

Above

**Conclusion:**

Shrinkage cracking was not a cause of the Laminar Cracks



## FM 2.5 – Concrete Construction

### **Description:**

Concrete construction methods may determine the structure's performance and properties.

Description of issues and conclusions follow.

### **Data to be collected and Analysed:**

Concrete Construction was evaluated based on original job specifications, review of inspection and NCR (Non-Conformance Report) records, review of photographic evidence, and analysis of industry standards and common practice.

Exhibit 4 (Specification C-26 - TECHNICAL SPECIFICATIONS FOR THE FORMING, PLACING, FINISHING AND CURING OF CONCRETE) provided guidelines for placing the concrete in the wall.

Exhibit 5 - QA and procedures slip form construction - Vendor Document 7749-C-38-3-1

Exhibit 6 (Specification C-38 - TECHNICAL SPECIFICATIONS FOR THE SHIELD BUILDING No 7749-C-38) includes description and instruction for the slip-form work.

Exhibit 27 is the ACI 347-63 Recommended Practice for Concrete Formwork.

Exhibit 28 is Fegles Drawing of Jack Rod layout plan.

### **Verified Refuting Evidence:**

#### **Vibration**

Specification C-26 (Exhibit 4) provided the requirements for methods and equipment to be used in the consolidation of the concrete. It stated that:

“Concrete shall be placed with the aid of mechanical vibrating equipment and supplemented by hand spading and tamping... The vibrator shall be operated in a near vertical position, and the vibrating head shall be allowed to penetrate under the action of its own weight and revibrate the concrete in the upper portion of the underlying layer. Neither form nor surface vibrators shall be used unless specifically approved. Vibrators shall not be used to move or spread concrete. A ratio of not less than one spare vibrator in good working condition to each three vibrators required for satisfactory vibration of the concrete being placed shall be kept available for immediate use at point of deposition. . .”

Thorough review of project documents, including daily inspection records, NCRs, and delivery tickets did not show any significant problem with the consolidation of concrete in the wall.

Visual analysis of cores revealed the presence of entrapped air bubbles of various sizes in the matrix. These voids are not expected to have a significant impact on the strength of the concrete and its ability to resist tensile stresses. They could, however, provide locations where water can accumulate and freeze and where cracks can initiate.

It can be concluded that vibration was not a cause of the laminar cracking

#### **Time between pours**

ACI recommendations and ASTM standards provide clear guidelines for timing concrete delivery so that new concrete can be integrated into existing concrete without creating cold joints.

Thorough review of project documents, including daily inspection records, NCRs, and delivery tickets did not show any significant problems with timing of concrete delivery.

It is concluded that the time between pours was not a cause of the laminar cracking.



### **Joints**

Exhibit 4 required that construction joints be prepared by sand blasting, bush hammering or other approved means.

“All concrete surfaces to receive new concrete shall be wet down two hours prior to placing concrete. All horizontal surfaces be thoroughly covered with approximately 1/2 inch of mortar immediately before the concrete is placed... The provision may be waived by the CONSTRUCTION MANAGER on slip-form work...”

Reviewed delivery tickets did not provide records of mortar meeting the specification requirements. However, visual observations of the completed wall show horizontal lines of darker concrete at various elevations. It is believed that these lines were caused by the application of ½ inch mortar as required by the specification in exhibit 4.

Thorough review of project documents, including daily inspection records, NCRs, and delivery tickets did not reveal any deficiencies with joint construction.

It is concluded that joints did not contribute to the laminar cracking.

### **Forms**

The concrete forms are expected to be straight and true, able to withstand the internal and external pressures without leaking or damaging the concrete. Exhibit 27 (ACI 347-63) provides basic guidelines for slip-formed forms. Exhibits 4, 5, and 6 are project specifications detailing the requirements and the QA system to monitor the forms.

Exhibit 4:

“The Shield Building walls will be constructed by the slip-form method as described in Specification No. 7749-C-38. Forms shall be constructed in accordance with the applicable Provisions of ACI 347 except as modified herein on the drawings. Forms shall be of wood, metal, structural hard board or other suitable material that will produce the required surface finish. Forms shall be constructed to conform to the shape, form, line and grade required, and shall be sufficiently rigid to prevent deformation under load and be so designed to be removed readily without injuring the concrete. Joints shall be mortar tight and arranged to conform to the pattern of the design required...”

Exhibit 5:

“The basic slip-forms will consist of a four foot high form on the inside and outside face of the wall, constructed of vertical staves (1" x 4" T&G flooring) with walor [sic] segments cut to the prescribed radius. The segments are cut from 2" lumber and are three laminations thick for each segment.

The form will be erected with a slight batter, that is, narrower at the top than at the bottom. This is to prevent the concrete from creating excessive friction on the form sides and allow the wall concrete to assume the proper width, approximately half way up in the form.”

Exhibit 6:

“Parting agent shall not be used in the slip-form operation.”

The design detailed in Exhibit 5 is intended to ensure that the forms slide over the fresh concrete with minimal friction and no damage to the setting concrete.



The observed finish of the wall surface shows no signs of damage due to leaking forms or "friction tear."  
It is concluded that forms design and operation did not cause the laminar cracking.

**Slip-form speed**

The rate of movement of the forms is specified in Exhibit 5 (ACI 347-63) as follows:

"When in the opinion of the Slip Form Superintendent the concrete in four foot section has attained its proper set the jacking operation will be initiated. Thereafter, the rate of the forms vertical movement will be controlled by the Slip Form Superintendent, based Upon the setting rate of the concrete, placing of reinforcing bars, placing of inserts and openings. A minimum of 13" to 20" of firm concrete must be attained in the lower part of forms to provide Support at all times for fresh concrete."

Thorough review of project documents, including daily inspection records, NCRs, and other communications did not show any problem with the slip-forming speed.

Slip-form speed is not considered a cause of the laminar cracking.

**Jacking Rods Locations/Dimensions**

The location/dimension of jacking rods is specified in Exhibit 5 (ACI 347-63) as follows:

"IN THE DESIGN OF THE FORMS IN WHICH JACKS ON VERTICAL RODS ARE USED, CARE MUST BE TAKEN TO PLACE JACKS IN SUCH A MANNER THAT THE VERTICAL LOADS ARE AS NEARLY EQUAL AS POSSIBLE AND DO NOT EXCEED THE SAFE CAPACITY OF THE JACKS. THE STEEL RODS OR PIPE ON WHICH THE JACKS CLIMB OR BY WHICH THE FORMS ARE LIFTED SHOULD BE ESPECIALLY DESIGNED FOR THIS PURPOSE. THESE RODS MUST BE PROPERLY BRACED WHERE NOT ENCASED IN CONCRETE. JACKING RODS OR PIPES MAY BE LEFT IN CONCRETE OR WITHDRAWN AS CONDITIONS PERMIT BUT SPLICES AND LOW BOND VALUE MUST BE GIVEN SPECIAL CONSIDERATION IF THEY ARE TO BE USED AS REINFORCEMENT."

Jack rod layout is detailed in Exhibit 28. Eighty (80) pairs of jack rods were spaced evenly around the structure, located inside the reinforcing mats. Photos taken during construction and observations made during demolition show jack rod installation in compliance with the specifications.

The Jacking Rods are 5/8 inch diameter, mild steel sections that extend from the foundation to the top of the vertical wall. No correlation was observed between the location of the laminar cracks and the Jack-Rods.

Thorough review of project documents, including daily inspection records, NCRs, and other communications did not show any problem with the Jack rods.

Jacking Rod Locations/Dimensions is not considered a cause of the laminar cracking.

**Verified Supporting Evidence:**

None

**Discussion:**

See above

**Conclusion:**

The Listed Construction Issues did not cause the Laminar Cracks



## FM 2.6 – Voids near Rebar

**Description:**

This potential failure mode will examine whether localized voids near the reinforcing steel caused or contributed to the identified laminar cracking.

When dense reinforcing bars are located in a structure where low-slump concrete with large aggregates is placed, there is a potential for deficient consolidation and resulting voids.

**Data to be collected and analysed:**

Observations during demolition process.

**Verified Supporting Evidence:**

None

**Verified Refuting Evidence:**

- During the hydro-demolition activities to create the 2011 construction opening there were numerous reinforcing steel bars exposed. Visual examination of the construction opening rebar did not identify any unusual voids near the rebar.
- For practical reasons it was not feasible to obtain core samples containing intact rebar/concrete interfaces. However, Petrographic analysis and voids analysis did not reveal significant difference between samples taken adjacent to steel and samples taken some distance from the steel.
- Analysis of the vibration methodology used (FM 2.2 – Concrete Placement) did not identify any deficiencies.

**Discussion:**

It is believed that except for the normal air trapped under horizontal bars during the placement process there were no unusual voids created near rebar.

**Conclusion:**

There were no excessive voids near rebar and such voids were not a cause of the Laminar Cracks



## FM 2.7 – Concrete Sealant

### **Description:**

Concrete sealants are recommended for use on concrete walls exposed to freezing conditions because concrete's porous nature allows external moisture to penetrate the concrete. Under wind driven rain conditions the depth of penetration and amount of water may be significant.

### **Data to be collected and Analysed:**

Exhibit 5 - QA and procedures slip form construction - Vendor Document 7749-C-38-3-1  
Slip form field data summary (Exhibit 20) provides information about the sealant used for curing.  
ACI 515 is the authoritative source of recommended practice for application of sealant to concrete.

### **Verified Refuting Evidence:**

According to Exhibit 20, Grace's Clear Seal #12 was applied to the concrete under the moving forms. There is no record of the product's composition or performance, but based on similar products it is believed that this was a curing/sealing compound intended to lock moisture inside the concrete during the curing period. These products are not intended for long term sealing of concrete against external moisture and they tend to lose effectiveness under environmental exposure.

### **Verified Supporting Evidence:**

There is no record of the application of a sealant to the vertical walls since the structure was constructed.

### **Discussion:**

ACI 515.1 R-79 (not available during construction) is 'A Guide to the Use of Waterproofing, Damp-proofing, Protective, and Decorative Barrier Systems for Concrete.' Section 2.2 sets the standard-of-care for using water proofing and makes the case for applying water-proofing or damp-proofing to the wall:

"2.2-When waterproofing is used

Waterproofing is normally used to prevent leakage of water into, through, or out of concrete under hydrostatic pressure. **If freezing and thawing conditions exist, as in above-grade applications** or if water is carrying aggressive chemicals which attack reinforcing steel or concrete, **then the waterproofing barrier will be used to prevent leakage into the concrete...**

Waterproofing is also used to minimize unsightly carbonates or efflorescence.

2.2.1 Water leakage into and through concrete - Water may be forced through concrete by hydrostatic pressure, water vapor gradient, capillary action, **wind-driven rain**, or any combination of these. This movement is aggravated by porous concrete, cracks or structural defects, or joints that are improperly designed or installed... Waterproofing membranes are intended primarily to prevent the passage of water in liquid form. They also retard the passage of water vapor in varying degrees depending on the type of membrane..."

According to Davis-Besse specification C-38 (Exhibit 5):

"9.2 Curing

The Shield Building concrete, except as otherwise approved by the CONSTRUCTION MANAGER, shall be cured by the liquid membrane method. The liquid membrane curing compound shall conform to Clear Seal No. 150 as manufactured by Grace and Company, Cambridge, Massachusetts, or approved equal. Application shall be in accordance with the manufacturer's instructions. The liquid membrane shall be applied to all slip-form wall surfaces. The membrane shall be applied to within 2 feet (two feet) of the bottom of the slip-form after the concrete surface has been finished."





The product used is no longer available, but similar sealants have limited life (need reapplication periodically) and are mainly intended to provide the concrete with protection for the curing period. This curing compound can be assumed to be inefficient after 12 months.

At Davis-Besse the contractor was instructed to remove the membrane by sand-blasting if paint or special coating application was required.

The Shield Building surface was inspected with the following results:

- Surface cracks appear to be tight
- No surface staining exist (no corrosion, carbonates, or efflorescence)
- No freeze thaw damage on the surface
- No or limited signs of spalling (one case identified at the flute corner, reference CR 2011-05648)

Based on the above there is no evidence of surface damage from water infiltration.

Although no signs of surface infiltration were found, the lack of concrete sealing can allow water ingress into the concrete. If the concrete was to achieve a high moisture content followed by sub-freezing conditions, it could create a situation where icing condition would exist. This icing condition could be a contributor to concrete cracking if the moisture content was sufficiently high and widespread.

**Conclusion:**

The inadequate Concrete Sealant was a contributing cause to the Laminar Cracks



## FM 2.8 – Concrete Rebar Adhesion

<b>Description:</b> This failure mode pertains the lack of adequate concrete to rebar adhesion may have caused/contributed to the formation of the laminar cracks.
<b>Data to be collected and analysed:</b> Observations during demolition process.
<b>Verified Supporting Evidence:</b> None
<b>Verified Refuting Evidence:</b> <ul style="list-style-type: none"><li>• Direct observation of the concrete/rebar adhesion was performed by the FENOC staff during the initial investigation of this issue. There were numerous examples of concrete strongly adhered to the rebar. There was at least one example where the concrete was adhered to the end of a rebar which posed a potential hazard to personnel working below.</li><li>• While it would not be unusual to have small localized areas where the concrete to rebar adhesion varies, there were no observed large scale areas of less than adequate concrete to rebar adhesion.</li><li>• In reinforced concrete design it is assumed that deformation bearing against the concrete, and not adhesion, facilitate the transfer of stresses between steel and concrete. Therefore, loss of adhesion and slippage is not expected to lead to failure.</li></ul>
<b>Discussion:</b> None
<b>Conclusion:</b> Deficient concrete to rebar adhesion was not a cause of the Laminar Cracks



## FM 2.9 – Amount of Rebar in the Structure

**Description:**

This potential failure mode will examine if the amount of rebar in the structure may have caused or contributed to the identified laminar cracks.

**Data to be collected and analysed:**

Exhibit 41 - Drawing C-110

Exhibit 40 - Drawing C-111

Exhibit 39 - Drawing C-112

**Verified Supporting Evidence:**

None

**Verified Refuting Evidence:**

Maximum reinforcement ratio:

For a member under axial force and bending, current ACI provisions limit the reinforcement ratio to 8%, while at the spring line the ratio is  $(1.56 \times 2 \times 3) / 30 / 12 = 2.6\%$ . Note that ACI 318-63 does not have limits the reinforcement ratio for members under axial force and bending.

The maximum reinforcement ratio for a single reinforced beam, which does not apply here (see section 1601 of ACI 318-63 where  $k_1$  is 0.85 for 4000 psi concrete).

Considering the spring line as a beam, they need to use the equations for double reinforced beams, in such case the maximum rebar ratio is given in ACI 318-63 section 1602, see below. Note that this ratio is always met since  $p = p'$ .

Minimum reinforcement spacing:

The regions with 2"-3" rebar spacing are localized and therefore should not affect the global behavior of the structure. In fact bars with such spacing can be considered a bundle. However it must be noted that per ACI 318-63 bundled rebar must be enclosed by ties or stirrups.

The majority of the cracking has occurred in areas where the reinforcing steel is #11 at 12" spacing, inside and outside face. This reinforcing pattern is not considered excessive.

Therefore, the rebar density does not seem uncommon or unusually high for this type of structure.

**Discussion:**

Refer to FM 1.5 for additional discussion

**Conclusion:**

Amount of rebar in the structure was not a cause of the Laminar Cracks



## FM 2.10 – Rebar Lap Splice

<b>Description:</b> This failure mode will review the potential for rebar lap splice to have caused/contributed to the laminar cracking issue.
<b>Data to be collected and analysed:</b> Exhibit 41 - C-0110 Roof plan wall section details Exhibit 43 - Calculation C-CSS-099.20-054
<b>Verified Supporting Evidence:</b> None
<b>Verified Refuting Evidence:</b> See FM 1.4
<b>Discussion:</b> None
<b>Conclusion:</b> Rebar lap splice did not cause the Laminar Cracks



## FM 2.11 – Small Rebar Spacing

**Description:**

This failure mode will be reviewed to determine if small rebar spacing caused or contributed to the laminar cracks in the Shield Building. The small rebar spacing reduces the quantity of concrete available to carry the tensile stresses that may act on the structure

**Data to be collected and analysed:**

Exhibit 41 - Drawing C-110

Exhibit 44 - Drawing C-111A

Exhibit 39 - Drawing C-112

Exhibit 51 – Rebar density sensitivity study by PII

**Verified Supporting Evidence:**

- Laminar cracks were observed at the top of the shield building
- Laminar cracks were observed around the construction opening
- Laminar cracks were observed around the main steam line penetration
- A 'Rebar Spacing Sensitivity Study' was performed by PII (exhibit 51). The study established that higher density of rebar could lead to more laminar cracking under a given stress condition.

**Verified Refuting Evidence:**

The identified laminar cracks are primarily located in the architectural shoulder areas of the Shield Building, Ref. Drawing C-111A. Cracks were also identified in two locations that had a higher density of reinforcement. The top 20 feet of the Shield Building wall has #11 horizontal rebar spaced at 6 inches on center, Ref. Drawing C-110. The lap splice locations would have even a smaller spacing between rebar. The other area of concentrated rebar is located at the two main steam line penetration areas. There is horizontal rebar spaced at about 6 inches per Detail 3 on Drawing C-112.

The identified rebar spacing is not unusually small for nuclear power plant structures. Therefore the small spacing is not considered to be the cause for the laminar cracks. The small rebar spacing described above may have contributed to the propagation of the cracks that originally formed in the shoulder areas.

**Discussion:**

A study to evaluate freezing failure and rebar spacing (exhibit 51) found that for a given motivating force, large laminar cracks form in regions with dense rebar and not in regions with sparse rebar.

**Conclusion:**

Small rebar spacing may be a contributing cause to laminar cracking



## FM 2.12 – Out-of-Plumb

### **Description:**

Dynamic construction of tall vertical walls requires special attention to plumbness control. If walls are allowed to shift beyond an allowed degree it can create a condition of excessive stresses for which the wall was not designed.

### **Data to be collected and Analysed:**

Plumbness specifications (Exhibit 6) (Specification C-38 - TECHNICAL SPECIFICATIONS FOR THE SHIELD BUILDING No 7749-C-38) includes description and instruction for the slip-form work;  
Plumb control QA specifications (Exhibit 5) (Specification C-38 - QUALITY ASSURANCE AND CONSTRUCTION PROCEDURES REACTOR SHIELD WALL SLIP FORM CONSTRUCTION METHOD);  
Plumb control measurements (Exhibit 18) from original QA during construction;  
Exhibit 19 - Out-of-plumb Interim Field Report.

### **Verified Refuting Evidence:**

Exhibit 6 (page 13 of 22) specifies construction tolerances for plumbness:

“The cylindrical wall of the completed Shield Building shall be plumb within 4 inches (four inches) from top to bottom and shall be not more than 1 inch (one inch) out of plumb in any 25 feet (twenty-five feet).”

Exhibit 5 provides the specifications for plumb control during wall construction:

“The wall plumbness will be measured at 16 equally spaced stations on the moving forms at the inside face of the wall with a Wild ZNL 16 optical plummet (sic). The instrument bases will be installed so that the wall face exposed by the form movement can be compared with a target at the bottom of the wall.

These readings will be taken by the Job Engineer at eight-hour intervals during the slip form operation, recorded, on the plumbness record form (see Form #2), and then submitted to the Quality Control Engineer for his use.

If the deviations from plumb, as plotted on the master control chart, indicate that corrective measures are necessary, the Quality Control Engineer will inform the Job Superintendent (see Fig. 1).

The slip form and working platform level will be adjusted as directed by the Slip Form Superintendent to allow the whole structure to go back to its original position. These adjustments will be made thru control of individual jacks by the jacking crew and/or use of a telescoping leg and guide wheel system mounted on the jacking yokes...”

Exhibit 18 is a plot of plumb measurements at the required 16 points during construction. It shows out-of-plumb measurements of up to 3-3/4”. In all cases the forms were brought back to plumb and construction continued.

Exhibit 19 - Out-of-plumb Interim Field Report concluded:

“Engineering has reviewed the Interim Field Report and its attached plumbness plots [Exhibit 18]. Out of tolerance exceeds the 1” in 25’ specified by 2-3/4”. The effects this has on the shield building structural integrity were found to be insignificant.

Engineering recommends that all interface work be adjusted to meet the as-built alignment of the structure.



The structure is accepted as is.”

It is concluded that out-of-plumb condition was not a cause of the Laminar Cracks.

**Verified Supporting Evidence:**

None

**Discussion:**

Documentation of the Out of Plumb condition was limited to the documents provided. We do not have information regarding the method of correcting the problem and whether it caused excessive friction forces.

- Attempts to correlate these locations to locations of cracking found no significant correlation. The out-of-plumb condition peaked at three distinct (Exhibit 18) elevations that did not correspond to cracking as determined by CTL.
- Exhibit 5 (Project specifications) provides information regarding design considerations that reduce friction.
- The rate of slip-forming (average about 4' per shift) is fast enough to minimize friction problems.
- The observed cracking through aggregates is further indication that the laminar cracking happened after the concrete reached sufficient maturity and not during placement.

**Conclusion:**

The out-of-plumb issues did not cause the Laminar Cracks



## Appendix VII Group 3 Failure Modes

### FM 3.1 – Earthquake

<p><b>Description:</b> Earthquake related movement has the potential to cause elevated stresses in any concrete structure. These stresses can, in combination with other existing stresses, contribute to cracking of concrete. This FM will review Earthquake (EQ) incidents at the Davis-Besse power plant and their effect on the structure. This failure mode hypothesizes that the oscillating forces from an earthquake may excite the shield building into large resonant vibrations at its fundamental frequency, 3.8 Hz. The resonant vibrations of the shield building may produce both shear stress and radial stress in the shield building, causing laminar cracks in outer rebar mat.</p>
<p><b>Data to be collected and Analyzed:</b> Classifiable Events records for Davis-Besse – Exhibit 37</p>
<p><b>Verified Supporting Evidence:</b> None</p>
<p><b>Verified Refuting Evidence:</b></p> <ul style="list-style-type: none"><li>• Davis-Besse Safety Related structures, including the Shield Building is designed for two types of earthquakes. The Operating Base Earthquake (OBE) with a ground acceleration of 0.08g and the Safe Shutdown Earthquake (SSE) with a ground acceleration of 0.015g.</li><li>• The site as a seismic monitor trigger station that senses very low ground accelerations. The threshold for the seismic trigger is 0.01g with a range of 1 - 10 Hz. Based on a review of historical seismic data recorded in the location near the shield building of the Davis Besse Nuclear Power Plant between 1971 to present, there has been no earthquake detected and registered. In addition, a review of the historical data in the vicinity of Davis-Besse also revealed no significant seismic activities</li><li>• Davis-Besse had only one classifiable event from seismic activity which was on 3/5/1986 (event #3837). Computer and annunciator alarms were received for an operating basis earthquake (OBE) - longitudinal and an Unusual Event was declared due to the seismic trigger actuation. No seismic activity was detected at Perry, Fermi, or the University of Toledo so the event was terminated after safety system walkdowns. Davis-Besse was in cold shutdown at the time of the seismic event from a loss of feedwater event that occurred eight months earlier on 6/9/1985.</li></ul>
<p><b>Discussion:</b> Above</p>
<p><b>Conclusion:</b> The Earthquake Classifiable Event at Davis Besse was not a cause of the Laminar Cracks</p>





## FM 3.2 – Lightning

**Description:**

This potential failure mode review will examine the effect of lightning strikes on the reinforced concrete Shield Building. There is a potential that a lightning strike could increase the temperature of the concrete which would cause a sudden expansion of the concrete which would result in a laminar crack.

**Data to be collected and Analysed:**

Exhibit 6 - Specification C-38

Exhibit 47 - Drawing E-401 Shield Bldg. Lighting and Lightning Protection

Exhibit 48 - 1995-0395 Lightning Potential Condition report

**Verified Supporting Evidence:**

Exhibits 48 reports on a single condition of potential lightning strike on 5/10/1995. The conclusion was that this was a non-reportable condition and that the observed spall is not likely to be lightning related.

**Verified Refuting Evidence:**

Specification C-38 Section 11 describes the temporary and permanent lightning protection system for the shield building. Drawing E-401 details the Shield Building lightning protection system. The Shield Building is well grounded. As shown on Drawing E-401, there are a total of 27 Air Terminals anchored to the top exterior of the shield building, 18 equally spaced around the parapet top, 8 equally spaced at the mid height of the dome, and one located at the top center of the dome. These Air Terminals are all interconnected and penetrate the concrete dome in 9 locations, 4 equally spaced near the parapet wall, 4 equally spaced at the mid height of the dome, and one at the top center of the dome. The grounding cable passes through the concrete and is then connected to the containment vessel at the nearest point. There are 9 interconnected locations provide a path for the lightning to immediately exit the structure without traveling down the sides of the building to ground.

These systems provide the needed protection against lightning strikes.

**Discussion:**

None

**Conclusion:**

Lightning Event at Davis Besse was not a cause of the laminar crack.



## FM 3.3 – Tornado

**Description:**

On June 24, 1998, a F2 tornado (113 – 157 mph wind speed) passed in close proximity to the shield building of the Davis Besse Power Plant. The pathway of the 1998 tornado was about 300 ft. north of the shield building. Note: Davis-Besse is design for a 300 mph tornado with a 3 psi differential pressure in addition to tornado generated missiles.

This failure mode hypothesizes that the vortex shedding from the tornado, as it passed by the shield building, could have excited the building into vibrations, resulting in low cycle fatigue cracks in the outer rebar mat. Moreover, the dynamic loading of the swirling wind from the tornado could have resulted in the observed the laminar cracking.

**Data to be collected and Analysed:**

Exam of core samples  
Wind related stresses – Exhibit 62

**Verified Supporting Evidence:**

None

**Verified Refuting Evidence:**

A detailed wind related stress modeling analysis was performed and reported in Exhibit 62. The analysis concluded that wind velocity of 105 mph resulted in stresses of less than 1 psi around the area where laminar cracks were observed. Clearly, scaling the wind velocity up to 150 mph (tornado wind) would not create significant stresses that would be sufficient to either initiate or propagate the laminar cracks. Moreover, PII did not observe any fine cracks near the main fracture surface. This evidence indicated that vibrations from tornado would not have been the cause to propagate the cracks.

**Discussion:**

Above

**Conclusion:**

The Tornado Event at Davis Besse was not a cause of the laminar cracks.



## FM 3.4 – Electrical Potential

<b>Description:</b> This failure mode hypothesizes that unbalance of electrical potential of the shield building was set up in different parts of the shield building due to failure of grounding system or different concrete/rebar material properties. The existence of the unbalance of electrical potential sets off accelerated rebar corrosion in certain areas of the shield building due to galvanic effects. The rebar corrosion, in turn, resulted in the cracking of concrete.
<b>Data to be collected and Analyzed:</b> Exhibit 49 - Photos from construction opening Exhibit 68 - Photometric's report that discusses corrosion
<b>Verified Supporting Evidence:</b> None
<b>Verified Refuting Evidence:</b> The Refuting Evidences against this failure mode are described below: <ul style="list-style-type: none"><li>• The rebar corrosion was observed to be minimum in all rebar visible during opening of the shield building and in one core sample that was inadvertently drilled to be in contact with an inner mat rebar (Exhibit 68 - ~18 mils of corrosion thickness in this sample). The observed level of corrosion is considered normal and is not sufficient to produce stress in the concrete and cracks near outer mat rebar,</li><li>• All electrical grounding system was functional without registering loss-of-grounding alarms since the plant operation.</li><li>• Based on construction records, the concrete mix and material properties of rebar were found to be the same throughout the building.</li></ul>
<b>Discussion:</b> Above
<b>Conclusion:</b> Electrical Potential was not a cause of the laminar cracks



## FM 3.5 – Hydro-Demolition Damage

### **Description:**

The process of hydro-blasting exploits the existence of micro-cracks, voids, capillaries and cracks to enable concrete demolition using high pressure water jets. This raises the question of potential damage to concrete in adjoining area through direct pressure, vibrations, or crack propagation.

This document is intended to determine if hydro-blasting can cause cracking and if any occurred at Davis-Besse

### **Data to be collected and Analysed:**

Review literature Exhibit 21 is a "Guide for the Preparation of Concrete Surfaces for Repair Using Hydrodemolition methods", Exhibit 22 includes selected pages from ACI 546R-04 "Concrete Repair Guide", Exhibit 23 includes selected pages from the book "Hydrodemolition of Concrete Surfaces and Reinforced Concrete" by Andreas Momber, Exhibit 24 is a published article "Hydrodemolition for Removing Concrete", and Exhibit 25 is a research report from Missouri Department of Transportation "Hydrodemolition and Repair of Bridge Decks");

### **Verified Refuting Evidence:**

1. Literature review shows a consensus that hydro-demolition does not cause significant damage to adjacent material (see highlighted sections of Exhibits 21, 22, 23 and 24). Alternative mechanical and impact methods can damage the residual concrete that is to be repaired (see for example Exhibit 21, pages 3 and 4 of 16);
2. Hydro-demolition removes concrete not by impact, but by introducing high-pressure water into existing voids (Exhibit 23). The high internal pressure in these voids causes the concrete to fail, spalling the surface material;

### **Verified Supporting Evidence:**

Hydro-demolition works through the introduction of high pressure water into cracks (Exhibit 23). If a delamination crack is encountered during demolition, the water will fill it and exert pressure internally, potentially accelerating propagation.

### **Discussion:**

Delamination cracks at Davis-Besse were found throughout the structure. This rules out hydro-blasting as the universal cause.

Delamination cracks in the demolition area were not spread around the opening, as would be expected if hydro-blasting was the cause.

The mechanism of hydro-blasting supports propagation of existing cracks as the result of the demolition. It is possible that some crack extension was caused by the hydro-blasting, but there is no evidence that this extended beyond the opening.

### **Conclusion:**

The hydro-blasting did not cause the Laminar Cracks



## FM 3.6 – Freezing of Water near Rebar in a Blizzard

### **Description:**

A blizzard is a severe storm characterized by sustained winds or frequent gusts that are greater than or equal to 35 mph, blowing or drifting snow which reduces visibility to ¼ mile or less and lasts for three hours or more.

The top three blizzards, in terms of freezing temperature and duration, occurred near the Davis-Besse Power Plant in 1977, 1978, and 1994.

The lowest temperatures registered during these blizzards are:

- -6 degree F (1977)
- -24 degree F (1978)
- -17 degree F (1994)

The event that is of particular interest to the analysis was the 1978 blizzard that struck the Toledo area on January 25th and lasted through January 27th 1978. According to NOAA records (Exhibit 66), this blizzard is one of the worst on record for the Great Lakes area with southwestern winds of 105 mph.

This failure mode hypothesizes that wind induced pressure during a severe storm caused water to penetrate the concrete and remain trapped in the voids around the outer mat rebar. Upon freezing during blizzards, the volume expansion near rebar would cause laminar cracks. There are two sub-modes for this failure mode. One is related to the freezing of water near outer rebar, and the other is related to the expansion of concrete due to ice formation (see discussion below).

### **Data to be collected and analyses to be performed:**

PII used the state-of-the-art concrete stress and fracture analysis modeling techniques to understand the feasibility of the failure mode. These modeling techniques were originally developed as a part of the Crystal River-3 (CR3) root cause investigation and calibrated against the CR3 fracture and temperature data. Note that the CR3 root cause investigation was extensively reviewed by the US Nuclear Regulatory Commission (NRC) over a period of more than one year and has received no negative comments from the NRC.

For the first sub-mode, detailed finite element analysis was performed to show the damage development in dense rebar areas due to the formation and accumulation of ice (Exhibit 51 and Exhibit 51 Appendix). Extensive finite element analyses (FEA) showed that the second sub-mode can be used to explain the increase in radial stress and the damage development in the shell during the blizzard. The coefficient of thermal expansion (CTE) of Davis Besse concrete was considered to be temperature dependent, which means the concrete expands in a certain low temperature range. PII continues to explore the CTE phenomenon and its effects on concrete expansion. The temperature dependent CTE is discussed in Exhibit 57. Exhibit 64 presents the results of finite element thermal analysis for internal



temperature fields in the structure. Exhibit 61 presents the results of finite element stress analysis. Exhibits 66 and 71 present meteorological information used in the analysis.

Exhibit 72 explains the sources of water used in the analysis.

Exhibit 73 describes the model and conclusions of FEA analyzing the effect of the 1978 blizzard.

- Exhibit 51 - Freezing-Failure-study-DRAFT-report-section-Rev-0\_95
- Exhibit 51 - appendix-Freezing Failure study Rev 0 95
- Exhibit 57 - Temperature dependent CTE - v04
- Exhibit 61 - 2012-02-11 Stress State during the 1978 and 1977 Blizzards
- Exhibit 64 - Thermal Stress Analysis with Gravity and Wind Load
- Exhibit 66 - Toledo 1978 weather
- Exhibit 71 - Comparison of Toledo Blizzards
- Exhibit 72 - Water and moisture transfer into concrete - v02
- Exhibit 73 - 2012-02-12-Laminar-Cracking-due-to-1978-Blizzard-Rev-0\_1-DRAFT

**Verified Supporting Evidence:**

The following are the supporting evidences:

1. The crack is considered a circumferential laminar crack and not a through-thickness crack.
2. The location of the crack is limited to the outer reinforcing (rebar) mat, not the inner mat rebar due to the fact that the water accumulated near outer rebar.
3. The cracking is prevalent in the flute shoulder areas.
4. The crack is also prevalent in the higher reinforcing areas at the top of the shield building and along the blockouts for the main steam line room penetrations
5. Cracking is more prevalent in the South and Southwest quadrant of the shield building
6. Cracking is less prevalent in the flute areas and the shell areas (between the shoulder areas).
7. The shield building exterior surface was not sealed with a water resistant sealer, so moisture can penetrate into the concrete.

**Verified Refuting Evidence:**

None

**Discussion:**

Analysis to evaluate Laminar Cracking due to 1978 Blizzard (exhibit 73) concluded that:

- Cracking is predicted due to the 1978 blizzard and not due to the 1977 blizzard:
  - The 1978 blizzard produced stresses and strain energy adequate to initiate cracks at the of rebar mat.
  - The 1977 blizzard did not produce conditions sufficient to initiate cracks in the concrete.
- The locations of the cracking are confined to the observed crack locations under the thick



sections of the shoulders and not in the thinner sections in the flute and panels.

Another study to evaluate freezing failure and rebar spacing (exhibit 51) found that only a small fraction of the voids under the rebar need to fill with water and freeze in order to get laminar cracks. It also determined that for a given motivating force, large laminar cracks form in regions with dense rebar and not in regions with sparse rebar.

The moisture diffusion and ice formation process in the shoulder area were not simulated by finite element model, because, as stated earlier, the moisture diffusion process is driven by two field variables: temperature and moisture. The two field variables are fully coupled. Moreover, the formation of ice in the pores of concrete changes moisture diffusivity of concrete since ice crystals in pores block the pathway of moisture and thus reduces the diffusivity; on the other hand, when an excessive amount of ice formed in pores, the ice generates cracks in concrete and thus increases the diffusivity of concrete (Eskandari-Ghadi et al. 2012; Xi and Nakhi 2005). Furthermore, the effect of high wind pressure on the outer surface of the wall makes the numerical modeling of moisture penetration process into concrete a very complicated task. Currently available commercial finite element programs can only handle such a sophisticated multi-physics problem with extensive customization to incorporate highly-specialized physics, which was not feasible within the scope of this project.

There are two small areas of laminar cracking in the shield building that are not exposed to blizzards due to their locations being inside the auxiliary building. The two areas are located 45 degree above the blockouts of the two steam line room penetrations. However, these two areas are connected to laminar cracks above the auxiliary building roof. It is believed that the laminar cracks in these two areas initiated above the auxiliary building roof, probably due a lower concrete tensile strength and a high density of rebar, and propagated downward into areas that were not exposed to blizzards.

#### **Sub-mode 1 - Freezing of water near outer rebar**

This sub-mode can be used to explain the laminar cracking in the shoulders. The damage process is shown in Fig. 1 by three stages:

1. As the environmental temperature drops below the freezing point during the beginning stage of a blizzard, the trapped water near the horizontal outer mat rebar would freeze first near the flute areas and in the shell area between two shoulders because, in these two areas, the horizontal rebar are closest to the cold surface (~ 3 inches), as shown in the upper figure in Fig. 1. The moisture in the pores of concrete behind shoulder remains in liquid or vapor states (no ice) because the shoulder keeps this area warmer.
2. As the blizzard continues, the temperature would continue to drop well below the freezing point of water. At this point, the water trapped near the outer mat horizontal rebar between the two first-freezing areas starts to freeze, i.e., in the areas directly behind the thick shoulders from the surface. The moisture behind the shoulder diffuses towards the ice fronts, which are located near the surface of the flute and shell wall. The diffusion directions of moisture are shown in the middle figure in Fig. 1. The moisture diffusion is driven by the maximum temperature gradient from the hottest area to the coldest area as well as by the maximum free energy gradient from the area with higher free energy (vapor and liquid) to the area with lower free energy (ice).



3. When the diffusing moisture reaches the ice fronts, it turns into ice. This is shown in the third part (the enlarged area) of Fig. 1. So, the ice fronts move from both sides (the flute and the shell wall) toward the middle of the shoulder. Due to the formation of ice at ice fronts and high density rebar in the shell wall, high pressure is generated there to push the crack to propagate in the shoulder.

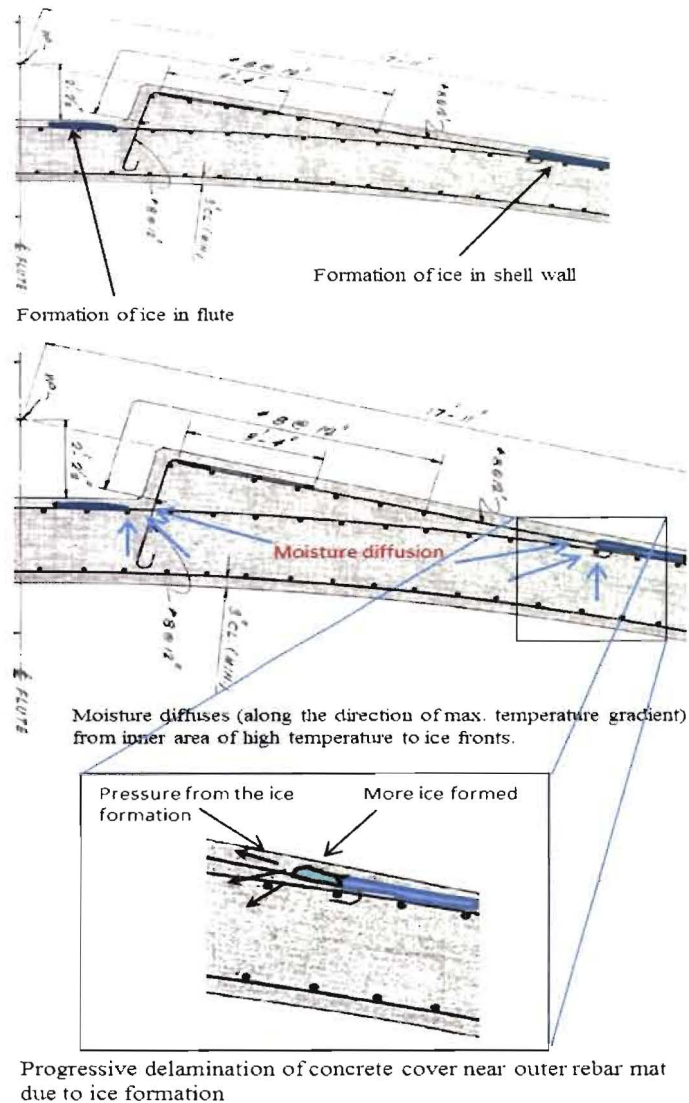
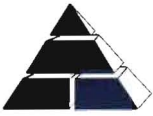


Fig. 1 Freezing damage near outer rebar mat in the shoulder

This failure mode would exist only under the following conditions in a severe blizzard:

- I. A significant amount of water is diffused into the gaps between outer mat rebar and the concrete due to wind induced surface pressurization.
- II. The environmental temperature is well below freezing point of water for a long period of time so that the





temperature near the outer rebar mat behind the shoulders (3 – 18 inches deep into the shield building) could drop below the freezing point (from a non-freezing state of a normal temperature range from 35 degree to 50 degree F).

- III. The temperature in the inside annulus of the shield building is low. Note that if the reactor is shut down during the blizzard, the inner surface temperature of the shield building will be in the range of 55 degree F, versus 105 degree F if the reactor is in operation.

### Sub-mode 2 - The expansion of concrete due to ice formation

Concrete may expand instead of contract during a cooling period. This is possible because of ice formation in the concrete. During the blizzard, as shown in Fig. 2, the temperature in outer layer of the cylindrical wall is lower than that of inner layer. So, the ice may form in the concrete of outer layer of the wall resulting in an expansion, while the inner layer of the wall has contraction. This special outer-expansion-and-inner-contraction deformation pattern may generate a tensile stress in the radial direction of the wall. Delamination cracking may occur in the case of high radial tensile strength. This failure mode was used to analyze the damage of concrete walls of more than 50 water tanks in Ontario, Canada (Grieve et al. 1987).

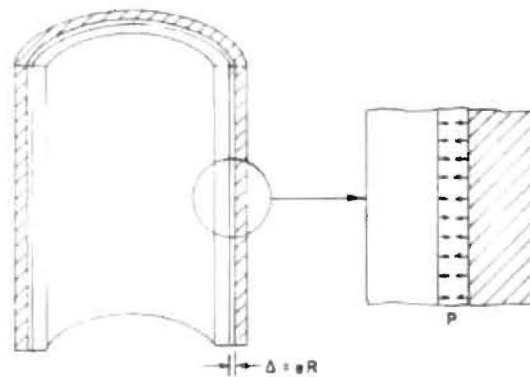


Fig. 2 Expansion of outer layer and contraction of inner layer of a concrete wall generate tensile stress in the radial direction (Grieve et al. 1987)

### References:

- Eskandari-Ghadi, M., Zhang, W.P., Xi, Y., and Sture, S. (2012) "Moisture Diffusivity of Concrete at Low Temperatures", *Journal of Engineering Mechanics, ASCE*, in press.
- Grieve, R., Slater, W.M., and Rothenburg, L. (1987) "Deterioration and Repair of Above Ground Concrete Water Tanks in Ontario, Canada", *Research Report to Ontario Ministry of the Environment*, Golder Associates and W.M. Slater & Associates, Inc.
- Weblink: [http://www.greatlakes.salsite.com/Toledo\\_Snowstorms.html](http://www.greatlakes.salsite.com/Toledo_Snowstorms.html)
- Xi, Y. and Nakhi, A. (2005) "Composite Damage Models for Diffusivity of Distressed Materials", *J. of Materials in Civil Engineering, ASCE*, May/June, 17(3), 286-295.

### Conclusion:

Freezing of water near rebar during the Blizzard of 1978 caused the Laminar Cracks.



## FM 3.7 – Long Term Thermal Stress Cycles

### Description:

This failure mode hypothesizes that solar exposure and repeated cycles of thermal expansion of the concrete near the surface cause radial stresses high enough to produce radial cracks near the outer rebar mat.

### Data to be collected and Analysed:

Data regarding the environmental conditions around the shield building was collected and analyzed for resultant stresses and strains. Details can be found in:

[Exhibit 64](#) - Thermal Stress Analysis with Gravity and Wind Load

[Exhibit 56](#) - structural and thermal analysis investigation

[Exhibit 78](#) - Test data of Photometric lab report

[Exhibit 26](#) - WJE Lab report

### Verified Supporting Evidence:

The supporting evidence is that the cracking in the south-west quadrant of the shield building, which is typically at a higher temperature due to solar heating, is more prevalent than the north-east quadrant of the shield building.

### Verified Refuting Evidence:

The refuting evidence is detailed below:

1. A detailed finite element analysis was performed ([Exhibit 64](#)) to determine the radial stresses near the outer rebar mat. It was determined that the resultant stresses were not high enough to cause damage.
2. Thermal and shrinkage strains ([Exhibits 56 and 64](#)) were not high enough to cause the cracking.

### Discussion:

#### Thermal fatigue damage

Thermal fatigue can be considered from three aspects:

- (1) Stress level caused by temperature gradient
- (2) Damage, such as cracking, due to thermal strain variation
- (3) Damage due to elevated temperature.

*The stress due to solar temperature variation.* The finite element thermal stress analysis (see [Exhibit 64](#)) showed that the maximum radial stress in the structure is about 300 psi during a record hot summer day. That is about 33% of the tensile strength of the concrete and well below the fatigue limit of concrete under cyclic loading, which is about 55% for  $10^7$  cycles (Mindess et al. 2003, p343). It is important to note the 300 psi radial stress is the maximum peak stress occurred in the structure due to solar heating, and it is not regular daily temperature variation. The cyclic stress due to regular daily temperature variation is below 300 psi, and the corresponding stress ratio is below 33%. Accordingly, thermal stress due to cyclic solar loading is not a root cause.

*The thermal strain.* The surface strain of concrete under solar heating is a combination of thermal expansion and drying shrinkage. Thermal expansion creates compressive stress in the surface of concrete. The stress level is well below the compressive strength of concrete (see [Exhibits 56 and 64](#)). The drying shrinkage creates tensile stress of concrete, which could generate cracking in concrete. This



is especially important for early age concretes. In some cases, solar heating cycles can combine with other factors to cause cracking in concrete. Bier et al (1991) showed that, in addition to solar heating cycles, repeated heating of hot exhaust gases of the auxiliary power unit of aircraft can generate significant shrinkage cracking in concrete pavement. In our case, there is no other cyclic loading that have continued for 40 years during the life span of the structure. The petrographic analysis results (see Exhibit 26 WJE report) showed that the depth of shrinkage cracking is not more than one inch after 40 years of exposure to the environment. This depth is relatively small comparing to the depth of concrete cover. More importantly, the internal surfaces of many concrete samples were examined by microscopes (see Exhibit 78), and there is no significant amount of microcracking in the concrete. This indicates that the small surface shrinkage cracks did not coalesce to form discrete large cracks. So, the thermal strain and shrinkage cracking due to cyclic solar loading is not a root cause.

*The damage due to elevated temperature.* It is well known that properties of concrete change under elevated temperatures (Phan 2002; Lee et al. 2008). There are phase changes taking place in concrete when the temperature is above 100°C (e.g. vaporization of water, decomposition of calcium hydroxide, etc.). Upon fast heat (e.g. 20°C/min.), the rapid increase of vapor pressure may cause spalling of concrete. In the case of solar heating and cooling, the temperature level and the rate of temperature variation are not sufficient to generate significant phase transformation and spalling damage in concrete. So, the elevated temperature due to solar heating is not a root cause.

#### References

- Bier, T.A., Wise, S., and Chang, P. (1991) "A Mechanistic Study of Failure of Concrete Subjected to Cyclic Thermal Loads", NCEL Contract Report CR91.008 by CEMCOM Research Associates, Inc., and University of Maryland.
- Lee, J.S., Xi, Y., and Willam, K. (2008) "Properties of Concrete after High Temperature Heating and Cooling", J. of Materials, ACI, July-Aug. 105(4), 334-341.
- Mindess, S., Young, J.F., and Darwin, D. (2003) "Concrete", Prentice Hall, 2nd Edition.
- Phan, L.T. (2002) "High-Strength Concrete at High Temperature—An Overview," Utilization of High Strength/High Performance Concrete, 6th International Symposium, Leipzig, Germany, Vol. 1, pp. 501-518.

#### Conclusion:

Long term thermal stresses cycling is not a contributor to the Laminar Cracks.



## FM 3.8 – Permafrost

**Description:**

This failure mode hypothesizes that the permafrost was formed in the outer rebar mat, causing the concrete to crack. Permafrost is a phenomenon that involves diffusion of water into warmer, but still under the freezing temperature, underground locations; and the water accumulated to amounts that may exceed the potential hydraulic saturation of the ground material (usual ground rocks). The consequential volume increase from over-saturated water produces cracks in parallel to the ground surface.

Permafrost will typically form in any climate where the mean annual air temperature is less than the freezing point of water. Exceptions are found in moist-wintered forest climates, such as in Northern Scandinavia and the North-Eastern part of European Russia, where snow acts as an insulating blanket. The bottoms of many glaciers can also be free of permafrost.

**Data to be collected and Analysed:**

Construction drawings:

Exhibit 44 - C-0111A

Exhibit 41 - C-0110

**Verified Supporting Evidence:**

None

**Verified Refuting Evidence:**

The Refuting Evidences include the following facts:

- The permafrost layer usually has a thickness much more than 0.01 inch, which is the average crack width of the cracks in the shield building. Typical permafrost thickness is greater than 2 ft.
- The mean air temperature near the Davis Besse Power Plant is greater than the freezing temperature of the water.
- All the identified laminar cracks are located a considerable distance above ground elevation.

**Discussion:**

None.

**Conclusion:**

Permafrost was not a contributor to the Laminar Cracks.







## FM 3.9 – Chemical Attack

### Description:

Concrete is vulnerable to multiple mechanisms of chemical attack that may lead to deterioration over time and potential failure. In porous materials, water can be the source of chemical processes of degradation by transporting aggressive ions. Therefore, controlling permeability is the main method for limiting chemical related damage. The two other factors affecting durability are the availability of aggressive ions, and the presence of concrete constituents that are vulnerable to these ions. Chemical attack may be prevented by reducing permeability, using non-reactive concrete components, and preventing aggressive ions from penetrating the concrete.

Chemical attack may be the result of Sulfate attack, acid and base attack, aggressive water attack, phosphate ion attack, Alkali Aggregate Reactions (AAR), Carbonation, efflorescence/leaching, and biological attack. A detailed discussion of these mechanisms is beyond the scope of this document and may be found in external sources (such as ACI 201).

The effects of chemical attack vary, but generally include loss of concrete cover accompanied by staining, erosion, reduction of concrete constituents, cracking, and spalling.

A visual survey is considered (ACI 349) an effective way of quantifying the effects of damage and identifying possible sources and composition of the aggressive chemicals.

This document will attempt to identify potential reactions and determine if any occurred in a way that impacted the observed failure.

### Data to be collected and Analyzed:

- Exhibit 1 - mix design
- Exhibit 2 - Lab Test results from CTL
- Exhibit 26 Test report from WJE
- Exhibit 29 Permeability vs Water Cement ratio
- Exhibit 32 - ACI 515 Protective systems
- Exhibit 55 - ACI 201.2R-08 table 6.3
- Reports of damage related to chemical attacks (exhaustive search of plant inspections was conducted)
- Exhibit 58 – Carbonation study of cores by PII

### Verified Supporting Evidence:

Test reports from WJE (Exhibit 26) describe:

“Secondary deposits thinly line virtually all the air voids throughout the concrete in Core F2. The deposits have an approximately equal thickness throughout and appear to consist of Ettringite and calcium hydroxide. The presence of these deposits in air voids typically suggests long term exposure to moisture migrating through the concrete...”

The same test report from WJE also states:

“Air voids in Core F4 contain secondary deposits linings in the same abundance and pattern as those of Core F2...”

### Verified Refuting Evidence:

1. The concrete meets industry standards for low permeability required for durability



## FM 3.9 – Chemical Attack

(Exhibit 55 - ACI 201.2R-08 table 6.3; Exhibit 1 – mix design; Exhibits 2 and 26 – representative Petrographic reports.

2. Petrographic report by CTL (Exhibit 2) for two concrete cores identified carbonation to a depth of 5-8 mm. Test report by WJE (Exhibit 26) for another two concrete cores identified carbonation of about 20 mm. These are small carbonation depths for the 40-year old concrete. More importantly, the thickness of concrete cover is much larger than carbonation depth and thus the current carbonation does not reduce the concrete's ability to protect the embedded steel.
3. Petrographic reports (Exhibit 2 and 26) found no evidence of destructive Alkali Aggregate Reaction (AAR). Nor were reactive components found in the aggregate.
4. There is no indication that the structure was exposed to significant levels of water borne aggressive chemicals.
5. Inspection of steel bars showed small corroded spots on rebars (Exhibit 33). Details are described in FM 3.10. The interface between rebars and surrounding concrete remains in good condition, with a small amount of rust on the surface of rebars. The limited corrosion and the small carbonation depths consistently indicate that carbonation and carbonation-induced steel corrosion did not cause the laminar cracking.
6. Inspections over the life of the structure did not detect any indication of damage due to chemical attack.

### Discussion:

#### Permeability

Industry standards, as demonstrated in Exhibit 31 from ACI 201.2R-08, use water to cement (W/C) ratio as an indication of concrete's permeability. It has been established that concrete with W/C of 0.4 or lower has voids system that is mostly made of disconnected discreet small voids – making it practically impermeable (Exhibit 29).

Based on data from all pour cards of concrete used in the containment structure it was established that the concrete was placed with W/C ratio average of 0.51. Exhibit 1 is a summary of mix designs used in the construction. These designs were prepared with W/C of 0.51.

Exhibit 2 is the CTL Petrographic report that made an attempt at estimating the W/C ratio. Estimates ranged from 0.45 to 0.55 which match the calculated values.

Based on the above it is concluded that the concrete has low permeability.

#### Alkali Aggregate Reaction

Alkali Aggregate Reaction (AAR) requires the presence of reactive aggregates in sufficient quantities to cause destructive expansion, as well as sufficient moisture. According to Petrographic reports (Exhibits





## FM 3.9 – Chemical Attack

2 and 26), the aggregates are composed of limestone, dolomitic limestone, argillaceous limestone, and other carbonate rocks. No potentially reactive materials were detected in the coarse or fine aggregates. Exhibit 2 concluded that:

“No alkali-silica reaction (ASR) gel is observed in the concrete, nor are any cracks observed associated with the particles.”

### Sulfate attack

Sulfate attack is a process of forming expansive products in the hardened concrete by converting cement components into Ettringite and/or Gypsum. This process requires permeable concrete, moisture, and availability of Sulfate ions.

As demonstrated above, the concrete has low permeability and there are no readily available sources of sulfate ions, either from the soil or the environment. The below-grade portion of the structure was constructed with Type II cement that would reduce its potential for sulphate attack.

Petrographic analysis found no evidence of Sulfate attack (Exhibit 2). A thin layer of secondary deposits reported by WJE (Exhibit 26) is not enough to create stresses of reduce strength and is likely the result of internal reactions (as opposed to external attack).

### Leaching and efflorescence

Leaching and efflorescence are a process and indication of moisture transfer through the concrete, resulting in the removal of dissolved salts. These salts crystallize into white powder on the exposed surface when the water evaporates. No significant incidences of such process were reported over the life of the structure, nor were any observed during visual inspections of the containment structure by PII in 2011.

### Acid

Exposure to acids has the potential to cause significant damage to concrete. There is no indication that the containment structure was directly exposed to acids during its lifetime.

### Carbonation

Carbonation is the result of the interaction of carbon dioxide gas in the atmosphere with the alkaline hydroxides in the concrete. Like many other gases carbon dioxide dissolves in water to form an acid. Unlike most other acids the carbonic acid does not attack the cement paste, but just neutralizes the



## FM 3.9 – Chemical Attack

alkalies in the pore water, mainly forming calcium carbonate that lines the pores.

Carbonation damage occurs most rapidly when there is little concrete cover of the reinforcing steel. It can also occur when the cover is high but the pore structure is open, pores are well connected together and allow rapid CO<sub>2</sub> ingress and when alkaline reserves in the pores are low. This occurs when there is a low cement content, high water cement ratio and poor curing of the concrete.

The concrete incorporated into the containment wall has low water/cement ratio, high cement content (Exhibit 1) and proper curing (see FM 2.2)

Virtually all the constituents of hydrated Portland cement are susceptible to carbonation. The results can be either beneficial or harmful, depending on the time, rate, and extent that they occur and the environmental exposure. Carbonation can improve the strength, hardness, and dimensional stability of concrete products, or it can result in deterioration and a decrease in the pH of the cement paste - allowing corrosion of reinforcement near the surface.

Petrographic reports (Exhibits 2 and 26) identified a limited layer of carbonated paste on the outside face of the concrete. Exhibit 2 states that on one core:

“Paste is fully carbonated along outer surface to depths of 5 to 8 mm (0.2 to 0.3 in.)...”

while the other core showed

“Paste is fully carbonated along outer surface to depths of 5 to 7 mm (0.2 to 0.3 in.)...”

These are very low carbonation levels for concrete that was exposed to the environment for over 40 years.

Exhibit 58 presents a study by PII on 17 cores to determine average carbonation depth on outside surface, and 23 cores to evaluate carbonation inside cracks. Its conclusion is similar to the previous petrographic studies with an average exterior carbonation depth of 8.6mm.

Evaluation of concrete cover in FM 2.2 concludes that the carbonation did not compromise the cover's ability to protect the reinforcing bars from corrosion.

### Moisture Migration

The WJE report (Exhibit 26) provides physical evidence of moisture migration uniformly through the concrete for the full depth of the cores (over 4 inches). The thin layer of secondary deposits after 40 year exposure is not considered an indication of attack since it does not create any stresses or strength



## FM 3.9 – Chemical Attack

reduction. The presence of deposits is not considered a strong indicator of moisture migration that should be pursued further with tests for Ettringite presence – especially since no environmental Sulfates were suspected. Ettringite may be present in concrete pores at different time periods and for different reasons, including sulfate attack and normal internal reactions.

### General Chemical Attack

1. **Exhibit 23 presents a list of chemicals known to have a deleterious effect on concrete. None of those chemicals is known to be present in significant quantities in contact with the concrete containment structure.**

### Conclusion:

The containment structure's concrete did not undergo chemical attack. Therefore, chemical attack was not a contributor to the Laminar Cracks. Specifically, carbonation depth is small comparing with the thickness of concrete cover for the 40-year old structure, and carbonation-induced steel corrosion is not a root cause.



## FM 3.10 – Corrosion of Rebar

### Description:

Corrosion of embedded metal is one of the main causes of failure of concrete structures (ACI 201.2R, ACI 222R). The critical elements needed for corrosion to occur are water, oxygen, and chloride ions, which in turn makes permeability the main concrete property that influences corrosion resistance. The high alkalinity ( $\text{pH} > 12.5$ ) of the concrete protects the thin iron-oxide film on the surface of the steel, thus making the steel passive to corrosion. The alkalinity can be reduced by carbonation or exposure to acidic solutions, allowing corrosion when oxygen and moisture are available. In the presence of chloride ions, the pH threshold for corrosion initiation is considerably higher than when chlorides are not present.

The initial stage of corrosion often produces cracking, spalling, and staining in the surrounding concrete. These can be detected by visual observations.

This document will attempt to identify basic properties of the concrete, type of exposure, and service conditions that affect its corrosion resistance.

### Data to be collected and Analyzed:

2. 1. Permeability of the concrete. (Exhibit 29 – correlation between W/C and permeability; Exhibit 1 – mix design)
3. 2. Design parameters that affect corrosion resistance (Exhibit 31 and 33 include a representative plan and enlarged detail).
4. 3. Availability of chloride ions (Exhibit 2)
5. 4. Petrographic analysis for extent of carbonation (Exhibit 2 and Exhibit 58)
6. 5. Visual observations of the rebar (Exhibit 33).

### Verified Supporting Evidence:

7. None

### Verified Refuting Evidence:

8. 1. The concrete meets industry recommendations for low permeability required for durability (Exhibit 29 – correlation between W/C and permeability; Exhibit 1 – mix design).
9. 2. Providing adequate cover of low-permeability concrete was part of the original design. Original plans called for concrete cover of 3" over the reinforcing bars (Exhibit 31 and 33 include a representative plan and enlarged detail).
10. 3. Measurements taken during the demolition in 2011 show cover size in line with the plan requirements and with ACI 117 (Standard Specifications for Tolerances for Concrete Construction and Materials) that allows cover variation of  $\pm \frac{1}{2}$ " in elements thicker than 12". Exhibit 33 is a photo where splicing of rebar resulted in cover of less than 1 inch. This is an unusual situation where construction limitations resulted in cover that is less than specified. However, there is no evidence that this condition resulted in corrosion after 40 years exposure (explanation follows).
11. 4. The containment structure does not have direct exposure to chloride ions from spray (it is located next to fresh water lake) or artificial sources (such as deicing salts). Test for chlorides in concrete cores found low chloride levels as reported in Exhibit 2.
12. 5. Petrographic analysis revealed a dense, low-permeability concrete with low depth of carbonation after over 40 years in service (Exhibit 2 – reported measured carbonation



## FM 3.10 – Corrosion of Rebar

depth of 5-8 mm). This level of carbonation is an indication that the concrete in the structure is not losing its ability to protect the metal inserts from corrosion. (See FM 3.9 for additional analysis of Carbonation)

13. 6. Visual inspections over the life of the structure did not detect corrosion related distress.
14. 7. Exhibit 33 includes a photo taken during hydro-demolition where corroded rebar are embedded in the concrete in the inside rebar mat. The corrosion appears to be surface rusting with no scaling or loss of material. It is likely that this level of corrosion was present during construction before the rebar was installed. It is not considered a problem.

### Discussion:

Industry standards use water to cement (W/C) ratio as an indication of concrete's permeability. It has been established that concrete with W/C of 0.5 has very low permeability levels (Exhibit 29). Exhibit 1 is a summary of mix designs used in the construction. These designs were prepared with W/C of 0.51. Based on the above it is concluded that the concrete has low permeability. Another source of moisture and chloride ingress can be surface cracks. Visual inspections did not identify open cracks through the surface concrete that exposed rebar or tendon. All rebar in the containment wall are protected by a low permeability cover of concrete, meeting design criteria and industry standards.

### Conclusion:

The concrete in the containment structure did not experience corrosion of rebar. Therefore corrosion was not a contributor to the Laminar Cracks.



## FM 3.11 – Rebar Creep

**Description:**

This failure mode hypothesizes that the material strength of the rebar is subject to creep under thermally induced radial stress over time in the hot summer days. During the winter days, the crept rebar could not shrink back, thus generating radial stresses and cracks the outer rebar mat.

**Data to be collected and Analysed:****Verified Supporting Evidence:**

None.

**Verified Refuting Evidence:**

The rebar are purchased and qualified under ASTM standards for material strength, not subject to creep. Moreover, the stress in the concrete produced by thermal effects is too low (less than 500 psi) that is well below the creep stress threshold for rebar (i.e., greater than 30,000 psi).

**Discussion:**

Above

**Conclusion:**

Rebar creep was not a contributor to the Laminar Cracks.



## FM 3.12 – Concrete Creep

<b>Description:</b> This failure mode hypothesizes that the concrete creeps under stress over long period of time. When the shield building was cut to install access opening, the crept concrete near the opening bounced back and redistributed the stress. The stress redistribution caused the laminar cracks near the outer reinforcing mat to occur.
<b>Data to be collected and Analysed:</b>
<b>Verified Supporting Evidence:</b> None.
<b>Verified Refuting Evidence:</b> The refuting evidences are listed below: <ol style="list-style-type: none"><li>1. Had this failure mode been responsible for the laminar cracking, the cracking would have limited only to the areas near the access opening, not over all shoulders and in areas far away from the opening.</li><li>2. The measured creep coefficient is about 2.2, which is considered in its normal range. This coefficient means that the permanent creep is only about 33% of the elastic strain. Since the concrete elastic strain is near zero due to a very low tensile stress, the amount of the creep recovery is minimum and not sufficient to cause any laminar cracks.</li></ol>
<b>Discussion:</b> Above
<b>Conclusion:</b> Concrete Creep was not a contributor to the Laminar Cracks.



## FM 3.13 – Excessive Snow/Ice Loading on the Dome

<b>Description:</b> This failure mode hypothesizes that during operation, heavy snow and rain accumulated on the top of the dome caused the observed laminar cracking.
<b>Data to be collected and Analysed:</b>
<b>Verified Supporting Evidence:</b> None.
<b>Verified Refuting Evidence:</b> The refuting evidences are listed below: <ul style="list-style-type: none"><li>• The dead weight of snow that could have caused any laminar cracking would have been greater than 2,000 ft of snow in height on top of the dome, which was not possible.</li></ul>
<b>Discussion:</b> Above
<b>Conclusion:</b> Excessive Snow/Ice Loading on the Dome was not a contributor to the laminar crack.





## FM 3.14 – Vibration

<b>Description:</b> There is a potential that long term low cycle vibration from rotating equipment may set up a failure mechanism
<b>Data to be collected and Analysed:</b> none
<b>Verified Supporting Evidence:</b> None
<b>Verified Refuting Evidence:</b> The Shield Building is a free standing reinforced structure that shares foundation with the Containment Vessel and the Containment Internals. This foundation bears directly on bedrock. There is no equipment located on or supported from the Shield Building. The only major rotating equipment in the Containment Internals is the four Reactor Coolant pumps and the three Containment Cooling Fan motors. These components are closely monitored by plant personnel for any out of tolerance vibration. There have been no unacceptable indications identified.
<b>Discussion:</b> Above
<b>Conclusion:</b> Vibration was not a cause of the Laminar Cracks



## FM 3.15 – Physical Attack

### Description:

Concrete is vulnerable to multiple mechanisms of physical attack that may lead to deterioration over time and potential failure. Physical processes include salt crystallization, freezing and thawing, abrasion and erosion, thermal exposure, and irradiation.

Thermal exposure, fatigue and settlement are discussed elsewhere in separate Failure Modes.

Salt crystallization is a process where dissolved salts move through the concrete by capillary action and crystallize on or under the surface as the water evaporates. The growing crystals can exert pressure on the “skin” of the concrete, resulting in spalling of the surface. This process can continue as long as there is a ready supply of moisture from the soil or atmosphere and the concrete experiences cycles of wetting and drying.

Abrasion and erosion are processes where surface material is removed from the concrete by either dry rubbing/grinding or impact of fluid carried particles.

Irradiation by either neutrons or gamma rays can cause changes to concrete’s physical properties and/or volume change of aggregates (a summary of concrete irradiation is provided Exhibit 30).

This document will attempt to identify potential processes and determine if any occurred in a way that impacted the observed failure.

### Data to be collected and Analysed:

1. Permeability of the concrete (Industry Standards - Exhibit 29 Permeability vs Water Cement ratio; mix design; Petrographic reports - Exhibit 2 - Lab Test results from CTL; Exhibit 26 Test report from WJE)
2. inspections record of damage related to physical attacks
3. Radiation exposure records (Exhibit 30 Irradiation effect)

**Verified Supporting Evidence:** None

### Verified Refuting Evidence:

1. The concrete has low Water to Cement (W/C) ratio (measured average of 0.51) and permeability (Exhibit 29 is a figure showing established relationships).
2. Petrographic reports did not detect salt crystallization inside the concrete (Exhibits 2 and 26).
3. Thorough review of inspection reports and NCRs over the life of the structure did not identify significant surface salt crystallization (efflorescence) or concrete spalling that is associated with salt crystallization. No damage typical of physical attack was reported.
4. The structure was not exposed to abrasion or erosion causing processes from mechanical abrasion or flowing water.
5. Irradiation levels are low at the concrete level and will not have a detrimental effect on the containment structure’s concrete.

### Discussion:

1. Industry standards use water to cement (W/C) ratio as an indication of concrete’s permeability. It has been established that concrete with W/C of 0.4 or lower has voids system



that is mostly made of disconnected discreet small voids – making it practically impermeable (Exhibit 29). At Davis-Besse, all the concrete was placed with 1.5” aggregate and W/C ratio of 0.51 (as calculated from actual delivery tickets). Based on the above it is concluded that the concrete has low permeability.

2. Some of the physical attack modes mentioned above require moisture transmission through the concrete. Impermeable concrete will be resistant to damage by salt crystallization.

3. W/C ratio is also a good indicator of concrete strength. The low W/C ratio resulted in strong concrete, able to resist higher stresses caused by physical attack.

4. Irradiation levels at the containment wall are very low and would not have significant effect on the concrete’s physical properties.

**Conclusion:**

Physical attack was not a contributor to the Laminar Cracks.



## FM 3.16 – Freeze-Thaw

**Description:**

Freeze-thaw is a collective name for several mechanical weathering processes induced by stresses created by the freezing of water into ice. The term serves as an umbrella term for a variety of processes such as frost shattering, frost wedging and cryo-fracturing. The process may act on a wide range of spatial and temporal scales, from minutes to years and from dislodging mineral grains to fracturing boulders. Freeze-thaw is mainly driven by the frequency and intensity of freeze-thaw cycles and the properties of the materials subject to weathering. It is most pronounced in high altitude and latitude areas and is especially associated with alpine, peri-glacial, sub-polar maritime and polar climates but occurs wherever freeze-thaw cycles are present.

This failure mode hypothesizes that water is diffused into the shield building concrete, filling up some small voids in the concrete. Inside the concrete, the water in the small voids gradually migrate to the big voids, such as gaps between the outer rebar and concrete, which have lower free energy to trap water. When the temperature drops below freezing point of water, the volume expansion of ice produced radial stresses and laminar cracks near the outer mat rebar.

**Data to be collected and Analysed:****Verified Supporting Evidence:**

None

**Verified Refuting Evidence:**

The refuting evidences is listed below:

- Had this failure mode been responsible for the laminar cracking near the outer rebar mat due to the degradation of the material strength, micro-cracking near small voids in one of the 83 samples would have been observed. No excessive micro-cracking has been observed in an extensive SEM (Scanning Electron Microscope) examination of the 83 samples.
- There is no sign of freeze-thaw (i.e., chipping of surface concrete) on the concrete surface for all the concrete cores (a total of 13) that contain laminar cracks near outer rebar mat.

**Discussion:**

Above

**Conclusion:**

Freeze-thaw was not a contributor to the laminar cracks.



## FM 3.17 – Containment Cutting

<b>Description:</b> This potential failure mode will examine if the action of cutting opening in the structure could have caused the observed delamination
<b>Data to be collected and analysed:</b> Extent of delamination (Exhibit 42 is a drawing by CTL of NDT testing for delamination cracks)
<b>Verified Supporting Evidence:</b> None
<b>Verified Refuting Evidence:</b> Delaminations were found throughout the structure including areas that are not directly linked to the opening.
<b>Discussion:</b> If opening cutting related stresses were the cause of the delamination we would see most of it happening adjacent to the opening.
<b>Conclusion:</b> Containment cutting was not a cause of the Laminar Cracks



## FM 3.18 – Modification Activities

<b>Description:</b> The only modifications to the shield Building have been the two temporary construction openings installed in 2002 and 2011. The evaluation of these mod activities is described above in FM 3.17
<b>Data to be collected and analysed:</b> See FM 3.17
<b>Verified Supporting Evidence:</b> None
<b>Verified Refuting Evidence:</b> See FM 3.17
<b>Discussion:</b> See FM 3.17
<b>Conclusion:</b> Modification Activities was not a cause of the Laminar Cracks



## FM 3.19 – Building Settlement

<b>Description:</b> This failure mode hypothesizes that the settling and its associated movement of the foundation of shield building was the cause to either initiate or propagate the observed laminar cracks.
<b>Data to be collected and analysed:</b> Exhibit 45 - C-0100 Shield Bldg. Foundation Seismic data
<b>Verified Supporting Evidence:</b> None
<b>Verified Refuting Evidence:</b> The entire Shield Building foundation rest directly on bedrock (reference drawing C-100 – 110) and precludes any differential settlement. Had the foundation settling caused the observed laminar cracks, both the inner and outer rebar mats would have shown laminar cracks. Note that the observed laminar cracks were only in the outer rebar mat. Moreover, foundation settling would have resulting cracks at building joints and/or corners. No such cracks were observed neither in the shield building nor in the adjacent auxiliary building.
<b>Discussion:</b> None.
<b>Conclusion:</b> Building settlement was not a cause of the laminar cracks



## FM 3.20 – Penetration Translation

<b>Description:</b> This failure mode will examine the potential for loads caused by the translation (movement) of piping penetrations in the Shield Building.
<b>Data to be collected and analysed:</b> See FM 3.21
<b>Verified Supporting Evidence:</b> None
<b>Verified Refuting Evidence:</b> As described in FM 3.21, the high energy piping lines that penetrate the Shield Building are structurally isolated (no physical connection). Therefore, there this potential failure mode is refuted.
<b>Discussion:</b> See FM 3.21
<b>Conclusion:</b> Penetration Translation was not a cause of the Laminar Cracks





## FM 3.21 – Piping Penetration (High Energy Loads)

<b>Description:</b> This failure mode will examine the potential for piping penetration loads on the Shield Building as a cause for the identified laminar cracks. High energy piping, if applicable, could cause vibration/fatigue stresses in the adjacent concrete.
<b>Data to be collected and analysed:</b> Exhibit 44 - Drawing C-111A Exhibit 69 - Drawing M-284A Exhibit 70 - Drawing M-284B
<b>Verified Supporting Evidence:</b> None
<b>Verified Refuting Evidence:</b> The high energy piping that penetrates the Shield Building is limited to the main steam and main feedwater lines. These high energy pipes are structurally isolated from the Shield Building, Ref. Drawings M-284A & M-284B. Therefore, there is no mechanism to transfer high energy piping loads to the shield Building. Also, these piping penetrations would only affect a relatively localized area of the building, which does not conform to the crack condition documented on drawing C-111A. Therefore, the high energy piping mechanism can be removed from the potential causes for the laminar cracks.
<b>Discussion:</b> If opening cutting related stresses were the cause of the delamination we would see most of it happening adjacent to the opening.
<b>Conclusion:</b> Containment cutting was not a cause of the Laminar Cracks



## Appendix VIII Exhibits



## Appendix IX Resumes

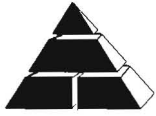


**Exhibit 1: Mix Design**

532106-87

645-3601

**TESTING AN ENGINEERING LABORATORY, INC.**

ENGINEERS AND CHEMISTS

402 GOWAN AVENUE, ST. PAUL, MINN. 55114



REPORT OF

CONCRETE MIX DESIGN

TOLSON-SPRISON POWER & LIGHT

DATE: October 2, 1970

TOLSON, MINN.

Enger Construction Company

FURNISHED BY: Nicholson Concrete & Supply Co.

2100 Sycamore Avenue

Minneapolis, Minnesota 55404

COPIES TO:

Attn: Mr. John Ellison

REPORT No. 6-7891

PROJECT

Concrete Strength @ 28 Days

C-2-SF-3

C-2-SF-4

Foundation Structure

5000 psi

4800 psi

Concrete Aggregate

Foundation Walls

Foundation Walls

over 12" Thick

over 12" Thick

1 1/2" - #4

1 1/2" - #4

5"

5"

3% - 6%

3% - 6%

AGGREGATE

Type I Portland Cement (ASTM C150)

Manufactured Sand furn. by Woodville Lime & Chem.

Crushed Limestone furn. by Woodville Lime & Chem.

1. Master Builders Pozzolith Type 200-N

2. MVA AEA furn. by Master Builders Company

Type 200-N Pozzolith

588#

588#

MVA AEA

17.6 ounces

17.6 ounces

1/4" - #4

3.8 ounces\*

4.8 ounces\*

3/4" - #4

1435#

1440#

Total

620#

620#

940#

940#

1560#

1560#

36.5 gal/yr

34.0 gal/yr

3.8 gal/yr

5.8 gal/yr

6"

6"

6.25 in/yr

6.35 in/yr

6.7%

6.7%

145.2 psi

144.8 psi

TEST RESULTS (6" Diameter x 12" High Cylinders)

(psi)

1970

1960

1945

2000

1910

2000



**Exhibit 2: Lab Test Results from CTL**



- Paste along the outer surface of the cores (i.e., exterior surface of the Shield Building wall) is fully carbonated to a depth of 5 to 8 mm. Carbonation in the body of the cores exhibits a mottled pattern with small areas of carbonated and non-carbonated paste; however, this feature does not appear to affect the overall integrity and performance of the concrete. Paste along the fracture surfaces of both cores, associated with those crack locations identified in the core holes, exhibits the same mottled carbonation pattern observed in the body of the cores; however, the paste does not appear to have carbonated due to exposure along the fracture surfaces.
- Estimated air content in Core A ranged from 1 to 3%. Estimated air content in Core D ranged from 1 to 3% at the outer end and 3 to 5% in the body of the core. Concrete appears air-entrained, but overall air contents are lower than specified in the original mix designs shown in Attachment C.

Water-soluble and acid-soluble (total) chloride ion tests were performed on concrete samples cut from various depths in each of the two cores. Testing was performed in accordance with ASTM C1218, "Standard Test Method for Water-Soluble Chloride in Mortar and Concrete" and ASTM C1152, "Standard Test Method for Acid-Soluble Chloride in Mortar and Concrete." Acid-soluble chloride ion tests measure the total (soluble and insoluble) chloride ion level in concrete. Chloride testing was performed at a 3/4 to 4 inch depth for Core A and at a 3/4 to 4 in. and 19-1/4 to 23 in. for Core D. Laboratory test report is included in Attachment E and results summarized as follows:

A	3/4 to 4	0.083	0.037
D	3/4 to 4	0.090	0.031
D	19-1/4 to 23	0.083	0.031

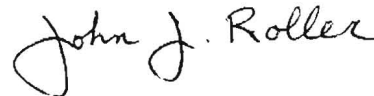
We appreciate the opportunity to assist First Energy on this project. If you have any questions or require additional assistance, please call.

Sincerely,



Carlton A. Olson  
 Principal & Group Manager

[COlson@CTLGroup.com](mailto:COlson@CTLGroup.com)  
 Phone: (847) 972-3244



John J. Roller, PE (Ohio - PE. 74103)  
 Structural Engineering & Mechanics

[Jroller@CTLGroup.com](mailto:Jroller@CTLGroup.com)  
 Phone: (847) 972-3178

COA #01178  
 Attachments- A through E

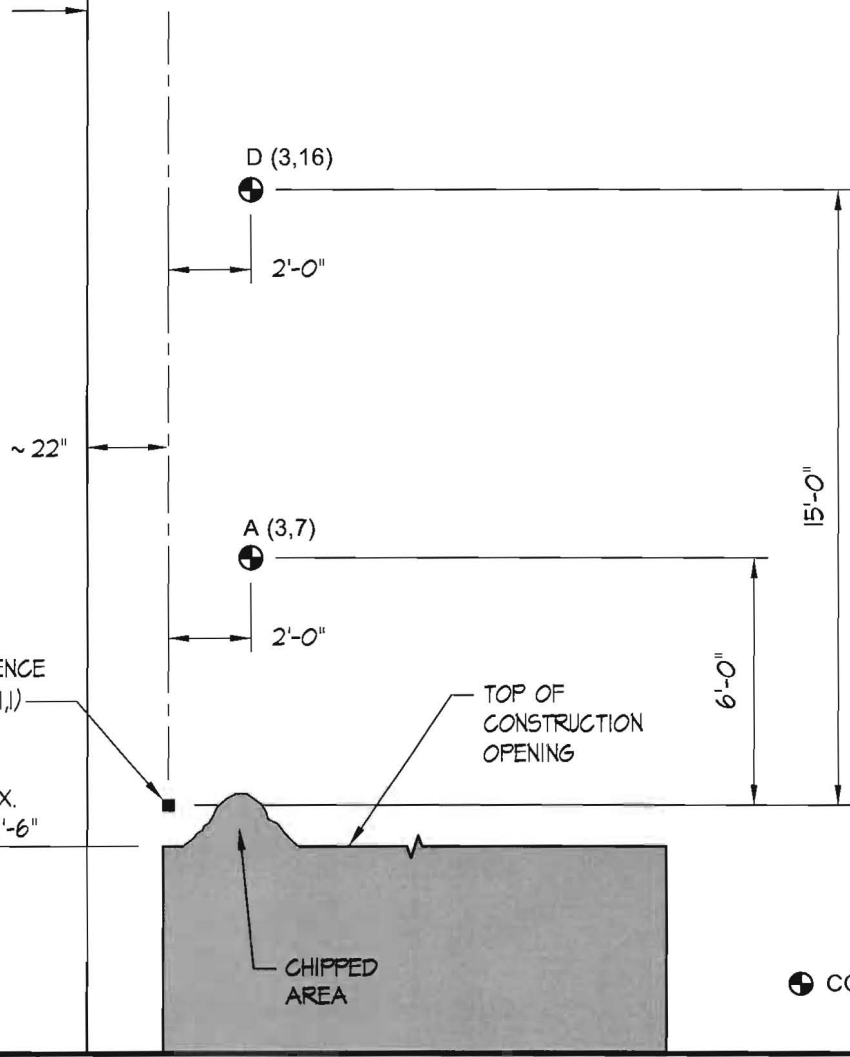


□

□□□□□**M**□□□□□

Location Sketch – Cores A and D

EDGE OF FLUTE 8



REFERENCE POINT (1,1)

APPROX. EL. 637'-6"

TOP OF CONSTRUCTION OPENING

CHIPPED AREA

⊕ CORE SAMPLE

**Location of Cores A and D - Shield Building Exterior**

**CTLGROUP**  
 CONSTRUCTION TECHNOLOGY LABORATORIES  
 ENGINEERS & CONSTRUCTION TECHNOLOGY CONSULTANTS  
 5400 Old Orchard Road • Skokie, IL 60077-1030  
 Phone 847-965-7500 Fax 847-965-6541  
 www.CTLGroup.com

Davis-Besse Nuclear  
 Power Station  
 Oak Harbor, OH

CTLGroup No.:	<b>262600</b>
Drawn:	<b>AMS</b>
Checked:	<b>CAO</b>
Date:	<b>27OCT11</b>
Scale:	<b>NTS</b>

Figure No.:

**1**

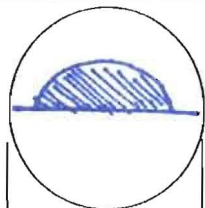
Laboratory Evaluation of Davis-Besse Shield Building Concrete  
CTLGroup Project No. 262600

October 27, 2011

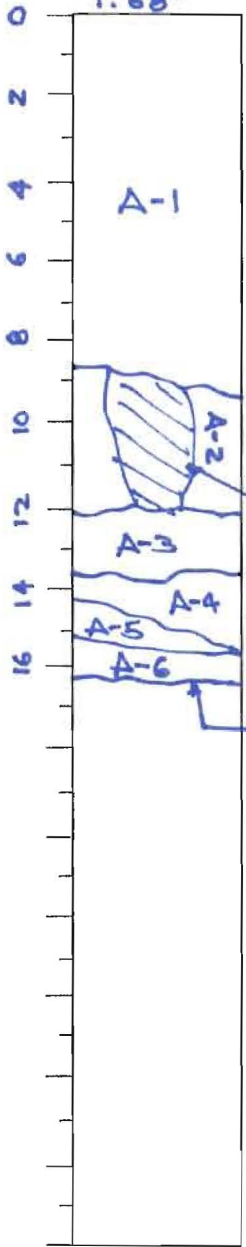
□

□□□□□**M**□□□□□

Core Logs – Cores A and D



3/8" NOM.  
0.68"  
1.68"

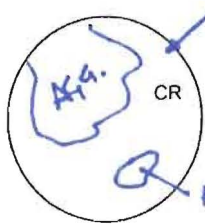


(TYP.)  
EXTRACTION  
FRACTURE THRU  
AGGREGATE

SURFACE  
CHIP EXTRACTION  
DAMAGE

FRACTURE  
SURFACE  
VERIFIED  
WITH BORESCOPE.  
FRACTURE  
ENCOMPASSES  
FULL CIRCUM-  
FERENCE OF  
CORE HOLE.

[SEE BORESCOPE  
PHOTOS 1-21  
AND 0-20]



SURFACE IS  
FLAT AND  
PROPAGATES  
THROUGH  
AGGREGATE.

CTLGROUP  
Building Knowledge. Defining Results.

CTLGroup  
Project No.  
262600

Core Designation:  
ALPHA "A"

Date Collected:  
18 OCT 2011

Examined By:  
DPD

Reviewed  
By:

CTLGroup  
Master No.:

Structure:

Orientation:  →  ↓  ↑

CORE DATA:

Max. Aggregate Size:  <0.5"  0.5"-1"  1"-1.5"  1.5"-2"  >2"  
Type of Aggregate:

CORE HOLE NOTES:

Hole Depth: "  
Visible Delaminations:  
@ " "  
@ " "  
@ " "  
@ " "  
@ " "

REINFORCEMENT:

ORIENTATION: Up  
1 |  
2 ○

DIA./#	DEPTH
1)	@ " "
2)	@ " "
3)	@ " "
4)	@ " "
5)	@ " "

Notes:

Notes:

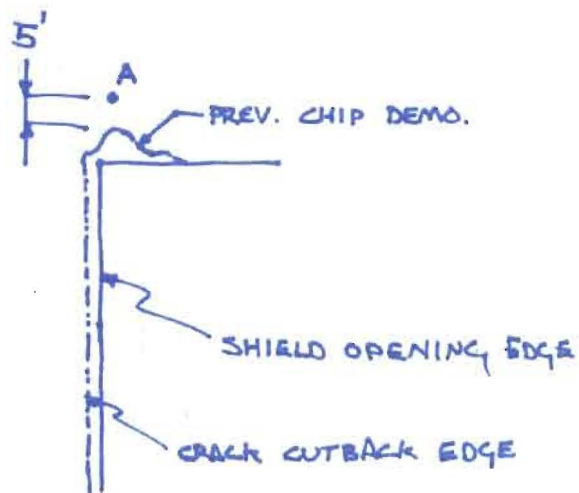
LEGEND:

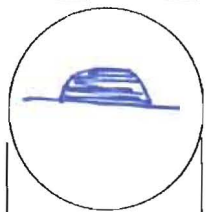
(CR) Crack  
XXX (R) Rubble  
~ (D) Delam  
~ (F) Fracture during coring  
☁ Void  
● Steel  
(DP) Deposits

LABORATORY TESTING:

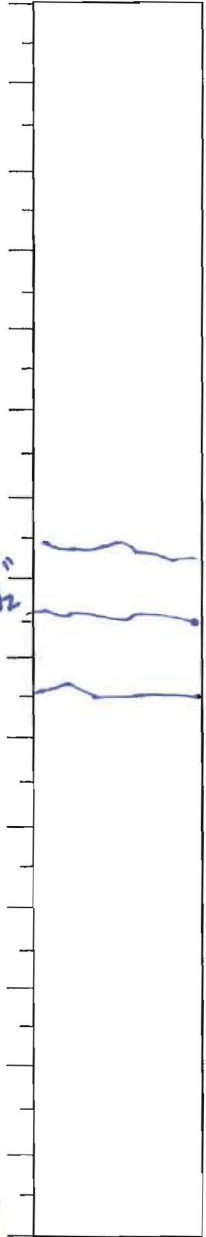
PORTION FROM FRONT FACE  
 f<sub>c</sub>: from " to "  
 Petro: from " to "  
 C1: @ " ; @ " ; @ "  
 None  
Notes:

LOCATION DIAGRAM:



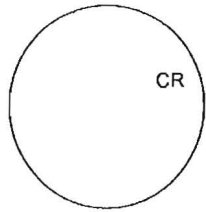


1 5/8"



14"  
15 1/2"  
16"  
26"

← LIKELY EXISTING CRACK LOCATIONS  
VERIFIED WITH BORESCOPE



CTLGROUP  
Building Knowledge. Delivering Results!

CTLGroup Project No. 262600

Core Designation: DELTA "D"

Date Collected: 18 OCT '11

Examined By: DPD

Reviewed By:

CTLGroup Master No.:

Structure:

Orientation:  →  ↓  ↑

CORE DATA:

Max. Aggregate Size:  <0.5"  0.5"-1"  1"-1.5"  1.5"-2"  >2"

Type of Aggregate:

CORE HOLE NOTES:

Hole Depth: "

Visible Delaminations:

@ " ;  
@ " ;  
@ " ;  
@ " ;  
@ " ;

Notes:

REINFORCEMENT:

ORIENTATION:

ORIENTATION	DIA./#	DEPTH
Up	1)	@ "
1	2)	@ "
2	3)	@ "
	4)	@ "
	5)	@ "

Notes:

LEGEND:

- ~ (CR) Crack
- XXX (R) Rubble
- ~ (D) Delam
- ~ (F) Fracture during coring
- Void
- Steel
- (DP) Deposits

LABORATORY TESTING:

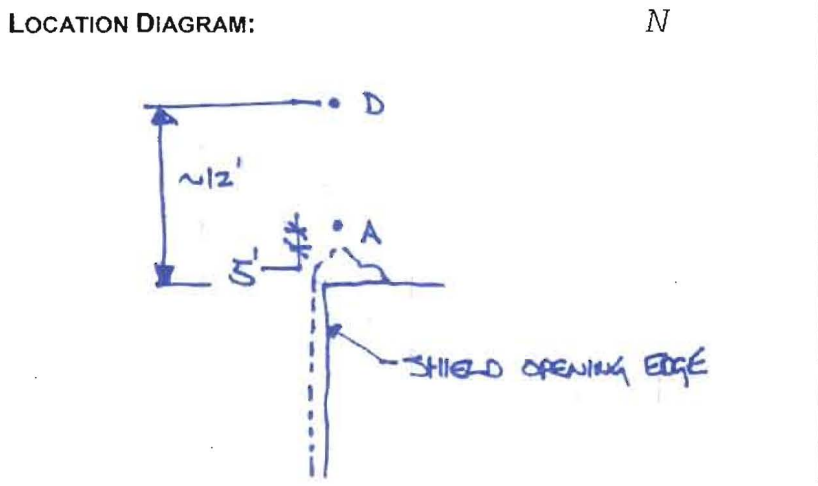
PORTION FROM FRONT FACE

f<sub>c</sub>: from " to "

Petro: from " to "

C1' @ " ; @ " ; @ "

Notes:



Laboratory Evaluation of Davis-Besse Shield Building Concrete  
CTLGroup Project No. 262600

October 27, 2011

□

□□□□□**M**□□□□□

Shield Building Concrete Mix Designs

0 5 3 2 1 0 6 8 7

645-3601

**TESTING AN ENGINEERING LABORATORY, INC.**

ENGINEERS AND CHEMISTS

602 Croswell Avenue - St. Paul, Minn. 55114

CONCRETE MIX DESIGN



REPORT OF  
**EDISON POWER & LIGHT**  
 TOLING, WISG  
 Taylor Construction Company  
 2110 Nicollet Avenue  
 Minneapolis, Minnesota 55404  
 Attn: Mr. John Ellison

DATE: **October 2, 1970**  
 FURNISHED BY: **Nicholson Concrete & Supply Co.**  
 COPIES TO:

TEST No. **6-7891**

Concrete Strength @ 28 Days	<b>C-2-SF-3</b> 4000 psi	<b>C-2-SF-4</b> 4000 psi
Use of Structure	Foundation Walls over 12" Thick	Foundation Walls over 12" Thick
Use of Coarse Aggregate	1 1/2" - #4	1 1/2" - #4
	6"	5"
	3% - 6%	3% - 6%

Type I Portland Cement (ASTM C150)  
 Manufactured Sand furn. by Woodville Lime & Chem.  
 Crushed Limestone furn. by Woodville Lime & Chem.  
 1. Master Builders Pozzoloth Type-200-N  
 2. MBVR AEA furn. by Master Builders Company

Type 200-N Pozzoloth	588#	588#
MBVR AEA	17.6 ounces	17.6 ounces
	3.8 ounces*	4.0 ounces*
	1435#	1440#
Water (14" - 3/4")	620#	620#
Water (2" - 1/4")	940#	940#
Water - Total	1560#	1560#
	36.5 gal/yd	36.5 gal/yd
	5.8 gal/ft <sup>3</sup>	5.8 gal/ft <sup>3</sup>
	6"	5"
Wet Weight	6.25 ex/ft <sup>3</sup>	6.25 ex/ft <sup>3</sup>
	5.5%	5.7%
Weight of Plastic Concrete	143.2 pcf	144.6 pcf

TESTS (6" Diameter x 12" High Cylinders)

Compressive (all)	1920	1960
	1900	2000
	1910	2000

Laboratory Evaluation of Davis-Besse Shield Building Concrete  
CTLGroup Project No. 262600

October 27, 2011

□

□□□□□**M**□□□□□

Petrographic Examination Report





Report for

[Redacted text]

CTLGroup Project No. 262600

[Redacted text]

October 26, 2011

Submitted by:  
Victoria A. Jennings

COA #01178

5400 Old Orchard Road  
Skokie, Illinois 60077-1030  
(847) 965-7500

Austin, TX • Chicago, IL • Washington, DC

[www.CTLGroup.com](http://www.CTLGroup.com)



Partnering Knowledge Delivering Results.

CTLGroup is a registered d/b/a of Construction Technology Laboratories, Inc.



As received, the core samples were transversely fractured into multiple segments, however only a few of the fractures reportedly represent cracks within the wall structure (Figs. 2 and 3). All of the observed fractures extend mainly through aggregate particles. Surfaces generally appear cleanly fractured, with no discoloration or debris, and few deposits (Fig. 5). In addition to the main transverse fractures, the cores exhibit a few microcracks (Fig. 6). Based on petrographic examination, no materials-related causes for the cracks and microcracks are observed. The concrete does not exhibit deleterious chemical reactions involving aggregates and paste constituents (such as alkali-aggregate reaction) nor other forms of chemical or physical deterioration.

On a small scale, concrete within the cores exhibits considerable variability in physical paste properties and paste microstructure. Within the body of the cores, paste ranges in color from light beige to medium-dark gray (Figs. 7 and 8). Where lighter in color, the paste tends to be moderately soft to soft, and moderately to highly absorbent, with dull to subvitreous luster. Where darker in color, the paste is moderately hard to hard, subvitreous, and moderately dense. Throughout the core samples, paste-aggregate bond is very tight. Given this variability, w/c within the concrete varies over small areas but is judged to be moderate overall, estimated in the range 0.45 to 0.55. This estimate is consistent with the provided mix designs, but is somewhat speculative due to the age of the concrete and the advanced degree of cement hydration.

Paste along the outer surface of each core is fully carbonated to depths of 5 to 8 mm (Figs. 9 and 10). pH staining suggests that paste at greater depths is non-carbonated but thin section examination indicates an unusual pattern of paste carbonation within the body of the cores. The paste is fully carbonated along the periphery of several aggregate particles (such areas generally appear lighter in color and exhibit weaker paste properties). Elsewhere within in the body of the concrete, the paste exhibits a mottled pattern of carbonation with small areas of

coarsely carbonated paste and small areas of non-carbonated paste (Fig. 11). The observed pattern of carbonation and variability in paste properties may have been influenced by: 1) the use of moist or wet aggregates at the time of mixing; 2) interaction (non-deleterious) between the carbonate aggregates and the paste; 3) incomplete mixing of the concrete constituents; and/or 4) the presence of moderate to large amounts of clay-sized carbonate fines within the concrete. While the observed pattern of paste carbonation is unusual and the paste is non-uniform, these features do not appear to have affected the overall integrity and performance of

concrete. Paste along interior fracture surfaces exhibits the same mottled carbonation pattern as observed elsewhere in the body of the concrete. Thus, the paste does not appear to have carbonated due to exposure along the fracture surfaces.

In general, the concrete consists of crushed carbonate rock coarse and fine aggregate in a hardened portland cement paste. Observed aggregate top size is 25 mm (1.0 in.). In Core A, air content is estimated at 1 to 3%. In Core D, the air content varies with depth, ranging from 1 to 3% at the outer end to 3 to 5% in the body of the core. The concrete appears air entrained based on the presence of small, spherical voids in the paste, but overall air contents are generally lower than specified by the mix designs. Additional findings and details of the examination are provided in the attached petrographic data sheets.

#### M

Petrographic examination of the provided samples was performed in accordance with ASTM C856, "Standard Practice for Petrographic Examination of Hardened Concrete." The samples were visually inspected and photographed as received. The outer two segments of Core A and the full length of Core D were then cut in half longitudinally, and one of the resulting halves of each core was ground (lapped) to produce a smooth, flat, semi-polished surface. Lapped and freshly broken surfaces of the concrete were examined using a stereomicroscope at magnifications up to 45X.

For thin-section study, two small rectangular blocks were cut from each core, and one side of each block was lapped to produce a smooth, flat surface. The blocks were cleaned and dried, and the prepared surfaces were mounted on ground glass microscope slides with epoxy resin. After the epoxy hardened, the thickness of the mounted blocks was reduced to approximately 20  $\mu\text{m}$  (0.0008 in.). The resulting thin sections were examined using a polarized-light (petrographic) microscope at magnifications up to 400X to study aggregate and paste mineralogy and microstructure.

Estimated water-cement ratio ( $w/cm$ ), when reported, is based on observed concrete and paste properties including, but not limited to: 1) relative amounts of residual (unhydrated and partially hydrated) portland cement clinker particles; 2) amount and size of calcium hydroxide crystals; 3) paste hardness, color, and luster; 4) paste-aggregate bond; and 5) relative absorbency of

paste as indicated by the readiness of a freshly fractured surface to absorb applied water droplets. These techniques have been widely used by industry professionals to estimate w/cm.

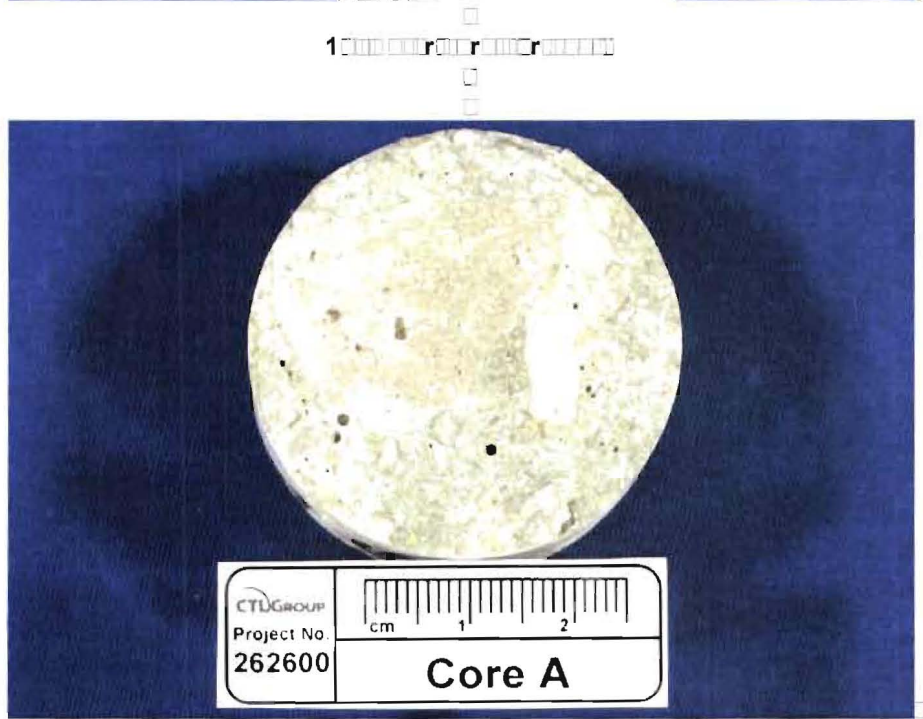
Depth and pattern of paste carbonation was initially determined by application of a pH indicator solution (phenolphthalein) to freshly cut and fractured concrete surfaces. The solution imparts a deep magenta stain to high pH, non-carbonated paste. Carbonated paste does not change color. The extent of paste carbonation was confirmed in thin-section.

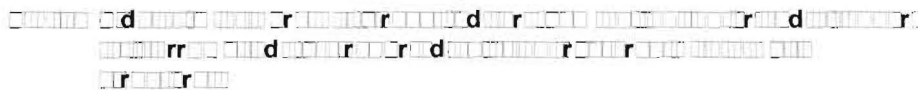
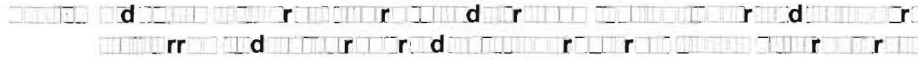
*Victoria A. Jennings*

Victoria A. Jennings  
Petrography Group

VAJ

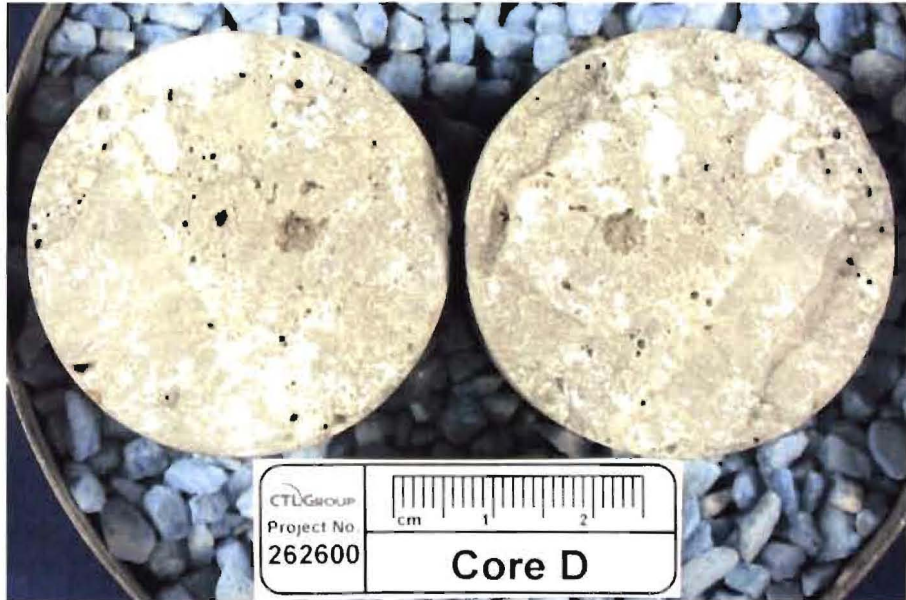
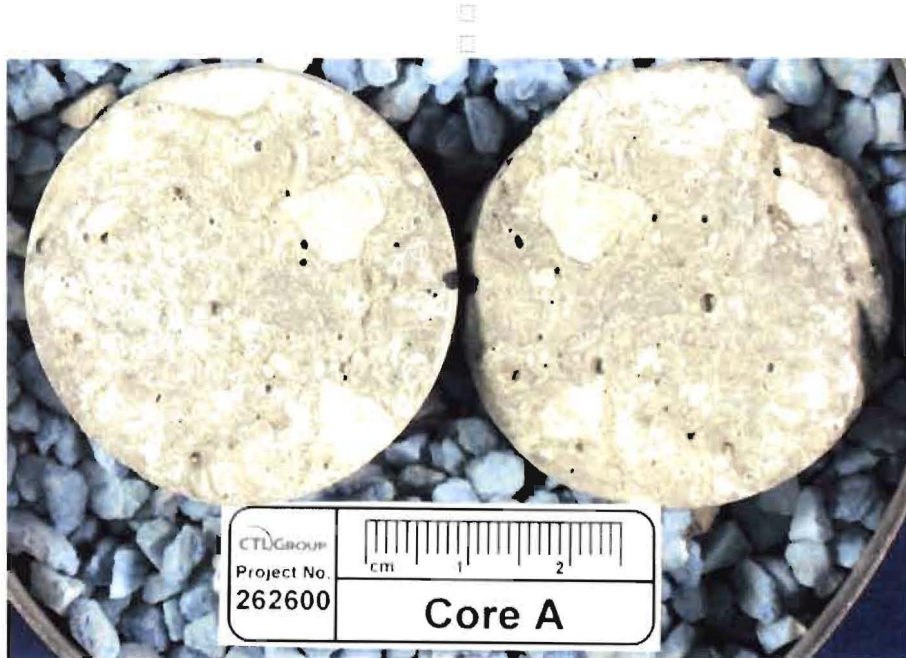
- Notes:
1. Results refer specifically to the samples submitted.
  2. This report may not be reproduced except in its entirety.
  3. The samples will be retained for 30 days, after which they will be discarded unless we hear otherwise from you.

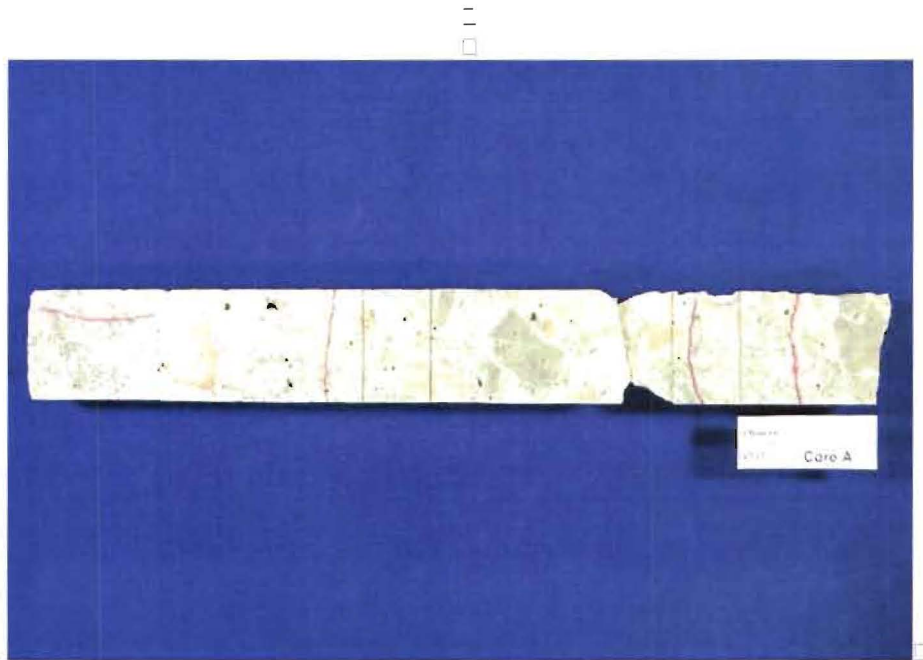




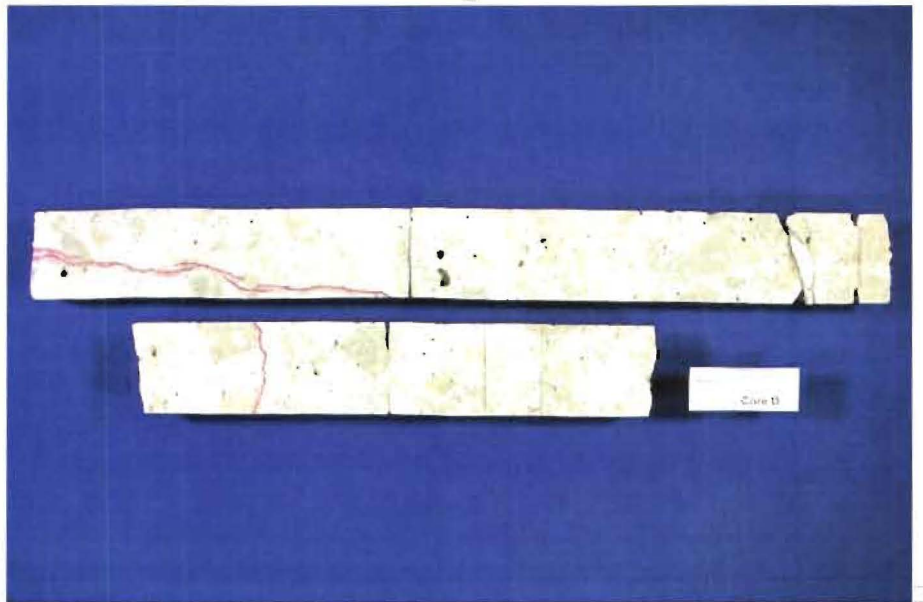






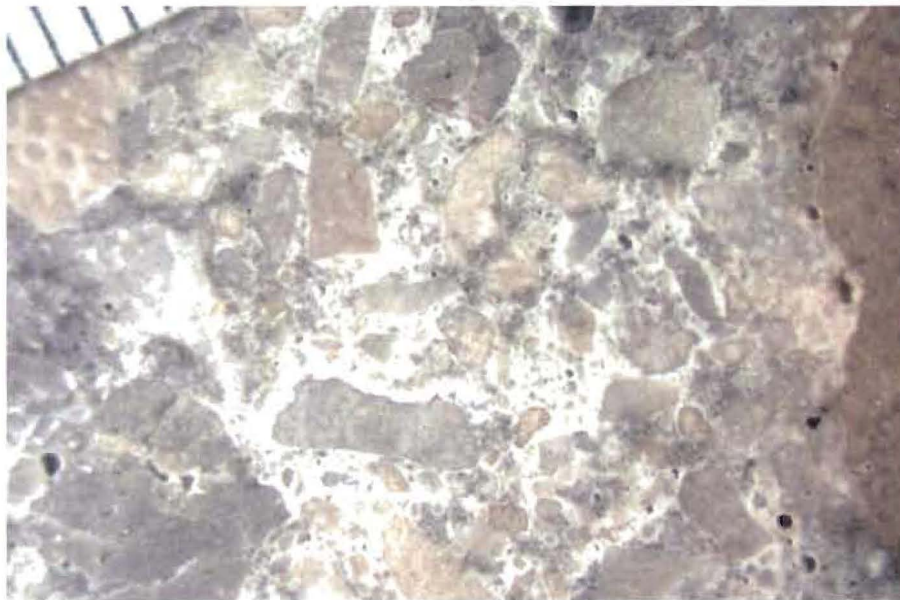


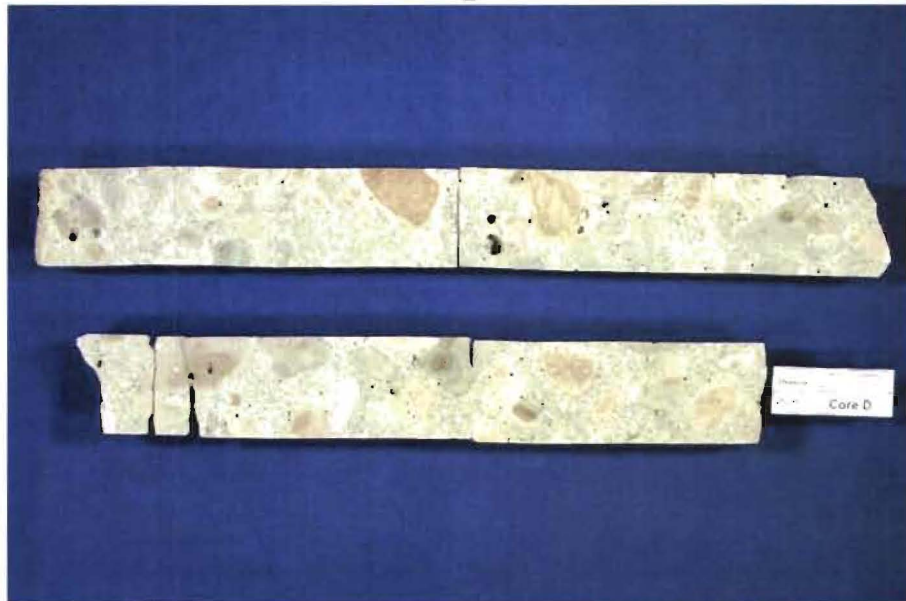
0 1 2 3 4 5 6 7 8 9 10 11 12 13 14 15 16 17 18 19 20 21 22 23 24 25 26 27 28 29 30 31 32 33 34 35 36 37 38 39 40 41 42 43 44 45 46 47 48 49 50 51 52 53 54 55 56 57 58 59 60 61 62 63 64 65 66 67 68 69 70 71 72 73 74 75 76 77 78 79 80 81 82 83 84 85 86 87 88 89 90 91 92 93 94 95 96 97 98 99 100



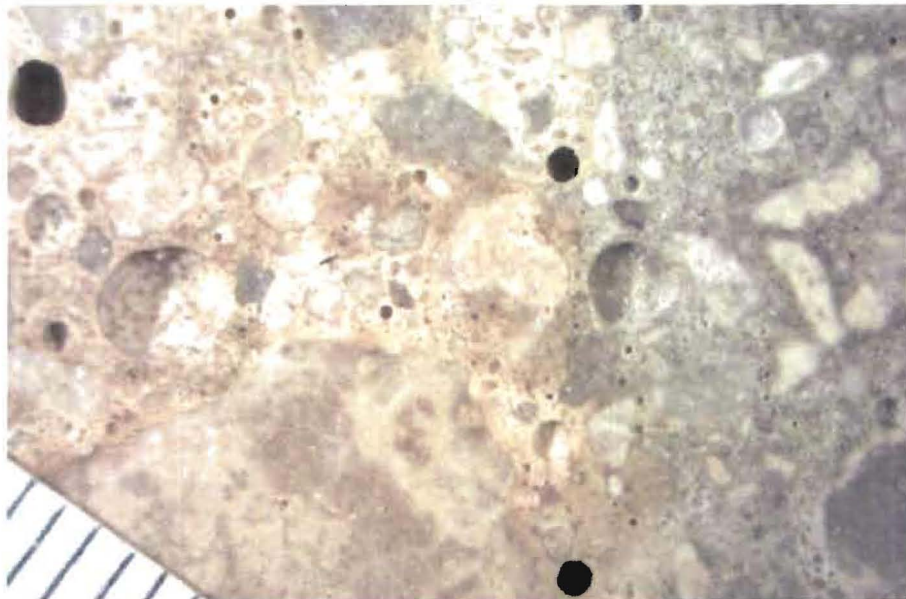
0 1 2 3 4 5 6 7 8 9 10 11 12 13 14 15 16 17 18 19 20 21 22 23 24 25 26 27 28 29 30 31 32 33 34 35 36 37 38 39 40 41 42 43 44 45 46 47 48 49 50 51 52 53 54 55 56 57 58 59 60 61 62 63 64 65 66 67 68 69 70 71 72 73 74 75 76 77 78 79 80 81 82 83 84 85 86 87 88 89 90 91 92 93 94 95 96 97 98 99 100

0 1 2 3 4 5 6 7 8 9 10 11 12 13 14 15 16 17 18 19 20 21 22 23 24 25 26 27 28 29 30 31 32 33 34 35 36 37 38 39 40 41 42 43 44 45 46 47 48 49 50 51 52 53 54 55 56 57 58 59 60 61 62 63 64 65 66 67 68 69 70 71 72 73 74 75 76 77 78 79 80 81 82 83 84 85 86 87 88 89 90 91 92 93 94 95 96 97 98 99 100



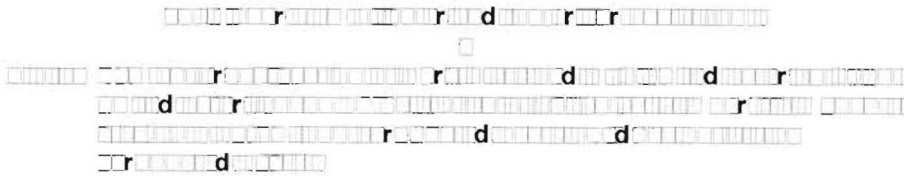
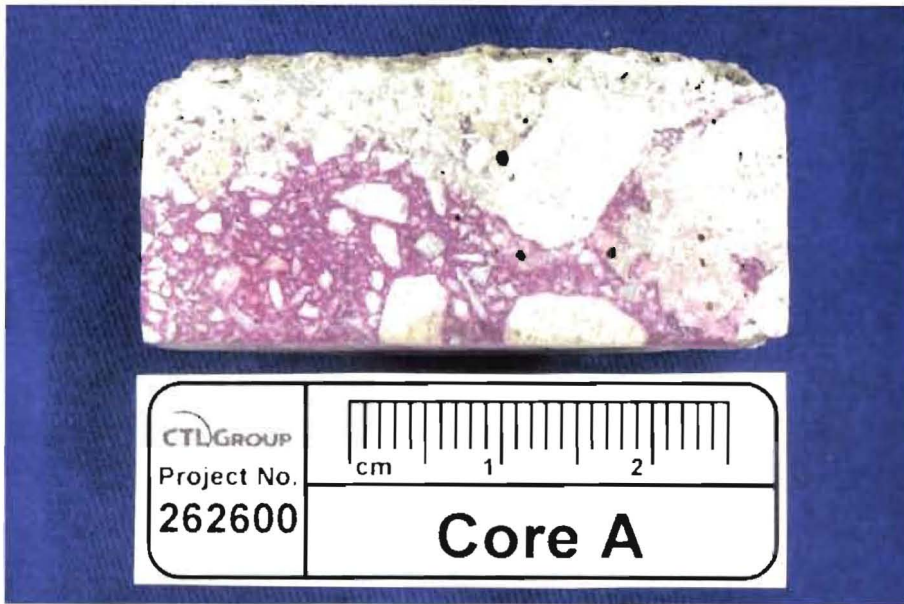
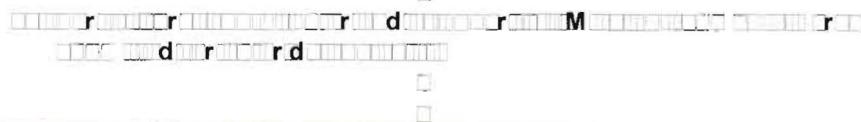
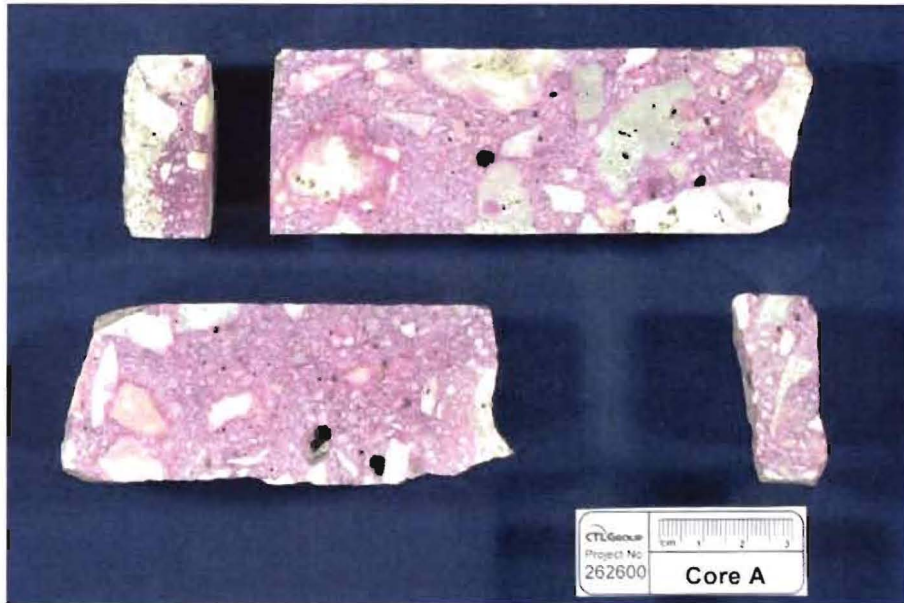


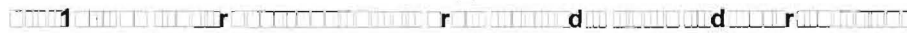
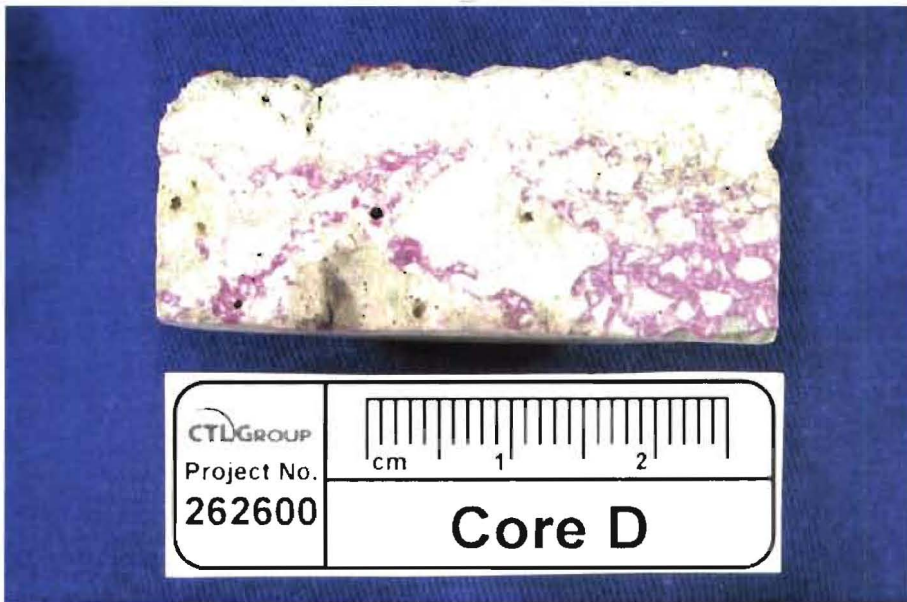
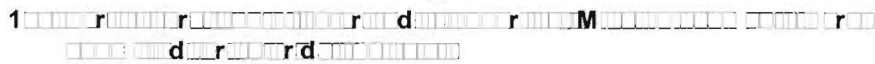
0 1 2 3 4 5 6 7 8 9 10 11 12 13 14 15 16 17 18 19 20 21 22 23 24 25 26 27 28 29 30 31 32 33 34 35 36 37 38 39 40 41 42 43 44 45 46 47 48 49 50 51 52 53 54 55 56 57 58 59 60 61 62 63 64 65 66 67 68 69 70 71 72 73 74 75 76 77 78 79 80 81 82 83 84 85 86 87 88 89 90 91 92 93 94 95 96 97 98 99 100  
r d r

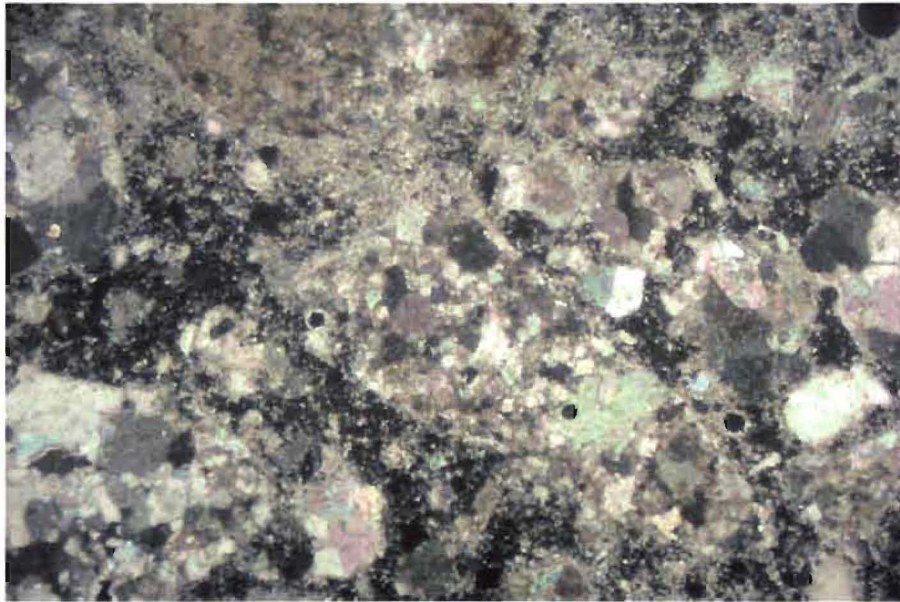


0 1 2 3 4 5 6 7 8 9 10 11 12 13 14 15 16 17 18 19 20 21 22 23 24 25 26 27 28 29 30 31 32 33 34 35 36 37 38 39 40 41 42 43 44 45 46 47 48 49 50 51 52 53 54 55 56 57 58 59 60 61 62 63 64 65 66 67 68 69 70 71 72 73 74 75 76 77 78 79 80 81 82 83 84 85 86 87 88 89 90 91 92 93 94 95 96 97 98 99 100  
M d r r r

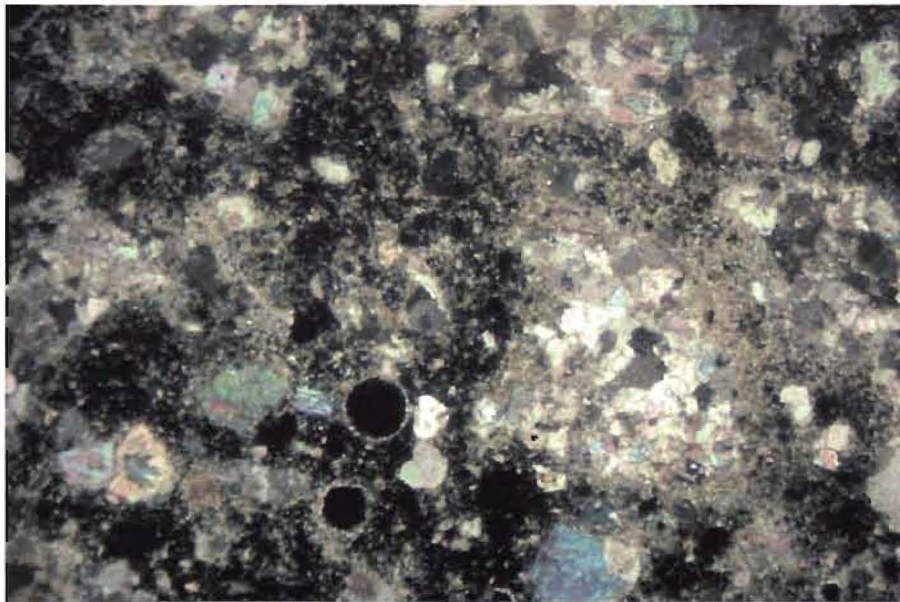
0 1 2 3 4 5 6 7 8 9 10 11 12 13 14 15 16 17 18 19 20 21 22 23 24 25 26 27 28 29 30 31 32 33 34 35 36 37 38 39 40 41 42 43 44 45 46 47 48 49 50 51 52 53 54 55 56 57 58 59 60 61 62 63 64 65 66 67 68 69 70 71 72 73 74 75 76 77 78 79 80 81 82 83 84 85 86 87 88 89 90 91 92 93 94 95 96 97 98 99 100  
d d r







11



11

11





□□□□□□

□□□□□□Variable. Paste is beige where carbonated along outer surface; color then appears mottled between light beige-gray and medium-dark gray to depths of approximately 50 mm (2.0 in.). At greater depths, color ranges from light beige to light gray to medium gray.

□□rd□□□□□□Variable from moderately soft to soft where lighter in color to moderately hard where darker in color.

□□□□□□□Generally subvitreous. Locally dull where lighter in color. Paste also locally appears resinous to waxy near some aggregate particles.

□□□□□□□□r□□□□□□□□d□Very tight; surfaces of freshly fractured concrete extend through nearly all coarse and fine aggregate particles.

□r□□□□□□□Estimated 1 to 3%. Concrete contains some small, spherical voids but is effectively non-air entrained.

□□□□□□□□r□□□□□□□□□□Paste is fully carbonated along outer surface to depths of 5 to 8 mm (0.2 to 0.3 in.). In body of core, paste is also fully carbonated along the periphery of several aggregate particles. Elsewhere in body of core, on a microscopic scale, paste exhibits a mottled pattern of carbonation with areas of coarsely carbonated paste and areas of non-carbonated paste. Paste along interior fracture surfaces exhibits similar mottled carbonation pattern as observed elsewhere in body of concrete, i.e., paste does not appear to have carbonated due to exposure along fracture surfaces.

□□□□□□□□dr□□□□□□□□□□Could not be evaluated due to unusual pattern of carbonation within body of concrete.

□□□d□□□□□□r□□□□d□□□□□□□□□□□□□□□□Estimated less than 1%. Relics of in-situ hydrated clinker particles are abundant; particles up to 150 μm (0.006 in.) are fairly common.

□□□□□□□□□□r□□□□□□□□□□□□□□□□None observed.

□□□□□d□□□□□□□□□□□□□□□□Relatively coarse calcite crystals line the surfaces of several voids. Inwardly-projecting ettringite crystals also line the surfaces of, or completely fill, some voids.

**M**□□□□□□□□□□□□□□□□Core exhibits one longitudinal microcrack, extending from outer surface to depth of approximately 55 mm (2.2 in.). Two outer segments of core also exhibit transverse microcracks at depths of approximately 115 mm, 250 mm, and 285 mm (4.5, 9.8, and 11.2 in.). Microcracks extend both around and through aggregate particles.

□□□**M**□□□□□□□□□□□□□□□□**M**□□□□□□□□□□□Variable throughout cement paste but overall estimated to be moderate (0.45 to 0.55). Numerical estimation is somewhat speculative given age of concrete, advanced degree of cement hydration, and unusual pattern of paste carbonation.

**M**□□□□□□□□□□□□□□□□

1. Outer surface of core is covered with mortar coating, up to 1 mm (0.04 in.) thick. Mortar contains siliceous sand aggregate in a soft, absorbent, cementitious paste.

2. Paste is highly absorbent along outer surface to depths of up to approximately 5 mm (0.2 in.). In body of core, paste is moderately absorbent to moderately dense. In general, paste is more absorbent where lighter in color.
3. Concrete contains a moderate to large amount of carbonate fines, likely crushing fines from aggregate.
4. Concrete exhibits some intermediate- to sand-sized, fine-grained and porous aggregate particles that appear darker and retain moisture longer than other particles. The cement paste adjacent to these particles often appears resinous or waxy. Despite the appearance of the adjacent paste, no other evidence is observed to suggest that the particles are reacting with alkalis in the cement paste. No alkali-silica reaction (ASR) gel is observed in the concrete, nor are any cracks observed associated with the particles.

\*percent by volume of paste





dense; paste is generally more absorbent where lighter in color and more dense where darker.

2. Concrete contains a moderate to large amount of carbonate fines, likely crushing fines from aggregate.
3. Concrete exhibits some intermediate- to sand-sized, fine-grained and porous aggregate particles that appear darker and retain moisture longer than other particles. The cement paste adjacent to these particles often appears resinous or waxy. Despite the appearance of the adjacent paste, no other evidence is observed to suggest that the particles are reacting with alkalis in the cement paste. No alkali-silica reaction (ASR) gel is observed in the concrete, nor are any cracks observed associated with the particles.

---

\*percent by volume of paste

Laboratory Evaluation of Davis-Besse Shield Building Concrete  
CTLGroup Project No. 262600

October 27, 2011

□

□□□□□□□□

Acid Soluble (Total) and Water Soluble Chloride Ion Test Reports

Client:	██	CTL Project No:	████████
Project:	██	CTL Project Mgr.:	████████████████████
Contact:	████████████████████	Analyst:	████████
Submitter:	████████████████████	Approved:	<b>R W Stevenson</b>
Date Received:	████████████████████11	Date Analyzed:	████████████████████11
		Date Reported:	████████████████████11

██

Sample Identification			Determined Chloride
CTL ID	Client ID	Description	(wt% sample)
2969001-02	Core A-- 3/4 to 4 in.	Concrete	0.083
2969002-02	Core D-- 3/4 to 4 in.	Concrete	0.090
2969002-03	Core D--19 1/4 to 23 in.	Concrete	0.083

- Notes:
1. This analysis represents specifically the samples submitted as received.
  2. Analysis by potentiometric titration with silver nitrate. (ASTM C 1152-04ε1)
  3. This report may not be reproduced except in its entirety.

Client:	██████████	CTL Project No:	██████
Project:	██████████	CTL Project Mgr.:	██████████
Contact:	██████████	Analyst:	██████████
Submitter:	██████████	Approved:	<b>R W Stevenson</b>
Date Received:	██████████11	Date Analyzed:	██████████11
		Date Reported:	██████████11

██████████

Sample Identification			Determined Chloride	
CTL ID	Client ID	Description	(wt% sample)	(ppm Cl)
2969001-02	Core A-- 3/4 to 4 in.	Concrete	0.037	370
2969002-02	Core D-- 3/4 to 4 in.	Concrete	0.031	310
2969002-03	Core D--19 1/4 to 23 in.	Concrete	0.031	310

**Notes:**

1. This analysis represents specifically the samples submitted as received.
2. Analysis by potentiometric titration with silver nitrate. (ASTM C 1218-99 (2008))
3. This report may not be reproduced except in its entirety.





**Exhibit 3: Lab Test Results from Twining**



DATE: 11/19/2011

TLSC JOB NO: 110889.1

Page 1 of 1

## M.O.E., SPLIT TESILE AND COMPRESSION TESTS ON CONCRETE CORES

**CLIENT:** Performance Integrity International  
 2111 S. El Camino Real,  
 Oceanside, Ca. 92054  
**JOB NAME:** Fenco - Davis - Dessl (as reported by Client)  
**SAMPLED FROM:** Davis-Besse Shield Building  
 (Location in Structure) Shoulder ( as reported by client)  
**Cored On:** N/A  
  
**Specified Strength:** See Attachment 4,000 psi  
**TAKEN BY:** Twining from client Office in Newport Beach, CA  
**Picked Up On:** 11/16/2011

CORE I.D.	S1 ( core #1)	S1 (core # 2)	Splitting Tensile on S3
DATE OF TEST	11/19/2011	11/19/2011	11/19/2011
DIAMETER, in.	3.67	3.67	3.67
LENGTH AS RECEIVED, in.	14.0	14.0	8.0
CAPPED LENGTH, in	6.00	6.00	N/A
AREA, sq.in.	10.58	10.58	10.58
LENGTH/DIAMETER	1.63	1.63	N/A
MAX. LOAD, lbf	75,347	98,000	27,450
Stress (psi)	7,123	9,260	935
MOD. OF ELAS., psi	5.90E+06	N/A	N/A

M.O.E. is rounded to the nearest 50,000 psi

TEST STANDARD: ASTM C42, ASTM C469, ASTM C 496

Notes: Core identified as S1 was cut into two pieces, sample # 1 was tested for M.O.E. ,test # 2 was tested for compression test.

Mike Fattal, Manage  
 Senior Project Engineer  
 Twining, Inc.

Review Engineer



**Exhibit 4: Spec C-26; Forming, Placing,  
Finishing, & Curing Concrete**



Power and Industrial  
Division

Specification No. 7749-C-26  
Job No. 7749  
Q-List No. 1.2220

2

THE TOLEDO EDISON COMPANY

AND

THE CLEVELAND ELECTRIC ILLUMINATING COMPANY

DAVIS-BESSE NUCLEAR POWER STATION

UNIT NO. 1 CONSTRUCTION

SECTION XIb

2

TECHNICAL SPECIFICATIONS  
FOR THE  
FORMING, PLACING, FINISHING AND CURING  
OF  
CONCRETE

*BT L 2002  
5-17-76*

RECEIVED  
JUN 7 1976  
DAVIS-BESSE

BECHTEL COMPANY  
GAITHERSBURG, MARYLAND

No.	Date	Revisions	By	G.L.	C.E.	P.E./	TECo
A	3-23-70	Issued for Client Approval and Bid					
0	8-7-70	Issued for Detailing and Material Purchase					
1	10-30-70	Issued for Construction & Addendum 3					
2	5-11-71	Issued for Addendum 4					
3	5/12/76	Issued for Addendum 5 and Revised Section 3.4 and Form ED6058	RJR	OK	TKH	TKY	Ecn

2  
3  
4

000162



Division

SPECIFICATION REV. 3

INDIVIDUAL PAGE REVISION INDEX SHEET

<u>Page No.</u>	<u>Latest Individual Page Addendum No.</u>
Cover Sheet	5
Individual Page Revision Index Sheet	5
Table of Contents	2
1	2
11	3
iii	3
1	2
2	4
3	5
4	3
5	4
6	4
7	3
8	3
9	3
10	3
11	4
12	4
13	4
14	3
15	3
Documentation Distribution Requirements	5

000102004



TECHNICAL SPECIFICATIONS

TABLE OF CONTENTS

Sections	Page	2
1.0 GENERAL	1	
2.0 ABBREVIATIONS	1	
3.0 QUALITY CONTROL REQUIREMENTS	2	
3.1 QC Records	2	
3.2 Shop Inspection	2	
3.3 Quality Control Documentation Required	3	
3.4 Handling, Shipping and Storage	3	
4.0 FORMS	3	
4.1 Construction	3	
4.2 Form Ties	4	
4.3 Form Parting Agent	4	
4.4 Removal	5	
5.0 EXPANSION JOINTS	5	
5.1 Expansion Joint Filler	5	
5.2 Joint Sealer	5	
5.3 Shear Keys	5	
5.4 Water Stops	5	
6.0 CONSTRUCTION JOINTS	6	
6.1 Cleaning Horizontal Construction Joints	6	
6.2 Cleaning Vertical Construction Joints	6	
6.3 Sandblasting or Water Blasting	6	
6.4 Air-Water Jet Cutting of Horizontal Joints	6	
6.5 Construction Joint Treatment	7	

00015200



Power and Industrial  
Division

Specification No. 7749-C-26

7.0	EMBEDDED ITEMS	7	
7.1	Reinforcement	7	
7.2	Inserts	7	
8.0	CLASSES OF CONCRETE AND MAXIMUM SIZE AGGREGATE	8	
9.0	CONVEYING AND PLACING	8	
9.1	Clean-up Preparation	8	
9.2	Deposition	8	
9.3	Control Joints	9	13
9.4	Time Between Adjacent Placement	9	
9.5	Placement Protection	9	
9.6	Segregation	9	
9.7	Placing Limitations	10	
9.8	Vertical Members	10	
10.0	CONSOLIDATION OF CONCRETE	10	
11.0	COLD AND HOT WEATHER CONCRETING	10	
11.1	Methods	10	
11.2	Moderate Weather Precautions	11	
11.3	Cold Weather Concreting	11	
11.4	Hot Weather Concreting	12	
12.0	CURING	12	
12.1	Moist Curing	12	
12.2	Blanketing Method	13	
12.3	Cotton Mat Method	13	3
12.4	Waterproof Paper Method	13	
12.5	Liquid-Membrane Method	13	
12.6	Plastic Membrane	13	
13.0	CONCRETE GROUT AND MORTAR	14	
13.1	Grout Classification	14	
13.2	Non-Shrink Grout	14	
13.3	Mixing Non-Shrink Grout	15	
13.4	Drypack Mortar	15	3



Power and Industrial  
Division

Specification No. 7749-C-26

14.0	SLUMP REQUIREMENTS	15	3
15.0	CONCRETE SURFACE FINISHES	15	
16.0	REPAIR OF CONCRETE	15	
17.0	MEASUREMENT AND PAYMENT	15	1

00010200107





Power and Industrial  
Division

Specification No. 7749-C-26

TECHNICAL SPECIFICATIONS

FOR

FORMING, PLACING, FINISHING AND CURING

OF

CONCRETE

1.0 GENERAL

1.1 This Specification covers the complete forming, placing, finishing and curing of concrete. It forms a part of Specification No. 7749-C-38, Shield Building, and Construction Document No. 7749-18.

1.2 The WORK includes the furnishing of all supervision, labor, materials, tools, and equipment and the performance of all operations and incidentals necessary to complete the forming, placing, finishing and curing of Portland cement concrete in accordance with this Specification and Specification No. 7749-C-38, Shield Building.

The WORK also includes furnishing documentation to the CONSTRUCTION MANAGER as specified in Paragraph 3.0 and Section XII of this Contract Document.

1.3 The intent of these Specifications is to establish criteria for the forming, placing of concrete, reinforcement and embedments, and finishing and curing of Portland cement concrete.

2.0 ABBREVIATIONS

The abbreviations listed below when used in these Specifications shall have the following meanings and shall refer to the latest revision in effect on the date of this Contract.

AASHO - American Association of State Highway Officials

ACI - American Concrete Institute

ASTM - American Society for Testing and Materials

0001320018

2



Power and Industrial  
Division

Specification, No. 77-49-C-26

### 3.0 QUALITY CONTROL REQUIREMENTS

#### 3.1 QC Records

The equipment or materials specified hereunder are Q-List items and are to perform critical functions in the Nuclear Power Plant. The CONTRACTOR shall furnish, for the benefit of the CONSTRUCTION MANAGER, Certified Records of Quality Control Inspections and Tests performed during production, as required in these Specifications and Section XII of this Contract Document.

Without altering responsibilities imposed by codes, these Specifications, applicable statutes, etc., and in addition to those otherwise required the CONTRACTOR shall provide copies of inspection and test reports, as listed below, in advance of material or equipment shipment. The CONTRACTOR agrees to provide access to basic inspection records, including those of non-destructive tests, and shall stipulate when originals will be released to the CONSTRUCTION MANAGER. Bidders shall submit with the Proposal, an outline of the quality control inspection and test procedures to be followed in furnishing the material or equipment. Within thirty days after receipt of an order, the CONTRACTOR shall furnish detailed quality control inspection and test procedures, and the schedule for accomplishing the activities. The CONTRACTOR'S inspection and test procedures shall provide for maintenance of a calibration system to control the accuracy of his measuring and test equipment. The same information shall be provided for all lower-tier SUBCONTRACTORS and Suppliers furnishing materials, components or services to the CONTRACTOR which require inspection or certification.

2

#### 3.2 Shop Inspection

The CONSTRUCTION MANAGER will not furnish a Shop Inspector for the water stops listed in Paragraph 5.4 but will require the CONTRACTOR to furnish letters of conformance or test reports for same governed by the Corps of Engineers Specifications in Paragraph 5.4.

2

3

4

6  
1  
0  
0  
2  
1  
0  
0  
0



3

3.3 Quality Control Documentation Required

3.3.1 The following documentation on forming, placing and curing concrete is required for the CONSTRUCTION MANAGER'S review and file.

2

- a. Completed placing inspector's clearance card.
- b. Placing inspector's report at end of each shift.
- c. Placing inspector's report at end of curing time.

3.3.2 The above documentation is required for the CONSTRUCTION MANAGER'S file for the following structures and supports:

2

- a. Shield Building including all embedded items.

3.4 Handling, Shipping and Storage

The CONTRACTOR shall maintain handling, storage, preservation, packing and shipping procedures to protect the quality of products and prevent damage, loss, deterioration, degradation, or substitution of products. Means shall be provided for necessary protection against deterioration or damage to products to be held in field storage. When products require special environments in storage, the CONTRACTOR shall label packages to indicate this condition. The procedures for handling, storage, preservation, packing, and shipping shall be submitted for approval in accordance with Form ED6058.

5

4.0 FORMS

4.1 Construction

00010240



The Shield Building walls will be constructed by the slip-form method as described in Specification No. 7749-C-38. Forms shall be constructed in accordance with the applicable Provisions of ACI 347 except as modified herein or on the drawings. Forms shall be of wood, metal, structural hardboard or other suitable material that will produce the required surface finish. Forms shall be constructed to conform to the shape, form, line and grade required, and shall be sufficiently rigid to prevent deformation under load and be so designed as to be removed readily without injuring the concrete. Joints shall be mortar tight and arranged to conform to the pattern of the design required. Forms placed for successive pours for continuous surfaces shall be fitted to accurate alignment to assure a smooth completed surface free from irregularities on exposed surfaces. Local defects, such as chipped plywood or kinks in steel forms, will not be permitted. Temporary openings shall be provided where required to facilitate cleaning, inspection and placing. Forms to be reused shall be thoroughly cleaned and carefully inspected for surface damage misalignment, etc., before re-use. Unless otherwise noted, chamfer strips shall be provided in the exterior angles of forms to produce clean, straight and uniform edges on any concrete that will be exposed in its permanent and finished state.

4.2 Form Ties

Form ties shall be of adequate strength and of a type suitable for the purpose. Ties shall be so arranged that, when forms are removed, all metal shall be not less than 2 inches from surfaces exposed to lake water and not less than one inch from surfaces subjected to ordinary weather exposure. Lugs, cones, washers, or other devices shall not leave a surface depression or hole larger than 7/8 inch in diameter on exposed surfaces.

4.3 Form Parting Agent

Forms for surfaces which will be exposed, except those surfaces to be painted, shall be coated with approved parting agent before the reinforcement is placed. Surplus and splattered coating material shall be removed from the forms, reinforcements and adjacent concrete surfaces prior to concrete placement. Care shall be taken that the parting agent does not get into concrete or reinforcement which is to bond with new concrete. Forms for exposed concrete surfaces to receive paint or similar coating shall be sprayed with lacquer, shellac, paint, or other suitable preparations that will leave the concrete surface free from oil, grease or residue from the parting agent. Such surfaces will be indicated in the Specification for Field Painting and on the Architectural Drawings. The parting agent selected shall be chemically compatible with the paint or protective coating to be applied. Forms for such surfaces shall not be placed prior to the CONSTRUCTION MANAGER'S approval of the parting agent. Wood forms for surfaces which will not be exposed may be thoroughly wetted with water in lieu of form coating, except that in cold weather with probable freezing temperatures, coating shall be used.

Parting agent shall not be used in the slip-form operation.

3

10002091000



4.4 Removal

Forms for columns, walls, sides of beams, slabs and girders, and other parts not supporting the weight of the concrete, shall be removed as soon as practicable in order to avoid delay in curing and repairing surface imperfections. Wood forms or insulated steel forms for members 2-1/2 feet or greater in thickness shall be stripped within 24 hours. Non-insulated steel forms used for members 2-1/2 feet in thickness, shall, if practicable, be stripped within 24 hours to allow for proper curing and repair of surface imperfection. In no case, however, shall forms be removed before approval by the CONSTRUCTION MANAGER. Forms shall remain in place until the concrete has reached sufficient strength to prevent exothermic cracking. Forms shall be removed in such a manner as will assure the complete safety of the structure and prevent damage to the concrete. Form work for beam and girder soffits, slabs and other parts that support the weight of the concrete shall remain in place until the concrete has reached sufficient strength to prevent exothermic cracking and has reached 80 percent of its specified 28 day strength or 60 percent of its specified 90 day strength. Accelerated form stripping time will be determined from the results of additional concrete cylinder strength tests.

5.0 EXPANSION JOINTS

Expansion joints shall be formed to agree with the details shown on the drawings and the material supplied in accordance with the following respective specifications or requirements.

5.1 Expansion Joint Filler\*

Preformed expansion joint filler shall conform to ASTM Designation D994 (Bituminous Type), D1751 (Bituminous Type), or D1752 (Nonbituminous Type) as indicated on the design drawings.

5.2 Joint Sealer\*

Joint sealer shall conform to ASTM Designation D1190 (Hot-Poured Type), D1850 (Cold-Application Type) or USAS Specification A116.1 (Multiple-Component Type) as indicated on the design drawings. Joint preparation and application of primer and joint sealant shall conform to sealant manufacturer's instructions.

5.3 Shear Keys

Shear key forms shall be made from metal to the sizes and shapes shown on the drawings, or be formed with lumber to proper dimensions.

5.4 Water Stops\*

Water stops shall be of rubber, polyvinylchloride, metal, or neoprene or as specified on the drawings and be located and installed as shown on the drawings. If the need arises, the CONSTRUCTION MANAGER will specify or change the location of the water stops.

Rubber and PVC finished water stops shall meet or exceed the physical properties of the Corps of Engineers Specifications CRD-C513 and CRD-C572 respectively.

\*The CONTRACTOR shall furnish a letter of conformance or test reports to the ENGINEER and CONSTRUCTION MANAGER for this material as shown in Form ED 6058.

2  
3  
4  
5  
6  
7  
8  
9  
10  
11  
12  
13  
14  
15

3  
4  
4  
3  
4



6.0 CONSTRUCTION JOINTS

Construction joints shall be made in accordance with ACI 318 except as may be modified herein or on the drawings. Joints in columns or piers shall be made at the underside of the deepest beam, girder or haunch framing. Proprietary shear keys and water stops shall be installed in accordance with the manufacturer's directions and the CONSTRUCTION MANAGER'S approval.

6.1 Cleaning Horizontal Construction Joints

When the surface of a lift is congested with reinforcing steel, or is relatively inaccessible, or if for any other reason it is undesirable to disturb the surface of a lift before final set has taken place, surface cutting by means of air-water jets will not be permitted unless approved by the CONSTRUCTION MANAGER. And the use of sand-blasting or light bush hammering or other means will be required. Surface set retardant compounds shall not be used.

6.2 Cleaning Vertical Construction Joints

Vertical construction joints, where required, shall be cleaned by sandblasting, by light bush hammering, or by other approved means. The existing surface shall be thoroughly wetted before placing of new concrete.

Where construction joints are made by means of expanded metal, adjacent pours shall not be made until all multiple laps of the expanded metal are removed and the laitance is removed to expose clean, sound concrete at the openings in the expanded metal.

Close inspection shall be performed to assure that no voids exist in the concrete on the opposite side of the welded wire mesh.

6.3 Sandblasting or Waterblasting

Sandblasting or waterblasting shall be employed in the preparation of the Shield Building wall construction joints. The operation shall be continued until all unsatisfactory concrete and all laitance, coating, stains, debris and other foreign materials are removed and solid aggregate is exposed. The surface of the concrete shall then be washed thoroughly to remove all loose material.

6.4 Air-Water Jet Cutting of Horizontal Joints

Air-water jet cutting may be performed upon approval by the CONSTRUCTION MANAGER. The surface shall be cut with a high pressure air-water jet to remove all laitance and to expose clean, sound aggregate without undercutting the edges of the large particles of aggregate.

0001000

3

4

2



6.5 Construction Joint Treatment

All concrete surfaces to receive new concrete shall be wet down two hours prior to placing concrete. All horizontal surfaces be thoroughly covered with approximately 1/2 inch of mortar immediately before the concrete is placed. For congested areas the mortar may be forced ahead of the concrete. The mortar shall have the same cement-sand ratio as used in the concrete being placed. The provision requiring placement of 1/2" mortar on horizontal construction joints may be waived by the CONSTRUCTION MANAGER on slip-form work when in his judgement the CONTRACTOR demonstrates that a satisfactory joint can be obtained without the use of mortar.

7.0 EMBEDDED ITEMS

7.1 Reinforcement

Reinforcing bars or mesh, at the time concrete is placed, shall be free from loose rust, scale, dirt, grease or other coatings that will destroy or reduce the bond.

7.1.1 Reinforcing shall be placed in accordance with ACI 318, ACI 301 and as called for on the drawings and shall be securely tied in both directions with No. 16 gage black annealed wire and securely held in position during placing by spacers, chairs, or other supports approved by the CONSTRUCTION MANAGER. For placements on grade, the reinforcement shall be supported on precast concrete blocks, spaced at intervals as required by the size of reinforcement, to maintain the specified cover.

7.1.2 The bending, lapping, splicing and offsetting of reinforcement and the concrete cover required for the various types of structures shall be as shown on the drawings.

7.1.3 Splicing by the Cadweld method, if required, shall be in accordance with Specification No. 7749-C-30.

7.1.4 Exposed reinforcement intended for bonding with future extensions shall be protected from corrosion by concrete, wrapping, or other adequate covering.

7.1.5 Reinforcing bars shall not be cut, welded or moved from the locations shown on the drawings except with prior approval from the CONSTRUCTION MANAGER.

7.2 Inserts

Anchor bolts, sleeves, drains, curb and trench angles, screen guides, door frames, conduits and outlet boxes, unistruts and other inserts, as shown on the drawings, shall be accurately placed or templated in and securely anchored prior to placing concrete.

0001023104



8.0 CLASSES OF CONCRETE AND MAXIMUM SIZE AGGREGATE

3

Concrete of the various classes and maximum aggregate sizes will be proportioned in accordance with Specification No. 7749-C-25, Central Concrete Mix Plant, and will be the responsibility of others. The actual concrete class and corresponding slump figure for the slip-form concrete shall be as shown on the drawings.

3

9.0 CONVEYING AND PLACING

Conveying and depositing of concrete shall be in accordance with ACI 301, ACI 304, ACI 318, ASTM C-94, and as follows: An interconnected telephone or radio system for the use of the batch plant inspector, placing inspector, and the concrete testing laboratory shall be maintained. The communication system at the location of placement shall be provided with a suitable annunciator and light to attract attention under working conditions. An annunciator and light shall be used to control conveying of concrete by a concrete pump or pneumatic placer. One set will be located at the point of deposition and one set at the concrete pump or pneumatic placer. No aluminum pipe shall be used to convey concrete from a concrete pump or pneumatic placer to point of placement.

3

9.1 Clean-up Preparation

Before depositing concrete, all placing equipment shall be cleaned. Debris (mud, snow and ice) shall be removed from spaces to receive concrete, and the reinforcement and other metal to be embedded shall be thoroughly cleaned of all loose rust, scale, and/or other coating which might impair the bond. All compacted soil, rock or concrete surfaces to receive concrete shall be thoroughly wetted before placement.

9.2 Deposition

Critical structural concrete shall be deposited in accordance with a schedule developed by the CONTRACTOR and approved by the CONSTRUCTION MANAGER showing the number, size and sequence of concrete pours. A concrete pour checkout card shall be completed prior to concrete deposition. Should additional water be added to the concrete in transit or at the point of placement, a minimum of (30) additional revolutions will be required in the mix truck. The time between introduction of mixing water and the start of discharge of concrete from the truck shall not exceed 45 minutes. However, the time from introduction of initial mixing water to the time of complete discharge of concrete from the truck shall not exceed that specified in ASTM C-94-68. Water introduced to the dry mix, either at a central plant, transit mixer, or transport mixer at point of deposition shall be the total volume of water designated by the design mix correlated to field conditions of aggregate and slump differential. Addition of tempering water will not be permitted except as approved by the CONSTRUCTION MANAGER and requires both slump test and test cylinders taken of the altered concrete at the point of placement.

3

3







9.7 Placing Limitations

Concrete shall be deposited in horizontal layers of not greater depth than 24 inches, and shall not be allowed or caused to flow a distance, within the mass, of more than 5 feet from point of deposition.

9.8 Vertical Members

Vertical members, such as walls and columns, shall be poured to a level approximately 1 inch above the soffit of beams, girders, haunches, or other superimposed construction or top of walls and then struck off to true level after settlement has taken place.

10.0 CONSOLIDATION OF CONCRETE

Concrete shall be placed with the aid of mechanical vibrating equipment and supplemented by hand spading and tamping. The vibrating equipment shall be of the internal type and shall at all times be adequate in number of units and power of each unit to properly consolidate all concrete. The vibration frequency shall be not less than 7000 cycles per minute. The duration of vibration shall be limited to the necessary time to produce satisfactory consolidation without causing objectionable segregation. In consolidating each layer of concrete, the vibrator shall be operated in a near vertical position, and the vibrating head shall be allowed to penetrate under the action of its own weight and revibrate the concrete in the upper portion of the underlying layer. Neither form nor surface vibrators shall be used unless specifically approved. Vibrators shall not be used to move or spread concrete. A ratio of not less than one spare vibrator in good working condition to each three vibrators required for satisfactory vibration of the concrete being placed shall be kept available for immediate use at point of deposition. Provisions shall be made for auxiliary power to provide continuity of vibration in case of power failure from the principal source. Experienced and competent operators shall be provided for each vibrator being used.

11.0 COLD AND HOT WEATHER CONCRETING

11.1 Methods

Methods and means of batching, mixing and delivery of concrete in cold and hot weather shall comply with the Technical Specification No. 77-49-C-25, "Central Concrete Mix Plant", and shall be the responsibility of others. Concrete for slip-form work shall not be considered mass concrete but shall be treated as concrete for "thin" sections.

000102007



Power and Industrial  
Division

Specification No. 7749-C-26

11.2 Moderate Weather Precautions

During moderate weather, fresh concrete shall not be placed at an ambient temperature lower than 45F. It shall be protected from extreme temperature variations for not less than 72 hours.

3  
2

11.3 Cold Weather Concreting

11.3.1 Concrete, as mixed during cold weather, shall have a temperature of not less than the following: (and as specified in Specification No. 7749-C-25, Central Concrete Mix Plant).

2

<u>Air Temp. Deg. F</u>	<u>Thin Sections Less than 2 1/2 feet in Least Dimension</u>	<u>Mass Concrete 2-1/2 feet or More in Least Dimension</u>
30F to 45F	60F	50F
0F to 30F	65F	55F
Below 0F	70F	60F

11.3.2 Heating of the mixing water or aggregates will be the responsibility of others.

4

11.3.3 All concrete members 2-1/2 feet or more in thickness, shall have a placing temperature of not more than 70F and not less than 45F with the exception of slip-form concrete which shall have a maximum placing temperature of 85F and a minimum placing temperature of 70 F. Concrete less than 2-1/2 feet in thickness shall have a placing temperature of not more than 85F and not less than 55F.

3

11.3.4 Before concrete is placed, all ice, snow, and frost shall be completely removed from surfaces which will be in contact with the concrete. The temperature of such surfaces, when ambient temperature is below 32F, shall be raised within 20F of the temperature specified in Paragraph 11.3.1 except that no concrete shall be placed upon a construction joint unless the construction joint has a temperature of at least 40F. No concrete shall be placed upon a frozen subgrade or one that contains frozen materials.

3

00010000



Power and Industrial Division

Specification No. 7149-C-26

11.3.5 Concrete, except slip-form concrete, shall be protected from freezing by adequate means for seven (7) days. Adequate equipment for protecting concrete from freezing shall be available at the jobsite prior to placing concrete. Particular care shall be exercised to protect edges and exposed corners from freezing. Forms shall be removed and the concrete member shall be completely enclosed in an ambient air temperature not more than 10F (more or less) than the temperature at which the concrete was placed. No curing water will be required if steam is employed. If heat is used, care shall be taken to insure that no part of the concrete becomes dried out or is heated to temperatures above 90F. When dry heat is used, the concrete shall be adequately cured by one of the methods specified in Paragraph 12.0. The housing, covering, or other protection used shall remain in place and intact at least 24 hours after the artificial heating is discontinued.

3

11.3.5.1 Concrete for slip-form work shall conform to ACI Standard "Recommended Practice for Cold Weather Concreting" (ACI 306-66). The concrete shall attain a minimum ultimate compressive strength of 1200 psi in two days when type II cement is used and 1600 psi in two days when type I cement is used. The CONTRACTOR shall certify and document by laboratory tests to the satisfaction of the ENGINEER that the specified concrete is not susceptible to freeze-thaw damage when exposed to cold weather. Cold weather protection of concrete shall be required for a minimum of two days.

3

11.4 Hot Weather Concreting

Concrete members for slip-form work shall not be considered as mass concrete and shall have a maximum placing temperature of 85F and a minimum placing temperature of 70F. To keep the temperature of the concrete from exceeding this limit during hot weather, the CONTRACTOR shall, at his expense, use approved means and measures for minimizing the temperature of the concrete, all as approved by the CONSTRUCTION MANAGER.

3

3

12.0 CURING

The entire concrete surface, except as specified otherwise, shall be cured by one or more of the following methods:

3

12.1 Moist Curing

Newly placed concrete shall be kept wet by the continuous application of water with a nozzle, soakers or wet burlap for the first 7 days after the concrete has been placed. The curing water shall be clean and free of contaminating substances that will discolor the concrete. Concrete members 2-1/2 feet or more in the least dimension and all concrete construction joints to receive additional lifts of concrete shall be water cured except in extremely cold weather when another method must be employed.

4

000102109



Power and Industrial  
Division

Specification No. 7749-C-26

12.2 Blanketing Method

The entire surface shall be covered with a blanket of sand or cattn not less than 2 inches in thickness. Immediately after placing, the blanket shall be thoroughly wetted and kept saturated for not less than 7 days after being placed.

12.3 Cotton Mat Method

The entire surface shall be covered with cotton mats laid directly upon the concrete. The cotton mats shall conform to AASHTO Designation M-73-67. Immediately after placing, the mats shall be thoroughly wetted and kept saturated for not less than 7 days.

12.4 Waterproof Paper Method

The entire surface shall be covered with waterproof paper laid directly upon the concrete. The paper shall conform to ASTM Designation C-171. The paper shall be lapped not less than 4 inches at edges and ends, and be sealed with mastic or pressure-sensitive tape not less than 1-1/2 inches in width. Paper shall be weighted to prevent displacement. Holes appearing during the curing period shall be immediately patched. Paper shall remain intact for not less than 7 days after placing. When tested according to ASTM Standard C-156, the loss in weight of water through the curing material shall not exceed 0.005 grams per square centimeter.

12.5 Liquid-Membrane Method

The liquid-membrane curing compound shall conform to clear seal No. 12 as manufactured by Grace and Company, Cambridge, Massachusetts, or equivalent approved by the CONSTRUCTION MANAGER. Application shall be in accordance with manufacturer's instructions and the CONSTRUCTION MANAGER'S approval. All wall surfaces of the Shield Building above the foundation slab shall receive the liquid membrane cure.

4  
3  
4

12.6 Plastic Membrane

The entire surface shall be covered with a polyethelene film laid directly upon the concrete. The film shall be lapped not less than four inches at edges and ends, and be sealed with mastic or pressure-sensitive tape not less than 1-1/2 inches in width. The film shall be weighted or otherwise fastened to prevent displacement. Holes appearing during the curing period shall be immediately patched. The film shall remain intact for not less than seven days after placing. When tested according to ASTM Standard C-156, the loss in weight of water through the curing material shall not exceed 0.055 grams per square centimeter.

0001021000



Power and Industrial  
Division

Specification No. 7749-C-26

13.0 CONCRETE GROUT AND MORTAR

13.1 Grout Classification

Grout and mortar shall meet the following requirements:

<u>Class</u>	<u>Strength</u>	<u>Aggregate</u>	<u>Location</u>
Non-Shrink	4000 psi 5000 psi	Concrete sand	As shown on design drawing
Standard mortar	Same sand-cement ratio used in concrete	Concrete sand	Construction joints, and patching

13.2 Non-Shrink Grout

13.2.1 Composition of interior Embeco non-shrink grout shall be as follows:

- 1 part Portland cement
- 1 part Master Builders Embeco Aggregate, or approved equal
- 1 part clean, well graded concrete sand
- 5.5 gallons of water per sack of cement

13.2.2 Interior and Exterior Non-Shrink Grout

- a. Aluminum Powder non-shrink grout shall consist of cement, concrete sand, Interplat "C" (as manufactured by Sika Chemical Corporation or equivalent approved by the CONSTRUCTION MANAGER), and water. Grout shall be mixed in accordance with the manufacturer's instructions. | 3
- b. Five Star Grout manufactured by U. S. Grout Corporation shall be mixed in accordance with the manufacturer's instructions.
- c. Test batches shall be made, tested and approved by the CONSTRUCTION MANAGER for expansion and compressive strength prior to use. | 3

1000132



13.3 Mixing Non-Shrink Grout

Non-shrink grout may be mixed by hand or mechanical mixer. The Embecco aggregate, or aluminum powder, and water shall be added to the mix immediately prior to use. Grout shall be mixed in small quantities so that all grout shall be completely placed within 20 minutes after mixing. Grout shall not be retempered by addition of more water.

13.4 Drypack Mortar

Drypack shall consist of a mixture (by volume) of 1 part cement to 2-1/2 parts of sand with gradation such that 100 percent shall pass the No. 16 sieve. Only enough water shall be used to produce a mortar, which when used, shall stick together on being molded into a ball by a slight pressure of the hands, and shall not exude water but will leave the hands damp. The proper amount of mixing water and the proper consistency shall be that which produce a filling which is at the point of becoming rubbery when the material is solidly packed. Any less water will not make a sound, solid pack; any more will result in excessive shrinkage and a loose repair. Drypack shall be placed and packed in layers. Each layer shall be solidly compacted over its entire surface by the use of a hardwood stick and a hammer.

14.0 SLUMP REQUIREMENTS

14.1 The slump as indicated in the Central Concrete Mix Plant, Specification No. 7749-C-25 shall be maintained at the point of delivery and discharge to this Shield Building CONTRACTOR. Slumps at the stationary mixer shall be gaged to provide these required slumps and will be the responsibility of others.

15.0 CONCRETE SURFACE FINISHES

15.1 See Specification No. 7749-C-38, Shield Building.

16.0 REPAIR OF CONCRETE

16.1 See Specification No. 7749-C-38, Shield Building.

17.0 MEASUREMENT AND PAYMENT

17.1 The Lump Sum Price for the complete WORK for the Shield Building shall include the concrete specified herein. The unit prices bid in Paragraphs 2.2 and 2.3 of the Proposal shall be used for additions to or deletions from the Lump Sum bid in Items 2.1.1 and 2.1.2 respectively of the Proposal. Only net changes in quantities as directed by the CONSTRUCTION MANAGER or the ENGINEER shall constitute additions to or deletions from the Lump Sum bids.

17.2 Net changes in quantities shall be calculated on the dimensions as detailed on the drawings.

0001020002

## FOR QUALITY ASSURANCE USE

(A) MR. H. W. WAHL PROJECT ENGINEER BECHTEL COMPANY 15740 SHADY GROVE ROAD GAITHERSBURG, MD. 20760	(B) MR. M. R. STEPHENS PROJECT CONSTRUCTION MANAGER BECHTEL CORPORATION P.O. BOX 449 PORT CLINTON, OHIO 43452	(C) MR. J. D. LENARDSON THE TOLEDO EDISON CO. P.O. BOX 929 TOLEDO, OHIO 43601
--	--	--

\* These required certified copies shall be furnished upon or prior to the arrival of the material at the jobsite.

2 Issued for Addendum 4  
 1 Issued for Construction Addendum 3  
 0 Issued for Detailing and Material Purchase  
 A Issued for Client Approval and Bid

REV.	DESCRIPTION	TYPE OF DRAWINGS AND OTHER REQUIREMENTS	REFER TO SPECIFICATION PARAGRAPH	COPIES WITH PROP PLUS 1 TO (C)	KIND OF COPIES (PLACE * WHERE REQ.)	COPIES FOR APPROVAL TO		CERTIFIED COPIES TO			
						(A)	(C)	(A)	(B)	(C)	
1		QUALITY CONTROL INSPECTION AND TEST PROCEDURES (OUTLINE)	3.1	1	REPRODUCIBLE PRINTS		2			2	
2		QUALITY CONTROL INSPECTION AND TEST PROCEDURES (DETAILED)	3.1		REPRODUCIBLE PRINTS	3	2	2		2	
3		PRODUCTION SCHEDULE	3.1		REPRODUCIBLE PRINTS	3	2	2	2	2	
4		COMPLETED PLACING INSPECTOR'S CLEARANCE CARD	3.3.1 (a)		REPRODUCIBLE PRINTS		2	1	2	2	
5		PLACING INSPECTOR'S END-OF-SHIFT REPORT	3.3.1 (b)		REPRODUCIBLE PRINTS		2	1	2	2	
6		PLACING INSPECTOR'S END-OF-CURING-TIME REPORT	3.3.1 (c)		REPRODUCIBLE PRINTS		2	1	2	2	
7		TEST CERTIFICATES FOR RUBBER WATER STOPS	5.4		REPRODUCIBLE PRINTS		2	1	2	2	
8		TEST CERTIFICATES FOR PVC WATER STOPS	5.4		REPRODUCIBLE PRINTS		2	1	2	2	
9		LETTER OF CONFORMANCE FOR EXPANSION JOINT FILLER	5.1		REPRODUCIBLE PRINTS		2	1	2	2	
10		LETTER OF CONFORMANCE FOR JOINT SEALER	5.2		REPRODUCIBLE PRINTS		2	1	2	2	
11		CERTIFICATION AND DOCUMENTATION BY LAB TESTS, FREEZE/THAW DAMAGE	11.3.5.1		REPRODUCIBLE PRINTS	3	2	2	2	2	
12		HANDLING, STORAGE, PRESERVATION, PACKING AND SHIPPING PROCEDURES	3.4		REPRODUCIBLE PRINTS		2		2	2	
13		TEST BATCH RESULTS	13.2.2c		REPRODUCIBLE PRINTS		2		2	2	
14					REPRODUCIBLE PRINTS						
15					REPRODUCIBLE PRINTS						
16											
17											
18											
19											
20		BASIC INSPECTION RECORDS AVAILABLE _____ TO BUYER PER SPECIFICATION (FORECAST DATE)									

THE TOLEDO EDISON COMPANY  
 AND  
 THE CLEVELAND ELECTRIC ILLUMINATING COMPANY  
 DAVIS-BESSE UNIT NO. 1 CONSTRUCTION  
 QUALITY ASSURANCE  
 DOCUMENTATION DISTRIBUTION REQUIREMENTS  
 CONSTRUCTION DOCUMENT NO. 7749-18

JOB NO. 7749  
 SPEC. NO. 7749-C-26  
 ITEM NO. CD-18  
 P. O. NO.





**Exhibit 5: QA and Procedures for  
Slip Form Construction**